

Dericht

1 Z 22174 F

September

Zeitschrift für Geophysik

Band 38

1972

Heft 3



Proceedings

Symposium on the Interpretation of Seismic Discontinuities



PHYSICA - VERLAG · WÜRZBURG

ZEITSCHRIFT FÜR GEOPHYSIK

als zweimonatliche Publikation herausgegeben im Auftrag der Deutschen Geophysikalischen Gesellschaft von

W. Dieminger, Lindau/Harz

und

J. Untiedt, Münster i. W. (als Stellvertreter)

unter Mitwirkung von

A. Defant, Innsbruck — W. Hiller, Stuttgart — W. Kertz, Braunschweig — Th. Krey, Hannover — E. A. Lauter, Kühlungsborn — H. Menzel, Hamburg — O. Meyer, Hamburg — F. Möller, München — St. Müller, Zürich — H. Reich, Göttingen — U. Schmucker, Göttingen — M. Siebert, Göttingen — H. Soffel, München

Veröffentlicht werden Originalarbeiten aus dem gesamten Gebiet der Geophysik und aus den Grenzgebieten in deutscher, englischer oder französischer Sprache. Außerdem erscheinen mehrmals im Jahr auf Einladung hin verfaßte Übersichtsartikel.

Für kurze Mitteilungen, bei denen Interesse an raschem Erscheinen besteht, gibt es neben den normalen Veröffentlichungen die „Briefe an den Herausgeber“ (ohne Zusammenfassung). Sie werden nach Möglichkeit im nächsten Heft gebracht.

Jede Originalarbeit beginnt mit einer deutschen und einer englischen oder französischen Zusammenfassung. Bei deutschsprachigen Aufsätzen und Briefen werden Titel der Arbeit und Abbildungsunterschriften zusätzlich in englischer oder französischer Sprache gebracht.

Die Autoren erhalten 50 Sonderdrucke ihrer Arbeit kostenlos. Weitere Exemplare können vom Verlag gegen Berechnung geliefert werden. Eine Honorierung der Beiträge erfolgt nicht.

Es wird gebeten, die Manuskripte in Maschinenschrift mit handschriftlich eingetragenen Formeln druckfertig einzureichen und gesondert eine „Anweisung für den Setzer“ beizufügen, aus der zu ersehen ist, wie kursiver, gesperrter oder fetter Satz und griechische, gotische oder einander ähnliche Typen und Zeichen kenntlich gemacht sind (z. B. durch farbige Unterstreichung). Die Vorlagen für die Abbildungen sollen reproduktionsfertig (Tuschzeichnung) möglichst im Maßstab 2:1 eingesandt werden.

Die Zitate sollen entsprechend folgendem Beispiel angefertigt werden:

Im Text: Bei der ersten Zitierung [JUNG, MENZEL und ROSENBACH 1965], bei jeder folgenden Zitierung [JUNG et al. 1965]
Im Literaturverzeichnis: JUNG, K., H. MENZEL und O. ROSENBACH: Gravimetermessungen im Nördlinger Ries. Z. Geophys. 31, 7—26, 1965.

Manuskripte sind zu senden an Prof. Dr. WALTER DIEMINGER, Max-Planck-Institut für Aeronomie, 3411 Lindau/Harz.

Anschrift der Deutschen Geophysikalischen Gesellschaft:

2 Hamburg 13, Binderstr. 22.
Tel. (0411) 441 97 29 77

Postscheckkonto: Hamburg 559 83
Bank: Neue Sparcasse, Hamburg 24/115 28

Aufgenommen werden nur Arbeiten, die weder im In- noch im Ausland veröffentlicht wurden und die der Autor auch anderweitig nicht zu veröffentlichen sich verpflichtet. Mit der Annahme des Manuskriptes geht das ausschließliche Nutzungsrecht an den Verlag über.

Es ist ohne ausdrückliche Genehmigung des Verlages nicht gestattet, fotografische Vervielfältigungen, Mikrofilme, Mikrofotos u. ä. von den Zeitschriftenheften, von einzelnen Beiträgen oder von Teilen daraus herzustellen.

Bezugspreis je Band (6 Hefte) 112,— DM, Einzelheft je nach Umfang. Abonnements verlängern sich jeweils um einen Band, falls keine ausdrückliche Abbestellung zum Jahresende vorliegt. Der Mitgliedsbeitrag schließt den Bezug der Zeitschrift ein.

Gedruckt mit Unterstützung der Deutschen Forschungsgemeinschaft.

Diesem Heft liegt ein Prospekt der Schweizerbart'schen Verlagsbuchhandlung, Stuttgart, bei.

Bekanntmachung lt. Bayer Pressegesetz: Verlag: PHYSICA-VERLAG Rudolf Liebing K.-G., D 87 Würzburg, Werner-von-Siemens Straße 5
Pers. haft. Ges.: Anulf Liebing und Hildgund Holler, sämtlich Buchhändler in Würzburg. Kommanditistin: Gertrud Liebing Würzburg

Druckerei: R. Oldenbourg, Graph. Betriebe GmbH, München

Printed in Germany



PHYSICA-VERLAG, Würzburg 1972

European Seismological Commission
Sub-Commission for the Interpretation of
Seismological Results

Seismic Modelling Working Group

Proceedings

Symposium on the Interpretation of Seismic Discontinuities

under the auspices of the European Seismological Commission and the
Czechoslovak Academy of Sciences

Castle of Liblice near Prague, 6–10 December 1971

List of Contents

Foreword, Program of the Symposium on the Interpretation of Seismic Discontinuities, List of participants	
VANĚK, J.: Seismological Evidence on Discontinuities in the Mantle (Invited Paper)	355
DAVYDOVA, N. I., I. P. KOSMINSKAYA, N. K. KAPUSTIAN and G. G. MICHOTA: Models of the Earth's Crust and M-Boundary	369
GIESE, P.: The Special Structure of the P^{MP} Traveltime Curve	395
TREGUB, F. S.: Relation between P-Wave Amplitudes and Discontinuities in the Earth's Crust	407
BERÁNEK, B., and A. DUDEK: The Results of Deep Seismic Sounding in Czechoslovakia	415
CHRISTOSKOV, L.: On the Amplitude Curves of Body Waves for Short Epicentral Dis- tances and Their Oscillatory Character	429
RUPRECHTOVÁ, L.: Recent Interpretation of the Core Discontinuities	441
CHOUDHURY, M. A.: P-Wave Attenuation in the Mantle	447
GALKIN, I. N., V. T. LEVSHENKO, V. I. MYACHKIN and A. V. NIKOLAYEV: Inhomoge- neity of the Earth with Respect to Physical Processes of Earthquakes	455
BABUŠKA, V.: Anisotropy in the Upper Mantle Rocks	461
ČERVENÝ, V.: Theory of Elastic Wave Propagation in Inhomogeneous Media (Invited Paper)	469
BEHRENS, J., R. BORTFELD, G. GOMMLICH and K. KÖHLER: Interpretation of Discon- tinuities by Seismic Imaging	481
ČERVENÝ, V., and J. ZAHRADNÍK: Amplitude-Distance Curves of Seismic Body Waves in the Neighbourhood of Critical Points and Caustics — A Comparison	499
RICHARDS, P. G.: Seismic Waves Reflected from Velocity Gradient Anomalies within the Earth's Upper Mantle	517
NEDOMA, J.: Investigation of Linear Harmonic Field of SH-Waves in a Stratified In- homogeneous Medium Using the Finite Difference Method	529
PLEŠINGER, A., and R. VÍCH: On the Identification of Seismometric Systems and the Correction of Recorded Signals for Identified Transfer Functions	543
PĚČ, K., and O. NOVOTNÝ: The Influence of the Low Velocity Zone on Phase Veloci- ties and Amplitudes of Love Waves	555
ČERVENÝ, V., and I. PŠENČÍK: Rays and Travel-Time Curves in Inhomogeneous Aniso- tropic Media	565
BEHRENS, J., O. G. SHAMINA and L. WANIEK: Interpretation of Discontinuities by Seismic Modelling Methods (Invited Paper)	579

KOZÁK, J.: Contemporary Possibilities of the Schlieren Method in the Study of Seismic Boundary Phenomena	595
SHAMINA, O. G.: Model Investigations of Inclusions in Medium	609
ČERVENÝ, V., and J. KOZÁK: Experimental Evidence and Investigation of Pseudo-spherical Waves	617
BEHRENS, J., and J. SIEBELS: Model Investigations on Low Velocity Layers	627
WANIEK, L.: Model Studies of Wave Propagation in Low Velocity Layers with Sharp Boundaries	647
BEHRENS, J., and G. GOMMLICH: Model Investigations with Respect to the Interpretation of Complicated Seismic Discontinuities	659

Foreword

The Symposium on the Interpretation of Seismic Discontinuities was held under the auspices of the European Seismological Commission in the Castle of Liblice near Prague from 6th to 10th December, 1971. It was organized by the Geophysical Institute of the Czechoslovak Academy of Sciences in Prague.

The present issue of the "Zeitschrift für Geophysik" presents the proceedings of the papers delivered at the Symposium. The impetus to organize the Symposium was given on the occasion of the XII Assembly of the ESC in Luxembourg in 1970. The discussions related to the problem of a correct interpretation of the Earth's structure indicated that the recent studies had signalized increasing uncertainty as to the physical properties of seismic discontinuities. The purpose of the Symposium was to bring together scientists working in the field of seismological observations, in the theory of wave propagation and in model seismology, and to provide them with the possibility of discussing and comparing their results.

The presented communications confirmed the importance of the confrontation of the results obtained along this line. The characteristic phenomena of low velocity layers, the M-discontinuity and other discontinuities within the Earth were critically elucidated and more realistic platforms for considering their actual properties were found.

The participants of the Symposium wish to express their thanks to the Publishers of the "Zeitschrift für Geophysik" for publishing the papers in a special issue. The manuscripts are presented in the form in which they were submitted. In a few cases the texts had to be slightly adapted in order to obtain a uniform form.

Prague—Clausthal, February 1972

L. WANIEK, J. BEHRENS

Program

The Symposium was opened on December 6, 1971 at the Castle of Liblice. The participants were addressed by the Vicepresident of the European Seismological Commission, Prof. Dr. R. TEISSEYRE and the Director of the Geophysical Institute of the Czechoslovak Academy of Sciences, Dr. V. BUCHA.

December 7, 1971

1st session — Seismology

Chairman: Prof. Dr. E. PETERSCHMITT, Convenor: Dr. J. VANĚK

VANĚK, J.: Seismological Evidence on Discontinuities in the Mantle (Invited Paper)

DAVYDOVA, N. I., I. P. ,KOSMINSKAYA, N. K. KAPUSTIAN and G. G. MICHOTA: Models of the Earth's Crust and M-Boundary

GIESE, P.: The Special Structure of the P^{MP} Traveltime Curve

TREGUB, F. S.: Relation between P-Wave Amplitudes and Discontinuities in the Earth's Crust

2nd session — Seismology

Chairman: Prof. Dr. I. P. KOSMINSKAYA, Convenor: Dr. J. VANĚK

BERÁNEK, B., and A. DUDEK: The Results of Deep Seismic Sounding in Czechoslovakia

CHRISTOSKOV, L.: On the Amplitude Curves of Body Waves for Short Epicentral Distances and Their Oscillatory Character

RUPRECHTOVÁ, L.: Recent Interpretation of the Core Discontinuities

December 8, 1971

3rd session — Seismology

Chairman: Prof. Dr. S. MÜLLER, Convenor: Dr. J. VANĚK

CHOUDHURY, M. A.: P-Wave Attenuation in the Mantle

MÜLLER, S.: The Nature of Seismic Boundaries within the Earth's Crust

GALKIN, I. N., V. T. LEVSHENKO, V. I. MYACHKIN and A. V. NIKOLAYEV: Inhomogeneity of the Earth with Respect to Physical Processes of Earthquakes

MÜLLER, S., and G. MÜLLER: An Example of an Iterative Process in Interpreting Crustal Seismic Data

In the afternoon an excursion to the Geophysical Institute of the Czechoslovak Academy of Sciences in Prague was organized.

December 9, 1971

4th session — Theory

Chairman: Prof. Dr. N. J. VLAAR, Convenor: Prof. Dr. V. ČERVENÝ

ČERVENÝ, V.: Theory of Elastic Wave Propagation in Inhomogeneous Media (Invited Paper)

BEHRENS, J., R. BORTFELD, G. GOMMLICH and K. KÖHLER: Interpretation of Discontinuities by Seismic Imaging

ČERVENÝ, V., and J. ZAHRADNÍK: Amplitude—Distance Curves of Seismic Body Waves in the Neighbourhood of Critical Points and Caustics—A Comparison

RICHARDS, P. G.: Seismic Waves Reflected from Velocity Gradient Anomalies within the Earth's Upper Mantle

5th session — Theory

Chairman: Dr. P. G. RICHARDS, Convenor: Prof. Dr. V. ČERVENÝ

NEDOMA, J.: Investigation of Linear Harmonic Field of SH-Waves in a Stratified Inhomogeneous Medium Using the Finite Difference Method

PLEŠINGER, A., and R. VÍCH: On the Identification of Seismometric Systems and the Correction of Recorded Signals for Identified Transfer Functions

PĚČ, K., and O. NOVOTNÝ: The Influence of the Low Velocity Zone on Phase Velocities and Amplitudes of Love Waves

ČERVENÝ, V., and I. PŠENČÍK: Rays and Travel-Time Curves in Inhomogeneous Anisotropic Media

BABUŠKA, V.: Anisotropy in the Upper Mantle Rocks

December 10, 1971

6th session — Models

Chairman: Dr. O. G. SHAMINA, Convenor: Dr. L. WANIEK

BEHRENS, J., O. G. SHAMINA and L. WANIEK: Interpretation of Discontinuities by Seismic Modelling Methods (Invited Paper)

KOZÁK, J.: Contemporary Possibilities of the Schlieren Method in the Study of Seismic Boundary Phenomena

SHAMINA, O. G.: Model Investigations of Inclusions in Medium

ČERVENÝ, V., and J. KOZÁK: Experimental Evidence and Investigation of Pseudo-spherical Waves

7th session — Models

Chairman: Prof. Dr. J. BEHRENS, Convenor: Dr. L. WANIEK

BEHRENS, J., and J. SIEBELS: Model Investigations on Low Velocity Layers

WANIEK, L.: Model Studies of Wave Propagation in Low Velocity Layers with Sharp Boundaries

BEHRENS, J., and G. GOMMLICH: Model Investigations with Respect to the Interpretation of Complicated Seismic Discontinuities

List of Participants

- V. BABUŠKA, Geofyzikální ústav ČSAV, Praha, ČSSR
J. BEHRENS, Institut für Geophysik der TU, Clausthal-Zellerfeld, GFR
B. BERÁNEK, Ústav užité geofyziky, Brno, ČSSR
R. BORTFELD, Prakla-Seismos GMBH, Hannover, GFR
I. BROUČEK, Geofyzikální ústav SAV, Bratislava, ČSSR
M. A. CHOUDHURY, Institut de Physique du Globe, Paris, France
L. CHRISTOSKOV, Institut po Geofizika BAN, Sofia, Bulgaria
K. CIDLINSKÝ, Ústav užité geofyziky, Brno, ČSSR
V. ČERVENÝ, Geofyzikální ústav KU, Praha, ČSSR
A. DUDEK, Ústřední ústav geologický, Praha, ČSSR
Z. FABIÁN, Geofyzikální ústav KU, Praha, ČSSR
P. GIESE, Institut für Meteorologie und Geophysik der TU, Berlin (W)
G. GOMMLICH, Institut für Geophysik der TU, Clausthal-Zellerfeld, GFR
J. JÁNSKÝ, Geofyzikální ústav KU, Praha, ČSSR
V. KÁRNÍK, Geofyzikální ústav ČSAV, Praha, ČSSR
K. KLÍMA, Geofyzikální ústav ČSAV, Praha, ČSSR
I. P. KOSMINSKAYA, Institut Fiziki Zemli ANSSSR, Moskva, USSR
J. KOZÁK, Geofyzikální ústav ČSAV, Praha, ČSSR
V. I. MYACHKIN, Institut Fiziki Zemli ANSSSR, Moskva, USSR
S. MÜLLER, Institut für Geophysik der ETH, Zürich, Switzerland
J. NEDOMA, Geofyzikální ústav ČSAV, Praha, ČSSR
O. NOVOTNÝ, Geofyzikální ústav KU, Praha, ČSSR
E. PETERSCHMITT, Institut de Physique du Globe, Strasbourg, France
K. PĚČ, Geofyzikální ústav KU, Praha, ČSSR
A. PLEŠINGER, Geofyzikální ústav ČSAV, Praha, ČSSR
J. PLOMEROVÁ, Geofyzikální ústav ČSAV, Praha, ČSSR
D. PROCHÁZKOVÁ, Geofyzikální ústav ČSAV, Praha, ČSSR
Z. PROS, Geofyzikální ústav ČSAV, Praha, ČSSR
I. PŠENČÍK, Geofyzikální ústav ČSAV, Praha, ČSSR
P. G. RICHARDS, Lamont-Doherty Geological Obs., Palisades, USA
B. RUNTÁK, Ústav užité geofyziky, Brno, ČSSR
L. RUPRECHTOVÁ, Geofyzikální ústav ČSAV, Praha, ČSSR
V. SCHENK, Geofyzikální ústav ČSAV, Praha, ČSSR

Z. SCHENKOVÁ, Geofyzikální ústav ČSAV, Praha, ČSSR
O. G. SHAMINA, Institut Fiziki Zemli ANSSSR, Moskva, USSR
C. SOBOTOVÁ, Geofyzikální ústav ČSAV, Praha, ČSSR
R. TEISSEYRE, Institut Geofizyki PAN, Warszawa, Poland
F. S. TREGUB, Institut Fiziki Zemli ANSSSR, Moskva, USSR
U. LUOSTO, Yliopiston seismologian laitos, Helsinki, Finland
J. VANĚK, Geofyzikální ústav ČSAV, Praha, ČSSR
N. J. VLAAR, Vening-Meinesz Institute, Utrecht, the Netherlands
L. WANIEK, Geofyzikální ústav ČSAV, Praha, ČSSR
I. ZAHRADNÍK, Geofyzikální ústav KU, Praha, ČSSR

Seismological Evidence on Discontinuities in the Mantle

J. VANĚK, Prague¹⁾

Eingegangen am 7. Februar 1972

Summary: Seismological methods of deriving the velocity distribution in the Earth are briefly reviewed including limitations in accuracy and difficulties in correct interpretation of data. The existence of possible discontinuities in the mantle is discussed in the light of recent seismological investigations.

Zusammenfassung: Die seismischen Methoden zur Bestimmung der Geschwindigkeitsverteilung im Erdkörper sind einschließlich ihrer Genauigkeitsgrenzen und Deutungsschwierigkeiten kurz beschrieben. Die Existenz möglicher Grenzflächen im Erdmantel wird im Lichte der jüngsten seismologischen Untersuchungen kritisch diskutiert.

1. Introduction

Seismological observations have the privilege among other geophysical data that they can provide substantial information on the internal structure of the Earth. This is caused by the fact that on the basis of the observation of seismic waves propagating through the Earth's body the distribution of velocity and attenuation in the Earth can be estimated. Although the attenuation of seismic waves is an important independent parameter, the evidence on the velocity distribution is at present incomparably more detailed and much more significant. Therefore this paper is mainly concerned with the problems of the velocity distribution. This distribution is not uniform and irregularities in this distribution may be connected to the internal structure of the Earth.

What are the irregularities in the uniform velocity distribution that are usually taken into account? It is assumed that a "normal" velocity distribution is characterized by gradually increasing velocity with depth. This idea is based on the fact that the velocity is an increasing function of pressure, which seems to be the governing thermodynamic variable for the velocity, the effect of temperature being usually less pronounced and appearing only in exceptional cases. The deviations from this uniformly increasing velocity idea are then assumed to be a clear evidence for some changes in the composition or state of materials in the Earth.

It is not simple to describe these deviations. In this connection usually the term "discontinuity" is used, discontinuity of the first order for a sudden change in velo-

¹⁾ Dr. Jiří VANĚK, Dr Sc., Geofyzikální ústav, ČSAV, Praha 4 – Spořilov, Boční II, ČSSR

city, or discontinuity of the second order for a sudden change in the gradient of the velocity-depth curve. In the classical meaning discontinuity is a geometric surface, an idea good for the geometric ray theory; real discontinuities in the Earth, however, are probably complicated transition zones with thickness of several kilometers. The discontinuities are very important from seismological point of view, being connected with specific types of seismic waves. Nevertheless, discontinuities are not the only irregularities in the uniform velocity distribution, because important peculiarities in the propagation of seismic waves may be also caused by layers with a specific velocity distribution, as low-velocity layers, layers with constant velocity, or layers with larger or smaller velocity gradients.

2. Methods

The classical method for obtaining seismological evidence on the velocity distribution in the Earth is based on the study of travel-time curves $T(\Delta)$ of seismic body waves. Both the GUTENBERG and JEFFREYS velocity distributions, which have formed the basis for the discussion of the properties of the interior of the Earth, were derived from the observed travel-time curves of P-, PKP-, and S-waves. Many recent attempts have been done to refine the velocity distribution. However, the efficiency of the method is limited by the accuracy of travel-time observations, which at present does not allow to determine uniquely the interesting details. To illustrate this indeterminacy YANOVSKAYA and ASBEL [1963] computed travel-time curves for 2400 different velocity distributions in the upper mantle, the parameters of which were varied by the Monte Carlo method, and found 115 cases satisfying the condition that the standard deviation between the computed and observed travel times was less than 1 second. In fact the indeterminacy of the travel times which permits the changes in the velocity distribution mentioned above could also be interpreted as permitting the segmenting of the travel-time curve due to the existence of discontinuities of either the first or second order. An example of this concept of segmenting of the travel-time curve can be seen in Fig. 1; the travel-time curves were derived by MAYER-ROSA [1969] for the region of south-eastern Europe. Besides the insufficient accuracy of observations another difficult problem is the correct coordination of the travel-time curve to the appropriate wave type, which must be usually presumed by the investigator. In most cases it is very difficult to determine the wave type on the basis of kinematic observations only.

To obtain more information on the details of the velocity distribution the travel-time gradient curves $p(\Delta) = dT/d\Delta$ have been applied in recent years. This method has been used especially with seismic arrays and enables to analyze thoroughly not only the first onsets but also later arrivals in the wave group in question. An example of the $p(\Delta)$ curve is given in Fig. 2; this $p(\Delta)$ curve was derived by JOHNSON [1967] from $dT/d\Delta$ measurements with the extended array at the *Tonto Forest Seismological Observatory* in Arizona. The method of gradient curves seems to be very effective

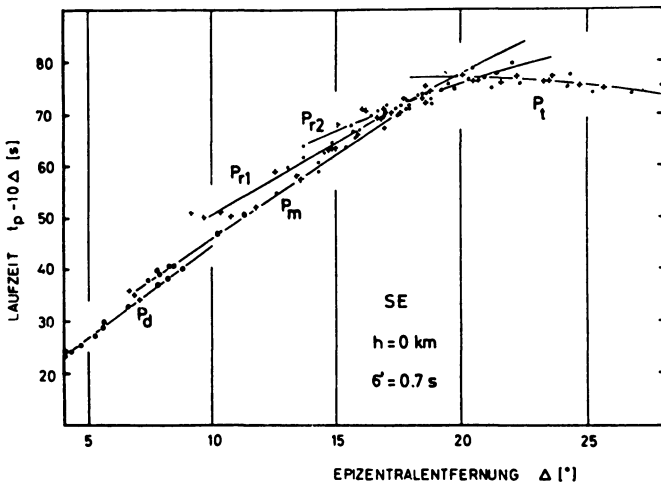


Fig. 1: Travel-time curves of P-waves derived by MAYER-ROSA [1969] for the region of south-eastern Europe.

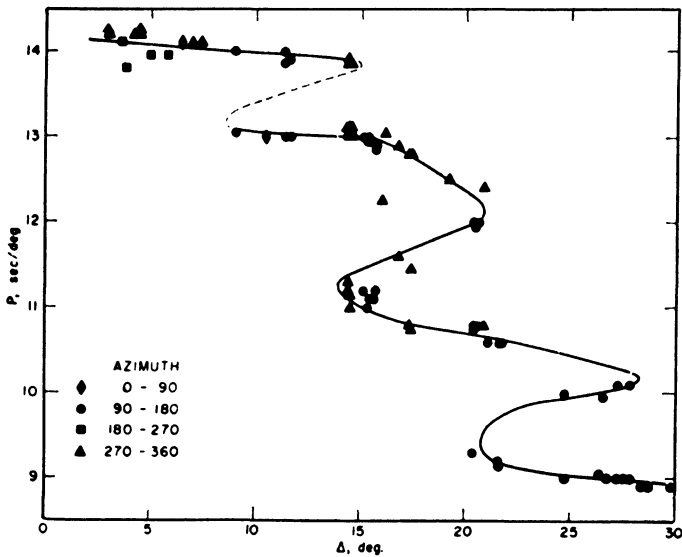


Fig. 2: Travel-time gradient curve $p(\Delta)$ of P-waves constructed from $dT/d\Delta$ measurements with the array at the Tonto Forest Seismological Observatory [JOHNSON 1967].

in some cases. However, it does not exclude the basic problem of interpretation, the necessary a priori presumption on the character of individual wave types.

Another source of information may be the amplitude-distance curves $A(\Delta)$. The amplitudes of seismic waves are sensitive to the velocity gradients near the bottom of their ray paths and therefore provide an independent check on the velocity distribution in the Earth. To a good approximation the logarithm of the amplitude is proportional to the second derivative of travel time according to distance $|d^2T/d\Delta^2|$ which is the absolute value of the slope of the travel-time gradient curve $p(\Delta)$. The application of dynamic parameters of seismic waves is, in general, much more complicated than that of kinematic data. Before constructing the amplitude curve the amplitude observations must be specially processed. The most substantial procedures appear to be the homogenization and normalization of data. The homogeneity of observations is very important because amplitude observations at two different stations are generally incomparable. Neglect of this fact leads to a large scatter of observations, which makes the derivation of the fine structure of the amplitude curve practically impossible. The normalization of data enables to exclude the influence of earthquake magnitude and mechanism on the amplitudes of seismic waves. Figure 3 is an example of the amplitude-distance curve for P-waves; this curve was derived for the region of south-eastern Europe [VANĚK 1969]. There is one especially weak point in the direct application of amplitude curves to the problem of the structure of the Earth. Amplitude curves are usually constructed for the maximum amplitude of the wave group in question. It appears that for example the P-wave group in the distance range between 5° and 30° [VANĚK and RADU 1964; VANĚK 1968b] is a mixture of many wave types, which are coming in comparable travel times and produce a complicated interference pattern of the P-wave group. At different epicentral distances different wave types are prevailing, thus forming the maximum of the P-wave group. A similar picture will apply to the formation of the S-wave group.

Similarly as in the case of travel times also the amplitude observations can be used for constructing the amplitude gradient curves $\alpha(\Delta) = dA/d\Delta$. In this case a system of near seismic stations or a seismic array is necessary for estimating the gradient α . The advantage of this method is that the amplitude observations have not to be normalized according to the earthquake magnitude and the shape of the amplitude-distance curve can be obtained by integration. Figure 4 shows an example of the amplitude gradient curve $\alpha(\Delta)$; the curve was constructed by VANĚK and TSKHAKAYA [1969] for P-waves from observations of the network of Caucasian seismic stations and is valid for the region of Central Asia.

Another independent method for the exploration of possible discontinuities is the observation of reflected waves with angle of reflexion smaller than the critical angle, i. e. observation of reflected waves near the source. This method, so frequently applied in seismic prospecting, is not simple to be used for deeper parts of the Earth because the energy of seismic waves generated by explosions is not sufficient and the reliable identification of this type of waves in the complicated earthquake records is very

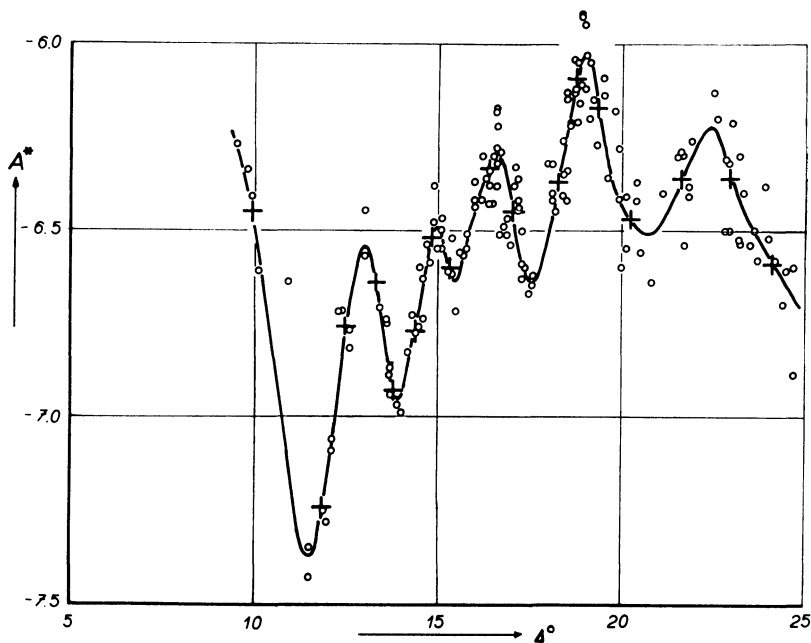


Fig. 3: Amplitude-distance curve $A^*(\Delta)$ of the horizontal component of P-waves for the region of south-eastern Europe [VANĚK 1969]. A^* —normalized amplitude, Δ —epicentral distance in degrees.

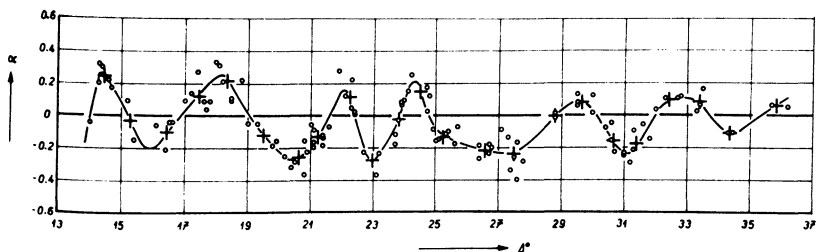


Fig. 4: Amplitude gradient curve $\alpha(\Delta)$ of the horizontal component of P-waves for the region of Central Asia [VANĚK and TSKHAKAYA 1969].

difficult. Recently, interesting efforts were done [POPLAVSKIJ 1971] to analyze statistically all the onsets appearing between P- and S-waves at epicentral distances smaller than 18° , and to try to coordinate the times of accumulation of data to waves reflected at deep discontinuities in the mantle. Again, this method is burdened by necessary presumptions of wave types correlated to times of accumulation. Comparison of theoretical and actual seismograms, as well as the study of spectra of seismic waves, can provide further valuable information, but only first attempts have been done and further research is necessary.

3. Discontinuities in the Mantle

During the history of seismological investigations many discontinuities were discovered. However, the existence of only three discontinuities of the first order seems to be quite certain. The first of them is the surface of the Earth, the second one is the boundary between crust and mantle, the MOHORoviČIĆ-discontinuity, and the third one is the boundary between mantle and core.

In the present report some details about possible discontinuities in the mantle are given. The MOHORoviČIĆ-discontinuity itself, although it was discovered by purely seismological methods, is studied at present by special methods of deep seismic sounding that are practically an extension of the methods applied in seismic prospecting. This is true also for the investigation of the internal structure of the Earth's crust. The structure of the crust is highly variable from one region to another and will be reported in other papers [KOSMINSKAYA, DAVYDOVA and MICHOTA 1972].

To have some basis for the discussion of the structure of the upper part of the mantle let us look at Fig. 5, where two schemes of the upper mantle structure are given: (a) the scheme derived for Central Asia by LUKK and NERSESOV [1965] on the basis of travel-time curves of earthquakes with intermediate focal depths, and (b) the scheme suggested from amplitude-distance curves of P-waves for south-eastern Europe [VANĚK 1968a]. The characteristic features of both schemes are the low-velocity channel starting at depths of about 100 km, and the discontinuity at about 400 km. There are also other discontinuities in both schemes between the MOHORoviČIĆ-discontinuity and the low-velocity channel, and between the low-velocity channel and the discontinuity at 400 km.

One of the main features of this part of the mantle is the low-velocity channel at depths around 100 km. In my opinion, the existence of this channel would be questionable, if we were using the travel-time data only. The main original argument of GUTENBERG [1948] for the existence of this low-velocity channel was the behaviour of amplitudes of seismic body waves. Actually, if we look at more recently derived amplitude-distance curves of both P- and S-waves [VANĚK and STELZNER 1962; VANĚK 1966, 1969; VANĚK and TSKHAKAYA 1969], we can see an anomalous increase in the amplitude level between 10° and 19° followed by a pronounced decrease in the

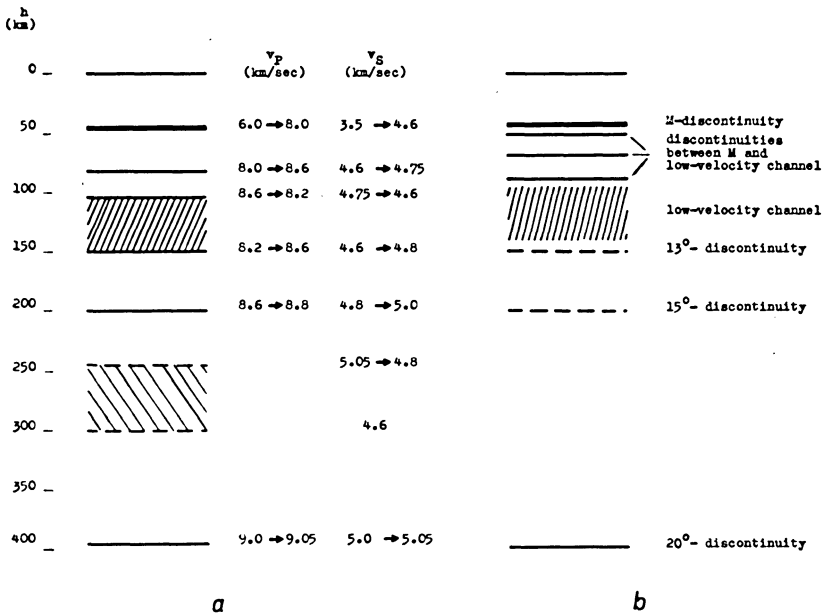


Fig. 5: Scheme of the upper mantle structure: (a) for Central Asia from deep earthquakes [LUKK and NERSESOV 1965]; (b) for south-eastern Europe from amplitude-distance curves of P waves [VANĚK 1968a].

distance range between 20° and 30°. The increase and decrease of amplitudes is not monotonous, several local maxima and minima appear on the amplitude-distance curve, but the general increasing and decreasing tendency in the above mentioned distance intervals can be very clearly observed. It is not possible that this behaviour of amplitudes in such a broad distance interval covering about 20° could be caused by any discontinuity; it must be an effect of a relatively thick layer in the upper mantle. The anomalous increase of amplitudes indicates the possibility of a decrease in the velocity, or, at least, in the velocity gradient within this layer. Also, all recent upper mantle models based on the study into the dispersion of seismic surface waves suggest the existence of a low-velocity channel (or low-velocity channels) in the upper mantle in most regions [DORMAN 1969]. However, the details on this channel, i. e. the velocity and attenuation distribution, nature and depth of its boundaries etc., are at present very obscure and uncertain and most data on the low-velocity channel have the character of assumptions.

The region between the MOHOROVIČIĆ-discontinuity and the low-velocity layer seems to have a rather complicated structure in continental areas. LUKK and NERSESOV

[1965] suggest the existence of a discontinuity with a velocity increase from 8.0 to 8.6 km/sec for P-waves at 85 km in Central Asia. A similar discontinuity with a velocity increase from 8.05 to 8.45 km/sec was assumed by MEREU and HUNTER [1969] for the region of the Canadian Shield at the depth of 84 km. The study of amplitude-distance curves of P- and S-waves disclosed that the structure of this part of the mantle could be even more complicated in some regions. This can be demonstrated by Fig. 6, where the amplitude-distance curve of P-waves is given in the distance range between 2° and 10° based on the observations of the seismic station Sofia [VANĚK and CHRISTOSKOV 1971]. The amplitude curve is characterized by large variations of amplitudes. Considering the amplitude curve as a smooth line, clear oscillations appear in this distance range. It is probable that these oscillations do not correspond to a single wave type. We suggest that these oscillations are a mixture of amplitude curves of different waves which are bound to different discontinuities between the MOHORoviČIĆ-discontinuity and the low-velocity channel. This suggestion is supported by a comparison with the shape of the amplitude curve previously derived from the observations of Bucharest for the same distance range [VANĚK and RADU 1964]. Whereas the observations of P-waves in Sofia were characterized by the mean period of 3 seconds, the mean period for the Bucharest observations was found to be 5.8 seconds. This phenomenon is probably caused by different filtering properties of the underground of both stations. If the interpretation that the amplitude-

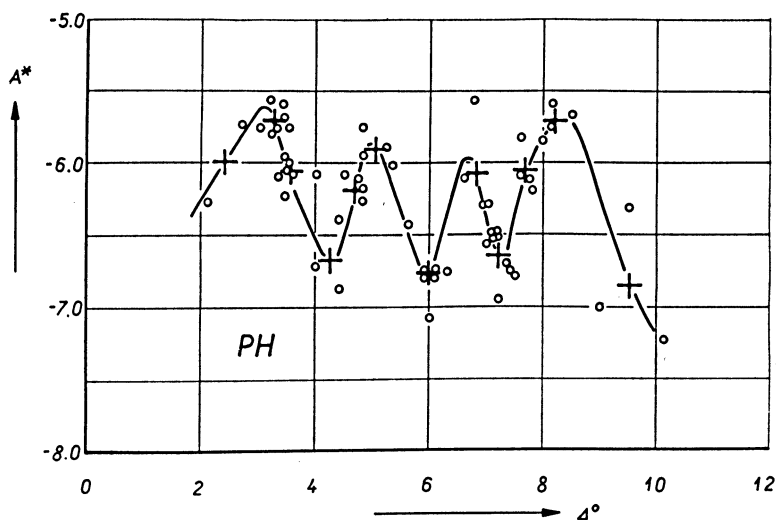


Fig. 6: Amplitude-distance curve $A^*(\Delta)$ of the horizontal component of P-waves derived from observations of Sofia for the region of south-eastern Europe [VANĚK and CHRISTOSKOV 1971].

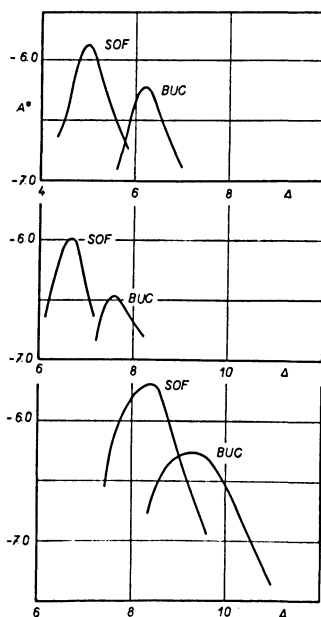


Fig. 7: Comparison of maxima of amplitude-distance curves of P-waves derived from observations of Bucharest (BUC, $T=5.8$ s) and Sofia (SOF, $T=3.0$ s).

distance curve is a mixture of amplitude curves of different reflected waves is correct, the shape of the amplitude curves in both frequency ranges should be similar but, according to the theory of spherical waves reflected at a plane interface by ČERVENÝ [1967], the maxima of the curves should occur at different epicentral distances. This is exactly the behaviour of the amplitude curves derived for Bucharest and Sofia (see Fig. 7). Three maxima of the amplitude curve are drafted in Fig. 7 for both stations; we see that in accord with theory the maximum for lower frequencies is shifted to longer epicentral distances in all three cases. It seems therefore that in the region of south-eastern Europe three discontinuities may exist between the MOHORoviČIĆ-discontinuity and the low-velocity channel. Similar results were obtained by RJABOJ [1966] on the basis of deep seismic sounding on the 625-km long profile between *Kopetdagh Mountains* and *Aral Sea*. From travel times and amplitude curves, the shape of which was quite similar to that shown in Fig. 6, he suggested the existence of three or four discontinuities in the depth of 45 and 120 km.

The structure beneath the low-velocity channel up to the depth of about 400 km is not clear. Some authors suggest the existence of a discontinuity at a depth of about 250 km, other investigators propose the existence of the second low-velocity channel

but, in general, no definite information on the detailed structure of this part of the mantle is available.

Another discontinuity may exist at the depth of about 400 km. This 400-km discontinuity was introduced by JEFFREYS as the famous 20° discontinuity. Although this discontinuity was rejected later by JEFFREYS himself, the existence of this discontinuity has been suggested by many authors on the basis of investigation of travel-time curves, travel-time gradient curves, as well as amplitude-distance curves; there are many unsolved problems with this discontinuity. In one of the most recent papers LEHMANN [1970] investigated the seismograms of the Nevada nuclear explosions recorded on the north-eastern profile and found that clear and well-marked later arrivals indicated the presence of a deep discontinuity, but for a precise determination of its depth more observations were required. In other regions the corresponding phases were less clearly marked. Miss Lehmann concludes that the nature of the deep discontinuity evidently varies, and it may not be present everywhere. The 400-km discontinuity is included also into the velocity distribution derived by

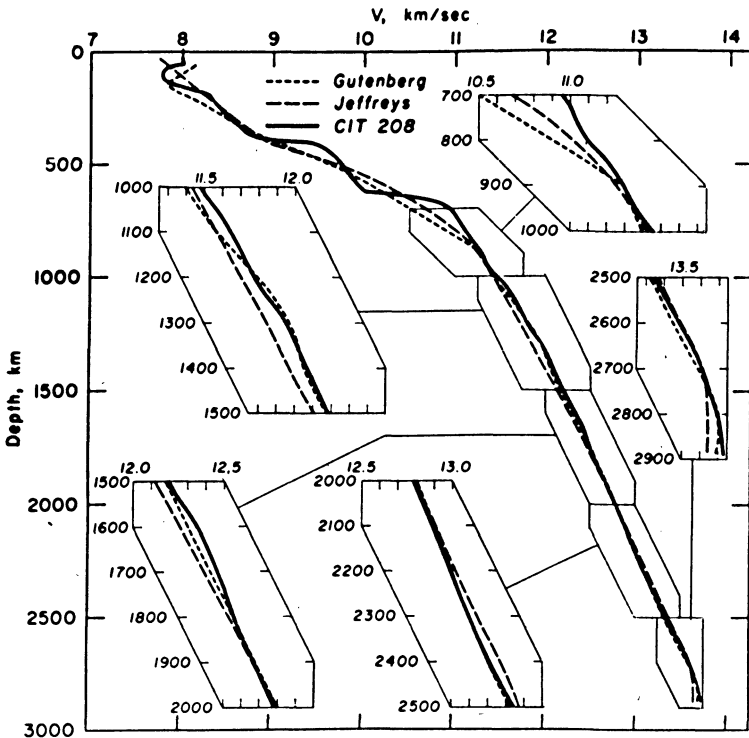


Fig. 8: Velocity distribution in the mantle given by JOHNSON [1969].

JOHNSON [1967, 1969] from the observations of the *Tonto Forest Seismological Observatory*; this velocity distribution, shown in Fig. 8 for the whole mantle, is one of the most recently derived models. In the upper part of the mantle it is very similar to the distribution given by ARCHAMBEAU, FLINN and LAMBERT [1969] on the basis of observations of nuclear explosions in the region of the North-American continent. According to this model another discontinuity appears near the depth of 650 km. It is interesting that the discontinuities are suggested as regions with high velocity gradients spread over 50 to 100 km. This concept was evidently influenced by the idea of possible phase transitions in the upper mantle. On the other hand, it seems that in both mentioned regions deviations from the uniformly increasing velocity very probably exist.

In contrast to the upper mantle the structure of the lower mantle seems to be much more uniform. This can be demonstrated by the velocity distribution by JOHNSON [1969] shown in Fig. 8. According to this distribution there are some possible irregularities in the lower mantle, but their magnitude is positively not so pronounced as at those in the upper mantle.

4. Conclusion

Before concluding this report I would like to demonstrate the high degree of indeterminacy in the details of the structure of the Earth. In Fig. 9 two schemes of

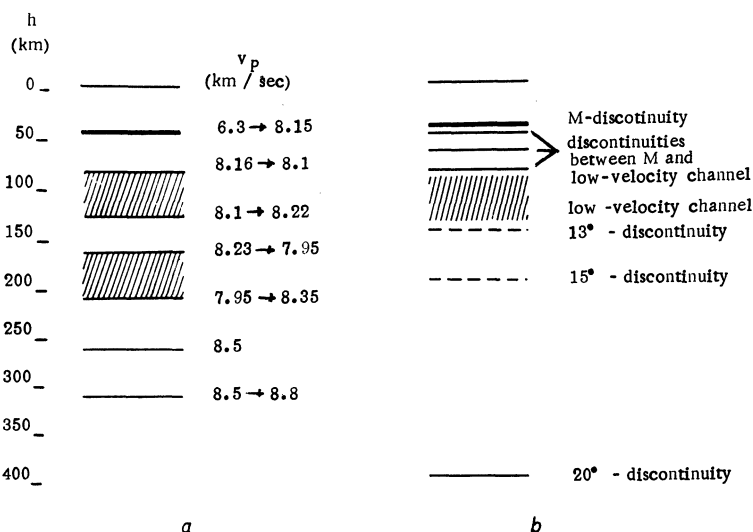


Fig. 9: Comparison of schemes of the upper mantle structure in south-eastern Europe: (a) from segmenting of the travel-time curves [MAYER-ROSA 1969]; (b) from amplitude-distance curves of P-waves [VANĚK 1968a].

the upper mantle structure are given, both proposed for the same region, for southeastern Europe. Scheme (a) was derived by MAYER-ROSA [1969] from segmenting of the travel-time curves (see Fig. 1), and scheme (b) was suggested as a possible scheme that could explain the shape of the amplitude-distance curves observed for this region [VANĚK 1968a]. It can be seen how different are the details, in spite of the fact that the schemes seemed to the authors to be the optimum solutions satisfying the observations. The actual situation is much more complicated, particularly in the upper parts of the mantle, due to the existence of lateral variations of the velocity and attenuation and to possible effects of elastic anisotropy.

In spite of this pessimistic tone, I think that much work has been done and new information on the structure of the Earth was obtained, especially in the last years. At the same time, it appeared almost in all papers that more and better observational data were urgently necessary. This is naturally nothing new, but it is the only possibility for improving our actual knowledge on seismic discontinuities in the Earth.

References

- ARCHAMBEAU, C. B., E. A. FLINN, and D. G. LAMBERT: Fine structure of the upper mantle. *J. Geophys. Res.* 74, 5825–5865, 1969
- ČERVENÝ, V.: The amplitude-distance curves for waves reflected at a plane interface for different frequency ranges. *Geophys. J.* 13, 187–196, 1967
- DORMAN, J.: Seismic surface-wave data on the upper mantle. *Geophys. Monograph No. 13, The Earth's Crust and Upper Mantle*, Amer. Geophys. Union, Washington, 257–365, 1969
- GUTENBERG, B.: On the layer of relatively low wave velocity at a depth of about 80 kilometers. *Bull. Seism. Soc. Am.* 38, 121–148, 1948
- JOHNSON, L. R.: Array measurements of P-velocities in the upper mantle. *J. Geophys. Res.* 72, 6309–6325, 1967
- JOHNSON, L. R.: Array measurements of P velocities in the lower mantle. *Bull. Seism. Soc. Am.* 59, 973–1008, 1969
- DAVYDOVA, N. I., I. P. KOSMINSKAYA, N. K. KAPUSTIAN and G. G. MICHOTA: Models of the Earth's crust and M-discontinuity. *Z. Geophys.* 38, 369–393, 1972
- LEHMANN, I.: The 400-km discontinuity. *Geophys. J.* 21, 359–372, 1970
- LUKK, A. A., and I. L. NERSESOV: Stroenie verchnej časti oboločki Zemli po nabljudenijam nad zemletrjasenijami s promežutočnoj glubinoj očaga. *Doklady AN SSSR* 162, 559–562, 1965
- MAYER-ROSA, D.: Die Geschwindigkeitsverteilung seismischer Wellen im oberen Erdmantel Europas. Dissertation, Universität Stuttgart, 1969

- MEREU, R. F., and J. A. HUNTER: Crustal and upper mantle structure under the Canadian Shield from Project Early Rise data. *Bull. Seism. Soc. Am.* 59, 147–165, 1969
- POPLAVSKIJ, A. A.: Statističeskoe issledovanie vremen prichoda vtoričnyh voln dalnevostočnyh zemletrjasenij. *Izvestija AN SSSR, Fizika Zemli* No. 9, 76–84, 1971
- RJABOV, V. Z.: Kinematičeskije i dinamičeskije charakteristiki glubinnych voln, svjazannyh s granicami v zemnoj kore i verchnej mantii. *Izvestija AN SSSR, Fizika Zemli* No. 3, 74–82, 1966
- VANĚK, J.: Amplitude curves of seismic body waves for the region of Asia Minor. *Travaux Inst. Géophys. Acad. Tchécosl. Sci.* No. 246, *Geofyzikální sborník, Praha*, 215–245, 1966
- VANĚK, J.: Amplitude curves of seismic body waves and the structure of the upper mantle in Europe. *Tectonophysics* 5, 235–243, 1968a
- VANĚK, J.: Amplitude curves of seismic body waves between 5° and 25° . *Bull. Seism. Soc. Am.* 58, 1035–1039, 1968b
- VANĚK, J.: Revised amplitude curves of seismic body waves for the region of South-Eastern Europe. *Studia geoph. et geod.* 13, 173–179, 1969
- VANĚK, J., and L. CHRISTOSKOV: Amplitude curves of P- and S-waves at short epicentral distances. *Bull. Intern. Inst. Seism. Earthq. Engin.* 8, 161–171, 1971
- VANĚK, J., and J. STELZNER: Amplitudenkurven der seismischen Raumwellen. *Gerlands Beitr. Geophys.* 71, 105–119, 1962
- VANĚK, J., and C. RADU: Amplitude curves of seismic body waves at distances smaller than 12° . *Studia geoph. et geod.* 8, 319–325, 1964
- VANĚK, J., and A. TSKHAKAYA: Amplitude curves of seismic body waves for the region of Central Asia. *UGGI, Assoc. Séismol., Comptes rendus* 15, 101–102, 1969
- YANOVSKAYA, T. B., and I. J. ASBEL: The determination of velocities in the upper mantle from the observations on P-waves. *Geophys. J.* 8, 313–318, 1963

Models of the Earth's Crust and M-Boundary

N. I. DAVYDOVA, I. P. KOSMINSKAYA, N. K. KAPUSTIAN and G. G. MICHOTA,
Moscow*)

Eingegangen am 22. Juni 1972

Summary: A review of the crustal models is presented. The conception of a generalized geological-geophysical model of the block-layered medium as a complicated spatial velocity function is introduced.

Dynamic criteria for the determination of the type of seismic boundary according to the properties of reflected and refracted waves are discussed. The boundary as a thin-layered zone with random structure is examined in detail. This structure of the *M*-boundary may be offered for such regions where the amplitudes of reflected waves near the shot points are comparable with those in critical points and have no sharp resonance properties.

Zusammenfassung: Eine Übersicht der Erdkrustenmodelle wird vorgelegt. Die Konzeption eines verallgemeinerten geologisch-geophysikalischen Modells, welches als Medium mit geschichteter Blockstruktur mit komplizierter räumlicher Geschwindigkeitsfunktion aufgefaßt werden kann, wird eingeführt.

Dynamische Kriterien zur Bestimmung des Grenzflächentypes auf Grund der Eigenschaften reflektierter und refraktierter Wellen werden diskutiert. Die Grenzfläche im Sinne einer heterogenen Zone mit dünnen Schichten wird eingehend geprüft. Ein solches Modell kann für die *M*-Diskontinuität in all den Gebieten angenommen werden, in denen die Amplituden reflektierter Wellen in der Nähe des Schußpunktes vergleichbar mit den in den kritischen Punkten beobachteten Reflexionsamplituden sind, wobei keine scharfen Resonanzeigenschaften auftreten.

1. Introduction

By the *structural seismic model* is understood the spatial distribution of seismic parameters. The seismic parameters of the structure, obtained from experimental data, are *P*- and *S*-wave velocities and their ratio, absorption and quality factor, velocity anisotropy and turbidity or transparency of the medium.

Moreover, such elements of seismic cross-sections as reflecting and refracting boundaries, their shape, the thickness of the transition layers and fracture zones are important for the structural description. All these elements are estimated from the combination of the kinematic and dynamic properties of individual waves, and of the wave field as a whole.

*) Dr. N. I. DAVYDOVA, Prof. Dr. I. P. KOSMINSKAYA, Dr. N. K. KAPUSTIAN and Dr. G. G. MICHOTA, Institut Fiziki Zemli ANSSSR, B. Gruzinskaya 10, Moskva, USSR.

Usually theoretical and experimental models are distinguished. The *theoretical model* is a certain distribution of seismic parameters, sufficient for the construction of the seismic field. The parameters of the medium may depend on one spatial coordinate, usually the depth.

The *experimental model* is the distribution of seismic parameters based on the kinematic and dynamic properties of the observed waves and theoretical conceptions of models founded on the methods of solution of the inverse problem of seismology.

Experimental models are also represented in one-dimensional scale as velocity stratification, in two-dimensional scale as seismic sections and maps and in three-dimensional scale as spatial diagrams.

For a long time there has been a tendency in seismology to construct some generalized models of the Earth [JEFFREYS, BULLEN, GUTENBERG] as well as some of its shells. We shall discuss the generalized models of the Earth's crust: both continental and oceanic.

2. Generalized seismic model of the Earth's crust

It is usually understood that the generalized seismic model is the synthesis of some conceptions of spatial distribution of the main properties of medium completed with hypothetical conceptions about the properties and structure of deep substances taken from geology and geochemistry.

The type of the crustal seismic model is determined first of all by the completeness of information about the medium, related directly with the precision of the observing system and with the level of theory, i. e. with the methods of interpretation.

A few records of near earthquakes allowed MOHORVIČIĆ to explain the main kinematic features of observed waves using the simplest one-layered crustal model.

CONRAD and WIECHERT discovered P^* waves by analysing all the near earthquakes and big shots, which led JEFFREYS and GUTENBERG to a two-layered crustal model.

This model explains fairly satisfactorily the main kinematic features of continental wave fields for distances from 100 to 300 km. As it is known the statistical travel-time curve by JEFFREYS-BULLEN is based on this model.

An essential stage in the determination of crustal properties was the one-layered gradient crustal model constructed by TUVE and TATEL. The main contribution of these investigators to the improvement of the crustal structure problem was the explanation of P^* waves as overcritical reflections from the M -boundary.

The appearance of Deep Seismic Sounding (DSS) methods using the principles of correlation of seismic waves (GAMBURSEV 1949) and a wide development of detailed observations led to constructing multilayered crustal sections with the boundaries of complicated shape. It was initially assumed that the correlatable waves were in general refracted waves corresponding to thick layers with high velocity.

Then, due to development of the wave propagation theory (PETRASHEN, ALEKSEEV, GELCHINSKY) and due to the use of dynamic properties of waves, a number of essential contradictions were brought to light. They were removed by the introduction of some gradient layers and layers with low or high velocity into the model (EGORKIN et. al.) In this connection a lot of crustal models with low velocity layers appeared (MÜLLER, LANDISMAN; MEISSNER; GIESE

and oth.). It is important to remember that GUTENBERG predicted this layer in the crust long ago.

The principal new information about the medium parameters were furnished by the observations near the shot point and allowed to detect subcritically reflected waves. This contributed to a more precise definition of the velocity distribution within the crust and enabled the beginning of the investigation into the structure of deep boundaries.

The interrupted character of the wave correlation on continuous seismic profiles allowed to put forward the suggestion of "partly-continuous" feature of seismic boundaries [KOSMINSKAYA 1966]. Distinctions in the wave field in different areas supplemented the idea of the block-layered structure of the crust and upper mantle. It was noticed that the regular components of the field could correspond to both the large blocks and smaller inhomogeneities in the medium, which could be conformed as a "grainy-blocked" model [RIZNICHENKO, KOSMINSKAYA 1963].

The recent generalized Earth's crust model (Fig. 1) contains all the now available peculiarities of the crustal structure obtained on the basis of all observed data. In such a model the velocity distribution with depth is complicated and includes high and low velocity zones. High velocity zones and thin-layered sections with interchanging parameters are more important because the most significant components of the wave field, the so-called main or predominant waves (reflected, refracted *P*- and *S*-waves), are connected with them. In some cases it is possible to obtain the data for v_S and $k = v_P/v_S$, characterizing the elastic properties of the medium. The absorption coefficient and the quality factor and their variation with depth are the additional parameters describing the medium. The turbidity factor or transparency factor [NIKOLAEV 1967, 1968] characterizes the diffusion properties of different parts of the crust and upper mantle and it express the influence of small inhomogeneities in the medium.

Of course now the stratification of the crust is understood in another way than in DSS sections made ten years ago. The main difference is that now the boundaries and layers are not so invariable across the area of observation as in the earlier DSS sections, the number of thick layers is smaller and in some cases velocities appeared to be larger because the reflected waves were interpreted as refracted.

The spatial distribution of velocity function $V(z, x, y)$ and other parameters of the medium consists in the existence of slight changes of parameters within blocks and strong variations at the flanks of adjacent blocks.

The generalized model of the continental crust contains the most typical structure elements (Fig. 1a). The oceanic crustal model (Fig. 1b) is less stratified probably due to the application of less detailed observations and lower frequencies used in the marine research.

The generalization of DSS data observed in different areas allows to assert that using the simplest recording system it is possible to obtain the main parameters as the average velocity in the crust and the shape and the velocities of the K_0 and *M*-boundaries. In some cases it is possible to obtain some data connected with regular intermediate boundaries.

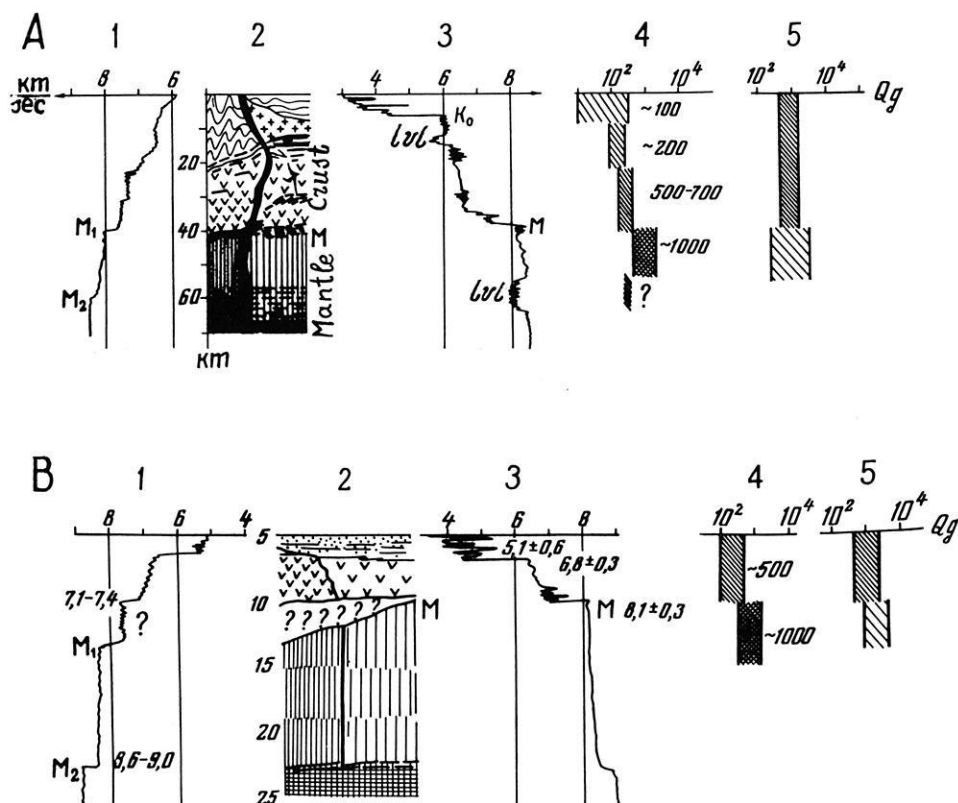


Fig. 1: Generalized models of the crust and upper mantle for A) continents and B) oceans, 1), 3) stratified velocity-depth distributions, 2) geological and geophysical structures, 4) quality factor distribution ($Q = \frac{2\pi}{\phi}$, where ϕ is the absorption coefficient), 5) transparency factor distribution $Q_g = \frac{2\pi}{g}$, where g is the heterogeneity factor characterizing the influence of small inhomogeneities in the crust and upper mantle at frequencies about 10 Hz for continents and 5 Hz for oceans [GALKIN, NIKOLAEV, STARSHINOVA 1971]. In B the stratified velocities at the right side correspond to results of SHOR and RAITT 1969, at the left side to [KOSMINSKAYA, ZVEREV 1969 and ZVEREV 1970].

Only using detailed observations such as continuous profiling and two-dimensional observations is it possible to obtain the information about the feature of the crustal structure: its stratification, fracture zones, the details of the relief of boundaries, steep discontinuities and low velocity zones.

Thus, in the interpretation of DSS data with a different degree of details we use different types of information and also different types of models in our calculations and we also construct seismic sections of different kinds.

Recently the main information has been yielded by two significant components of the seismic field: the first arrivals of refracted waves and the second arrivals of reflected waves.

Combining these two types of information it is possible to construct crustal sections as isolines of velocity $V(x, z) = \text{const}$ and seismic cross-sections with reflecting and refracting boundaries as usual. Effective methods of concordance of these types of data have not been sufficiently worked out up to now. Thus it often seems that these two types of information are independent, but, in principle, they are mutually controlled due to the possibility to determine the reflected wave properties by the use of velocity data obtained from first arrivals.

Agreement between them based on the direct problem solution is worked out by selecting such crustal sections that satisfy the experimental travel-time curves of reflected and refracted waves. The general structure of the crust section is obtained by solving the inverse problem of seismic prospecting based on rather simple crustal models e. g. [PAVLENKOVA 1971].

The use of wave dynamics is essential for detailed investigations of the crustal structure. Theoretical data connected with the wave dynamics for different models are necessary in order to ascertain the conformity of the medium properties to the dynamic characteristics of the wave field.

The description of wave properties using the ray theory of propagation was possible in previous thicklayered models. The introduction of thin layers into the generalized seismic model made the theory more complicated and other approximations had to be taken into account.

Now more and more complicated models of the crust and its individual elements are constructed to explain the observed dynamic features of seismic waves. Probability and statistical approaches were also applied to describe the properties of the wave field and the medium [GELCHINSKY 1971]. Combining the results of seismic prospecting with acoustical and vertical profiling data it was possible to construct the so called effective seismic model (ESM).

The idea of this method is that each system of data includes its specific information about the medium and that these three systems of observations must satisfy in the main parameters the kinematics and dynamics of the seismic wave field. According to DSS observations the parameters of the ESM have to depend on frequency in such a manner that when we move from the source, the general character of the seismic

field has to be simpler and the correlation properties of the predominant waves have to improve.

NIKOLAEV [1967] used the probability idea to estimate the influence of small inhomogeneities causing small fluctuations of dynamic and kinematic properties of the wave field. For this purpose all changes of the parameters connected with those features of the medium, which we are able to study using non-statistical models, are excluded.

Physically, both these methods overlap, i. e. in the model proposed by NIKOLAEV the inhomogeneities of average dimensions can be included under certain conditions in the term of turbidity. In the model by GELCHINSKY these inhomogeneities are considered as random ones and represent an important part of the effective model.

The probability method is used by BERZON et al. [1972] to study the properties of seismic boundaries. The statistical set allows to construct a group of thinlayered inversional models and the statistical properties of reflected waves connected with zones of random structure are examined.

This brief review of the Earth's crustal models shows that the actual geological medium is very complicated and varied. It is still difficult to describe it as a whole even if detailed observation data are available.

3. The models of *M*-boundary and criteria for its determination

The properties of seismic boundaries, where strong changes of physical parameters occur, are estimated from such main components of the wave field as reflected and refracted waves.

Morphology of deep boundaries. Data about the morphology, shape and depth of boundaries are obtained using the travel-time curves of seismic waves or special time field, drawn up by means of the results of discrete soundings. If a simplified system of observations is used, seismic boundaries are interpreted as almost horizontal or weakly sloped, plane and continuous with a velocity jump.

At the first stage of the application of continuous seismic profiling when most of the observed waves were considered as refracted, the deep boundaries were drawn up also as continuous and generally close to horizontal boundaries. Further detailed observations of the upper mantle and the crust employed the reflected waves and this allowed to establish the presence of abruptly sloped, reflecting, partly continuous boundaries. This fact confirmed that the observing system usually used in DSS reasonably chose the horizontal boundaries. For this purpose the special spatial observing systems [LITVINENKO, LENINA 1968] are necessary to detect and to trace the abruptly sloped boundaries. A close examination of the character of the wave field observed by means of the continuous profiling in different geological areas allowed to establish reliably the partly continuous character of the deep wave correlation (essentially in the subcritical area) and, thus, to pay attention to the partly continuous character of seismic boundaries. The study of reflected waves dynamics led to the conclusion that it was impossible to consider the individual parts of seismic boundaries as smooth reflecting elements and that they seemed to be characterized by a complicated structure. Other types of boundary models had to be considered.

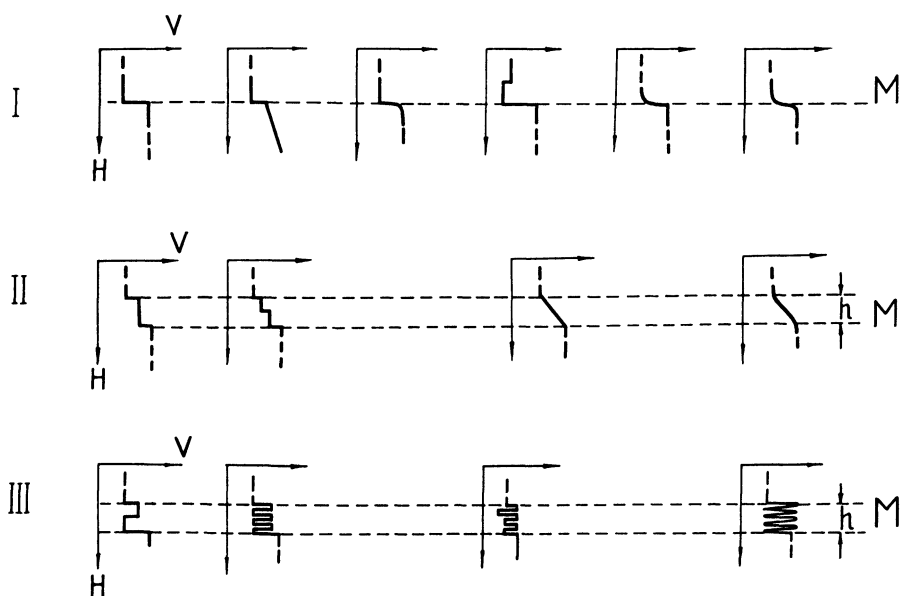


Fig. 2: Main types of M -boundary models. I—1st order boundaries, II—transition layers, III—thinlayered inversional zones.

3.1 The main types of M -boundary models

Fig. 2 illustrates the stages of the development of M -boundary conceptions. Three lines representing three main types of M -boundary models are shown. For a long time (approximately till 1960) the idealized model for the M -area as a first order boundary with a rather intense velocity jump (about 1,0–1,5 km/sec) was taken. Then, the transition from the crust to the upper mantle was considered as a comparable thin layer ($h < 2 \lambda$) with a sharp velocity gradient within the layer and a low jump of properties in its upper and lower parts [e. g. NAKAMURA, HOWELL 1964]. Recently (approximately since 1967) some investigators have begun considering a thin layered structure with interchanging elastic properties (inversional zones) as the model for the M -area [MEISSNER 1967, FUCHS 1968, 1969, 1970; DAVYDOVA et al. 1970, KOSMINSKAYA, DAVYDOVA 1971; DAVYDOVA et al. 1972].

Models of inversional zones can be divided into two groups: 1 (the *analytic model*) based on the usual interpretation of seismological data - the simple or complex periodical zone - and 2 (the *probability model*) the zone of a random structure. The mathematical basis and the numerical methods for this zone are well known in seismic prospecting and are described by [BERZON et al. 1972].

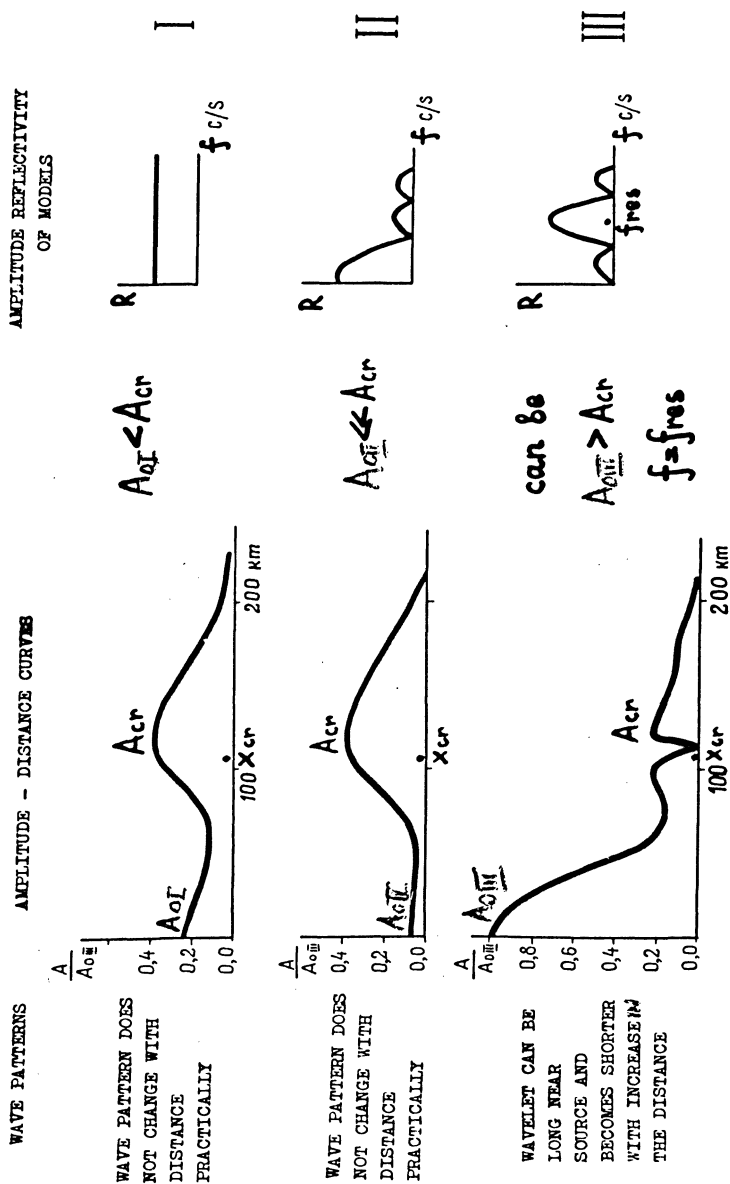


Fig. 3: Dynamic criteria for M-boundary models using reflected waves.

3.2 Criteria for determination of M -boundary model

Dynamic criteria for body waves, reflected and refracted waves are used now to determine the seismic boundary model.

In Fig. 3 the results of theoretical researches of the dynamic features of reflected waves are shown schematically for the main three models, obtained by different authors [GUPTA 1966, MISHENKIN 1969, FUCHS 1968, 1969 et al.]. The synthetic seismograms computed by RATNIKOVA-LEVSHIN program [1967] are exhibited to illustrate the features of the wave pattern and its changing with distance. As it can be seen the wave pattern becomes shorter and less complicated at overcritical distances than at subcritical ones in the case of multilayered zones.

It is clear from Fig. 3 and Fig. 4 that models of the third type differ from the models of the first and the second type by the character of records, amplitudes and spectra. They are characterized by a more narrow spectrum and higher main frequencies and higher level of amplitude A_0 near the shot point (approximately in 2–4 times). In the subcritical area the amplitude A_0 can be higher than the amplitude A_{cr} .

The calculations show that dynamic characteristics of reflected S -waves are close to those of P -waves in the case of thin layered inversional zones. The difference is that the spectra of S -waves are more narrow and are moved towards lower frequencies.

In Fig. 5 the reflectivity is shown as the frequency function for reflected P - and S -waves at the distance $x=61$ km to illustrate this thesis. The same conclusion about the properties of P - and S -waves reflected from M_1 and M_2 boundaries in the upper mantle (Fig. 6) can be drawn by using the data observed by PAVLENKOVA [1971]. It is possible to suppose from the similarity of the observed and calculated dynamics of P - and S -waves that in this area the reflecting boundaries M_1 and M_2 are thin layered zones.

It can be said that the determination of the type of the model using the dynamic criteria is fairly reliable, particularly if the records in subcritical and overcritical areas are available. If the model is of the third type, there is a chance of determining the concrete structure of the M -zone. However, there are some very reliable statistical data, concerned with possible limits of v_p and v_s variation in the layers of the M -zone. These limits restrict the uncertainty of zone properties. It is also possible to receive some ideas about the number of layers and their thickness by examining the wave spectra and the length of the wave pattern. Thus, the thin-layered models represented in different papers cannot be considered as a certain possibility of the determination of the boundary structure.

3.3 Review of the papers including the determination of M -boundary models

The results observed in different areas by different authors who tried to determine the M -boundary structure, are represented in three tables.

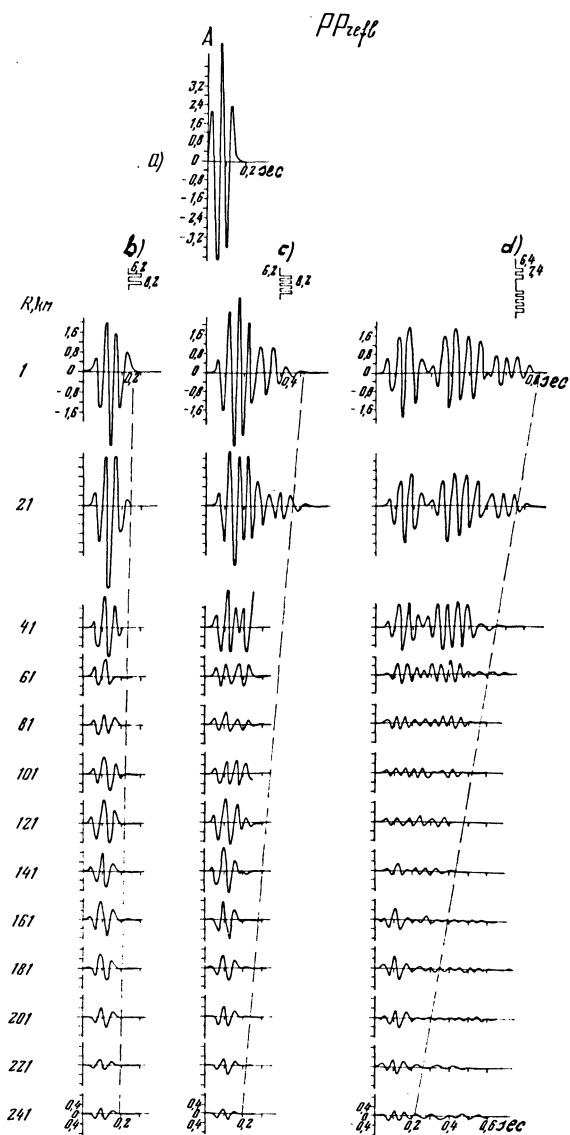


Fig. 4: Synthetic records illustrating the features of the wave pattern and its changes with distance for a different structure of thinlayered inversional zones.

Україна

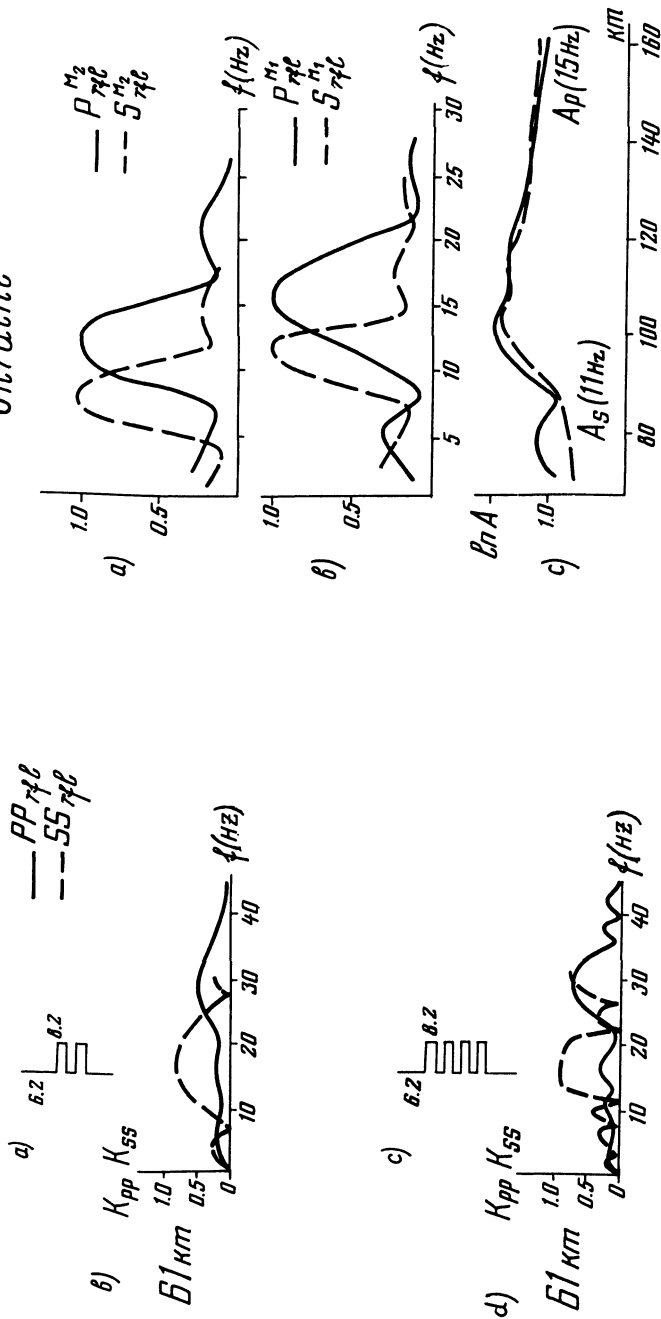


Fig. 6: Observed dynamic data of waves reflected from M_1 and M_2 in the upper mantle in the Ukraine [PAVLENKOVA 1971]. a - spectra of $P_{M_1}^{M_2}$ and $S_{M_1}^{M_2}$ waves, b - spectra of $P_{M_1}^{M_1}$ and $S_{M_1}^{M_1}$ waves, c - amplitude curves of $P_{M_1}^{M_1}$ and $S_{M_1}^{M_1}$ waves.

Fig. 5: Computed spectra of PP and SS waves reflected from two types of thinlayered inversional zones (distance 61 km). a - and c - velocity distribution, b - and d - reflectivity versus frequency.

Table 1. D S S DATA on the M-DISCONTINUITY (REFRACTED WAVES P_{fr}^M)

Region	DATA	MODEL	Author
Gift of Main	<p>Comparison of the first wave spectra</p>	<p>$\frac{dv}{dh} = 4 \text{ sec}^{-1}$</p>	Nakamura, Howell 1964
Lake Superior	<p>Comparison of the first wave spectra</p>	<p>$\frac{dv}{dh} = 5.2 \text{ sec}^{-1}$</p>	Howell 1966
N-W part of Pacific Ocean	<p>Comparison of amplitude curves $A(x)$</p>		Kosminskaya, Zverev 1969
Bering Sea a) N. Aleutian Basin b) S. Aleutian Basin	<p>Comparison of synthetic and observed recordings for the first arrivals ($t = 1.5 \text{ s.}$)</p>		Helmberger 1968
Hawaii	<p>Comparison of synthetic and observed records at 50-120 km</p>		Helmberger, Morris 1969
Canada	<p>Comparison of synthetic and observed wave fields at 100-350 km</p>		Berry, Fuchs 1971

In Table 1 the works, using dynamic characteristics of refracted waves P_{rfr}^M to determine the *M*-boundary are gathered. NAKAMURA and HOWELL used the frequency features of P_{rfr}^M waves; they suggested the *M*-boundary as a gradient transition layer whose thickness was according to their estimation equal to 0.5 km and the velocity gradient was 4 sec^{-1} .

KOSMINSKAYA and ZVEREV have interpreted the amplitude curves of P_{rfr}^M waves for different frequency components. They explain the observed differences by different sharpness of the transition from the crust to the upper mantle. The thickness of the transition zone was estimated as 1–1.5 km.

HELMBERGER, MORRIS, BERRY and FUCHS studied the *M*-boundary models by the use of the synthetic records and their comparison with observed data. BERRY and FUCHS adopted the *M*-boundary model as a thick gradient layer (about 10 km) with the velocity change from 7.2 to 8.4 km/sec. In the other case HELMBERGER and MORRIS considered it possible to adopt the *M*-boundary either as one homogeneous layer or as two homogeneous layers with velocity values intermediate between of the velocities of the overlying crust (6.8 km/s) and underlying mantle (8.2 km/s). They estimated the thickness of transition zone from 1.0 to 4.5 km.

In Table 2 are summarized results based on the interpretation of amplitude curves [KOSMINSKAYA et al. 1964, BERZON et al. 1969, RYABOI 1966], of spectra [MEISSNER 1967] and of the ratio of amplitudes of reflected and refracted waves [KRYLOV 1971]. Observations of reflected waves in critical and overcritical areas were used. In the first case a 1-st order boundary with a velocity jump was established as the model of the *M*-boundary, in the second and third cases a gradient transition zone was determined as the *M*-boundary. Its thickness was estimated to 6–7 km; the *M*-boundary as a layer with a negative velocity gradient was considered by BERZON et al.

In Table 3 the works using the subcritical, critical and overcritical reflections are represented. The different authors used different dynamic characteristics to determine the *M*-boundary: the amplitude-distance curves $A(x)$, the frequency features (spectra, resonance frequencies), the character of records and its variation with distance.

As can be seen, all the authors considering the subcritical reflections assume a thinlayered inversional zone, often a simple one with a low number of layers. Naturally, if the observed dynamics were used more completely, the model obtained was more reliable.

From Table 1–3 it can be concluded that the records of P_{rfr}^M waves are most informative and have the highest resolution power in the subcritical area.

The resolution power of refracted and reflected waves in the overcritical area is lower; the waves P_{rfl}^M characterize the structure of the upper part of the *M*-zone and the waves P_{rfr}^M -its lower part only.

The agreement of refracted and reflected wave dynamics allows to create a more detailed conception of the boundary and the medium over and under the boundary.

Table 2. M-DISCONTINUITY STRUCTURE on the BASIS of DATA of the CRITICAL and OVERCRITICAL AREA

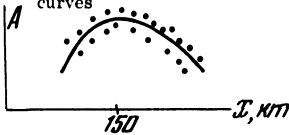
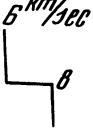
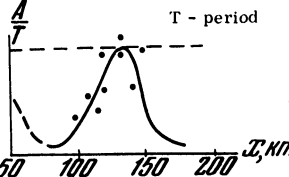
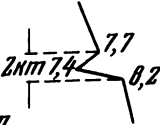


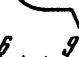
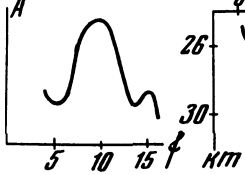
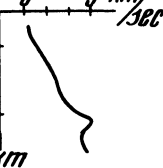
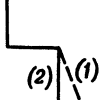
Region	DATA	Model	Author
Kopetdag - Aral Sea	Amplitude - distance curves 	6 km/sec 	Ryabov 1966
Seismic device 0.2 - 30 Hz	T - period 		Berzon et al. 1964
Northern part of Sea of Okhotsk	$\frac{A(P_{rfl}^M)}{A(P_{rfr}^M)}$ 5 - 10		Kosminskaya et al. 1964
South of Sea of Okhotsk	1		
S - W part of Pacific Ocean	sharp decrease of overcritical reflections		
Bavarian Molasse Basin	$\frac{A(P_{rfl}^M)}{A(P_{rfr}^M)}$ 1-3 	6 9 km/sec 	Meissner 1967
West Siberia	1) Hanti - Tobolsk 2) Tobolsk - Omsk $\left. \begin{matrix} 2.5 \\ 10-20 \end{matrix} \right\} = \frac{A(P_{rfl}^M)}{A(P_{rfr}^M)}$		Krylov 1971

Table 3. DSS DATA on the M-DISCONTINUITY

Region	Peculiarities of P_{r11}^M wave dynamics			Suggested model	Author
	Wave pattern	Amplitudes	Spectra		
Ukranian Shield					Pavlenkova Smelanskaya 1970 Pavlenkova 1971
East Coast of Caspian Sea			$f_{zes} = 35 \text{ Hz}$		Vozzhzova Chamo 1972
Inter-Caucasion Depression					Michota 1969
Russian Platform			$f_{zes} = 13 \text{ Hz}$		Druzhinin et al 1970
West Uzbekistan	 		$f_{zes} = 16 \text{ Hz}$		Davydova et al 1972
Canada		<p>Quality factor $Q = 200 - 3000$</p>	<p>Autopower spectra</p>		Clowes Kanasewicz 1971

4. Thinlayered inversional zone with random structure as the M -boundary model

The typical features of the wave field caused by a zone with random structure and the application of this model to the explanation of observed data in seismic prospecting and DSS was discussed by BERZON et al. [1972]. In this article the analysis of the waves reflected from a lot of thin boundaries in the crystalline part of the crust was made. It was concluded that the observed $P_{r/t}^M$ waves were similar to the waves reflected from a inversional zone with random structure. The average parameters of these boundaries were equal to the parameters of the adjacent medium. A practically homogeneous medium can be assumed and the boundaries within it have no influence on the average velocities of the adjacent medium.

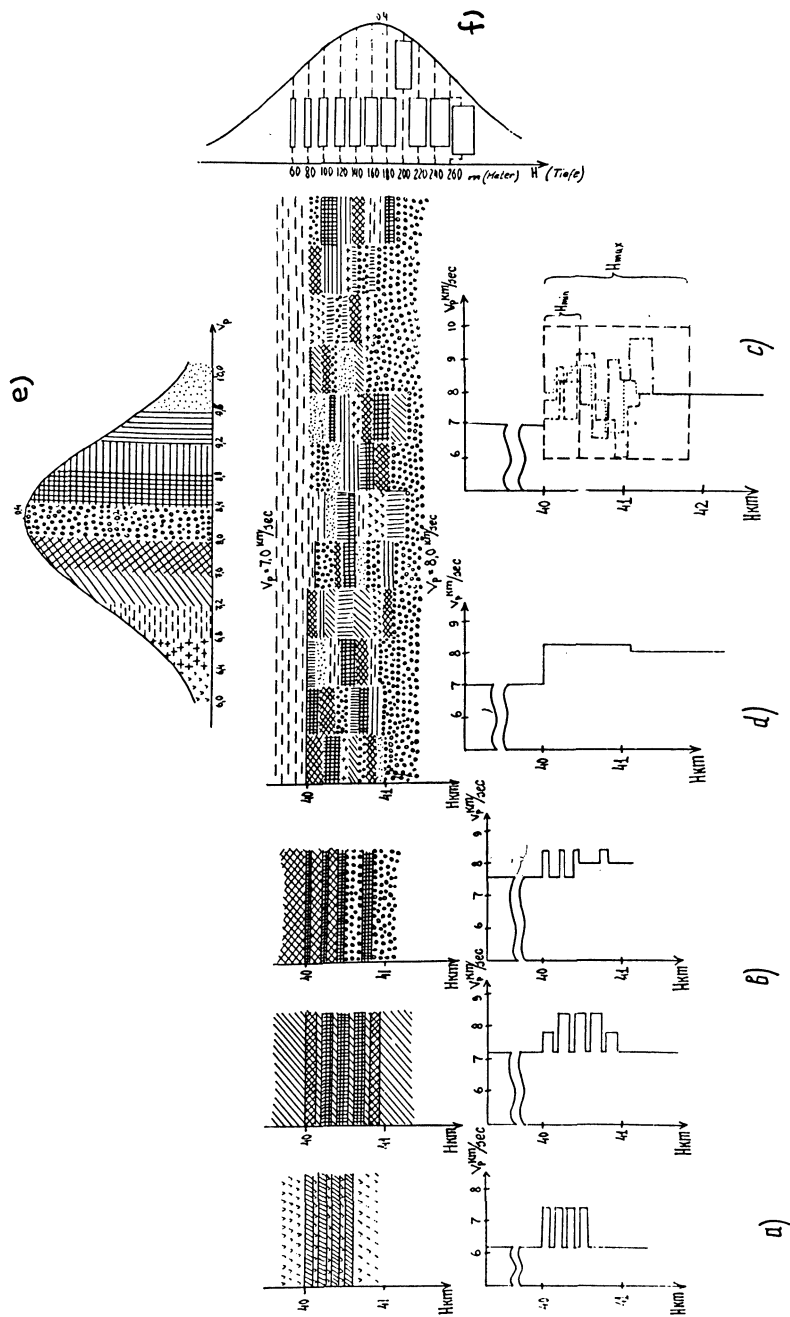
4.1 Description and properties of the generalized M -boundary

The method of interpretation and the computer program from the article mentioned above were used to calculate the properties of reflections from a special zone, which could be also considered as the M -boundary. We assumed that the average parameters of this zone rather differed from the crustal parameters (overlying medium) but were similar to the parameters of the underlying medium, i. e. the upper parts of the mantle (Fig. 7).

This zone can be described as follows: the zone is a system of layers, the P -wave velocity and thickness are random values with normal distribution (Fig. 7), the ratio of velocities is $v_p/v_s = \sqrt{3}$, the density is proportional to the velocity [MAGNITSKY 1966]. The average velocity in the zone is constant and equals to 8.2 km/sec. The depth of the upper boundary of the bundle is 40 km. The number of layers is 7, the average thickness of the layers is $0.3 \lambda_p$ where λ_p is the wavelength of the incident P -waves.

The reflectivity spectra were computed for each realization of the random zone and then the average reflectivity was obtained assuming that these spectra have also normal distribution. The average reflectivity $|H(\omega, x)|$ was calculated for the variations of frequency from 0 to 30 Hz and for distances from 2 to 82 km. Then one equivalent layer was considered. The parameters of this layer are the same as the average parameters of the random zone: $v_p = 8.2$ km/s, $h = 1.1$ km.

Fig. 7: Velocity-depth distributions (lower part) and cross sections of blocks with thinlayered structure (upper part): the block with a random zone is represented by 12 realisations. a – periodical zone, b – quasi-periodical zone, c – complicated zone, d – equivalent layer (its parameters are equal to the average parameters of the random zone), e – velocity distribution in the random zone, f – thickness distribution for the random zone.



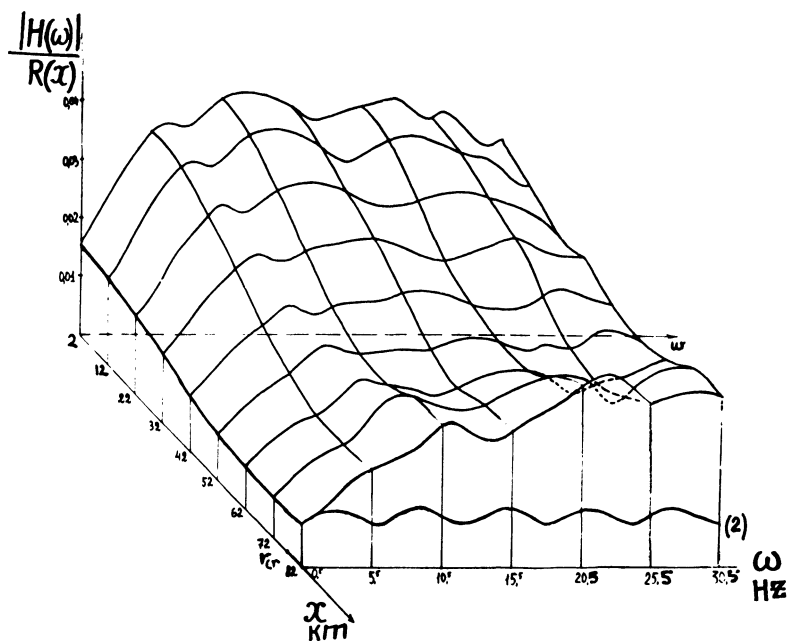


Fig. 8: Spatial diagram of the random zone reflectivity with divergence factor $R(x)$. The sinusoidal line at $x=82$ km is the reflectivity from the equivalent layer (see Fig. 7d).

First of all let us consider the main features of reflectivity for the arbitrary zone and then compare them with the reflectivity for individual realizations.

The dependence of the function $|H(\omega, x)| \cdot 1/R(x)$ on distance (where $R(x)$ is the divergence of the refracted wave) is shown in Fig. 8. The consideration of the whole complex of these spectra shows the stability of their shape and their slight variations if one moves away from the source. This fact indicates that in the case of a random zone we can expect a good correlation of refracted waves in the subcritical area. Let us compare these characteristics with the characteristics of the equivalent layer and of the individual realizations. The individual realizations are also complicated inversed thin-layered zones with a defined structure.

As can be seen in Fig. 8 and Fig. 9 the amplitude spectra for some realizations possess a quasi-sinusoidal shape and the level of these spectra is lower than the level of the amplitude spectra for the random zone by 2–3 times.

The amplitudes of some components of the spectrum for individual realizations change with distance in a complicated manner: they can decrease and increase (Fig. 10), or can have an oscillatory character (curve 4). The curves $|H(\omega = \text{const.}, x)|$ for the equivalent layer are like those for the random zone.

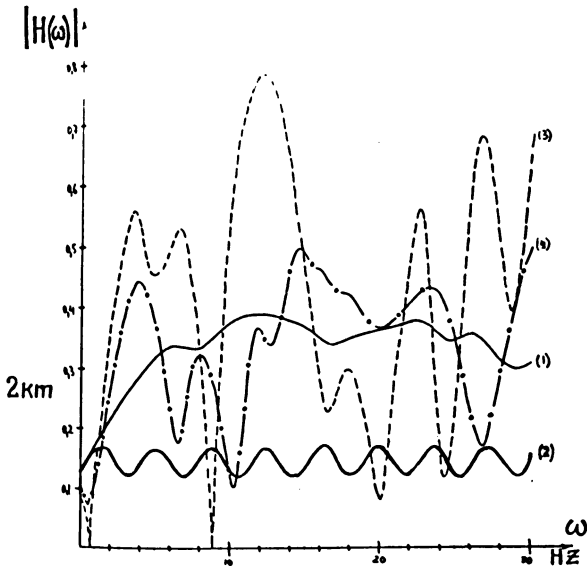


Fig. 9: Spectra of different *M*-boundary models. 1 — random zone; 2 — equivalent layer, 3 — and 4 — individual realizations, shown in Fig. 7e.

Thus, it can be expected that a random zone forms the reflected waves with a slight change in the shape of the records and with a rather variation of the reflectivity with distance and with a shallow minimum of amplitudes in the middle of the distance between the shot points, and the critical point in contrast to the zone with defined parameters. As it is known, these properties are like those for waves reflected from sharp boundaries and also from the thick equivalent layer. The most typical feature of a random zone is the higher intensity of subcritical reflections (approximately by 2 times).

The influence of absorption was not taken into account in these calculations, it will make the spectra more resonant.

4.2 Geological interpretation of the zone with random structure

In some cases the periodical or quasi-periodical zones allow to explain the observed dynamic features of seismic waves, reflected from the *M*-boundary. However, these models seem to be far from the real geological conditions. It is difficult to assume that structures represented by periodical thinlayered zone does not change for several

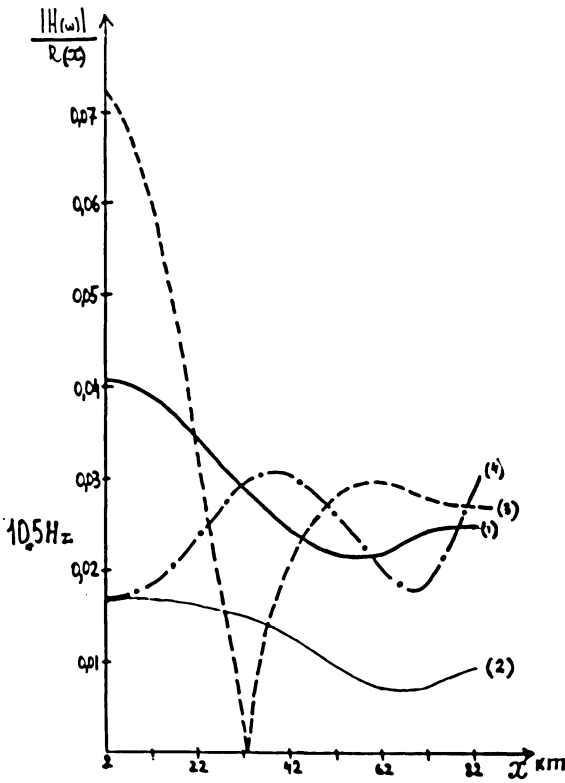


Fig. 10: Amplitude distance curves for frequency 10 Hz. The curves are denoted as in Fig. 9.

kilometers. The model with random structure seems therefore to be more probable. The geological interpretation of this type of boundary will be discussed in detail.

From the theory it is known that the dynamic properties of a certain wave depend not only on the medium structure in the point of reflection but also on the medium structure in the vicinity of this point. The dimensions of this area are estimated to 8 Fresnel zones*). If the *M*-boundary depth is 40 km and the distance $x=10$ km, the overall dimensions of this area are about 10 km.

If in each point of observation the reflected wave is formed by an random zone, i. e. by all blocks with the normal distribution of parameters, then the dimensions of

*) $A\gamma = 1/\cos \Theta \gamma \lambda l$, where $A\gamma$ is the half of ellipsis diameter, l is the half of ray length of the reflected wave, λ is the wave length equal to 0.6 km, Θ is angle of incidence.

an individual block are about 0.3 km, in our case of 30 realizations. Such a medium will form the "random wave" (Fig. 7).

It is possible to give an example of the explanation of a partly continuous correlation of subcritical strong reflections. Let us assume that the crust and the *M*-boundary is represented by large crustal blocks (length about 10 km), each containing a layered zone, whose parameters are interchangeable at 10 km length of profile. Let us consider the wave processes on 3 block zones forming the large block structure. For this case the dynamic travel-time curve of reflected waves (frequency 10.5 Hz) is shown in Fig. 11. The velocity-depth distribution of the proper zones are shown under the travel-time curve. It is seen clearly that if the average level of seismic noise is equal to the amplitude of reflected waves at the distance 40 km, it will be possible to detect the reflections only from the 1-st and 3-rd blocks. The reflections from the blocks with number 2 will be detected only near the critical point. Such a situation, observed in many regions, is typical for the partly continuous character of the wave field in the subcritical area.

The discussed possibilities of the *M*-boundary lead to the conclusion that it is necessary to assume a complex *M*-boundary with zones of layers in those regions where the reflections near the shot point are stronger or equal to the reflections in the critical area.

The partly continuous correlation of the subcritical reflections can be connected either with the discontinuities in these zones, or with a sharp variation of their properties, i. e. with the block character of the *M*-boundary. In this case the blocks should not be very small, their length must be of several kilometers.

If the strong reflected wave form short groups in the subcritical area and their characteristics are qualitatively close to the characteristics of the 1-st order boundaries it can be assumed that the *M*-boundary is represented by a random zone. In this zone a statistical alternation of very small blocks can be assumed. The parameters of zones are equal to these of small blocks which are distributed in such a manner that in each reflection all of the realizations take part.

In those regions where the reflections in the subcritical area are absent it is necessary to estimate the ratio of the seismic noise level with respect to the intensity of critical reflections. If this ratio is a small one it can be assumed that the critical reflections are much higher than the subcritical ones and the *M*-boundary can be represented by the 1-st or 2-nd type of boundary model (Fig. 2).

The presented estimation of the boundary type is, of course only the first step in a new tendency in DSS connected with the investigation of the fine structure of seismic discontinuities in general. Its development is conditioned by the success of new methods in seismic prospecting, in particular of a new technique to detect and correlate the subcritical reflections. Further development of numerical methods of the wave dynamic analysis and of the methods of solution of the inverse problem of seismology seems to be important for the study of the discussed types of media.

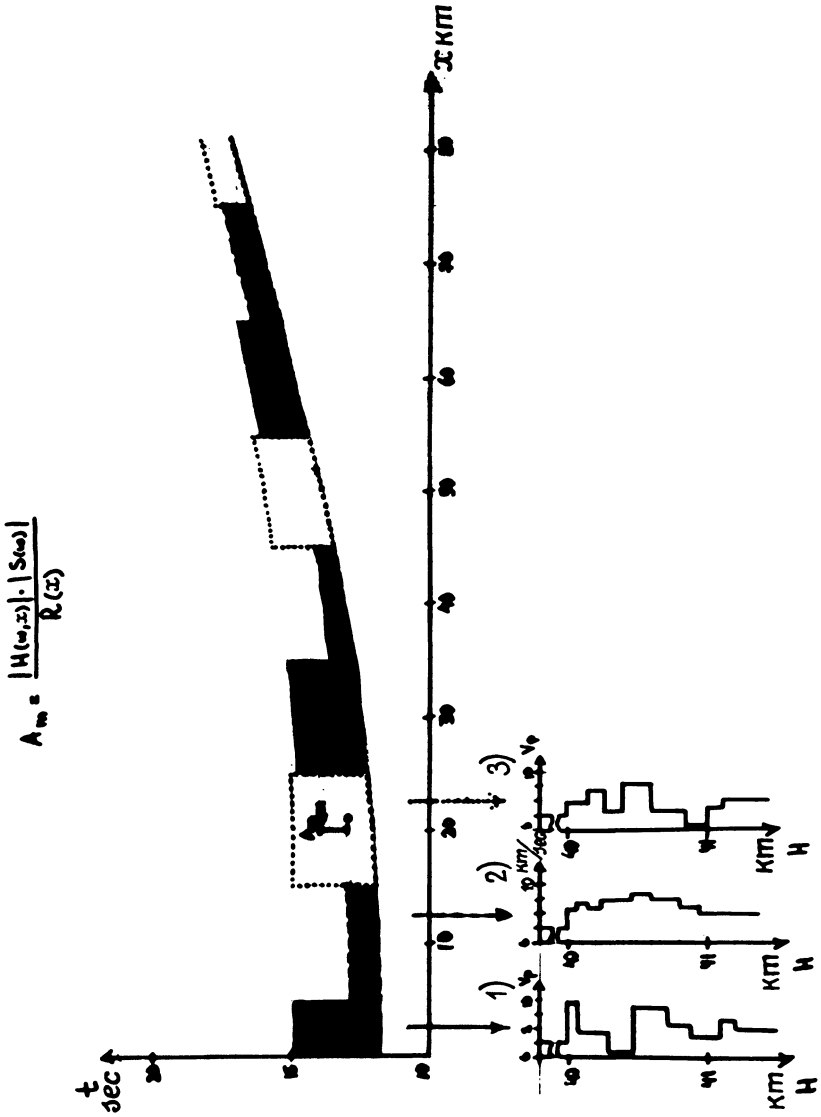


Fig. 11: Dynamic travel-time curve for subcritical reflections from the *M*-boundary represented by blocks with complicated inversional zones. Sections 1, 2 and 3 correspond to individual realizations of the random zone. The conventional seismic noise is drawn by dashed line.

References

- BERZON, I. S., S. A. KATZ, V. I. KOSTENITCH, and L. I. RATNIKOVA: Reflected and transient waves from layers with random structure in quasihomogeneous medium (in Russian), In: *Seismicheskie volny v tonkosloistych sredach*, Nauka, Moscow, 1972
- BERZON, I. S., P. S. VEITZMAN, I. P. PASECHNIK, and L. I. RATNIKOVA: Wave field from thin-layered models of the transition between crust and mantle (in Russian). *Geophys. Sbornik*, 31, Naukova dumka Kiev, 1969
- CLOWES, R. M., and E. R. KANASEWICH: Seismic attenuation and the nature of reflecting horizons within the crust. *J. Geophys. Res.*, 75, No 32, 1970
- DAVYDOVA, N. I., Yu. F. IVANTZOV, B. B. TAL-VIRSKY, A. N. FURZOV, and G. A. YAROSHEVSKAYA: Seismic properties of deep discontinuities in West-Uzbekistan (in Russian). *Seismicheskie svoystva granitzy Mohorovichicha*, Nauka, Moscow, 1972
- DAVYDOVA, N. I., I. P. KOSMINSKAYA, and G. G. MICHOTA: The thickness and nature of seismic discontinuities based on deep seismic sounding data. *Tectonophysics*, No. 10, 1970
- DRUZHININ, V. S., V. M. RYBALKA, and D. A. BELIKOVA: Reflecting properties of the *M*-boundary in the eastern part of the Russian platform. *Bull. (Izv.) Acad. Sci. USSR, Earth Physics*, No 8, 1970
- FUCHS, K.: Das Reflexions- und Transmissionsvermögen eines geschichteten Mediums mit beliebiger Tiefenverteilung der elastischen Moduln und der Dichte für schrägen Einfall ebener Wellen. *Z. f. Geophys.* 34, 389—415, 1968
- FUCHS, K.: On the properties of deep crustal reflections. *Z. f. Geophys.*, 35, 133—149, 1969
- FUCHS, K.: On the determination of velocity depth distribution of elastic waves from the dynamic characteristics of the reflected wave field. *Z. f. Geophys.*, 36, 531—548, 1970
- GALKIN, I. N., A. V. NIKOLAEV, and E. A. STARSHINOVA: Fluctuations of wave characteristics and diffuse heterogeneity of the Earth's crust. *Bull. (Izv.) Acad. Sci. USSR, Earth Physics*, No 2, 1970
- GELCHINSKY, B. Ya.: Wave propagation in media with effective random parameters-formulation of problems (in Russian). *Trudy Mat. Inst. Acad. Sci. USSR*, No 45, 1968
- GUPTA, R. N.: Reflection of elastic waves from a linear transition layer. *Bull. Seism. Soc. Am.*, 56, 2, 1966
- HELMBERGER, D.: The crust-mantle transition in the Bering sea. *Bull. Seism. Soc. Am.*, 58, 179—214, 1968
- HELMBERGER, D., and G. MORRIS: A travel time and amplitude interpretation of a marine profile: Primary waves. *J. Geophys. Res.*, 74, No. 2, 1969
- HOWELL, B. F.: Lake superior seismic experiment: Frequency spectra and absorption. In: *The Earth beneath the Continents*, *Geophys. Monograph*. 10, Am. Geophys. Union, 227—233, 1966
- KOSMINSKAYA, I. P.: Contemporary problems of deep seismic sounding (in Russian). In: *Sbornik, posvyaschennyi 60-letiu S. I. Subbotina*, Naukova dumka, Kiev, 1966

- KOSMINSKAYA, I. P., and N. I. DAVYDOVA: Crustal velocity models and structure of seismic boundaries. XIIe Assemblée Générale de la CSE, Luxembourg, 1970, Bruxelles, 1971
- KOSMINSKAYA, I. P., R. M. KRASCHINA, and I. P. PAVLOVA: North and central parts of the Ochotsk sea (in Russian). In: Stroenie zemnoi kory v oblasti perechoda ot Aziatskogo kontinenta k Tichomu okeanu. Edit.: E. I. Galperin and I. P. Kosminskaya, Nauka, 1964
- KOSMINSKAYA, I. P., and S. M. ZVEREV: Problems of seismic investigations in transition zones between continents and oceans (in Russian). In: Stroenie i razvitie zemnoi kory na sovetском Dalnom Vostoke, Nauka, 1969
- KRYLOV, S. V.: Deep seismic sounding in Sibiria-methods and results (in Russian). Novosibirsk, 1971
- LITVINENKO, I. V., and I. S. LENINA: Some results of deep seismic sounding in the Pechenga structure (in Russian). In: Geologia i glubinnoe stroenie vostochnoi chasti Baltiiskogo schita, Nauka, Leningrad, 1968
- MAGNITSKY, V. A.: The structure of the Earth's interior and physics of the Earth (in Russian). Nedra, Moscow, 1965
- MEISSNER, R.: Explored deep interface by seismic wide angle measurements. Geophys. Prospecting, 15, No 4, 1967
- MISHENKIN, B. P.: Synthetic seismograms of seismic waves reflected from a plane slowly dipping transition layer (in Russian). In: Glubinnoe seismicheskoe zondirovanie v Zapadnoi Sibiri, Nauka, 1969
- MICHOTA, G. G.: Spectra and intensity of deep submerging waves (in Russian). Edit.: Kosminskaya I. P., Sollogub V. B., Pavlenkova N. I., Naukova dumka, Kiev, 1969
- NAKAMURA, J., and B. F. HOWELL: Main seismic experiment: frequency spectra of refraction arrivals and the nature of the Mohorovičić Discontinuity. Bull. Seism. Soc. Am., 54, No 2, 1964
- NIKOLAEV, A. V.: Seismic turbidity of geological media and possibility of its investigation (in Russian). Doklady Acad. Sci. USSR, 177, No 5, 1967
- NIKOLAEV, A. V.: Seismic properties of turbulent media. Bull. (Izv). Acad. Sci. USSR, No 2, 1968
- PAVLENKOVA, N. I.: Application of longitudinal and shear waves in deep seismic sounding (in Russian). Razvedochnaya geofizika, 47, Nedra, Moscow, 1971 a
- PAVLENKOVA, N. I.: Correlation of velocity-depth functions of the Earth's crust in Ukraina. Methods and results. Part I. (in Russian). Geophys. Sbornik, 39, Naukova dumka, Kiev, 1971 b
- PAVLENKOVA, N. I.: Correlation of velocity-depth functions of the Earth's crust in Ukraina-method and results. Part II. (in Russian). Geophys. Sbornik, 42, Naukova dumka, Kiev, 1971 c
- PAVLENKOVA, N. I., and T. V. SMELYARSKAYA: Nature of group registration of waves reflected from the lowest crustal boundaries. Bull. (Izv). Acad. Sci. USSR, Earth Physics, No 2, 1968
- RATNIKOVA, L. I., and A. L. LEVSHIN: Calculation of spectral characteristics of thinlayered media. Bull. (Izv). Acad. Sci. USSR, Earth Physics, No 2, 1967

- RIZNICHENKO, YU. V., and I. P. KOSMINSKAYA: On the nature of the layered Earth's crust and upper mantle (in Russian). Doklady Acad. Sci. USSR, 155, No 2, 1963
- RYABOV, V. Z.: Kinematic and dynamic features of submerging waves connected with discontinuities in the Earth's crust and upper mantle. Bull. (Izv). Acad. Sci. USSR, Earth Physics, No 3, 1966
- SHOR, G., and R. RAITT: Explosion seismic refraction studies of the crust and upper mantle in the Pacific and Indian Oceans. The Earth's crust and upper mantle. Geophys. Monograph 13, Am. Geophys. Union, 1969
- VOZHKOVA, N. N., and S. S. CHAMO: Reflectivity of seismic boundaries in the West-Turkmenia depression zone (in Russian). In: Priroda seismicheskikh granitz, Nauka, Moscow, 1971
- ZVEREV, S. M.: Problems connected with seismic investigations of the Earth's crust and oceans. Bull. (Izv). Acad. Sci. USSR, Earth Physics, No 4, 1970

The Special Structure of the P^{MP} Traveltime Curve¹⁾

P. GIESE, Berlin²⁾

Eingegangen am 6. März 1972

Summary: One of the most prominent phases in crustal record sections is the P^{MP}-traveltime curve which is interpreted as wave bottoming the deeper crust and the M-discontinuity. A closer examination reveals that this P^{MP}-group can be composed by a sequence of separated segments. The time delay between the segments can exceed one second. Therefore, in a first approximation, the application of the ray theory seems to be justified. The resulting velocity depth functions show strong velocity reversals in the lower crust which are most intensive under the Central Alps, indicating the possible existence of completely or partly molten material in the crust/mantle transition.

Zusammenfassung: Die P^{MP}-Welle, die die unterste Kruste und die M-Diskontinuität erreicht, ist eine der wichtigsten Phasen in der Krustenseismik. Eine detaillierte Untersuchung zeigt, daß die zugehörige Laufzeitkurve in mehrere Äste zerfallen kann. Die Verzögerung der aufeinanderfolgenden Äste kann größer als 1 s sein. Daher erscheint die Anwendung der Strahlentheorie in erster Näherung gerechtfertigt. Die sich ergebende Tiefen-Geschwindigkeitsfunktion zeigt intensive Geschwindigkeitsverringierungen in der untersten Kruste, insbesondere im Bereich der Zentralalpen. Partiiell oder vollständig aufgeschmolzenes Material im Grenzbereich Kruste/Mantel ist hier daher möglich.

1. Introduction

One of the most important phases observed in crustal seismology is the so-called P^{MP}-phase. The corresponding rays are bottoming the crust/mantle boundary or its transition and the traveltime curve is reversed. The subcritical range is defined by apparent velocities greater than the velocity of the P_n-wave (8.0–8.2 km/sec) whereas the overcritical one is characterized by dx/dt -values smaller than $v(P_b)$.

From the study of the observed amplitudes and frequencies of subcritical waves it becomes evident that the model which most satisfies the observation is one in which the boundaries are represented by a zone of thin diverse lamellae which produce localized velocity inversion. [MEISSNER 1966 and 1967; DAVYDOVA, KOSMINSKAYA, and MICHOTA 1970; FUCHS 1970.]

¹⁾ Contribution within a joint research program of the Geophysical Institutes in West-Germany, sponsored by Deutsche Forschungsgemeinschaft (German Research Association).

²⁾ Prof. Dr. P. GIESE, Institut für Geophysik, Freie Universität Berlin, D 1 Berlin 33, Rheinbabenallee 49.

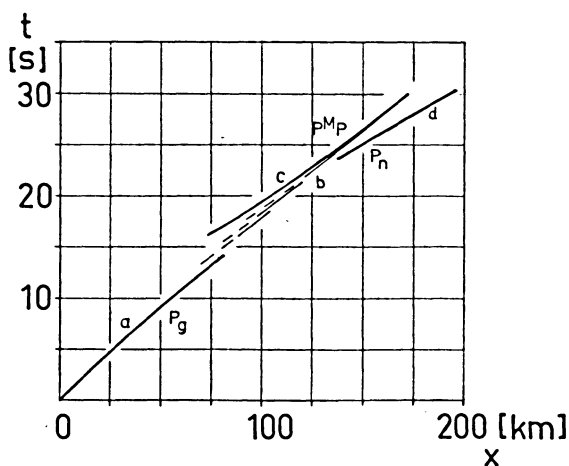


Fig. 1: Traveltime diagram showing the main phases of crustal waves.

The overcritical branch extends over a distance of about 100 km or even more. Hitherto, the overcritical PMP -curve is regarded as continuous and uninterrupted (fig. 1). From the theoretical point of view, the reversed PMP -curve can be generated by reflected waves and/or by penetrating ones as well. In the vicinity of the critical point, the waves are nearly a pure reflection whereas at greater distances, they are of a diving nature [GIESE 1966, 1968; MEISSNER 1967; PAVLENKOVA 1968]. From this behaviour results a more or less wide transition between crust and mantle which is characterized by an increasing velocity with increasing depth.

So two models are existing for the deeper crust and the transition to the upper mantle. The near vertical reflections require a lamination with velocity reversals whereas the overcritical PMP -waves imply a transition zone with positive velocity gradients. This contradicting picture is caused by the different resolution powers of the sub- and overcritical waves. In general, in the deeper crust, the velocity increases with depth, but there exist narrow zones of reversals which are only detectable by impulses with short wave length (some hundred meters).

On the other hand, many examples demonstrate a more or less intensive velocity reversal of complex structure in the middle part of the crust or even in its lower part with a thickness up to 10–20 km. It is, therefore, obvious to look for velocity reversals of intermediate thickness. This question requires a detailed study of the PMP curve that gives more information about the nature of the MOHORoviČIĆ-discontinuity.

2. Area under investigation and description of the material used

From the shotpoint Eschenlohe, a quarry situated in Southern Bavaria between Murnau and Garmisch-Partenkirchen at the northern margin of the Alps, refraction profiles are radiating to the foreland as well as into the Alps (fig. 2).

For the following considerations, the record sections of the profiles Eschenlohe-NNE, Eschenlohe-E, Eschenlohe-SE, and Eschenlohe-S will be used. The amplitudes in the records are uncalibrated, and they can be used only for getting a qualitative picture of energy recorded in the different wave groups.

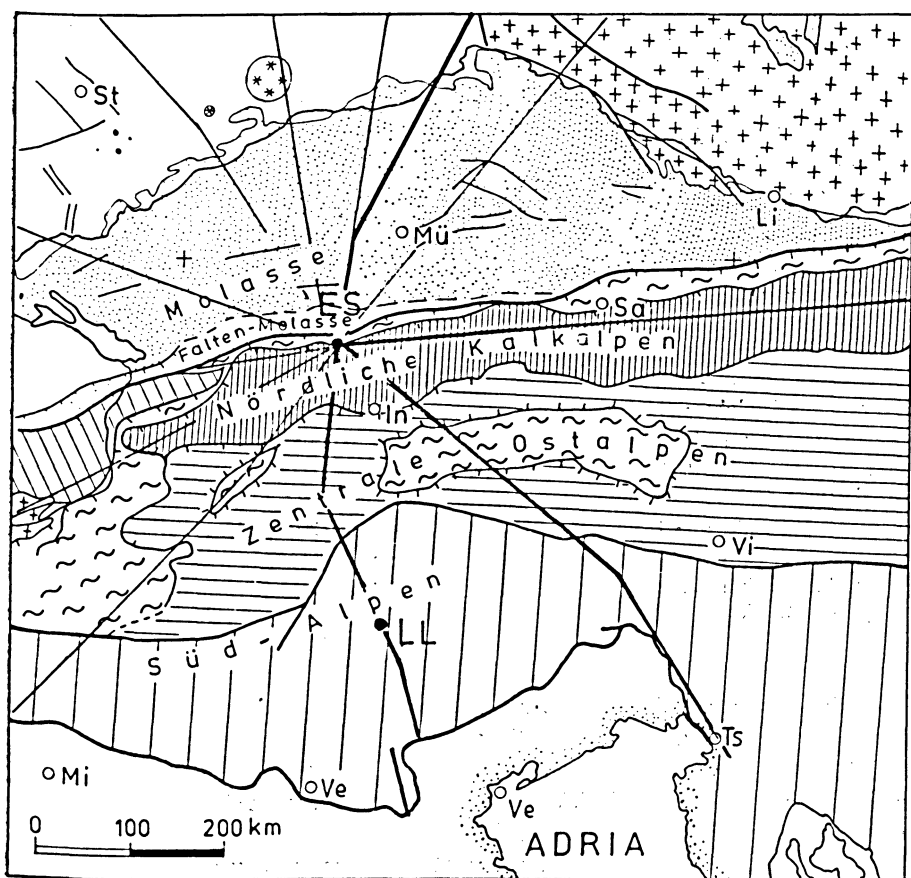


Fig. 2: Area under investigation—thick lines: profiles used in the present paper.
ES: Eschenlohe, LL: Lago Lagorai.

All four record sections show clear second arrivals of the P^MP-wave which are characterized by large amplitudes. In previous interpretations, attempts were made to fit the beginning of the secondaries by one branch of concave curvature. A closer inspection, however, reveals that this one curve does not catch the onsets of the P^MP-wave in all records; sometimes, the actual arrivals occur later. Under the aspect of the following points, a better fitting can be obtained if the one P^MP branch is splitted in separated segments.

1. phase correlation, if possible
2. correlation of the groups characterized by the largest amplitudes
3. correlation under the condition that the resulting apparent velocity increases with a decreasing angle of emergence within the range of possible values.

The four record sections (fig. 3, 4, 5, and 6) show the plotted correlation based on the criteria just mentioned. A splitting of three or even more segments is the result.

In some of his previous publications the author has introduced a phase b located between the branch P_g (a) and P^MP (c). The nature of this phase b—direct or reversed—was not entirely clear. [GIESE 1966, GIESE and STEIN 1971.] Here, the former phase b is the first segment of the P^MP-group and, of course, of reversed character.

Table I shows the distance range of each segment taken from the correlation in the record sections. Due to the fact that the overtaking parts of the segments are approximately parallel, the time delay Δt between them is also presented.

Table I

1. Profile Eschenlohe — NNE	3. Profile Eschenlohe — SE
c_1 : 70—165 km 0,3 sec	c_1 : 95—125 km 0,3 sec
c_2 : 120—200 km 0,3 sec	c_2 : 120—170 km 0,5 sec
c_3 : 170—250 km	c_3 : 140—200 km
2. Profile Eschenlohe — E	4. Profile Eschenlohe — S
c_1 : 80—125 km 0,4 sec	c_1 : 95—120 km 0,8 sec
c_2 : 115—160 km 0,3 sec	c_2 : 120—145 km 0,5 sec
c_3 : 145—215 km	c_3 : 130—205 km 0,6 sec
	c_4 : 135—220 km

Additionally, it should be remarked that the feature of splitting of the P^MP-curve becomes even more accentuated in the record sections of the two profiles radiating from the shotpoint Eschenlohe in SW direction [BEHNKE 1969]. A total time difference of about 4 sec is reached. Here, the time delay (in reduced time scale) between the beginning and the end of the P^MP traveltime group is mainly caused by the splitting effect and less by the normal curvature of a reversed segment.

From the examples presented here it can be stated that the effect of splitting becomes more intensive from north to south and in the Alpine area probably also from east to west.

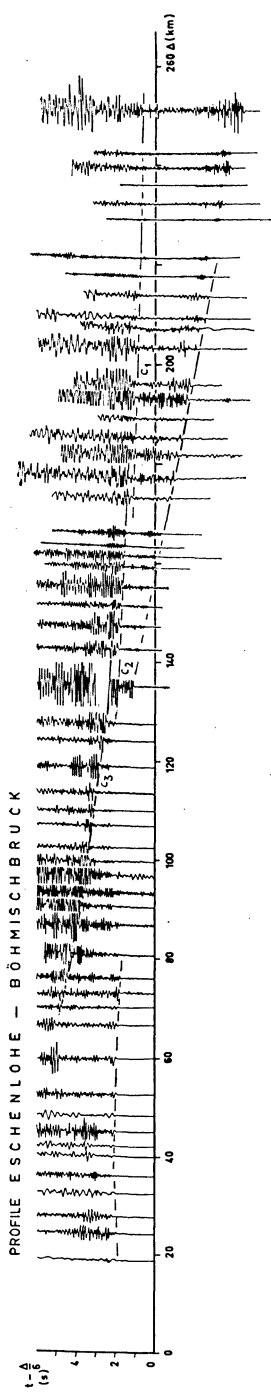


Fig. 3: Record section of the profile Eschenlohe-NNE.
[GIESE and STEIN 1971]

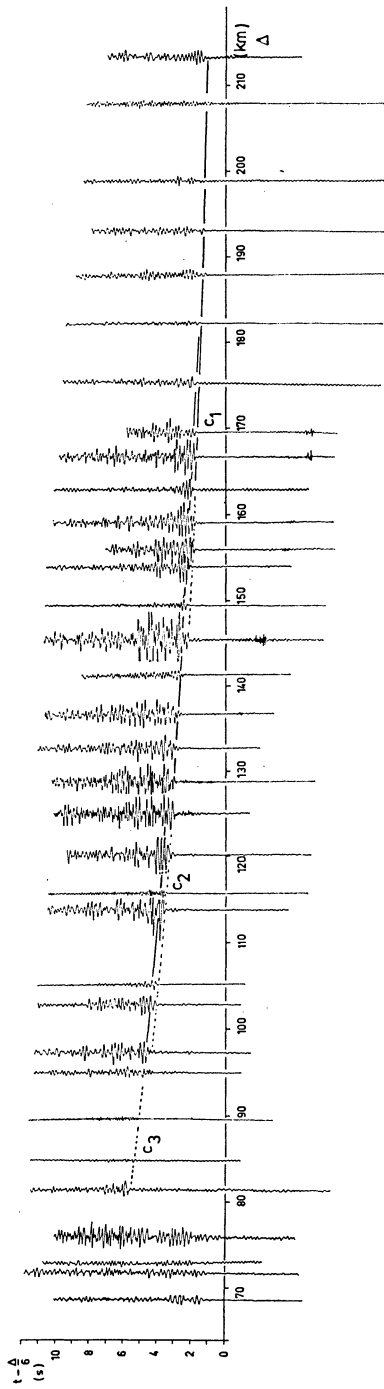


Fig. 4: Part of the record section of the profile Eschenlohe-E.
[KOSCHYK 1969]

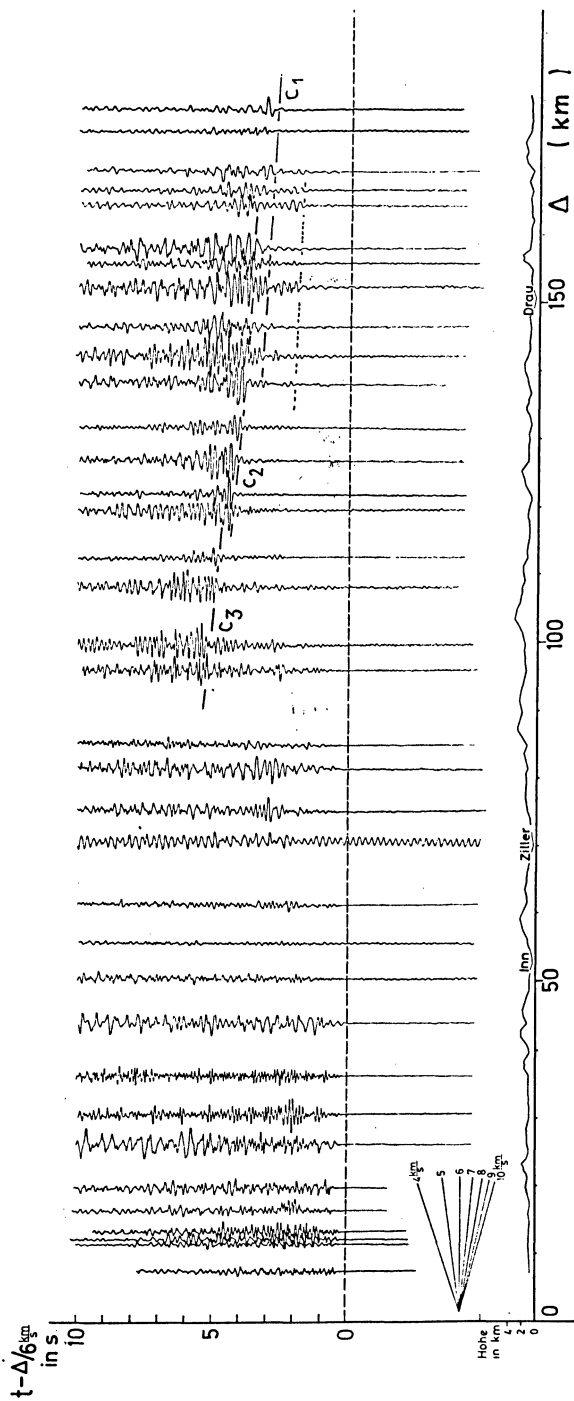


Fig. 5.

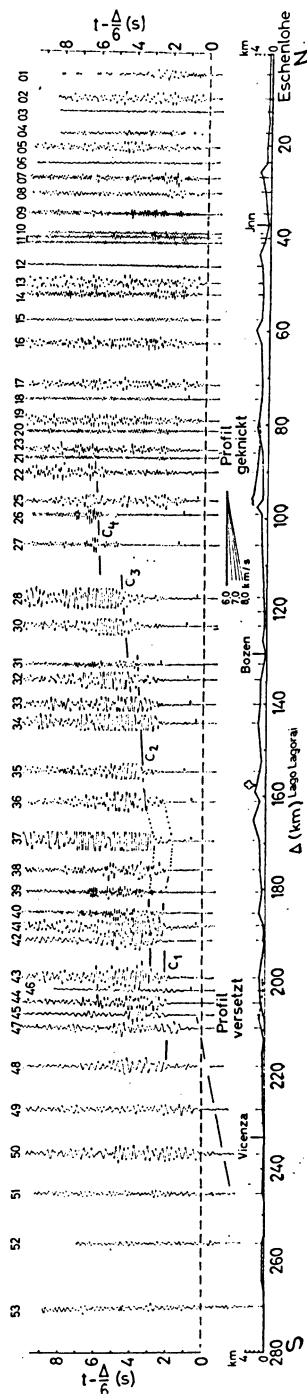


Fig. 6.

Fig. 5: Record section of the profile Eschenlohe-SE.
[ANGENHEISTER 1970]

Fig. 6: Record section of the profile Eschenlohe-S (Lago Lagorai).
[PRODEHL 1965]

Which possibilities are imaginable in trying to explain this splitting of the PMP curve? If the time delay is in the magnitude of one or two wavelengths, it is obvious to look for an effect caused by the wave nature of the seismic impulse. The period of the waves recorded is about 0.2 sec. The time delay in the record sections Eschenlohe-NNE and Eschenlohe-E ist about 0.3 sec, that means in the same size. The time delay, however, becomes stronger in the record sections of the Alpine profiles, therefore suggesting an effect caused by a complicated velocity distribution in the crust/mantle transition. Since there exists a time delay of more than one or two periods, the attempt seems justified to explain this splitting in a first approximation by using the ray theory.

3. Velocity depth function

The following considerations presume no lateral velocity variation, that means the velocity function is only dependent on the depth z . As mentioned above, the segments are regarded as of reversed nature. It is obvious to apply the x^2, t^2 method for depth calculation. But this method is less useful for overcritical reflection observed at large distances from the shotpoint.

Therefore, an empirical method was used to determine the velocity function. The apparent velocity was calculated by the formula [STEWART 1966]:

$$\frac{dx}{dt} = \frac{1}{f'(x_2)} \quad \text{where}$$

$$f'(x_2) = \frac{x_2 - x_3}{(x_1 - x_2)(x_1 - x_3)} f(x_1)$$

$$+ \frac{2x_2 - x_1 - x_3}{(x_2 - x_1)(x_2 - x_3)} f(x_2)$$

$$+ \frac{x_2 - x_1}{(x_3 - x_2)(x_3 - x_1)} f(x_3)$$

for the case $x_3 - x_2 = x_2 - x_1$ follows

$$f'(x_2) = \frac{f(x_3) - f(x_1)}{x_3 - x_2}.$$

In order to explain the interruption of the PMP-group, a corresponding number of low velocity layers is required. For this inversion zone, a triangular form of velocity distribution has been assumed. As shown by KOSCHYK [1969], only the thickness Δz and the maximum velocity decrease Δv are of importance. The position of the point of minimum velocity does not influence the traveltimes of waves penetrating deeper.

The greatest possible depth given by the expression

$$z_{\max} = \frac{x}{2} \sqrt{\frac{dx/dt}{x/t} - 1}$$

has been calculated in order to get a first rough model. Generally, the segments taken from the record sections have been interpreted as overcritical reflections including also the possibility of diving waves. The method for obtaining traveltimes

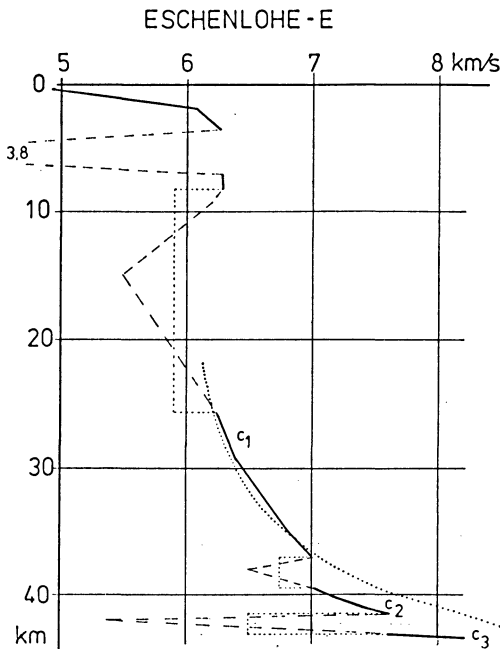


Fig. 7: Velocity-depth-function for the profile Eschenlohe-E. The velocity reversal in the uppermost crust is caused by the molasse beds which have been overthrust here by the Northern Calcareous Alps. Dotted line in the lower crust: velocity-depth-function resulting from an uninterrupted PMP-curve.

[GIESE and STEIN 1971, KOSHYK 1969]

from a velocity model is based in a piecewise linear continuous velocity function of depth [STEINHART and MEYER 1961].

The velocity-depth-functions presented in figs. 7 and 8 have been obtained by comparing the observed and the calculated traveltimes (fig. 9). For each record section about 20 functions have been calculated. From the example in fig. 9 it could be argued that the agreement must be improved. From experience, however, it can be pointed out that the general form of the velocity function remains untouched, only minor modifications are possible.

From the calculations result velocity reversal zones in the lower crust, characterized by only a few km in thickness but a very intensive decrease up to 1–3 km/sec. So the “missing link” seems to have been found between the wide reversal zones in the middle crust given by the delay of the P^{MP}-group as compared with the P_g one and the narrow low velocity zones in the lower crust indicated by the subcritical reflections.

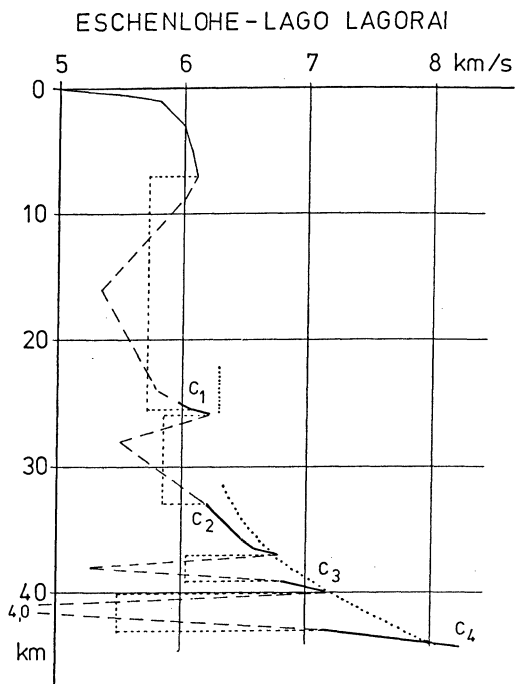


Fig. 8: Velocity-depth-function for the profile Eschenlohe-S – dotted line in the lower crust: velocity-depth-function resulting from an uninterrupted P^{MP}-curve. [GIESE 1966]

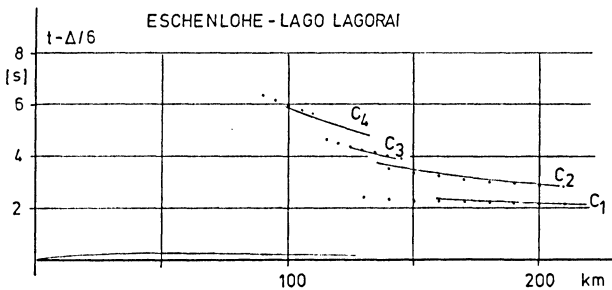


Fig. 9: Example of the profile Eschenlohe-S showing the comparison between the traveltimes taken from the record section and the times computed from the velocity-depth-function presented in fig. 8.

4. Conclusions

The intensity of the reversals in the lower crust and in the transition crust/mantle increases from north to south, that means from the foreland of the Alps to the Central Alps, and with thickening of the crust.

If these results can be confirmed by further observations, they would imply some new aspects for geologic and petrologic considerations.

The strong reversals cannot be explained by a change of rocks in solid state only, i. e. between acid and basic material. A decrease of 3 km/sec requires the existence of molten or at least partly molten rocks in the deepest crust. Assuming a temperature gradient of 20°C/km, a temperature of 800°C would exist in 40 km depth. Acid and intermediate material must be fluid. Taking a gradient of 30°C/km, this results in a temperature of 1200°C, and then even basic rocks must be molten.

In several previous publications it was pointed out that, in the central parts of the Eastern Alps, there is a connection between the zone of low velocity and density in the depth range between 10 and 20 km and the tertiary Tauern crystallization. [BOTT 1954; GIESE 1966; MAKRIIS 1971; ANGENHEISTER, BÖGEL, GEBRANDE, GIESE, SCHMIDT-THOMÉ, and ZEIL 1972].

The heat source for the granitization must be situated deeper. The present study reveals now molten and/or partly molten material in the deeper crust under the Central Alps which may cause the granitization in the higher crust.

These examples should demonstrate the complex nature of "discontinuities". Summarizing it must be stated that a "discontinuity" is not only characterized by a strong positive velocity gradient zone but that more or less wide reversal zones can be intercalated additionally.

References

- ANGENHEISTER, G.: Die Erforschung der tieferen Erdkruste. Untersuchungs-Methoden und Ergebnisse. Physik in unserer Zeit, 1, 59–66, 1970
- ANGENHEISTER, G., H. BÖGEL, H. GEBRANDE, P. GIESE, P. SCHMIDT-THOMÉ, and W. ZEIL: Recent investigations of surfacial and deeper crustal structures of the Eastern and Southern Alps. Geol. Rundschau 61/2, in press
- BEHNKE, C.: Meßdaten seismischer Untersuchungen in den Alpen 1959–1969 (unpublished report; unveröffentlichter Bericht), Niedersächsisches Landesamt für Bodenforschung, 15 p. with 17 fig., 1969
- BOTT, M. H. P.: Interpretation of the gravity field of the Eastern Alps, Geol. Mag., 91, 377–383, 1954
- CHOUDHURY, M., P. GIESE, and G. de VISINTINI: Crustal structure of the Alps—some general features from explosion seismology. Report I.U.G.G.—General Assembly (1967), 15 p., Boll. Geofis. teor. ed appl., 1972, in press
- DAVYDOVA, N. J., J. P. KOSMINSKAYA, and G. G. MICHOTA: The Thickness and Nature of Seismic Discontinuities Based on Deep Seismic Sounding Data. Tectonophysics, Vol. 10, 561–571, 1970
- FUCHS, K.: On the Determination of Velocity Depth Distributions of Elastic Waves from the Dynamic Characteristics of the Reflected Waves Field, Z. Geophys. 36, 531–548, 1970
- GIESE, P.: Versuch einer Gliederung der Erdkruste im nördlichen Alpenvorland, in den Ostalpen und in Teilen der Westalpen mit Hilfe charakteristischer Refraktions-Laufzeitkurven sowie eine geologische Deutung. Habil. Schrift, Math.-Nat. Fak. d. Freien Universität Berlin, 143 p., 1966, Publ. d. Inst. f. Meteorologie und Geophysik, Freie Universität Berlin, Bd. 1, H. 2, 202 p., 1968
- GIESE, P., and A. STEIN: Versuch einer einheitlichen Auswertung tiefenseismischer Messungen aus dem Bereich zwischen der Nordsee und den Alpen. Z. Geophys. 37, 237–272, 1971
- KOSCHYK, K.: Beobachtungen zur Erforschung der Erdkruste mit der Methode der Refraktions-Seismik längs der beiden Profile Eschenlohe-SE und Eschenlohe-E in den Ostalpen 1965–1969. Dipl.-Arbeit Inst. f. Angewandte Geophys., Universität München, 48 p., 1969
- MAKRIS, J.: Aufbau der Kruste in den Ostalpen aus Schweremessungen und Ergebnissen der Refraktions-Seismik. Dissertation Universität Hamburg, 65 p., Hamburg 1971
- MEISSNER, R.: An Interpretation of the Wide Angle Measurements in the Bavarian Molasse Basin. Geophys. Prospect. 14, 7–17, 1966
- MEISSNER, R.: Zum Aufbau der Erdkruste, Ergebnisse der Weitwinkelmessungen im bayerischen Molassebecken. Gerlands Beitr. Geophys. 76, 4, 211–314, 1967
- PAVLENKOVA, N. H.: Methods of Velocity Determination from Seismic Crustal Studies. Report at the meeting of the Study Group on Explosion Seismology, 22., Leningrad 1968
- PRODEHL, C.: Struktur der tieferen Erdkruste in Südbayern und längs eines Querprofils durch die Ostalpen, abgeleitet aus refraktionsseismischen Messungen bis 1964. Boll. Geofis. teor. ed appl. 25, 35–88, 1965
- STEINHART, J. S., and R. P. MEYER: Explosion Studies of Continental Structure. Carnegie Institution of Washington, Publ. 622, Washington D. C., 409 p., 1961
- STEWART, S. W.: Seismic Ray Theory Applied to Refraction Surveys of the Earth's Crust in Missouri. Doctor-Thesis, Saint Louis University, 189 S., 1966

Relation between P-Wave Amplitudes and Discontinuities in the Earth's Crust

F. S. TREGUB, Moscow¹⁾

Eingegangen am 11. Dezember 1971

Summary: The method of interpretation yields quantitative evaluation of the influence of layered structures in the upper part of the Earth's crust on the amplitude of longitudinal waves. The use of the statistical velocity model made it possible to zone and stratify the consolidated crust by the value of the "heterogeneity factor" and to single out a "transparent" layer.

Zusammenfassung: Es wird eine Interpretationsmethode vorgelegt, die es ermöglicht, den Einfluß von Schichtstrukturen im oberen Teil der Erdkruste auf die P-Wellenamplituden quantitativ zu bestimmen. Mit Hilfe einer angenommenen statistischen Geschwindigkeitsverteilung gelingt es, an Hand des „Heterogenitätsfaktors“ die Erdkruste in Zonen aufzugliedern und einzelne Schichten zu bestimmen, für welche dieser Faktor den Wert Null erreicht, d. h. die Schicht „durchlässig“ erscheint.

1. Introduction

Recently the seismologists have turned more often to statistical models of a medium to interpret seismic fields. First of all it is due to the fact that the solution of the inverse seismic problem in the framework of horizontal layered inhomogeneous media is very ambiguous. Further a great number of data of field investigations are still unused, such as fluctuations of amplitudes, times of observation, interruption of wave correlation and other characteristics which cannot be described quantitatively.

2. Method

We used the most simple statistical medium model suggested by NIKOLYAEV [1968]. Here are the basic relations:

$$V(x, y, z) = \bar{V}(z) + V_n(x, y, z) + \delta V(x, y, z) + \Delta V(x, y);$$

$$\ln A(x, y) = \ln \bar{A}(r) + \ln A_n(x, y) + \ln \delta A(x, y) + \ln \Delta A(x, y);$$

$$T(x, y) = \bar{T}(r) + T_n(x, y) + \delta T(x, y) + \Delta T(x, y).$$

¹⁾ Dr. F. S. TREGUB, Institut Fiziki Zemli ANSSSR, B. Gruzinskaya 10, Moskva, USSR.

Velocity field of P-waves is formed by four basic factors:

1. Determined horizontally layered velocity depth distribution $V(z)$, and amplitude distance curve $\ln \bar{A}(r)$ corresponding to the period-distance curve $\bar{T}(r)$, whereas \bar{T} varies smoothly along a profile.
2. Inhomogeneities near the seismic source expressed by $V_n(x, y, z)$, $\ln A_n(x, y)$ and $T_n(x, y)$ respectively. The latter term contains a constant component for a given direction from the source and changes smoothly along a profile.
3. Random field which is homogeneous and isotropic within the limits of single intervals of depths expressed by $\delta V(x, y, z)$, $\ln \delta A(x, y)$ and $\delta T(x, y)$ respectively. They change sharply as a summary effect of a random field of inhomogeneities along the whole wave path.
4. Inhomogeneities below the point of registration expressed by $\Delta V(x, y)$, $\ln \Delta A(x, y)$ and $\Delta T(x, y)$ respectively which are correlated to the place of registration causing an overlapping of graphs.

In the presence of a detailed system of observations using spatial characteristics of each component we can separate their influence by means of experimental data processing.

The relation between random and determined parameters of amplitude and time has the following form:

$$D\delta \ln A = 4\pi^2 f^2 D\delta T; \quad \ln \bar{A}(x) = C(x) + \frac{K \cdot d^2 \bar{T}}{dx^2}$$

The "heterogeneity factor" g , a quantitative parameter which describes the random field caused by inhomogeneities has been introduced. This coefficient is determined by the mean square variation of the amplitude fluctuation due to the increase of the travel path of the seismic wave:

$$g = \frac{[(D\delta \ln A)_{M_2} - (D\delta \ln A)_{M_1}]^2}{L(M_1, M_2)}$$

The expression for a reverse system of observations is:

$$g = \frac{D\delta \ln A}{2L}$$

3. Results

Such a statistical model of the velocity depth distribution was adopted as the basis of interpretation of deep seismic sounding data of one of the Kazakhstan profile.

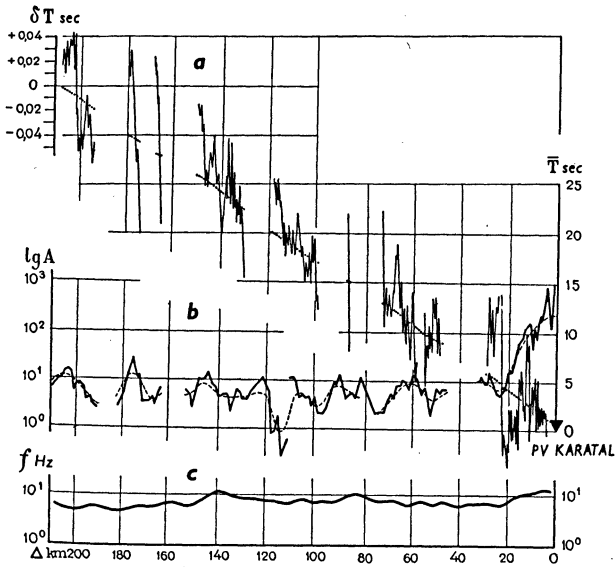


Fig. 1: Kinematic and dynamic parameters of the first wave group.

- a) Travel-time graph, observed (solid line) and smoothed (dotted line).
- b) Amplitude-distance curve, observed (solid line) and smoothed (dashed line).
- c) Frequency variation along the profile.

The length of the profile was 220 km. The first arrivals correspond to the wave refracted in a consolidated crust. At a distance of 200 km this wave changes into the wave from the M-discontinuity. This boundary was fixed according to the first arrivals and to the reflected wave. The attempt to single out overlying intermediate boundaries in the Earth's crust failed.

Fig. 1 shows kinematic and dynamic parameters of the first wave group observed from the same point of explosion. In this figure experimental values and results of spatial filtration smoothed by GAUSSIAN weighting function are given. In such a way smoothly varying components of amplitude and time functions can be separated from the sharp variations.

The relation between the internal geological structure and the amplitude of seismic signal was found in accordance to the summary effect of the first two components of the field of velocities $V(z)$ and $V_n(x, y, z)$ (Fig. 2).

Smoothed amplitude graphs normalized to the same energy of the source proved the correlation in conjugated points. The influence of the inhomogeneity $V_n(x, y, z)$ near the shotpoint "Ili" (Fig. 6) broke this regularity by decreasing the amplitude of the signal by 10 times in the north direction.

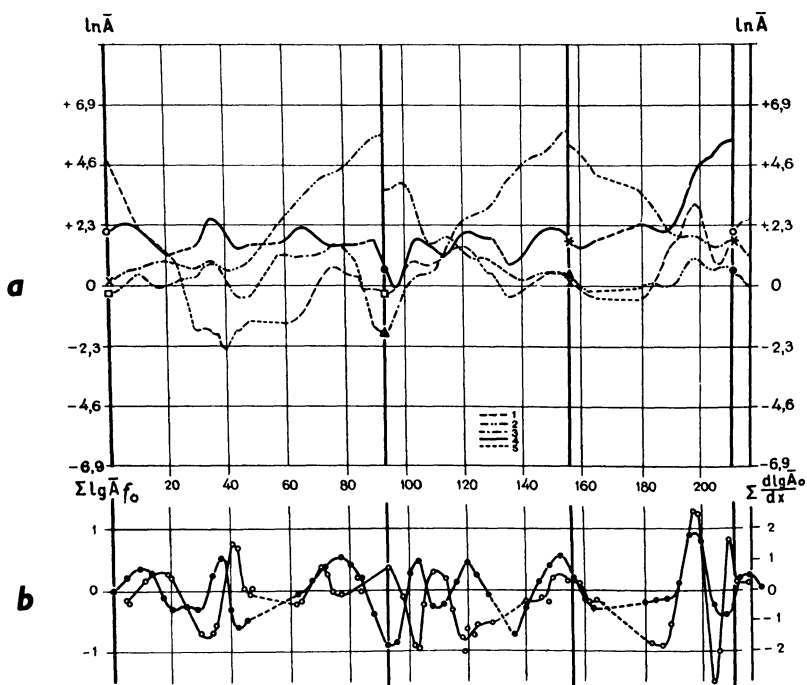


Fig. 2: Amplitude variations of seismic signals along the profile.

- a) Smoothed experimental amplitude-distance curves, 1, 2, 3, 4—obtained from different shotpoints, 5—interpolated intervals.
 b) Summary effect of local variations of the gradient of the amplitude along the profile.

Fluctuations of smoothed amplitude curves are correlated with the geological structure of the upper part of the profile: the increase of the amplitudes—on an average by half of the order—is registered within the area of lowlands and an amplitude decrease can be observed with crystalline rocks.

A relation between the first derivative of amplitude curves and the near surface tectonics is apparent. It is possible to single out the influence of the structure of deep boundaries from the background of distortions considering the upper part of the geological section.

The interpretation of the horizontal component of the velocity profile $V(z)$ is possible using the amplitude-distance curves reduced to one energy level only (Fig. 3). According to the attenuation of a signal a conclusion can be drawn that up to a depth of 10 km the structure of the medium is essentially different along the profile, in greater depths the structure becomes practically the same and is characterized

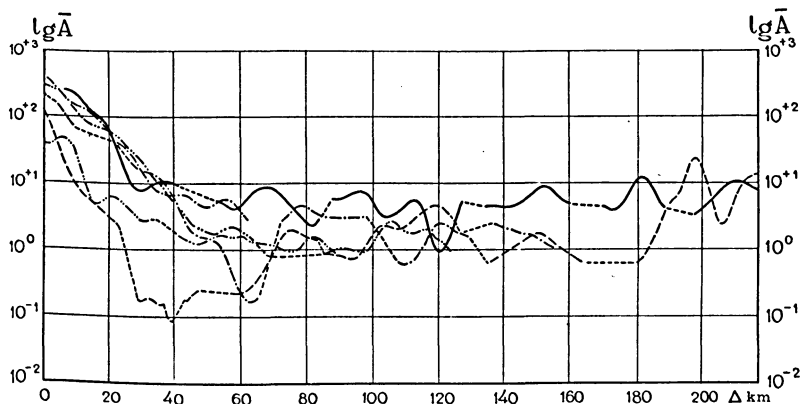


Fig. 3: Observed amplitude distance curves.

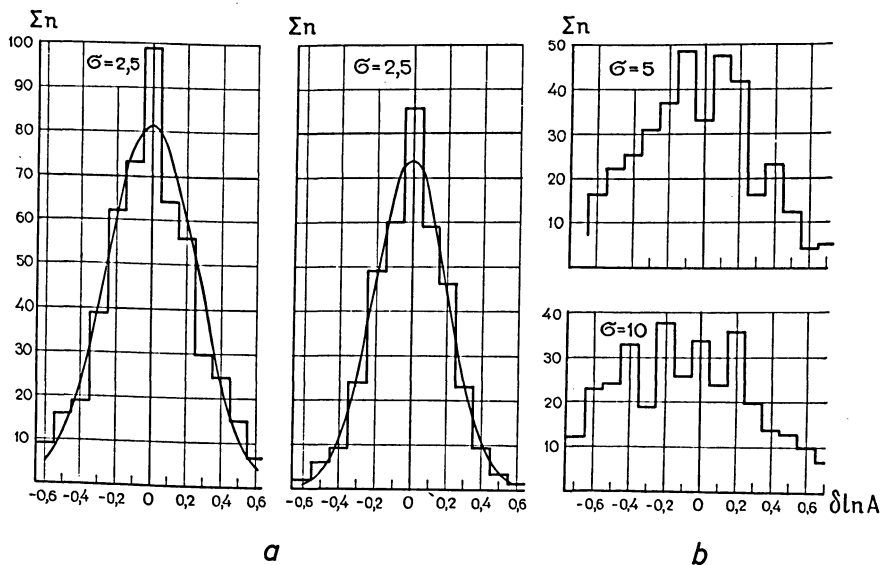


Fig. 4: Histograms of the natural logarithm of the random component of the amplitude curves.

- a) Zero mean of heterogeneity.
- b) Distribution with heterogeneity-effect.

by a very weak increase of the velocity with depth. At a distance of 180 km an increase of the amplitudes can be observed. Probably, this increase is related to the existence of a wave which can be singled out by kinematic parameters at a distance greater than 200 km.

Analyzing the system of smoothed curves, local increases and decreases of the amplitude can be interpreted by the geological structures in the upper part of the geological section. This fact causes the change of waves in the first arrivals.

Let us now consider the amplitude data which were filtered and not involved in the earlier interpretation. Histograms of fluctuations of amplitude logarithm (Fig. 4) confirm that separating the determinable components from random components optimum conditions for spatial filtration can be found. The ordinary law of distribution of $\delta \ln A$ (Fig. 4a) corresponds to the homogeneous field of $\delta v(x, y, z)$.

At the places of registration of $\Delta V(x, y)$ inhomogeneities can be singled out by the correlation of reverse and overlapping graphs (Fig. 4b). These inhomogeneities can change the amplitude of a signal some times.

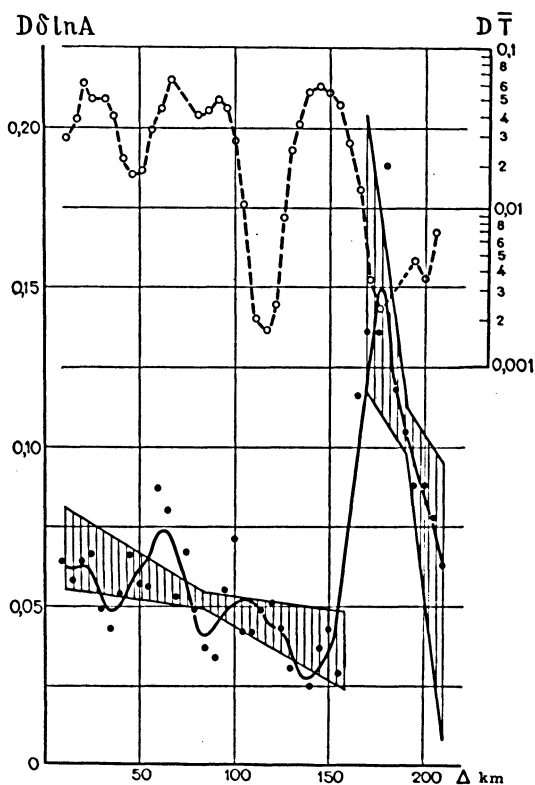


Fig. 5: Mean squares of fluctuations of amplitudes and times along the profile.

In Fig. 5 variations of mean squares of fluctuations of the logarithm of amplitudes and of the time of registration with distance are demonstrated.

It follows that the consolidated crust is strongly differentiated with respect to inhomogeneous velocity-depth distribution. The increase of amplitude fluctuations is not followed by the decrease of time fluctuations. This may be connected with the fact that the dimensions of inhomogeneities are essentially different at different depths.

Variations of the value of the heterogeneity factor along the profile and with depth are presented in Fig. 6. Calculations were carried out by means of reverse systems:

$$g_i = \frac{D\delta \ln A_i - \frac{1}{2} \sum_1^{i-1} Lg}{2 \left(L_i - 2 \sum_1^{i-1} L \right)},$$

and by means of the dependence of $D\delta \ln A$ on distance:

$$g_i = \frac{D\delta \ln A_i - 2 \sum_1^{i-1} Lg}{L_i - 2 \sum_1^{i-1} L}.$$

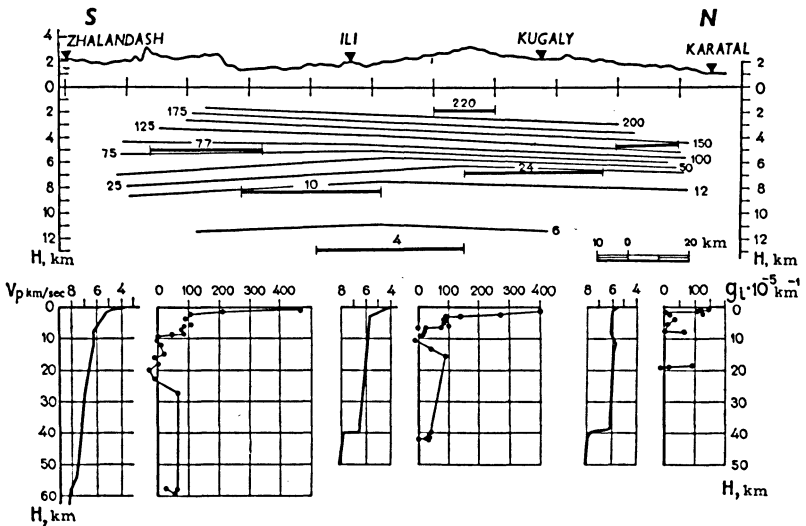


Fig. 6: Depth-distribution of velocity and of heterogeneity factor along the profile.

In all the cases the influence of the overlying layers was taken into account.

In the foothills of North-Tyan-Shan the heterogeneity of the consolidated crust uniformly decreases from the surface up to the depth of 10 km, at the south end of the profile the same decrease can be noted in a more narrow interval of depths between 4–6 km (Fig. 6). From the depth of 6–8 km the crust becomes more homogeneous. A layer of zero meaning of the heterogeneity factor can be singled out at a depth of about 10 km. This fact can be interpreted as the absence of velocity inhomogeneities for the observed wavelength of about 600 m. This "transparent" layer might be related to a low velocity layer. Such an interpretation is not in contradiction to experimental data and agrees well with different components of amplitude and time graphs.

It is believed that the suggested method can be used in seismic survey and in modelling and seismology as well.

References

- GALKIN, I. N., and A. V. NIKOLAYEV: Investigation of the heterogeneity of the Earth's crust and upper mantle by recording the amplitudes of refracted waves. *Bull. (Izv.) Acad. Sci. USSR, Earth Physics* 8, 481–487, 1968
- NIKOLAYEV, A. V.: Seismic properties of weakly heterogenous media. *Bull. (Izv.) Acad. Sci. USSR, Earth Physics* 2, 83–87, 1968
- NIKOLAYEV, A. V., and F. S. TREGUB: The results of the study of the statistical models of the crust (in Russian). *Doklady Acad. Sci. USSR*, 189, No. 6, 1969

The Results of Deep Seismic Sounding in Czechoslovakia

B. BERÁNEK, Brno¹⁾ and A. DUDEK, Prague²⁾

Eingegangen am 12. Februar 1972

Summary: The paper deals with the results of deep seismic sounding in Czechoslovakia in three international profiles (V, VI, VII) and presents their geological interpretation. Besides the course of the Moho-discontinuity, there were seismically confirmed or newly established deep-seated fault zones, which separate or limit main geological units (blocks) of the Bohemian Massif and the West Carpathians. The results of deep seismic sounding, first of all the course of the deep fault zones, are correlated with magnetic and gravimetric anomalies and with the seismic active zones.

Zusammenfassung: Der Aufsatz behandelt die Auswertung der tiefenseismischen Messungen in der Tschechoslowakei auf drei internationalen Profilen (V, VI, VII) und unterbreitet ihre geologische Interpretation. Neben der Bestimmung des Verlaufes der Moho-Diskontinuität wurden seismisch mehrere Tiefenstörungen bestätigt oder neu ermittelt, welche die geologischen Haupteinheiten (Blöcke) der Böhmisches Masse und der Westkarpaten trennen oder begrenzen. Die Ergebnisse der tiefenseismischen Messungen, hauptsächlich der Verlauf der Tiefenstörungen, wurden mit den gravimetrischen und magnetischen Anomalien und mit seismisch aktiven Zonen verglichen.

1. Introduction and description of Profiles

The exploration of the Earth's crust over the Czechoslovak territory using the method of explosive seismology has been carried on since 1964 as a part of the project for southeastern Europe. This project, originally planned for the Carpathian-Balkan region, investigates the structure of the Earth's crust even in its wider surroundings in ten international profiles (Fig. 1).

In Czechoslovakia, the exploration of the Earth's crust using the deep seismic sounding method followed successful works of Czechoslovak seismologists, especially that of Professor A. ZÁTOPEK. Three international profiles, namely V, VI and VII (Fig. 2), had been measured up by the end of 1970 in cooperation with geophysicists from the neighbouring countries (Poland, Hungary and the German Democratic Republic).

The profile V runs from Poland (east of Warsaw) across the Czechoslovak territory to Hungary. From the Polish Paleozoic platform it passes into the Carpathian foredeep, penetrates the Outer and Central Carpathians and terminates in the Pan-

¹⁾ Dr. BŘETISLAV BERÁNEK, Ústav užité geofysiky, Ječná 29a, Brno, ČSSR.

²⁾ Dr. ARNOŠT DUDEK, Ústřední ústav geologický, Hradební 9, Praha 1, ČSSR.

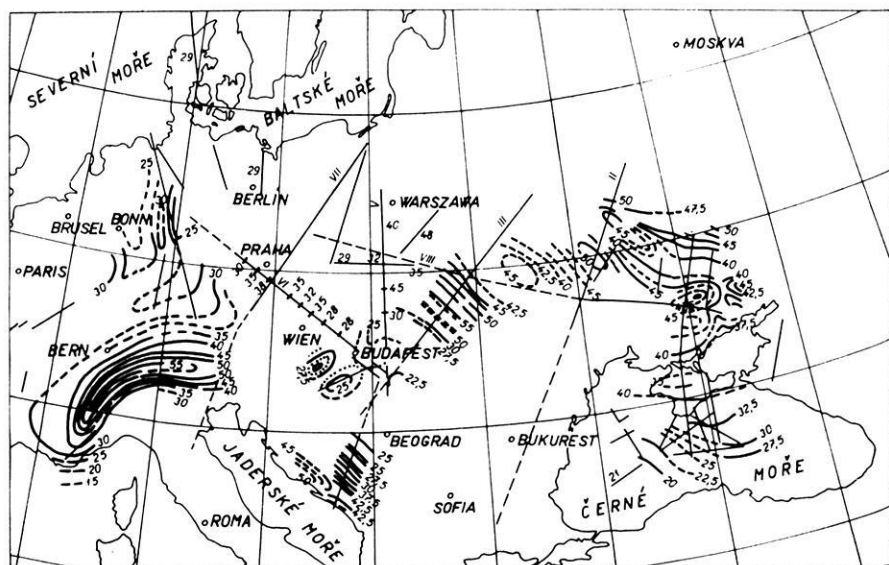


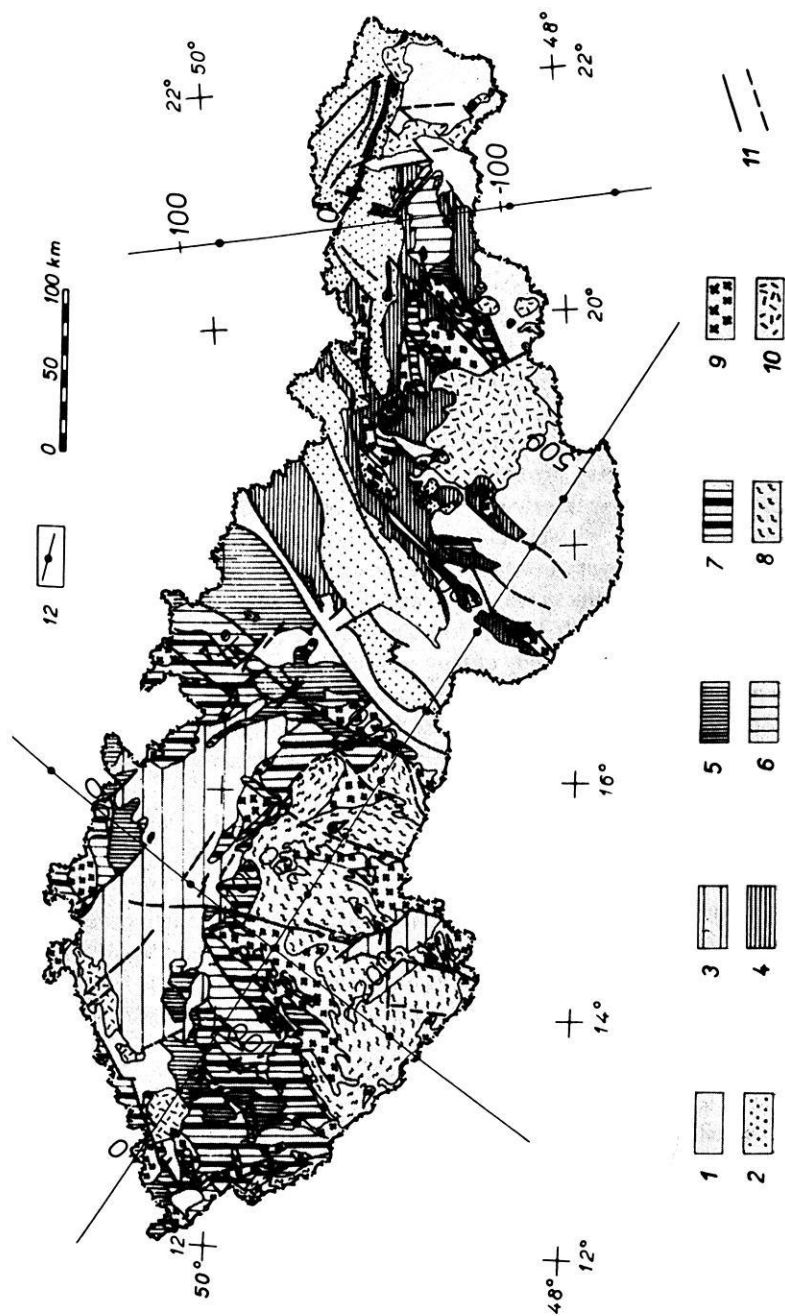
Fig. 1: International profiles in South-Eastern and Eastern Europe.

nonian Massif.—The profile VI runs from the G.D.R. to the Bohemian Massif, proceeds over the Carpathians to the area of the Pannonian Massif.—The profile VII is drawn from the Polish Paleozoic platform across the Sudeten, the Czech Cretaceous Basin and the Central Bohemian Pluton, and farther it passes into the southern part of the Moldanubicum and, on the Bavarian side, across the Bavarian molasse into the Alps.

The measurements on the profiles make it possible to trace the course of the M-discontinuity with the aid of reflected waves in the region of the critical point and beyond it. The velocity corresponding to this boundary (velocity of the Upper Mantle) was ascertained from the frontal waves in the profile VI in the Krušné hory Mts. and in the Moldanubicum, amounting on average 8.2 km/sec.

Fig. 2: International profiles V, VI and VII in Czechoslovakia with simplified geological situation.

1=Neogene, 2=Paleogene of the Carpathians, 3=Cretaceous of the Bohemian Massif, 4=Mesozoic of the Carpathians, 5=Late Paleozoic, 6=Early Paleozoic, 7=Algonkian, 8=Moldanubicum, 9=plutonic rocks, 10=neovolcanics, 11=principal faults, 12=international profiles with shot points.



The object of observation were mainly the waves, which, owing to their origin, are bound to the surface of the M-discontinuity or some other boundaries within the Earth's crust. We did not manage to discern exactly frontal waves from the Conrad discontinuity. The CONRAD-boundary seems to be found by reflected waves at certain places. From the travel-time curves of reflected waves or the refracted ones mean velocities were calculated; from them the velocity depth diagrams $\bar{v}(z)$ were constructed for certain areas (Moldanubicum, Central Bohemian pluton, Bohemian Massif and Carpathian block). From those diagrams layer velocities $v(z)$ were derived in dependence on depth and some models of the Earth's crust were constructed. These models consist of horizontal layers with constant velocity or constant vertical velocity gradient [BERÁNEK, ZOUNKOVÁ, HOLUB 1971]. In addition, a section of mean velocities $v(x, y)$ was constructed along the profiles VI and VII in dependence on depth.

To distinguish deep faults in individual profiles a number of criteria were used. Those of the first category are the anomalous phenomena in wave pattern, the disturbance of correlation of base waves by the occurrence of diffracted waves and establishment of their sources, as well as the sudden damping of energy of P^M waves. The second category of criteria involves sudden changes in the dip of the reflecting boundary within the crust and sudden changes in the course of isoline of mean velocities along individual profiles. It should be pointed out that velocity sections $\bar{v}(x, z)$ contribute considerably to the study of fault tectonics. Individual blocks (units) separated by deep faults can be characterized by a different distribution of mean velocities. Sedimentary areas manifest themselves by decreased velocities in the Bohemian Massif, however, the metamorphosed rocks display decreased mean velocities, if compared with granitic rocks.

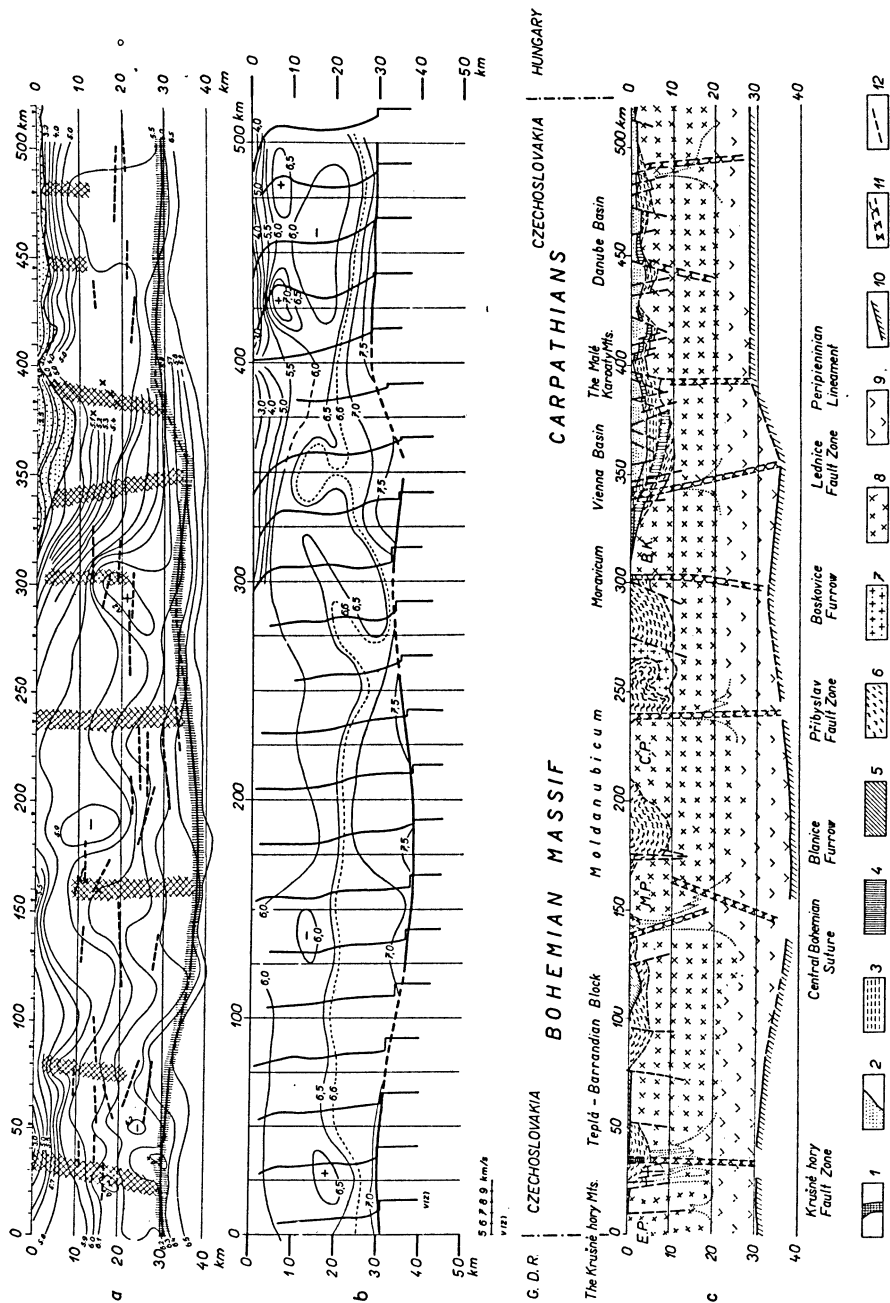
In the following, the essential results accomplished in individual profiles are given:

1.1 Profile VI

This profile indicates that the Bohemian Massif, except for its northwestern part, submerges deeply into the mantle, compared with the Pannonian Massif in the south-east and with the Saxo-Thuringian region in the north (Fig. 3). It is of interest that the greatest thickness of the Earth's crust in the Bohemian Massif has been found

Fig. 3: Results of deep seismic sounding on the profile VI.

- a) Cross section with seismic boundaries and M-discontinuity, with foci of diffracted waves and iso-velocity lines (mean velocities).
- b) Course of layer velocities. The CONRAD-discontinuity is drawn as a boundary at velocity 6.6 km/sec.
- c) Geological interpretation: 1 = neovolcanics, 2 = Neogene sediments, 3 = flysch belt, 4 = Mesozoic, 5 = Paleozoic, 6 = crystalline schists, 7 = durbachites, 8 = granite zone, 9 = basalt zone, 10 = M-discontinuity, 11 = deep faults, 12 = principal regional faults.



in the area of the Moldanubicum and in the Central Bohemian pluton. Here the M-discontinuity lies at a depth of 38 km. Elevations of the Moho-discontinuity were ascertained in the area of the Doupovské vrchy Mts. and at the east edge of the Moldanubicum.

The Bohemian Massif itself is divided by a number of faults which are physically indicated and can be correlated with dislocation structures known at the surface; nevertheless, only the results of geophysical measurements make it possible to distinguish their importance and deep foundation. The profile VI confirmed the first-order magnitude of the Krušné hory fault zone, which, in the west, bounds the block of increased crust thickness in the Bohemian Massif. From the geological point of view this block is formed by the Teplá-Barrandian region, Moldanubicum and the Brunia region. The Krušné hory fault zone is characterized by most of the geophysical criteria, from the geological point of view among other things by persistent magmatic activity from Proterozoic to Quaternary. The gravity, magnetic and volcanic data make it possible to presume also the elevation of basalt layer on its eastern flank. A fault zone of similar importance, was identified further in the Central Bohemian fault zone, at the northwestern border of the Central Bohemian pluton, in the Příbryslav fault zone at the eastern border of the Central Moldanubian Massif and in the Lednice fault zone at the western border of the Vienna Basin.

The principal importance of the Peripieninian lineament which, in the east, borders the block of the increased crust thickness and forms the deep boundary between the Bohemian Massif and the Carpathians, could be confirmed only with the help of deep seismic sounding. On the other hand, the depth extent of some major fault systems of Rhinish trend (the Blanice and Boskovice furrows) has not been evidenced.

Of great interest are the low-velocity channels found in the area of the Danubian lowland and in the Bohemian Massif, which can be observed at depths of about 10–20 km. According to some geological information from the Bohemian Massif they can be explained as a manifestation of partial anatexis.

Remarkable is the unusually complicated course of the iso-velocity lines at the eastern border of the Moldanubicum. In the deep structure (about 20 km) complexes characterized by higher velocities lie on those with lower velocities and they seem to be thrust over the latter. In this region, the existence of horizontal overthrust has been discussed for several decades. The found picture is similar to the velocity sections in the western Alps (Ivrea zone) [GIESE, MORELLI, STEINMETZ 1971], where regional horizontal overthrusts are unquestionable. Seismic exploration has thus provided a relevant argument for the existence of regional horizontal overthrusts in the Variscan or older orogeny on our territory.

In the course of the profile VI inexpressive mountain "roots" can be observed in the region of the Krušné hory Mts., where also prominent negative gravity anomalies were established, and in the area of the Vienna Basin below the Outer Carpathians. Here, the "roots" are less pronounced than in other sections across the Carpathian Arch.

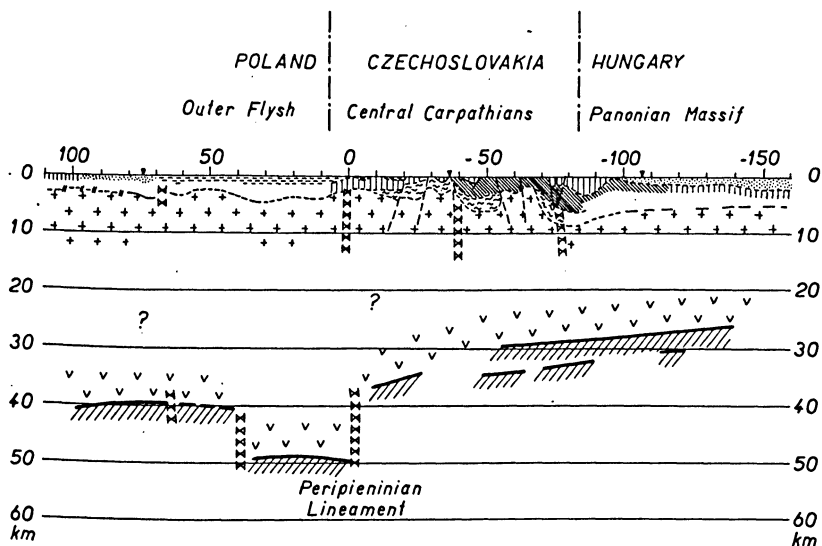


Fig. 4: Results of deep seismic sounding on the profile V. For explanations see Fig. 3.

1.2 Profile V

In this profile (Fig. 4), the study of which has not yet been completed, the greatest depths were found in the area of the Outer Flysch belt (Earth's crust thickness = 50 km). In this profile, an important fault was established at the boundary between the Outer and the Central Carpathians with a jump of about 15 km (Peripieninian lineament). It seems that the Central Carpathians form a block with the Pannonian Massif, where the thickness of the Earth's crust is relatively small. At the northern border of the Central Carpathians, however, there can be observed an increased thickness, which amounts to 36 km; farther southward it decreases to about 27 km.

An interesting result is the location of two boundaries of the M-discontinuity in the area of the Central Carpathians and the Pannonian Massif. One of them can attest to an old, the other to a newly forming boundary between the Upper Mantle and the crust according to SOLLOGUB's theory [1971].

1.3 Profile VII

Of importance for the Bohemian Massif is also the profile VII, which has not yet been measured uniformly over the whole extent (Fig. 5). The greatest thickness of the crust in the Massif (about 42 km) was found in the SSW part of the section. Towards the north, at the intersection with the profile VI, the crust decreases slowly to 38 km. The smallest thickness was found in the area of the Czech Cretaceous

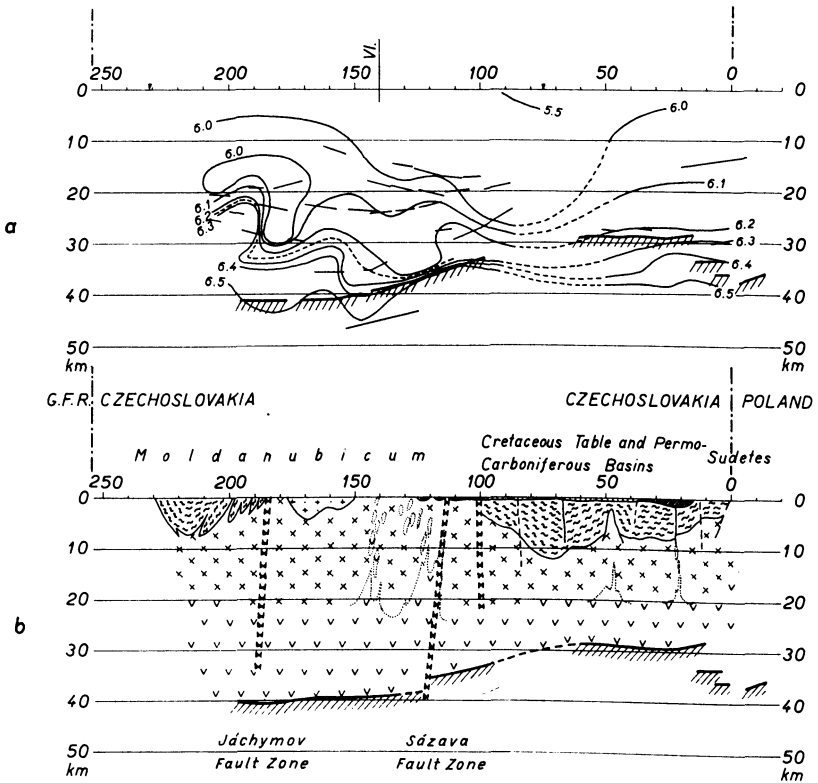


Fig. 5: Results of deep seismic sounding on the profile VII. For explanations see Fig. 3.

Basin—28 km. In the area of the Sudetes, a stepwise increasing of the crust thickness can be followed so that under the Krkonoše Mts. the depth of the M-discontinuity amounts to about 36 km. In the mean velocity section, a velocity decrease in the area of the Czech Cretaceous Basin is apparent. A number of geophysical effects make it possible to determine deep reaching Jáchymov and Sázava fault zones. From the course of mean velocities and from a large depression of iso-velocity lines in the Cretaceous, we can infer not only the presence of the Cretaceous and the Permo-Carboniferous sediments, but also the existence of thick complexes of Late Paleozoic, Proterozoic and crystalline schists.

Simultaneously with the measurements in Czechoslovakia, the Bavarian part of the profile was measured. Preliminary results enable us to state that the thickness of the crust decreases towards the south to about 35 km on the boundary between the Moldanubicum and molasse. Measurements in the profile VII make it possible to correlate the results from southeastern Europe and the Alps.

2. Qualitative comparison with results of gravimetry and magnetometry

Comparing the regional course of gravity anomalies with the course of the M-discontinuity we can see, in rough features, that the major negative anomalies correspond to the increased thickness of the Earth's crust and, conversely, that the positive regional anomalies correspond to the decreased Earth's crust thickness. This indicates a certain isostatic balance of the blocks in the Bohemian Massif and in the Carpathians as well. A comparison of regional gravimetry with the results of deep seismic sounding is given in the map of residual deflections of the vertical, compiled by BURŠA [1970]. The depression of the M-discontinuity is reflected in the map by the directions of deflections, which run from the area of the greatest thickness of the crust to the areas where the M-discontinuity ascends nearer to the surface. In the profile VI it is thus possible to indicate the depressions in the area of the Krušné hory Mts., in the Moldanubicum, etc. In the profile V, a gradual decrease of crust thickness in the north-southern direction is remarkable. Analogically in the profile VII, the vectors point out the greatest thickness of the crust in the area of southern Bohemia (Fig. 9).

Positive magnetic anomalies may indicate zones with basic masses nearer to the surface. The intrusion of basic masses along certain fault zones should be manifested by linear arrangement of positive magnetic anomalies. Fig. 6 shows the regions with regional magnetic anomalies and deep fault zones which were established by means

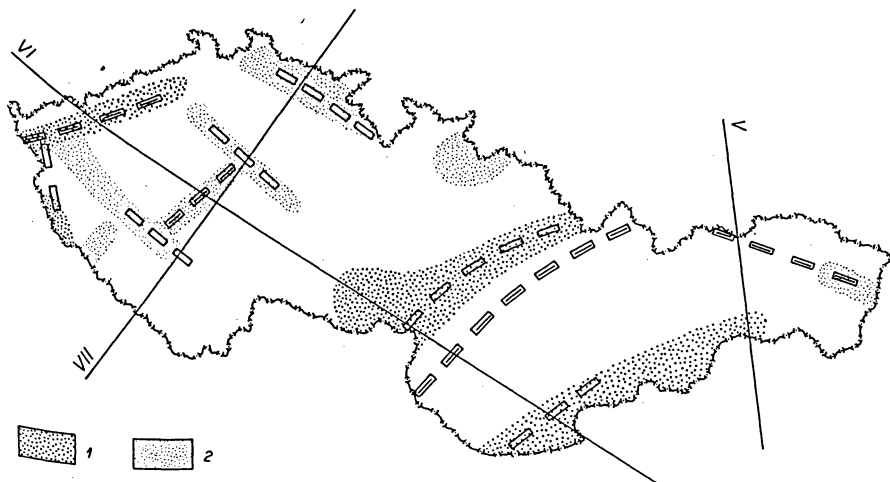


Fig. 6: Selected magnetic anomalies which correlate with the deep fault zones discovered by deep seismic sounding. 1=regional magnetic anomalies, 2=local magnetic anomalies.

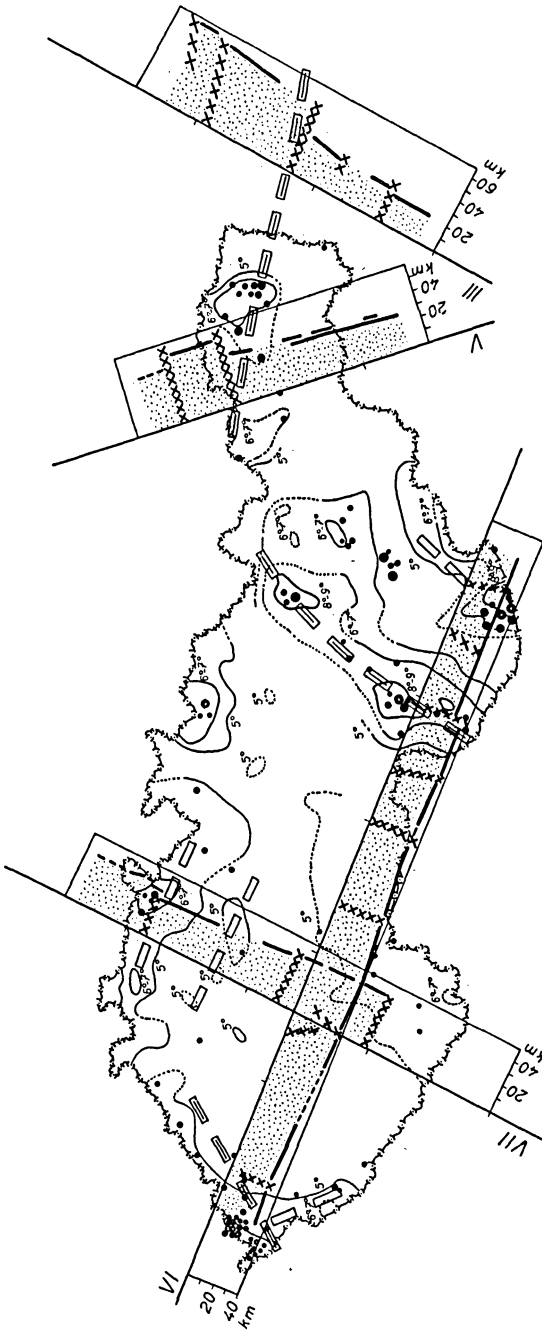


Fig. 7: Correlation of deep fault zones detected by deep seismic sounding with zones of maximal earthquake intensities and macro-seismic earthquake foci (according to V. KÁRNÍK 1959) on the Czechoslovak territory. The deep fault zones are in projection in the profiles II, V, VI and VII.

of deep seismic sounding. A good coincidence in the area of the Krušné hory, Central Bohemia, Lednice, Lužnice and Jáchymov fault zones and in the region of Komárno can be observed. In eastern Slovakia, the Peripieninian lineament is marked by a magnetic anomaly only in its eastern part. In the magnetic picture it is possible to follow also the Labe line and the fault system of Mariánské Lázně.

3. Comparison with results of earthquake activity observations

The deep zones found in the profiles V, VI and VII can be compared with the map of maximal intensities of earthquakes for the years 1851—1956 and of microseismic earthquake foci (Fig. 7). The zones of increased seismic activity can be found in the area of the Krušné hory Mts. and the Český les Mts., and also in the Sudeten; in Slovakia between the Outer and the Inner Carpathians, in the area of Central Slovakian neovolcanics and in the vicinity of Komárno. Two less important lines, namely the zones within the Bohemian Massif (probably the Labe line and the line running across the Central Moldanubian Massif) can be seen. Comparing these results with those obtained by deep seismic sounding, it is apparent that the live,

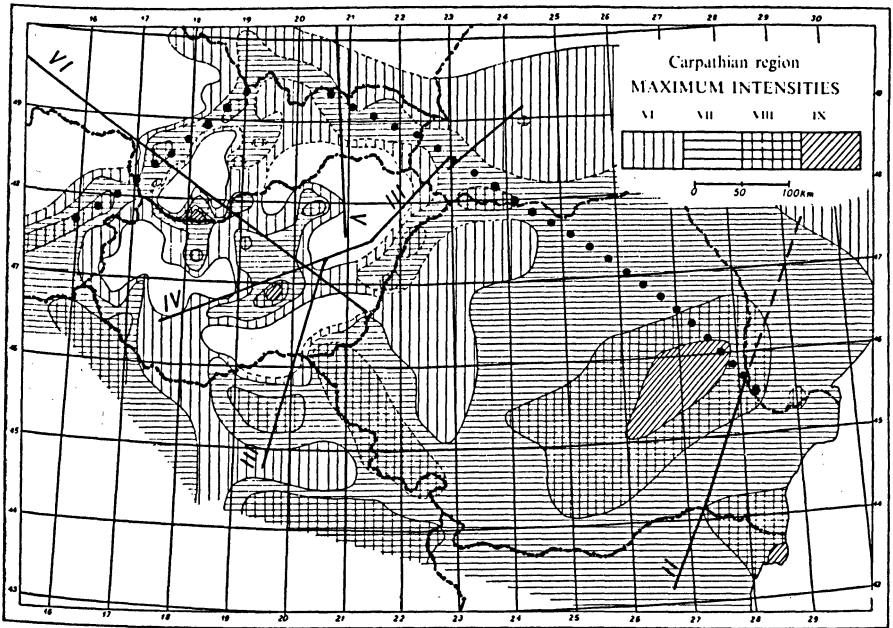


Fig. 8: Maximal earthquake intensities in the Carpathian region (according to V. KÁRNÍK and L. RUPRECHTOVÁ 1964) with the Peripieninian lineament.

seismically active zones can be correlated with the Krušné hory zone, the Lužice fault zone and perhaps with the Mariánské Lázně fault zone. The Labe lineament has not been confirmed by seismic methods as yet, because measurements in that area have not yet been concluded. In Slovakia, the earthquake seismic zones manifest themselves most markedly in the area of the so-called Peripieninian lineament (i. e. in the area of the Klippen belt).

Comparing further the map of maximal earthquake intensities (compiled by KÁRNÍK, RUPRECHTOVÁ [1964]) in the Carpathian area we can see that the structure of the Peripieninian lineament originated really by interaction of two lineaments of NE and WNW directions as presumed by MÁŠKA, ZOUBEK [1960]. The continuation of the Peripieninian lineament, which separates the Central and the Outer Carpathians, is observed in the U.S.S.R. in the profile III and in Romania in the profile II (Fig. 8). In the west, this deep-seated fault zone continues to the southwest into the Alps, where it runs probably below the border of Upper Austro-Alpine and Lower Austro-Alpine units and farther along the valley of the river Mur.

4. Structural scheme of the M-discontinuity

Using the map of the horizontal component of residual deflections of the vertical, the results obtained in three international profiles make it possible to compile a preliminary map of the course of the M-discontinuity in our territory. Fig. 9 shows a deep submersion of the crust in the area of the Moldanubicum and a small

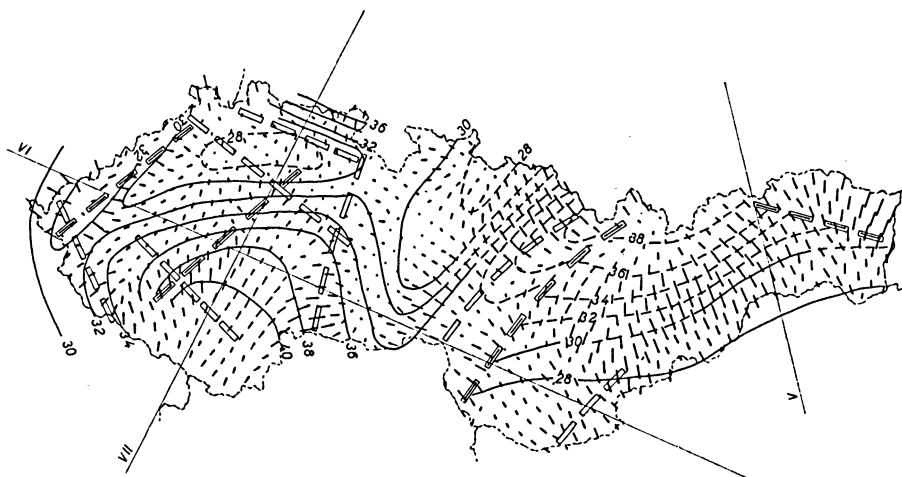


Fig. 9: Structural scheme of the M-discontinuity with deep fault zones confirmed by deep seismic sounding in the Czechoslovak territory. Arrows represent the horizontal component of the residual deflection of the vertical (according to M. BURŠA 1970).

depression of the M-discontinuity in the area of the Krušné hory Mts. In the western part, the measurements were tied to the results obtained in the Alpine area. The Cretaceous Basin, the eastern edge of Moldanubicum and the Nízky Jeseník Mts. manifest themselves by a decreased crust thickness. In the sketch, there is a remarkable increase of the thickness of the crust under the Outer Flysch zone of the Carpathian Arch; the Central Carpathians and the Pannonian Massif manifest themselves as homogeneous blocks, where the thickness decreases in the N-S direction. The results in the southern part were correlated with those obtained in Hungary.

The sketch in Fig. 9 is preliminary and gives only the first ideas of the course of M-discontinuity in the territory of Czechoslovakia. Recently, a new geophysical project has been started, the result of which will help us to acquire a new picture of the Earth's crust structure.

References

- BERÁNEK, B., M. ZOUNKOVÁ, and K. HOLUB: Results of deep seismic sounding in Czechoslovakia. — U.M.P. Czechoslovakia 1962–1970, Final Report, Prague, 94–115, 1971
- BURŠA, M.: On the correlation between deflections of the vertical and axes of zones of increased macroseismic mobility. — *Studia geoph. et geod.* 14, 1970
- DUDEK, A., and M. SUK: The deep relief of the granitoid plutons of the Moldanubicum. — *N. Jhb. Geol. Pal., Abh.* 123, 1–19, 1965
- GIESE, P., C. MORELLI, and L. STEINMETZ: Crustal structure of Western and Southern Europe. — Report I.U.G.G. General Assembly, Moscow, 1971
- IBRMAJER, J.: Gravimetrická mapa ČSSR 1:1000000, Praha, 1966
- KÁRNÍK, V.: Neue seismische Karten der Tschechoslowakei. — *Geofys. sborník* 1958, No. 88, 233–257, 1959
- KÁRNÍK, V., and L. RUPRECHTOVÁ: Seismicity of the Carpathian region. — *Geofys. sborník* 1963, No. 182, 143–187, 1964
- MAN, O.: Aeromagnetic map of Czechoslovakia 1:1000000, Praha, 1968
- MÁŠKA, M.: The main features of the structure and the development of the Czech Massif. In: *Tectonic development of Czechoslovakia*, Praha, 1960
- MÁŠN, J.: The regional aeromagnetic anomalies in Czechoslovakia. — *Věstník Ústř. úst. geol.* 41, 55–57, 1966
- RÖHLICH, P., and N. ŠŤOVÍČOVÁ: Die Tiefenstörungstektonik und deren Entwicklung im zentralen Teil der Böhmschen Masse. — *Geologie* 17, 670–694, 1968
- SOLLOGUB, V. B., D. PROSEN, and H. MILLITZER: Crustal structure of Central and South-Eastern Europe by the data of explosion seismology, Kiev, 1971

On the Amplitude Curves of Body Waves for Short Epicentral Distances and Their Oscillatory Character

L. CHRISTOSKOV, Sofia¹⁾

Eingegangen am 14. März 1972

Summary: The problem of the construction of the amplitude curves for the Balkan region and Japan at epicentral distances up to 20–25° is considered. The probable reasons are discussed for the oscillatory character of the amplitude curves at short epicentral distances. The variations in the shape of the amplitude curves are connected with the change of the velocity gradient of body waves in the Earth's interior. On the basis of the amplitude-distance curves an attempt is made to construct a probable scheme of the upper mantle structure for the Balkan region and Japan.

Zusammenfassung: Es werden Fragen der Konstruktion von Amplitudenkurven bis zu Epizentralentfernungen von 20–25° im Bereich des Balkans und in Japan behandelt. Weiter werden die wahrscheinlichen Ursachen des oszillatorischen Charakters von Amplitudenkurven für kleine Epizentralentfernungen diskutiert. Die Form der Amplitudenkurven ist mit der Veränderung des Geschwindigkeitsgradienten für die Raumwellen in Abhängigkeit von der Tiefe verbunden. Auf der Basis der Amplitudenkurven für Raumwellen wurde versucht, die wahrscheinliche Struktur des oberen Mantels für den Balkan und Japan aufzuzeichnen.

1. Introduction

At present the investigation into seismic wave amplitudes at short epicentral distances is of great practical importance. The normalized amplitude-distance curve is the basis for the local magnitude scales as well as for studying the attenuation of the body waves in the Earth's crust and the upper mantle. There is no doubt that the amplitude-distance curves of body waves contain also a very important information about the media in which the waves are propagated. It can be stated that the real shape of the amplitude-distance curve is approximately a transformed "representation" of the medium structure. In fact, the amplitude curves at short epicentral distances are used by different authors to determine and specify the structure of the Earth's crust and mantle (VANĚK 1968; ALEKSEEV, NERSESOV 1966; ASBEL, KEILISBOROK, YANOVSKAYA 1966; GOLIKOVA 1966).

The construction of an amplitude curve, particularly that for short epicentral distances, is usually accompanied with some difficulties connected with the deter-

¹⁾ Dr. LUDMIL CHRISTOSKOV, Institut po Geofizika BAN, Moskovska 6, Sofia, Bulgaria.

mination of the station corrections and the normalization of the curve itself [CHRISTOSKOV 1967, CHRISTOSKOV 1970]. The definition of the normalized amplitude curve $A^*(\Delta)$ follows from the basic magnitude equation:

$$M = \log\left(\frac{A}{T}\right)_k + \sigma_k(\Delta) + \delta M_s^k \quad (1)$$

where: A/T is the maximum ground velocity amplitude at a certain epicentral distance Δ (the amplitude A is given in microns and the corresponding period T in seconds); $\sigma(\Delta)$ is the calibrating function; δM_s is the station correction and k indicates the type of the wave group used for the determination the magnitude M . Obviously, the maximum velocity amplitude depends on the magnitude M as well as on the epicentral distance Δ . Using M as a normalizing quantity the amplitude curve is defined as a function of Δ :

$$A_k^*(\Delta) = \log\left(\frac{A}{T}\right)_k + \delta M_s^k - M \quad (2)$$

2. On the nature of the oscillatory character of the amplitude curves

It is typical of the earlier investigations of the amplitude-distance curves that they study only the general character of the amplitude curve without considering the oscillatory behaviour and the fine structure of these curve. After the improvement of the observation and normalization methods it was possible to discover the detailed structure and the oscillatory character of the amplitude curves [VANĚK, STELZNER 1960]. It is a very important fact because only in this case could the amplitude curve be accepted and used as an indicator for the structure of the media. The detailed investigations corroborated the fine structure and the oscillatory character of the amplitude curves for short epicentral distances [VANĚK, RADU 1964; ALEKSEEV, NERSESOV 1966; CHRISTOSKOV 1967]. Moreover, it was pointed out that this behaviour of the amplitude curve was due to the peculiarity and complexity of the media and to this effect the amplitude data could be very useful for the correct interpretation of the seismic discontinuities in the crust and the mantle.

It was found [ASBEL et al. 1966, GOLIKOVA 1966] that the amplitude-distance curves $A^*(\Delta)$ are roughly similar to the velocity gradient curves $g(r)$:

$$g(r) = -rd[v(r)/r]/dr \quad (3)$$

The function $g(r)$ for the sphere is analogous to the vertical velocity gradient dv/dh for half-space. Besides, each peculiarity in the behaviour of the gradient curve $g(r)$ at some interval of depths corresponds to the similar behaviour of the amplitude curve within a certain epicentral distance interval. If the function $g(r)$ is increased

or decreased a similar alteration is observed for the amplitude curve $A^*(\Delta)$. This correspondence is an important circumstance which elucidates to a certain extent the oscillatory character of the amplitude-distance curves.

For the multilayered media the sequence of the variations in the shape of the amplitude curve $A^*(\Delta)$ with the epicentral distance does not always correspond to the consequent variations in the velocity gradient with the depth, i. e. to the real consequence of the interfaces under the Earth's surface. This is due to the complicated character of the dependance between the shape of the amplitude curve and the depth on which the change in the gradient exists and the magnitude of the gradient before and after this change.

Let us denote the depth at which the change in the velocity gradient appears or an interface exists with h_m , and the corresponding epicentral distance at which the respective effect in the shape of amplitude curve is observed with Δ_m . The limits for h_m are defined as follows [ASBEL et al. 1966]:

$$h(\Delta_m - \delta_1) \leq h_m \leq h(\Delta_m) \quad (4)$$

when at $h=h_m$ the velocity gradient decreases and at $\Delta=\Delta_m$ respectively a "minimum" on the amplitude curve is observed, and

$$h(\Delta_m + \delta_2) \geq h_m \geq h(\Delta_m - \delta_3) \quad (5)$$

when at $h=h_m$ the velocity gradient increases and a "maximum" appears on the amplitude curve at $\Delta=\Delta_m$. For the upper mantle it was found that $\delta_1=4^\circ$ and $\delta_2=\delta_3=2^\circ$ [ASBEL et al. 1966].

From formulae (4) and (5) it follows that Δ_m characterizes the cross-section of the media non-uniquely i. e. the bottom of the ray path h_m could be determined in a very inaccurate manner in multilayered media.

Additional complications arise in the shape of the amplitude curves because it is impossible in practice to make an absolutely correct identification of the wave groups at different epicentral distances. The frequent change of seismic waves especially at the short distances presents serious problems in the correlation of the identical arrivals at different stations and at the different distances [ALEKSEEV, NERSESOV 1966].

It seems, however, that one fact is indisputable: the most remarkable variations and oscillations in the shape of the amplitude-distance curve are connected with the velocity distribution with the depth and the structure of the media. This conclusion is corroborated by the results obtained in the seismic modelling on both two-dimensional [RIZNICHENKO, SHAMINA 1964, SHAMINA 1966] and three-dimensional models [WANIEK 1966, VANĚK 1966]. These investigations are of practical importance because the applicability of the theoretical investigations to inhomogeneous media is limited.

3. Amplitude curves for the regions of Balkan and Japan

According to the definition (see eq. (2)) given above, the amplitude curves of body waves were constructed by the author for the Balkan region [CHRISTOSKOV 1967, CHRISTOSKOV 1969] and for Japan and her vicinity¹⁾. The main purpose of these investigations was to improve the accuracy of the magnitude determinations at the short epicentral distance for both regions.

The earthquake magnitudes used in these studies as a normalizing quantity in equation (2) were determined using the Central European network into which the central station Sofia was included during 1964. In the both cases the construction of the amplitude curves is based on the readings from the records of the mechanical WIECHERT's seismographs.

¹⁾ In collaboration with Dr. M. ICHIKAWA from J. M. A., Tokyo.

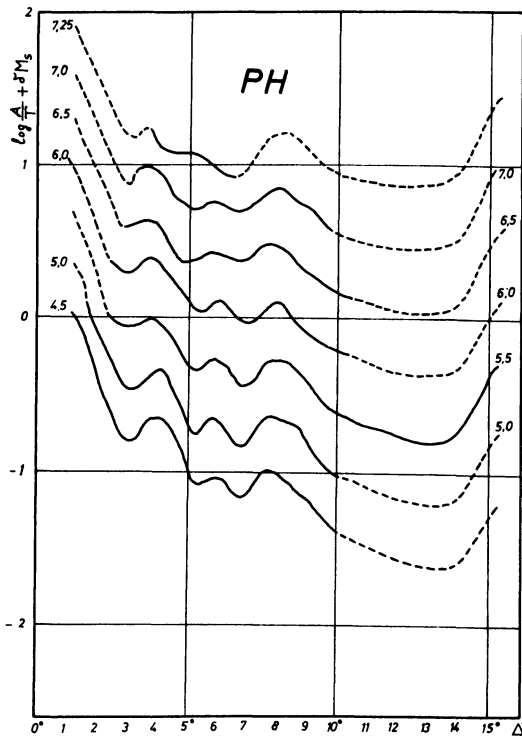


Fig. 1: Amplitude-distance curve $A^*_{PH}(\Delta)$ of PH wave for different energy levels (the number of each curve corresponds to the mean magnitude of the earthquakes used).

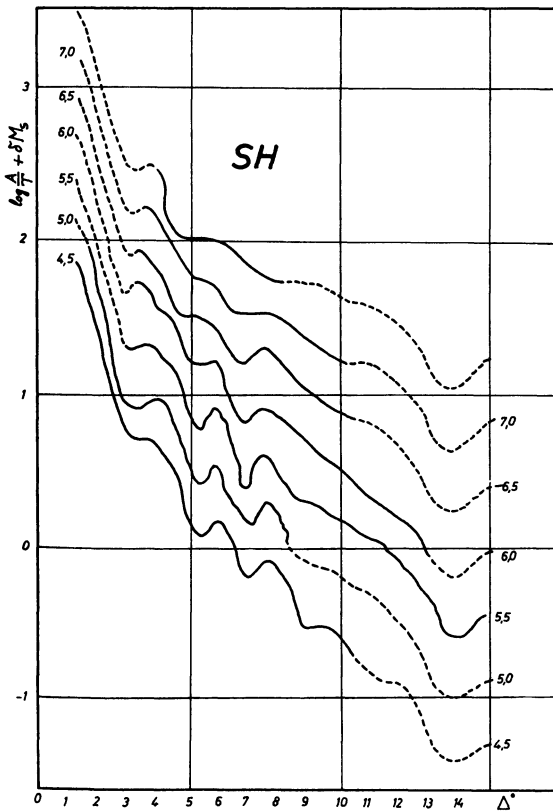


Fig. 2: Amplitude-distance curve $A^*_{SH}(\Delta)$ of SH wave for different energy level (the number of each curve corresponds to the mean magnitude of the earthquakes used).

For the Balkan region the records of more than 300 shallow earthquakes at the station Sofia were used for obtaining the amplitude curves $A_{PH}(\Delta)$ and $A_{SH}(\Delta)$ for PH and SH waves and over 150 earthquakes for the amplitude curves $A_{PgH}(\Delta)$, $A_{PbH}(\Delta)$, $A_{SgH}(\Delta)$ and $A_{SbH}(\Delta)$ of PgH, PbH, SgH and SbH waves respectively. The complicated shape and the oscillatory nature of these curves can be seen in Fig. 1, Fig. 2 and Fig. 3. The amplitude curves for PH and SH waves are evidently dependent on the magnitude of the earthquakes. The numbers given for each curve in Fig. 1 and Fig. 2 correspond to the mean value of the magnitude for these earthquakes whose records are used for deriving the respective amplitude curve. The "mean" amplitude curves for PH and SH waves are given in Fig. 3, and they are constructed from all the data without dividing them into groups according to the magnitude of

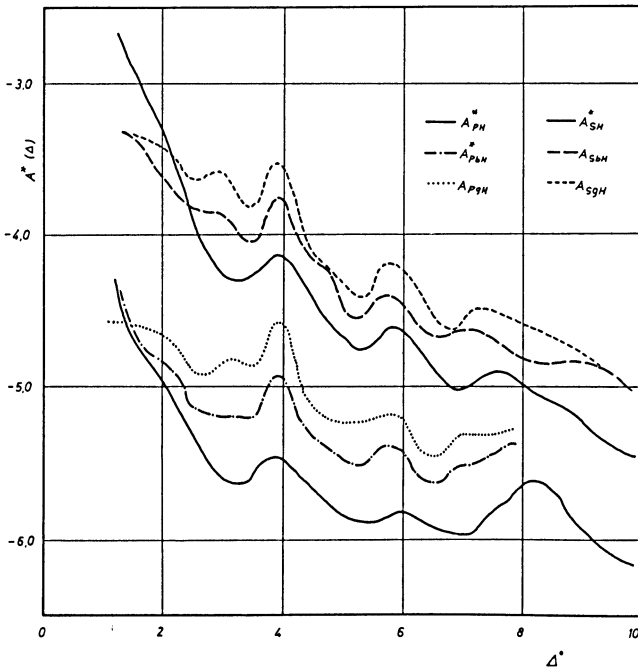


Fig. 3: Comparison of the amplitude curves $A^*_{PgH}(\Delta)$, $A^*_{PbH}(\Delta)$, $A^*_{SgH}(\Delta)$ and $A^*_{SbH}(\Delta)$ with the mean amplitude curves $A^*_{PH}(\Delta)$ and $A^*_{SH}(\Delta)$.

the earthquakes. It appeared that the amplitude curves derived for $M=4.5, 5.0, \dots, >7.25$ are similar to each other. They have the same shape and common oscillatory character. The most important fact is that the alternation of all the observed maxima and minima coincides for the amplitude curves $A_{PH}(\Delta)$ and $A_{SH}(\Delta)$ within a certain epicentral distance interval. Moreover, the typical extremes of $A_{PH}(\Delta)$ and $A_{SH}(\Delta)$ are in good correlation with the respective maxima and minima characteristic of the other amplitude curves given in Fig. 3. This circumstance indicates that the generally accepted mechanism of propagation for Pg, Pb, Sg and Sb waves is not very correct and probably the observed oscillatory character of their amplitude curves is a result of the interferential nature of these waves.

In table 1 are given the summarized results for the alternating maxima and minima of the amplitude curves for the Balkan region. The maxima and minima for the different amplitude curves appear within a certain epicentral distance interval whose average value is indicated as the mean epicentral distance.

The amplitude-distance curves for Japan and her vicinity were constructed from the data of 220 earthquakes recorded at 9 selected seismic stations: Nemuro, Sapporo,

Table 1: Maxima and minima of amplitude curves for Balkan region (maxima and minima are denoted by the signs plus (+) and minus (-) respectively).

type of extremum	mean distance Δ°	type of extremum	mean distance Δ°
-	3,1	-	6,8
+	3,8	+	8,0
-	5,3	-	12,5
+	5,9	+	15,8

Morioka, Tokyo, Nagano, Matsushiro, Kyoto, Abuyama and Miyazaki. They are situated on an almost straight line which is directed approximately from north-east to south-west direction. The station corrections are performed with respect to the Middle European network and station Sofia. The large set of initial data (50 to 80 points for one degree distance interval) were processed by means of a digital electronic computer, which gives more precise and independent results.

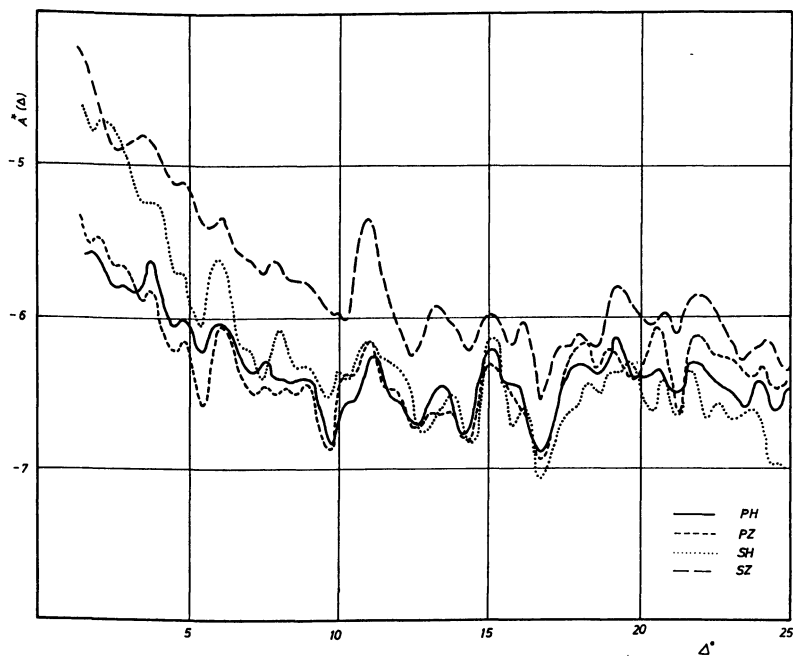


Fig. 4: Amplitude-distance curves $A^*(\Delta)$ of PH, PZ, SH and SZ waves for Japan and her vicinity.

Table 2: Maxima and minima of amplitude curves for Japan (maxima and minima are denoted by the signs plus (+) and minus (-) respectively).

type of extremum	mean distance Δ°	type of extremum	mean distance Δ°
-	3,3	-	14,3
+	3,8	+	15,1
-	5,4	-	16,7
+	6,1	+	18,2
-	7,1	-	18,6
+	7,7	+	19,4
-	9,7	-	20,0
+	11,3	+	20,6
-	12,6	-	21,3
+	13,4	+	21,7

The amplitude-distance curves of PH, PZ, SH and SZ waves for distances up to 25° are shown in Fig. 4. As it is apparent, an oscillatory character with alternation maxima and minima is typical for these amplitude curves as it was already established for the amplitude curves in south-eastern Europe. The position of the maxima and minima for P-waves is in good agreement with the extreme position of S-waves. This coincidence suggests that the properties and the characteristic peculiarities in the medium structure form the general shape of the amplitude curves. An important fact is that the amplitudes of the oscillations exceed considerably the level of the mean standard errors in the amplitude curves. A generalization in the situation of maxima and minima of the amplitude curves shown in Fig. 4 is given in Table 2.

4. Amplitude curves and the probable structure of the upper mantle

The comparison of the data from Table 1 and Table 2 shows a rough coincidence in the position of the maxima and minima for the Balkan region and Japan, especially at distances less than 10° . This coincidence points to a similarity in the structure of the medium immediately below the M-discontinuity in both regions.

From the correlation between the variations in the gradient curve $g(r)$ and the amplitude curve $A^*(\Delta)$ it is possible to determine the probable number of the interfaces in the mantle. According to the formulae (4) and (5) the bottom of the ray path h_m could be estimated with a considerable error. On the amplitude curves shown in Fig. 1—Fig. 4 an alternation of several maxima is observed through epicentral distance intervals of about 2° (see also Table 1 and Table 2). The length of these intervals is commensurate with the value of δ_2 and δ_3 in formula (5). This fact allows us to suppose that in our case the sequence of the probable discontinuities below the surface may correspond to the alternation of the maxima of the amplitude-distance curves, i. e. the epicentral distance Δ_m at which a certain maximum is observed may

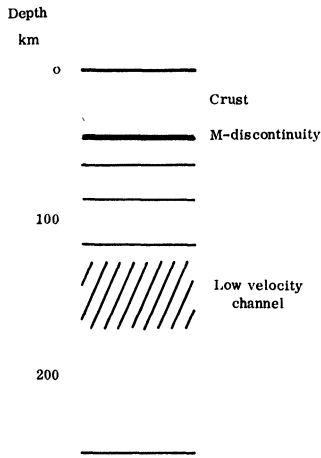


Fig. 5: Probable scheme of the upper mantle structure for the Balkan region.

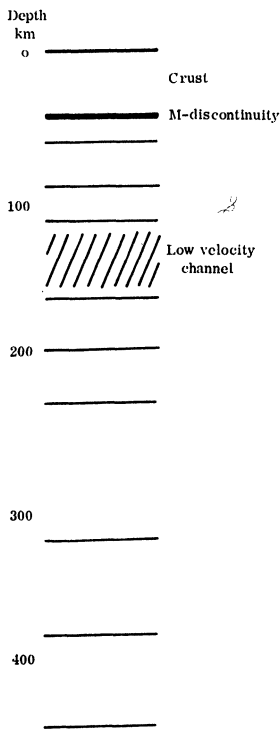


Fig. 6: Probable scheme of the upper mantle structure for Japan and her vicinity.

be used for a rough estimation of the depth h_m at which the change of the velocity gradient exists. Thus, an attempt was made to derive the probable structure of the upper mantle for the Balkan region and Japan from the amplitude-distance curves. Fig. 5 and Fig. 6 give one schematic version of the upper mantle structure for the Balkan region and Japan respectively. The indicated horizontal lines may be considered only as a possible and not as an accurate determined location of the real interfaces below the M-discontinuity. In this sense the scale of the depth has to be adopted as an orientation scale which gives an idea about the sequence of the interfaces in the depth.

The scheme shown in Fig. 5 is similar to the scheme of the upper mantle structure derived by VANĚK [1968] on the basis of the amplitude curves for south-eastern Europe.

Both schemes presented in Fig. 5 and Fig. 6 give only a preliminary idea of the probable structure for the Balkan region and Japan. Their reliability must be checked in the some more accurate studies when a joint interpretation of the travel-time curves and the amplitude-distance curves is realised.

References

- ALEKSEEV, A. S., and I. L. NERSESOV: Travel-times and amplitudes of waves in Central Asia—theory and experiments. *Studia geoph. et geod.*, 10, 172–176, 1966
- ASBEL, I. YA., V. I. KEILIS-BOROK, and T. B. YANOVSKAYA: A technique of a joint interpretation of travel-time and amplitude-distance curves in the upper mantle studies. *Geoph. J.* 11, 25–55, 1966
- CHRISTOSKOV, L.: Calibrating functions for PH- and SH-waves at epicentral distances up to 21° (in Bulgarian). *Bull. Geophys. Inst. Bulg. Acad. Sci.* 10, 85–98, 1967
- CHRISTOSKOV, L.: On the standardization of magnitude determinations of small epicentral distances. *Bull. I. I. S. E. E.* 6, 1–10, 1969
- CHRISTOSKOV, L.: Construction of amplitude curves and determination of station correction for a seismic network located in the epicentral area. *Bull. Earthquake Res. Inst.* 68, 19–28, 1970
- GOLIKOVA, G. B.: Some problems of using the dynamic parameters of P-waves for the study of the velocity distribution in the upper mantle (in Russian). *Vychisl. Seism., Vypusk 2*, 46–55, 1966
- RIZNICHENKO, YU. V., and O. G. SHAMINA: A comparison of amplitude curves obtained on a wave-guide model of the mantle with seismic data. *Bull. (Izv.) Acad. Sci. USSR, Ser. Geophys.* No. 8, 1129–1141, 1964
- SHAMINA, O. G.: Experimental investigation of necessary and sufficient characteristics of a wave-guide. *Studia geoph. et geod.* 10, 341–350, 1966

- VANĚK, J., and J. STELZNER: Oscillatory character of amplitude curves of seismic body waves. *Nature*, 187, 491–492, 1960
- VANĚK, J., and C. RADU: Amplitude curves of seismic body waves at distances smaller than 12° . *Studia geoph. et geod.* 8, 319–325, 1964
- VANĚK, J.: Amplitude curves of longitudinal waves for several three-dimensional models of the upper mantle. *Studia geoph. et geod.* 10, 350–359, 1966
- VANĚK, J.: Amplitude curves of seismic body waves and the structure of the upper mantle in Europe. *Tectonophysics* 5 (3), 235–243, 1968
- WANIEK, L.: Fabrication and properties of three-dimensional seismic models of the upper mantle. *Studia geoph. et geod.* 10, 290–299, 1966

Recent Interpretation of the Core Discontinuities

L. RUPRECHTOVÁ, Prague¹⁾

Eingegangen am 12. Februar 1972

Summary: The development of hypotheses on the Earth's core structure is briefly summarized. The variation of amplitude ratios of the core waves with the epicentral distance is investigated and the observed data are compared with the relative amplitudes calculated for three models of the Earth's core structure.

Zusammenfassung: Die Entwicklung von Hypothesen über die Struktur des Erdkerns wird in Kürze zusammengefaßt. Die Variation der Amplitudenverhältnisse von Kernwellen in Abhängigkeit von der Epizentralentfernung wird untersucht. Die beobachteten Daten werden mit den relativen Amplitudenwerten verglichen, die aus drei Typen von Erdkernmodellen berechnet wurden.

1. Introduction

The existence of discontinuities in the Earth's deep interior has been supposed and verified in accordance with the information provided by seismic body waves. The travel times of the P waves travelling through the Earth's core are the primary data from which all the hypotheses on the core structure have proceeded.

In the process of improving devices of the seismological stations new groups of core waves have been detected on the records. Simultaneously, our knowledge about the Earth's core structure has become more detailed. The original GUTENBERG's notion [GUTENBERG 1914] about the fluid core surrounded by the solid mantle had to be changed after the discovery of the PKIKP wave [LEHMANN 1936]; a two-layered model consisting of the fluid outer core and the solid inner core with a transition layer above the inner core boundary became a classic one [JEFFREYS 1939; GUTENBERG et al. 1939].

New evidence involving changes of the core model has been accumulated since the forerunners of the PKIKP wave at distances of 120° to 140° were found on the records. Their travel-time curve may be prolonged to larger epicentral distances forming a new branch between PKIKP and PKP₂. The weak onsets observed at distances smaller than 140° were interpreted by GUTENBERG [1957; 1958] as waves dispersed within the transition layer between the outer and inner core where the velocity gradient increases discontinuously, the velocity itself remaining continuous.

¹⁾ Dr. LIBUŠE RUPRECHTOVÁ, Geofyzikální ústav ČSAV, Praha 4 – Spořilov, Boční II, ČSSR.

The postulate of a sharp discontinuity on the bottom of the outer core was supported when the waves reflected on this boundary were found on the records [CALOI 1961; BOLT et al. 1968; ENGDahl et al. 1970] and is respected by all recent models of the Earth's core. BOLT [1963, 1964] proposed a simple model of the core compatible with the whole set of available travel times observations. He supposes another discontinuous jump in the P velocity inside the core, 450 km above the inner core boundary. Having chosen a suitable velocity distribution BOLT succeeded to fit the early P arrivals preceding the PKIKP wave at distances smaller than 140° and the onsets occurring after PKIKP behind the caustic as well. Ever since the character of the transition zone between the outer and inner core has been discussed on the basis of BOLT's improved model of the core.

The selection of a model of the Earth's interior must be sure in conformity not only with the seismological observations, but also with other physical implications which must be respected. BULLEN [1969] analysed some proposed core models and suggested the possibility of changes in chemical composition and phase within the outer core. The possibility of choosing the model only pertaining the observational data is limited quite narrowly.

Dynamic properties of core waves have been also investigated in order to decide which model of velocity distribution in the core is more or less compatible with the observations. ERGIN [1967] attempted to corroborate his rather complicated model of core structure with the observed amplitudes. Theoretical amplitude-distance curves of the waves reflected and refracted on the discontinuities in two-, three- and four-layered core models were derived by ANTONOVA [1971]. YANOVSKAYA [1971] investigated the ratio of amplitudes PKIKP and PKHKP in the distance interval $145^\circ - 151^\circ$. Observed amplitudes and theoretical amplitude values of the waves refracted and reflected in the inner core are given in the recent paper of BUCHBINDER [1971].

2. Comparison of observed and theoretical core wave amplitudes

The records of the Czechoslovak stations Průhonice and Kašperské Hory were used for an attempt to investigate the energy distribution among the individual wave groups at distances behind the caustic. The earthquakes from the Tonga, Fiji, Samoa and New Hebrides epicentral regions recorded during the year 1966 yielded a fairly numerous set of data.

The amplitude ratio of three most outstanding phases on the record belonging to the core wave group was investigated to avoid the influence of different magnitudes and depths of individual shocks and the local parameters of the station which must be taken into account if the real values of amplitude are considered. The dependence of the amplitude ratios on the epicentral distance is shown in Fig. 1, 2 and 3 (amplitudes of the PKIKP, PKHKP and PKP₂ wave are denoted A_1 , A_2 and A_3 , resp.). The observed values are compared with the relative amplitudes calculated for two models of the core structure fitting best the observed travel times [RUPRECHTOVÁ

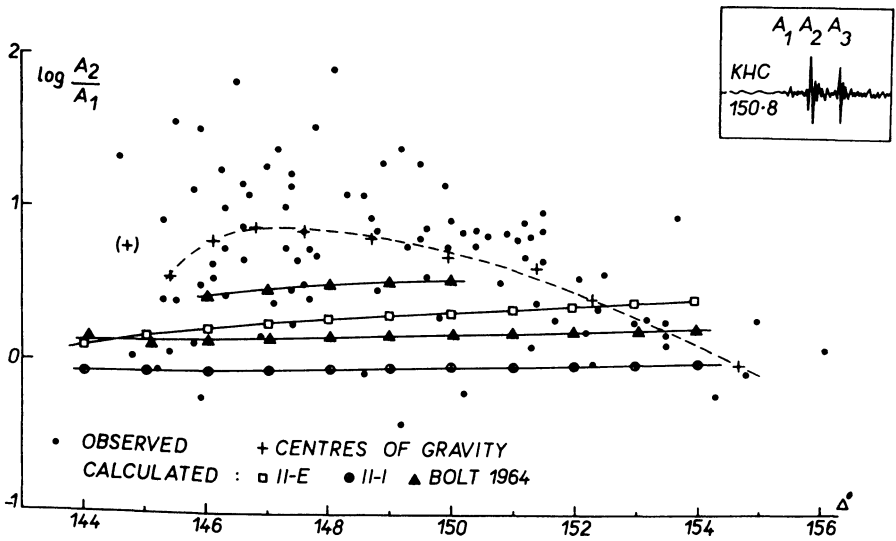


Fig. 1: Variation of the amplitude ratio PKHKP to PKIKP with the distance.

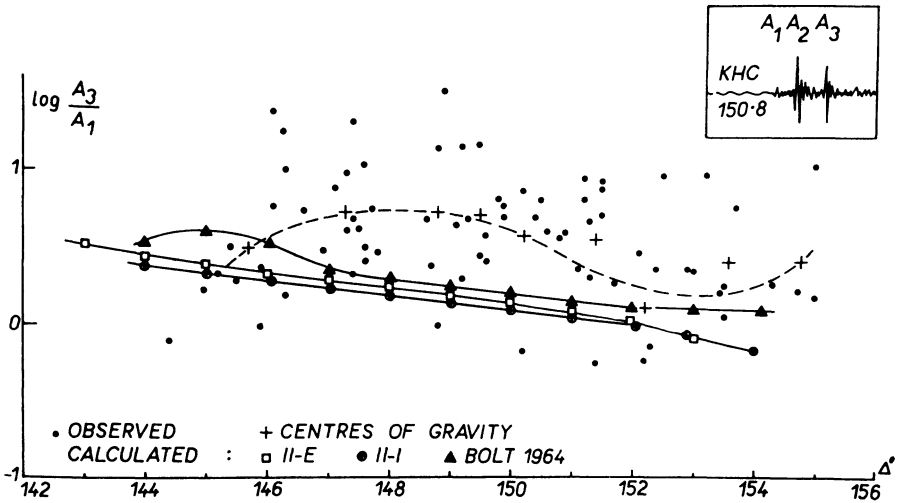


Fig. 2: Variation of the amplitude ratio PKP_2 to PKIKP with the distance.

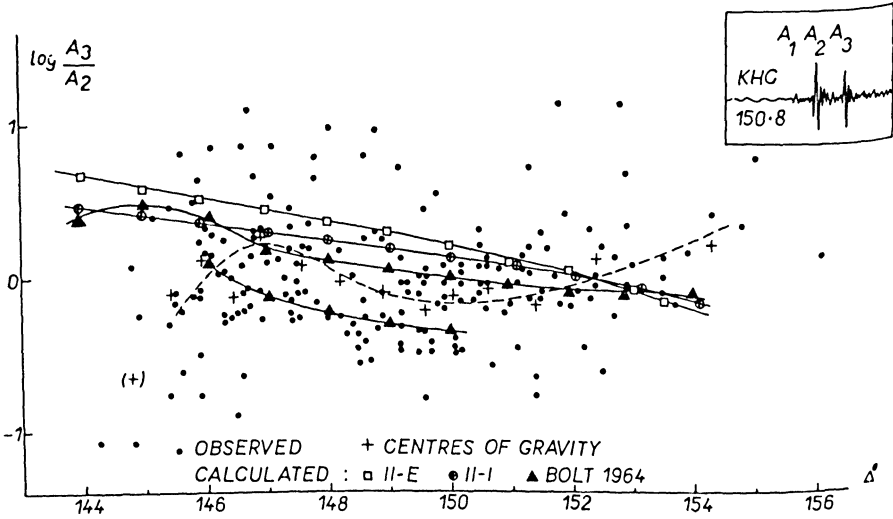


Fig. 3: Variation of the amplitude ratio PKP₂ to PKHKP with the distance.

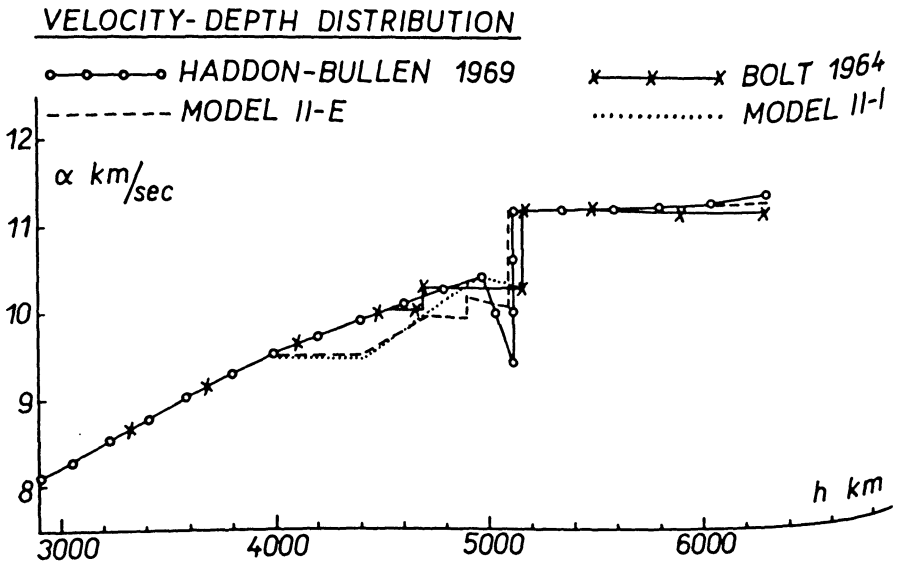


Fig. 4: Four models of the P velocity distribution in the Earth's core.

and KÁRNÍK 1971]. BOLT's model 1964 was also used for calculating the relative amplitudes. The velocity-depth function for all three models is shown in Fig. 4 together with one of the latest models of HADDON and BULLEN [1969]. It is evident from the graphs that the scatter was not removed by using the amplitude ratios. The influence of magnitude and focal depth, if any, was not systematic; it was then unnecessary to distribute the data according to these earthquake parameters. The whole set of $(A_i: A_j, \Delta)$ -values was represented by the centres of gravity. A certain trend may be observed to follow the theoretical curves (with the exception of the $A_2:A_1$ ratio), but from all three graphs it may be deduced that the energy of the second onset (PKHKP) from the core wave group is underestimated and the first one (PKIKP) is slightly overestimated.

3. Conclusions

In order to find an appropriate model of the core structure fitting the observed data concerning the travel times and amplitudes as well, it is necessary to obtain smaller PKIKP amplitudes beyond the caustic and larger amplitudes of the PKHKP wave, or to admit that two wave groups can overlap in the distance interval $146^\circ - 153^\circ$. It means that another branch must exist between the PKIKP and PKP₂ travel time curves near enough to the PKHKP that in the particular distance interval both waves cannot be separated and the energy is summarized. Such possibility is suggested by BOLT's model where the branch BC of the family of travel time curves is quite near and parallel to the PKHKP branch in the distance interval beyond the caustic to 151° . Summarizing the relative amplitude values of BOLT's BC and GH branch we obtain the section of the $(A_i: A_j, \Delta)$ -curve in the interval $146^\circ - 150^\circ$ (see Fig. 1 and 3) fitting well the observed data. It seems that BOLT's simple model of the core with two discontinuities is able to explain the main features of both core wave travel times and amplitudes.

4. Acknowledgements

I should like to thank Dr. J. JANSKÝ of the Geophysical Institute of the Charles University, Prague, for preparing the computer programme, and I. PŠENČEK for performing the computations.

References

- ANTONOVA, L. M.: On the depth distribution of seismic parameters in the transition zone between the outer and inner core. *Vychisl. seismol.* 5, 260–272, 1971 (in Russian)
- BOLT, B. A.: Gutenberg's Early PKP Observations. *Nature* 196, 122, 1962
- BOLT, B. A.: Velocity of Seismic Waves Near the Earth's Centre. *Bull. Seism. Soc. Am.* 54, 191–208, 1964

- BOLT, B. A., M.E. O'NEILL, and A. QAMAR: Seismic Waves Near 110°. *Geophys. J.* 16, 475–487, 1968
- BUCHBINDER, GOETZ G. R.: A Velocity Structure of the Earth's Core. *Bull. Seism. Soc. Am.* 61, 429–456, 1971
- BULLEN, K. E.: Compressibility – Pressure Gradient and the Constitution of the Earth's Outer Core. *Geophys. J.* 18, 73–79, 1969
- CALOI, P.: Seismic Waves from the Outer and Inner Core. *Geophys. J.* 4, 139–150, 1961
- ENGDAHL, E. R., and C.P. FELIX: Array Analysis of Core Phases (Abstract). *Trans. Am. Geophys. Union* 51, 4, 1970
- ERGIN, K.: Seismic Evidence for a New Layered Structure of the Core. *J. Geophys. Res.* 72, 3669–3689, 1967
- GUTENBERG, B.: Über Erdbebenwellen. *Nachr. Ges. Wiss. Göttingen*, 166–218, 1914
- GUTENBERG, B.: The "Boundary" of the Earth's Inner Core. *Trans. Am. Geophys. Union* 38, 750–753, 1957
- GUTENBERG, B.: Wave Velocities in the Earth's Core. *Bull. Seism. Soc. Am.* 48, 301–314, 1958
- GUTENBERG, B., and C.F. RICHTER: P' and the Earth's Core. *Monthly Notices Roy. Astron. Soc., Geophys. Suppl.* 4, 363–372, 1939
- HADDON, R. A. V., and K.E. BULLEN: An Earth Model Incorporating Free Earth Oscillation Data. *Phys. Earth Planet. Interiors* 2, 35–49, 1969
- JEFFREYS, H.: The Times of Core Waves. *Monthly Notices Roy. Astron. Soc., Geophys. Suppl.* 4, 548–561, 1939
- LEHMANN, I.: P'. *Publ. Bureau Central Intern. Séismol., Trav. Sci.* 14, 87–115, 1936
- RUPRECHTOVÁ, L., and V. KÁRNÍK: Core Waves Recorded in Central Europe. *Studia geoph. et geod.* 15, 299–315, 1971
- YANOVSKAYA, T. B.: Some properties of seismic waves in the Earth's core. *Vychisl. seismol.* 5, 272–282, 1971 (in Russian)

P-Wave Attenuation in the Mantle

M. A. CHOUDHURY, Paris¹⁾

Eingegangen am 20. März 1972

Summary: Relatively simple P-waves generated by earthquakes originating from a given region show overlapping spectra at frequencies between 0,4 and 1 Hz. Assuming that ground acceleration spectra at the source for such P-waves are flat within these frequencies, values of T/Q at 53°, 73° and 85° epicentral distances are found to lie around 1. An intermediate focus ($h=112$ km) earthquake at 95° does not show a larger value of T/Q as found elsewhere from long period differential attenuation data. For this shock, relative slopes of P, pP and PP suggest that most of the attenuation occurs in the upper mantle.

Zusammenfassung: Relativ einfache P-Wellen, die durch Erdbeben in einem bekannten Gebiet erzeugt werden, zeigen ein Überlappen der Spektren bei Frequenzen zwischen 0,4 und 1 Hz. Vorausgesetzt, daß an der Quelle die Boden-Beschleunigungs-Spektren solcher P-Wellen für diese Frequenzen flach sind, werden Werte von T/Q für 53°, 73° und 85° epizentraler Entfernungen bei ungefähr 1 gefunden. Ein Beben mit mittlerer Herdtiefe ($h=112$ km) bei 95° zeigt keinen größeren Wert für T/Q als anderswo von langperiodischen charakteristischen Dämpfungsdaten gefunden wurde. Für dieses Beben weist das Verhalten der spektralen Amplituden von P, pP und PP darauf hin, daß die größte Dämpfung im oberen Mantel stattfindet.

1. Introduction

Interpretation of seismic discontinuities are generally made in terms of changes in the velocity distribution $V(R)$ of elastic waves. The $V(R)$ distribution is known to show few discontinuous or almost discontinuous variations inside the Earth. Their natures are inferred from the form of $T(\Delta)$ curves and associated amplitudes. The amplitude parameter depends on the geometrical spreading of rays and the anelastic attenuation. In recent years attempts have been made to arrive at models revealing the attenuation properties ($Q(R)$ distribution) of the mantle.

Several $Q(R)$ models have been derived from free oscillation, surface wave and body wave data. These models show important differences. The differential attenuation method applied by TENG [1966] remains the main source of $Q(R)$ models for medium and long period P-waves. The method is identical to that used in deriving $V(R)$ by direct measurement of $dt/d\Delta$. Although the advantage of the method is that it eliminates the source effect when observing stations and the epicentre are aligned, the large scattering of measured differential attenuation [TENG 1966, and MIKUMO and

¹⁾ Dr. M. A. CHOUDHURY, Institut de Physique du Globe, Université Paris VI, France.

KURITA 1968] suggests however that the method is highly sensitive to factors on which sufficient control can not easily be exerted.

One could think of applying the less sensitive method in which a $\bar{Q}(\Delta)$ curve (identical to $T(\Delta)$ curves) would first be fitted (\bar{Q} is the mean value along the ray) from P-wave spectra of individual earthquakes recorded by a large number of stations. KURITA [1968] has used this method and has discussed the difficulties involved.

One could also use observations of different earthquakes at a single station eliminating thereby the inconveniences arising from differences in instrumental and crustal responses but in that case a similitude among different earthquakes, at least in a part of their spectra must be admitted. P-waves from earthquakes of magnitude around 6 or larger are in general complex. This, undoubtedly, is due to time and space dependence of faulting process. The history of this process depends on the magnitude of stress drop in the focal region. The source spectrum over a wide frequency range will, therefore, show significant differences, particularly at low frequencies. A complex P-wave may be considered as generated by a number of elementary dislocations each producing a simple P-wave. Records from wideband systems show that simple P-waves exist only for periods shorter than few seconds, suggesting that rupture propagation during each elementary dislocation is of short duration. If we assume that the rupture velocity is the same in all regions (a rough approximation), the onsets of P-waves from small and large earthquakes will have similar high frequency content which is a measure of the rise time of the onset. Provided that successive elementary dislocations are not too close together, the negative gradient of spectra will give a measure of attenuation. To evaluate quantitative values of attenuation it will be necessary to know the exact nature of the source spectrum.

2. Method

The method is briefly as follows: If we consider different transfer functions between the source and the record as linear filters, we can write the spectral components of the observed ground acceleration, $\ddot{A}(f)$, as

$$\ddot{A}(f) = \ddot{A}_0(f) \cdot \ddot{A}_M(f) \cdot \ddot{A}_C(f) \cdot \ddot{A}_I(f) \quad (1)$$

where the factors on the right hand side are the spectral components of the source and, the mantle, the crustal and the instrumental transfer functions respectively. In our recording system, the instrumental response is flat between 0.07 and 1 Hz. We have assumed the crustal response, $\ddot{A}_C(f)$, as constant. This is justified when the section of the seismogram analysed is not contaminated by reflexions inside the crust. Spectra within the frequency band 0.4–1 Hz have been obtained by analog filtering. This technique permits to isolate, in the case of complex shocks, a single wave down to a certain low frequency.

Taking the logarithm of (1) and differentiating with respect to frequency, f , and denoting d/df by a prime, we obtain,

$$\ddot{A}'(f)/\ddot{A}(f) = \ddot{A}'_0(f)/\ddot{A}_0(f) + \ddot{A}'_M(f)/\ddot{A}_M(f) \quad (2)$$

The quantity $\ddot{A}_M(f)$ can be separated into two terms corresponding one to a frequency independent geometrical spreading factor, G , and the other to a frequency dependant attenuation, $1/Q$.

$$\ddot{A}_M(f) = G \cdot \exp\left(-\pi f \int_{\text{ray}} \frac{ds}{Q(R)V(R)}\right) \quad (3)$$

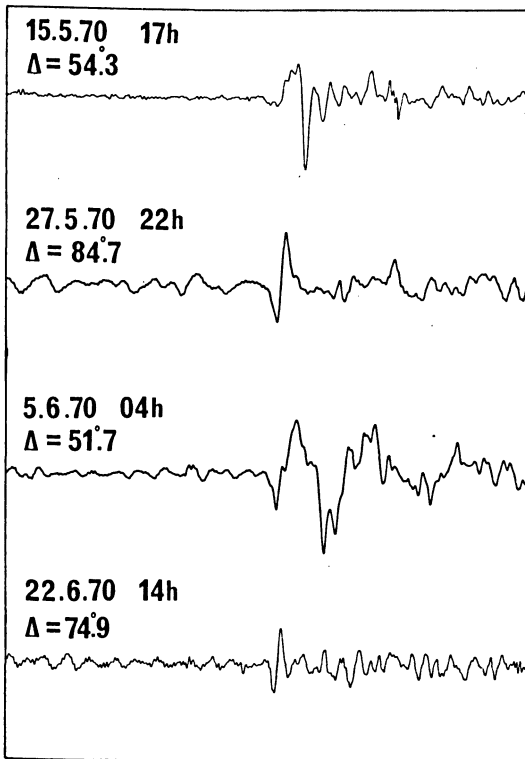


Fig. 1: Record sections showing the type of P-waves suitable for spectral slope determination.

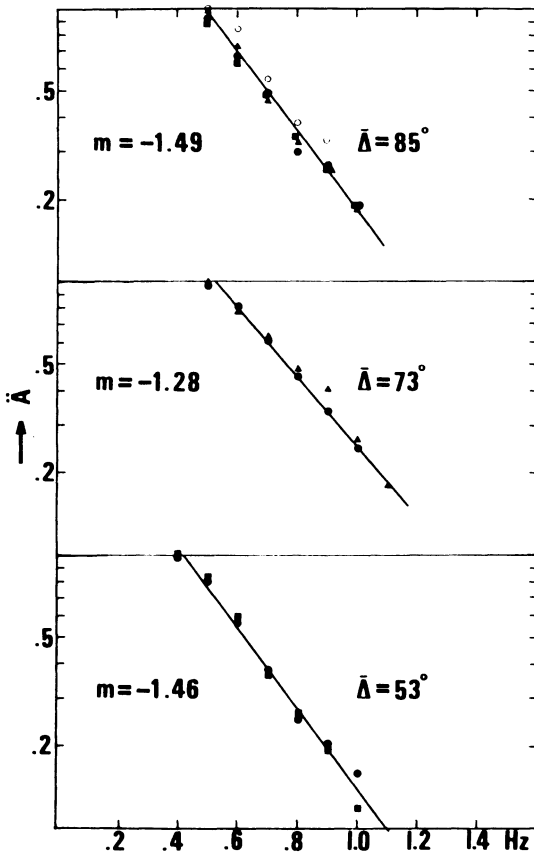


Fig. 2: Logarithmic plot of amplitude as a function of frequency at the mean distances of 53° , 73° and 85° . The slope, m , is indicated for each case. Open circles for $\Delta = 85^\circ$ correspond to the Amchitka nuclear explosion of Nov. 6, 1971.

where ds is a ray element, $V(R)$, the P- or S-wave velocity distribution and $Q(R)$, the quality factor distribution.

Replacing $\bar{A}_M(f)$ in (2) by its value in (3) we obtain,

$$\bar{A}'(f)/\bar{A}(f) = \bar{A}'_0(f)/\bar{A}_0(f) - \pi \log e T(\Delta)/\bar{Q}(\Delta) \quad (4)$$

where $T(\Delta)$ is the travel-time at distance Δ and $\bar{Q}(\Delta)$ is the mean value of Q at the same distance. The quantity $\bar{A}'(f)/\bar{A}(f)$ is the slope m (fig. 2) of logarithmic amplitude plots. To deduce $T(\Delta)/\bar{Q}(\Delta)$ from (4) we need to know the ground acceleration spectra at the source.

Spectral analysis of underground nuclear explosion records shows that the ground acceleration near the source is flat and the low cutoff frequency depends on the yield [MUELLER and MURPHY, 1971]. For the event "Greely" of large yield, the spectrum is flat down to 0.5 Hz. At the far field, acceleration spectra of large events show a maximum at about 0.5 Hz, the amplitude falling rapidly both at lower and higher frequencies. This characteristic of large nuclear explosions is well known, though the rapid amplitude fall at low frequencies remains still to be explained [MOLNAR, 1971]. The amplitude diminution at high frequencies as shown by the slope of acceleration spectra, must be attributed to anelastic attenuation.

The source time functions of nuclear explosions and earthquakes of equivalent magnitude are certainly different. But if we utilise only frequencies higher than 0.4 Hz, we analyse mainly the rise time of the signal. Without searching arguments from an examination of explosion and earthquake source functions, we shall derive a working hypothesis by comparing the negative spectral slopes from the two types of events.

3. Results

As mentioned earlier certain earthquakes with complex P-wave records are difficult to utilise in determining the slope of spectra. P-waves of relatively simple form have, therefore, been selected. The fig. 1 shows an example of few record sections. In this paper, data concerning only three distance groups are presented. The table below gives the parameters of earthquakes utilised:

Date	Longitude	Latitude	Origin time	Depth	MB	Δ°
15. 5. 1970	91,3	50,2	17 13 15,1	33	5,9	54,3
5. 6. 1970	78,8	42,5	04 53 06,4	20	6,0	51,7
11. 3. 1970	-153,9	57,5	22 38 34,6	29	6,0	72,2
22. 6. 1970	-156,5	55,2	14 39 30,6	N	5,5	75
27. 5. 1970	143,0	40,3	19 05 39,0	33	5,7	84,7
27. 5. 1970	143,2	40,2	22 35 46,4	16	5,5	
27. 5. 1970	143,0	40,3	23 56 40,0	38	5,4	

In the fig. 2 are presented the logarithmic amplitude spectra of the three distance groups. The scatter, as shown in the figure, is not large. For the distance group of 85°, in addition to the three earthquakes, the figure shows also the ground acceleration (open circle) from the Amchitka nuclear explosion of Nov. 6, 1971 situated at the same epicentral distance as that of the three shocks. The slopes are practically the same. As the ground acceleration spectra for large nuclear explosions are flat within the frequency band considered in this study [MUELLER and MURPHY, 1971], we assume that in the equation (4), $\ddot{A}_0'(f)/\ddot{A}_0(f)=0$. With the slopes as given in the fig. 2, we obtain for T/\bar{Q} the values of 1.07, 0.94 and 1.12 at the mean distances of

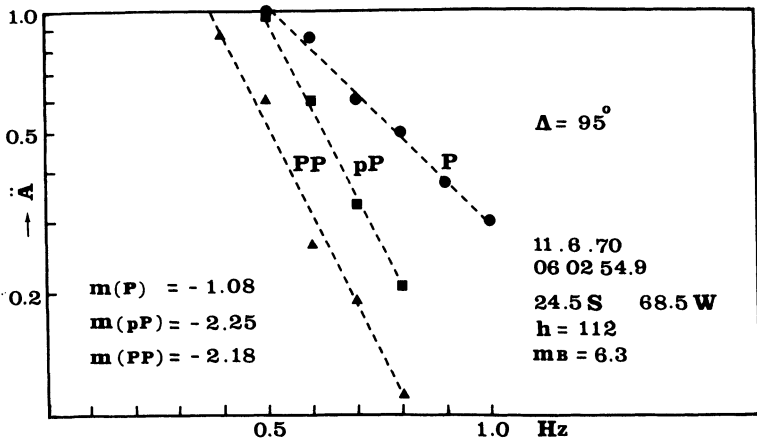


Fig. 3: Logarithmic plot of P, pP, and PP amplitudes from an intermediate focus earthquake showing the relative attenuation of the three phases.

53°, 73° and 85° respectively. This result is in approximate agreement with that of the model 11 of MIKUMO and KURITA [1968] except that at 85° the short period P waves do not show a noticeable increase in T/\bar{Q} values. Recent works suggest that the part of the lower mantle near the core boundary has low shear wave velocity. Differential attenuation results also show low Q values in this region for long period P-waves. The part played by diffraction around the core boundary and the interference by PcP at $\Delta > 80^\circ$ on the long period attenuation data is not yet well explained. Awaiting further observations, we consider that Q values in the lower mantle needs revision using short period data. This idea is supported by the data presented in the fig. 3.

The rise time of a signal is effected only by the attenuation properties in a linear system. If we assume that high frequency attenuation in different phases depends only on the attenuation properties of the medium, we can use phases like pP, PP, etc. to gain information about mean Q values in different parts of the mantle.

We have, so far, ignored the possibility that rays might travel partly in the dipping lithosphere (high Q) and partly in the surrounding low Q media. In the case of intermediate or deep focus earthquakes circumstances for P and pP might correspond to that for the maximum amplitude contrast (P travelling in the plate while pP in the low Q -zone). Quantitative estimation of the influence of different Q -zones on the P-wave amplitude in the frequency range 0.4–1 Hz is yet difficult. Should this be shown important, spectral slopes of P and pP will constitute an efficient tool to study the attenuation properties of the three Q -zones postulated by the plate tectonic theory.

The fig. 3 shows the logarithmic amplitude spectra of P, pP and PP from the June, 11, 1970 intermediate shock ($h=112$ km). The slopes are respectively -1.08 , -2.25 , -2.18 . pP and PP have almost the same slope, about twice that of P, suggesting that most of the attenuation occurs, in this particular case, in the top 100 km of the Earth and that the mantle near the focal region does not attenuate more than the mantle far away. The slope of P (-1.08) indicates no increase in the value of T/\bar{Q} at 95° .

4. Conclusion

From a judicious choice of earthquakes it is possible to construct $\bar{Q}(\Delta)$ curves with relatively small error. The negative gradient of logarithmic acceleration spectra of simple P-waves is proportional to the attenuation. The value of T/\bar{Q} for shallow focus earthquakes at 53° , 73° and 85° lie near 1. The low Q region at the bottom of the mantle as revealed by long period differential attenuation data for $\Delta > 80^\circ$ could not be confirmed for short period P-waves.

References

- KURITA, T.: Attenuation of Short Period P-waves and Q in the mantle, *J. Phys. Earth* 16, 61–78, 1968
- MIKUMO, T., and T. KURITA: Q distribution for Long Period P-waves in the mantle, *J. Phys. Earth* 16, 11–29, 1968
- MOLNAR, P.: P-wave Spectra from Underground Nuclear Explosions, *Geophys. J.* 23, 273–286, 1971
- MUELLER, R. A., and J. R. MURPHY: Seismic Characteristics of Underground Nuclear Detonations, Part I, Seismic Spectrum Scaling, *Bull. Seism. Soc. Am.* 61, 1675–1692, 1971
- Teng, T. L.: Body wave and Earthquake Source Studies, Thesis, California Institute of Technology, 1966

Inhomogeneity of the Earth with Respect to Physical Processes of Earthquakes

I. N. GALKIN, V. T. LEVSHENKO, V. I. MYACHKIN and
A. V. NIKOLAYEV, MOSCOW¹⁾

Eingegangen am 21. Februar 1972

Summary: In the present paper the results of deep seismic sounding considering also the dynamic parameters of the recorded signals are described. The elastic properties of the medium especially its transparency to seismic waves are characterized by the "heterogeneity factor". The evaluation of this factor shows that in the transition area from the continent to the ocean the Earth's crust is more inhomogeneous than the upper mantle.

Zusammenfassung: In der vorliegenden Arbeit werden die Ergebnisse seismischer Tiefensondierungen vorgelegt, die unter besonderer Beachtung der dynamischen Parameter der registrierten seismischen Signale gewonnen wurden. Die elastischen Eigenschaften des Mediums, speziell jedoch seine Durchlässigkeit gegenüber seismischen Wellen, werden durch die Einführung des „Heterogenitätsfaktors“ charakterisiert. Bei der Betrachtung dieses Faktors für verschiedene Gebiete zeigt es sich, daß in Übergangsbereichen zwischen ozeanischer und kontinentaler Krustenstruktur die Inhomogenität der Kruste größer ist als die des oberen Erdmantels.

1. Introduction

The object of the present communication is to show the importance of the study of small inhomogeneities in the Earth's crust. Lately relatively much work has been done in the study of the physics of earthquake foci. By this we mean the physics of the disturbance of great masses of rocks under thermodynamic conditions occurring in the Earth's interior.

It is well known that the inhomogeneity of the material determines the basic parameters of the disturbance process. Consequently also the basic earthquake characteristics, the energy and recurrence depend on inhomogeneity.

NIKOLAYEV [1967, 1968] developed a new model of medium. It includes the determined and the random components of the seismic wave field. For a layered model the determined part of the wave field represents the average values of parameters inside several layers. The variations of measured values from the average ones are described by a homogeneous and isotropic random field. These fluctuations are,

¹⁾ Dr. I. N. GALKIN, Dr. V. T. LEVSHENKO, Dr. V. I. MYACHKIN and Dr. A. V. NIKOLAYEV, Institut Fiziki Zemli ANSSSR, B. Gruzinskaya 10, Moskva, USSR.

however, much smaller than the average values of the parameters in question. The determined part is in good correlation with the space components of the observed wave field, contrary to the random part which is in bad correlation with these components. A new parameter of the medium has been introduced — the “heterogeneity factor” — characterizing the scattering of wave energy on small random heterogeneities. The value of the heterogeneity factor (g) is determined by the variation of scattering of amplitudes ($\ln A$) related to the wave path (R):

$$g = \frac{(\ln A_2)^2 - (\ln A_1)^2}{R_2 - R_1}.$$

A more detailed description of the new model of the medium and of the method of interpretation is given by TREGUB [1972].

The efficiency of the method was clearly evidenced by the results of deep seismic sounding at the sea and land [GALKIN, NIKOLAYEV 1968; GALKIN, NIKOLAYEV, STARSHINOVA 1970; NIKOLAYEV, TREGUB 1969] and by the results of ultrasonic modelling [NIKOLAYEV, AVERYANOV 1970]. The possibility of characterization of the vertical distribution of layering and the corresponding area zoning of media by the value of heterogeneity factor was shown in these papers.

2. Results

In the present paper some new results obtained during the investigations into small inhomogeneities in the region of Kamchatka will be given. In this region comprehensive studies of the physics of earthquakes and their prediction are being performed [MYACHKIN, SOBOLEV, DOLBILKINA, MOROZOV, PREOBRAZHENSKY 1971]. A part of this work are the investigations into changes of the field of velocity and amplitudes of seismic waves in time and space.

The system of observation will be briefly described. At fixed points situated in the ocean explosions are carried out and seismic waves generated are being recorded by five terrestrial seismic stations. The maximum profile length is 200 km. The conditions of generation and registration of seismic waves are constantly checked [GALKIN, DOLBILKINA, MYACHKIN 1969; GALKIN, LEVSHENKO, MYACHKIN in press].

Fig. 1a represents the amplitude curves of the first and dominant phase. The dotted lines mark the determined components of amplitudes after filtering. The random component of the amplitude curve is shown in Fig. 1b and the result of the determination of the heterogeneity factor is drawn in Fig. 1c.

In Fig. 2 the distribution of the logarithm of random fluctuation of amplitudes and the corresponding space intervals can be seen. In conformity with theory [GALKIN, LEVSHENKO, MYACHKIN in press] the interval of longitudinal correlation can be expressed by

$$\Delta r_e = \pi a^2 \lambda;$$

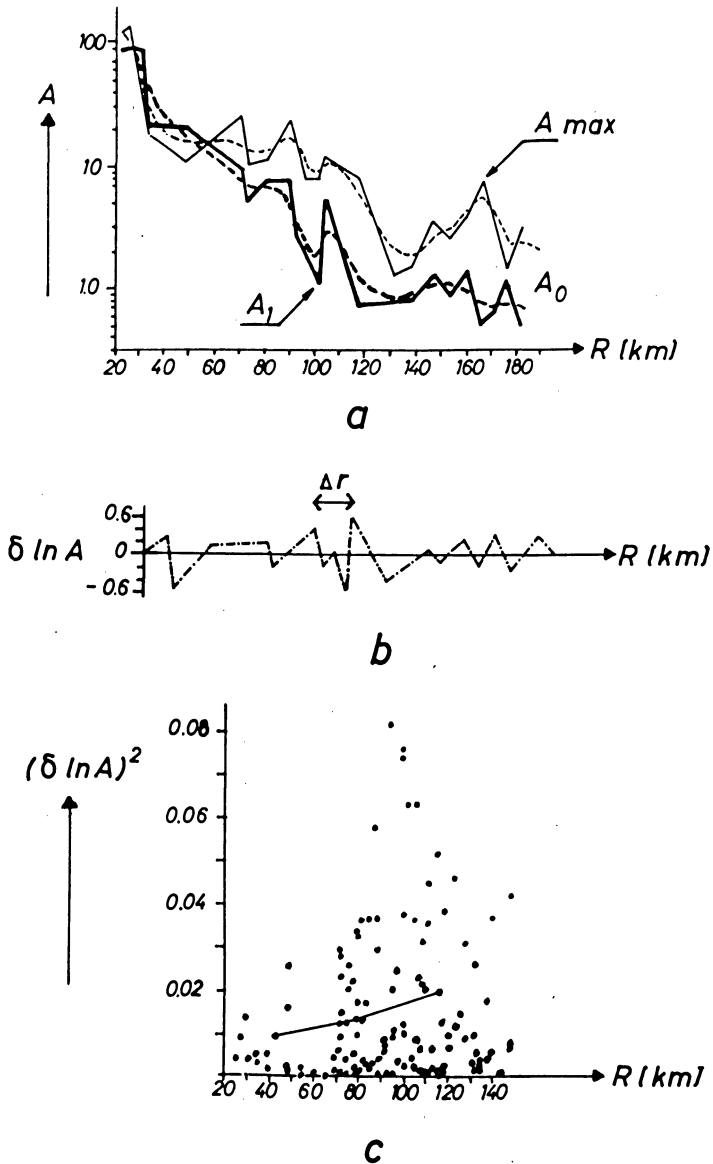


Fig. 1: a) Amplitude curves $\ln A(R)$ of the first A_1 (thick line) and dominant A_{max} phase (thin line). The dotted lines mark the determined component $\ln A_0(R)$ of the amplitude curve after low frequency filtering.
 b) Random component of the amplitude curve in dependence on distance.
 c) The heterogeneity factor in the region of Avacha Bay derived from refracted waves.

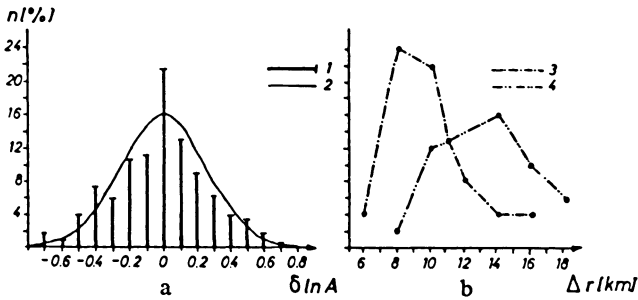


Fig. 2: The distribution of the logarithm of random fluctuations of amplitude.
 1. experimental data,
 2. normal curve (Fig. 2a) and corresponding space intervals at nonlongitudinal (3) and longitudinal (4) profiles (Fig. 2b).

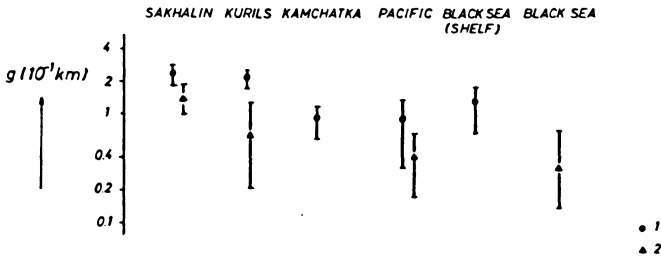


Fig. 3: The values of the heterogeneity factor at different regions of the transition areas for Pacific and Black-sea (1 - crust, 2 - mantle).

the interval of transversal correlation is $\Delta r_t = a$, where a is the predominant linear dimension of inhomogeneity and λ the wavelength.

From Fig. 2a it can be seen that the mean respective space interval in the non-longitudinal profile (8 km) is shorter than in the longitudinal profile (14 km). The basic physical finding obtained by experimental data processing is that the linear dimension of an inhomogeneity is about 8 km.

The other important result refers to the heterogeneity factor obtained from the observation of waves refracted in the crust

$$g = (0.8 - 1.2) \cdot 10^{-3} \text{ km}^{-1}$$

and from reflected waves

$$g = (0.7 - 1.0) \cdot 10^{-3} \text{ km}^{-1}.$$

Comparing the magnitude of both values we can draw the conclusion that the surface of the M-discontinuity is smooth for the wavelength under consideration.

In Fig. 3 the values of the heterogeneity factor obtained from deep seismic sounding on sea in the frequency range of 5 c/s are summarized.

3. Conclusion

The data clearly show a difference between the crust and the mantle: the crust is more heterogeneous than the mantle in all regions. This is a further evidence that in the transition area from the continent to the ocean the medium is more "transparent".

In conclusion it should be pointed out that the study of inhomogeneity is essential for further progress in the earthquake physics and that the study of the heterogeneity factor represents a step towards a quantitative determination of the influence of the medium on seismic processes.

References

- ALIOSHIN, A. S., and A. V. NIKOLAYEV: The method of the study of media with random inhomogeneities (in Russian). 5. Nauchnaja konferencija MGU, 1970
- GALKIN, I. N., and A. V. NIKOLAYEV: Investigation of the heterogeneity of the Earth's crust and upper mantle by recording the amplitudes of refracted waves. Bull. (Izv.) Acad. Sci. USSR, Earth Physics 8, 481 – 487, 1968
- GALKIN, I. N., N. A. DOLBILKINA, and V. I. MYACHKIN: The accuracy of amplitude measurement in seismic research at sea. Bull. (Izv.) Acad. Sci. USSR, Earth Physics 11, 721 – 724, 1969
- GALKIN, I. N., A. V. NIKOLAYEV, and YE. A. STARSHINOVA: Fluctuations of wave characteristics and small scale inhomogeneities of the Earth's crust. Bull. (Izv.) Acad. Sci. USSR, Earth Physics 11, 709 – 713, 1970
- GALKIN, I. N., V. T. LEVSHENKO, and V. I. MYACHKIN: Identification of small inhomogeneities of the crust in the region of the Avacha Bay (in Russian). In press.
- MYACHKIN, V. I., G. A. SOBOLEV, N. A. DOLBILKINA, V. N. MOROZOV, and V. B. PREOBRAZHENSKY: The study of variations in geophysical fields near the focal zone of Kamchatka. Program and abstracts of the 15th General Assembly IUGG, Nauka, Moscow, 1971
- NIKOLAYEV, A. V.: The heterogeneity of real media and the possibility of studying them (in Russian). Doklady Acad. Sci. USSR, 177, No. 5, 1967
- : Seismic properties of weakly heterogeneous media. Bull. (Izv.) Acad. Sci. USSR, Earth Physics 2, 83 – 87, 1968
- NIKOLAYEV, A. V., and F. S. TREGUB: The results of the study of the statistical models of the crust (in Russian). Doklady Acad. Sci. USSR, 189, No. 6, 1969

NIKOLAYEV, A. V., and A. G. AVER'YANOV: A study of longitudinal wave amplitudes in a plane model of a medium with random fluctuations of the absorption coefficient. Bull. (Izv.) Acad. Sci. USSR, Earth Physics 10, 624–628, 1970

TREGUB, F. S.: Relation between P-wave amplitudes and discontinuities in the Earth's crust. Z. Geophys. 38, 407–414, 1972

TSHERNOV, L. A.: Propagation of waves in the medium with random inhomogeneities (in Russian). Press of the Acad. Sci. USSR, Moscow, 1958

Anisotropy of the Upper Mantle Rocks

V. BABUŠKA, Prague¹⁾

Eingegangen am 7. Februar 1972

Summary: From the investigation of ultrasonic velocities and anisotropy, the ultramafic xenoliths studied are divided in two groups. Lherzolites (6 samples) are characterized by higher average velocities ($v_P = 8.03$ km/s) and anisotropy (4–12%) than pyroxenites (3 samples, $v_P = 7.73$ km/s, anisotropy 1–4%), although the average densities of both groups are almost identical. Applied to the upper mantle structure this indicates that increasing content of pyroxenes and garnet may reduce the seismic velocities and the anisotropy, but increase the density of the hypothetical olivine-rich uppermost mantle zone.

Zusammenfassung: Aus Untersuchungen von Ultraschallgeschwindigkeiten und Anisotropie lassen sich die ultrabasischen Xenolithen in zwei Gruppen aufteilen. Die Lherzoliten (6 Proben) unterscheiden sich durch höhere durchschnittliche Geschwindigkeiten ($v_P = 8,03$ km/s) und höhere Anisotropie (4–12%) von den Pyroxengesteinen (3 Proben, $v_P = 7,73$ km/s, Anisotropie 1–4%), obwohl die durchschnittlichen Dichten beider Gruppen beinahe identisch sind. Für die Struktur des Mantels ergibt sich damit, daß ein zunehmender Gehalt an Pyroxen und Granat möglicherweise die seismischen Geschwindigkeiten und die Anisotropie verringert, dagegen aber die Dichte der hypothetischen olivinreichen obersten Mantelzone vergrößert.

1. Introduction

From the seismological point of view two types of anisotropic media may be distinguished. The first one is the transversely isotropic medium with vertical axis of symmetry. Such a medium shows no variation of P-wave velocities in different directions, some differences in the arrival times of SV and SH waves should show up in this case [CHRISTENSEN and CROSSON 1965].

The second type of the anisotropy may be recognized from P-wave velocity differences in dependence on azimuth of their propagation. This corresponds to an anisotropic medium with orthorhombic or lower symmetry, or to a transversely isotropic medium with its axis of symmetry otherwise than vertical. This second type of seismic anisotropy was determined at several places under parts of the oceanic bottom. MORRIS et al. [1969], using refraction profiles oriented in different directions, observed in the region of Hawaii that the upper mantle immediately beneath the MOHORoviČIĆ-discontinuity is anisotropic with respect to the compressional waves, the maximum difference in velocities being 0.6 km/s (over 7% of the mean velocity).

¹⁾ Dr. VLADISLAV BABUŠKA CSc, Geofyzikální ústav ČSAV, Praha 4 – Spořilov, Boční II, ČSSR.

The anisotropy of the oceanic uppermost mantle near the Californian coast was 0.3 km/s [RAITT et al. 1969], in the area west of Vancouver even 8% of the observed velocity [KEEN and BARRETT 1971]. A seismic refraction study carried out by KEEN and TRAMONTINI [1970] on the Mid-Atlantic ridge at 45° N revealed velocity deviation of 0.5 km/s, which means anisotropy of 6%. In all cases the direction of the maximum velocity is situated more or less close to the east-west direction and to the general direction of the sea floor spreading.

The present paper reports briefly about the investigation of elastic properties of ultramafic xenoliths which probably represent original upper mantle materials. The detailed investigation of ultrasonic velocities, elastic anisotropy and fabric of the xenoliths will be a subject of a special study [BABUŠKA, under preparation].

2. Data

The cylindrical specimens were cut in different directions from 12 xenoliths suitable for ultrasonic measurements. The specimens were jacketed in a copper foil and both compressional and shear wave velocities were measured at pressures up to 10 kb. The apparatus and techniques of the velocity measurements are similar to that described by BIRCH [1960]. The method enabled to investigate the spatial distribution of elastic velocities and its changes at different pressures. In several cases the elastic anisotropy patterns were compared with the preferred orientation of olivine.

From the investigation of ultrasonic velocities and anisotropy the ultramafic xenoliths may be divided in two groups. Lherzolites are characterized by higher velocities of compressional and shear waves than other types with increased content of pyroxenes, although both groups have densities very close each to other (Fig. 1). Similarly elastic anisotropy is significantly higher (from 4% to 12%) with olivinic types (Fig. 2).

Figures 3 and 4 show examples of the olivine orientation patterns and the elastic anisotropy diagrams of lherzolites. The sample SB 1, lherzolite of San Bernardino, California (Fig. 3), is typical by a strong lineation expressed by the maximum of compressional wave velocities corresponding to the maximum of olivine *a* axes. The area of velocity minimum corresponds to *b* axes concentration. Such a pattern is in accord with the *P*-wave velocities in a single crystal of olivine, which are, according to KUMAZAWA and ANDERSON [1969], 9.89 km/s along *a* axis and 7.72 km/s along *b* axis. The highest difference of compressional velocities in the lherzolite SB 1 is 0.63 km/s, which means anisotropy of 7.5%.

Lherzolite KH 2 of Kilbournes Hole, New Mexico (Fig. 4) shows slightly different pattern. The maximum of crystallographic *a* axis again corresponds to the maximum of *P*-wave velocity, the velocity minimum is somewhat shifted aside from the maximum of *b* axes. The velocity plane in both lherzolites can be characterized by deformed triaxial ellipsoid with the shortest axis normal to the foliation plane and the longest axis parallel to the lineation.

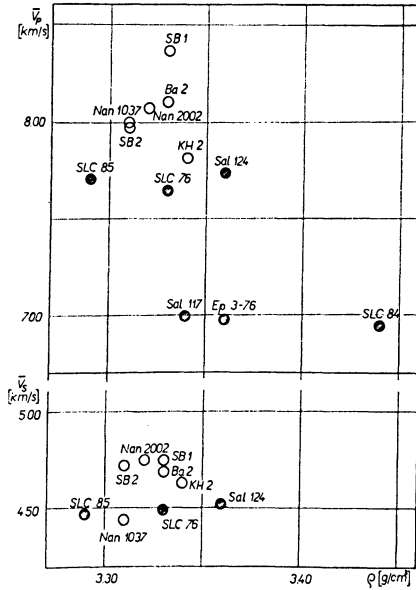


Fig. 1: Average velocities of compressional and shear waves at 10 kb versus true density. Open circles represent lherzolites SB 1, SB 2 (San Bernardino, Calif.), Ba 2 (Dish Hill, Calif.), KH 2 (Kilbournes Hole, New Mexico), Nan 1037, Nan 2002 (Nunivak, Alaska). Shaded circles represent pyroxenites (SLC 74, SLC 84, SLC 85) and garnet websterites (Sal 124, Sal 117), all from Salt Lake Crater, Hawaii, and pyroxene wehrilite Ep 3-76 (Kilbournes Hole, New Mexico).

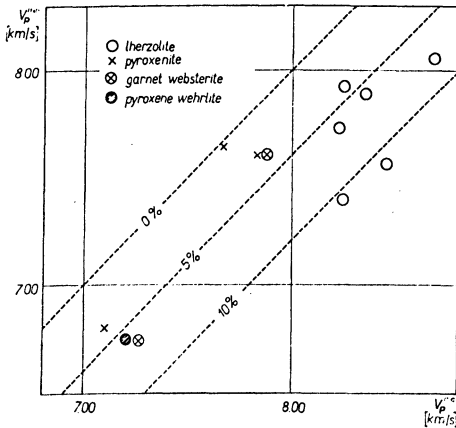


Fig. 2: Velocity anisotropy of compressional waves in xenoliths.

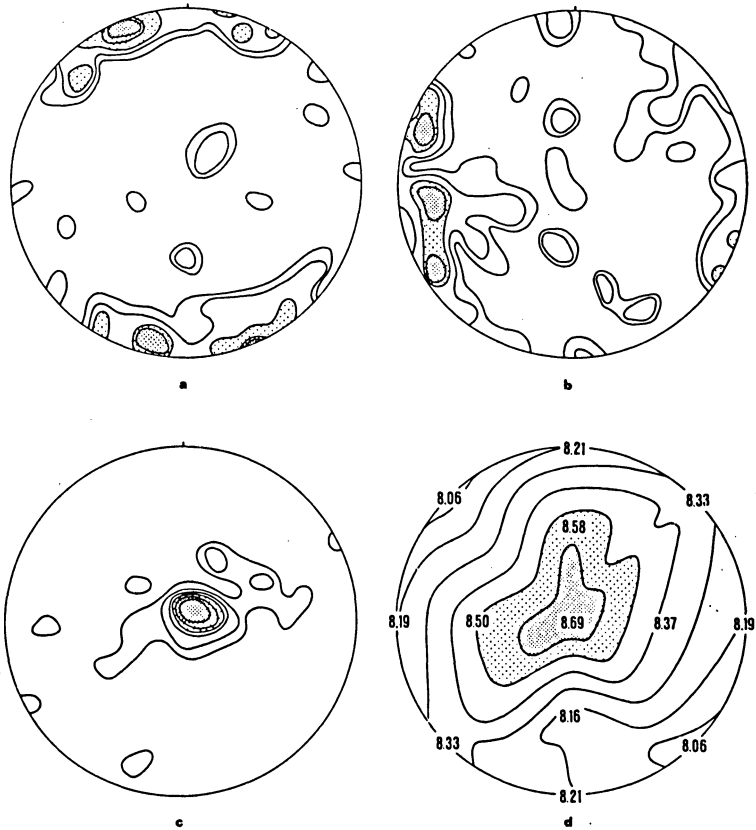


Fig. 3: Lherzolite SB 1 (San Bernardino, Calif.) — the equal-area projections of 150 olivine grains and the diagram of elastic anisotropy: a) *b* axes, contours 8%, 6%, 4%, 2% and 1% per 1% area; b) *c* axes, contours 6%, 4%, 2% and 1% per 1% area; c) *a* axes, contours 12%, 10%, 8%, 4% and 2% per 1% area; d) diagram of elastic anisotropy, isolines of compressional velocities are constructed from 8.10 km/s to 8.60 km/s in steps of 0.1 km/s.

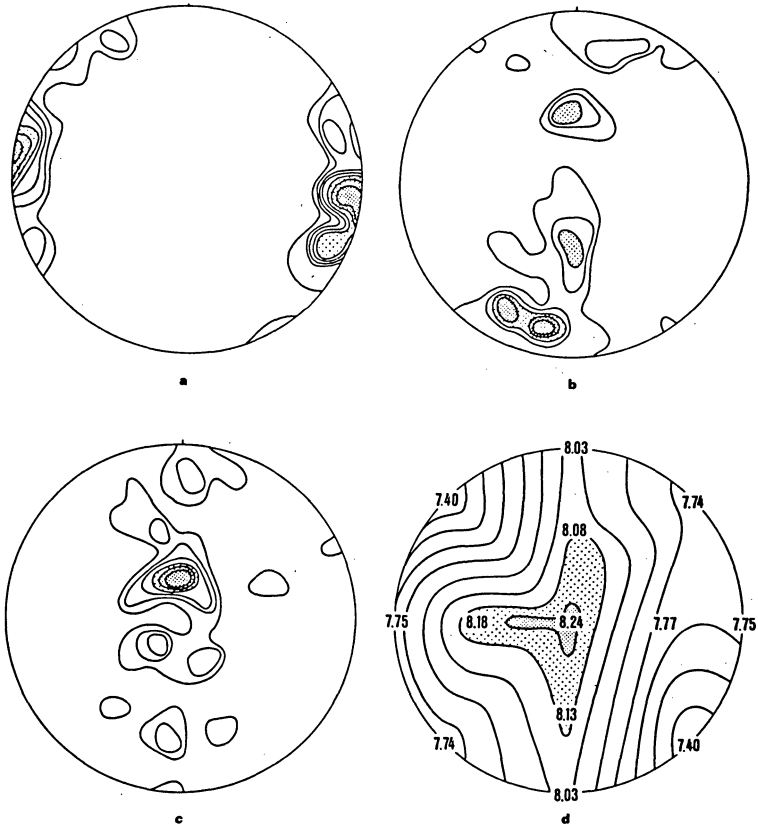


Fig. 4: Lherzolite KH 2 (Kilbournes Hole, New Mexico) — the equal area projections of 105 olivine grains and the diagram of elastic anisotropy: a) *b* axes, contours 14%, 12%, 10%, 8%, 6%, 4% and 2% per 1% area; b) *c* axes, contours 10%, 8%, 6%, 4% and 2% per 1% area; c) *a* axes, contours 12%, 10%, 8%, 6%, 4% and 2% per 1% area; d) diagram of elastic anisotropy, isolines of compressional waves from 7.50 km/s to 8.20 km/s in steps of 0.1 km/s.

3. Discussion

The average of the highest compressional velocities at the pressure of 10 kilobars in the six investigated lherzolite xenoliths is 8.36 km/s, the average of the lowest velocities under the same pressure is 7.76 km/s. The velocity difference is 0.6 km/s which is the same anisotropy as revealed by the seismic refraction measurements in the Pacific Ocean near Hawaii. It is probable that the seismic anisotropy of the uppermost mantle observed by refraction profiles is caused not only by the preferred orientation of olivine, but also by other oriented structural phenomena. Nevertheless, it is also highly probable that only a rock with a high content of olivine can provide such a high anisotropy as was observed e.g. near Hawaii. All xenoliths investigated show lower symmetry than the transversely isotropic medium. The observed symmetries can be characterized as monoclinic or triclinic, in the sample Ba 2 as orthorhombic.

The averages of the mean compressional velocities in the lherzolites and in the second group—pyroxene-rich rocks (two pyroxenites SLC 76, SLC 84, and one garnet websterite Sal 124) are 8.03 km/s and 7.73 km/s respectively. The remaining three xenoliths from the second group (Sal 117, Ep 3—74, SLC 84) are partly altered having porosities between 4% and 9%.

The comparison of densities, seismic velocities and anisotropy of both groups supports the model of the upper mantle structure proposed by JACKSON and WRIGHT [1970] for the region of Oahu, Hawaii. According to this model the uppermost mantle is composed of dunite or olivine-rich peridotite with velocities of compressional waves over 8 km/s. The present study indicates that rock complexes in this layer may be strongly anisotropic as follows from the high rate of preferred orientation of olivine in lherzolite xenoliths and gneissic structure of xenoliths from island Nunivak, Alaska (samples Nan 1037, Nan 2002).

Below the olivine-rich layer JACKSON and WRIGHT suppose rocks enriched by pyroxene and garnet. Such a petrologic model is in good agreement with the elasticity investigation. Pyroxenites of Salt Lake Crater may be suitable representatives of the material below the olivinic uppermost mantle. They have lower velocities of elastic waves and lower anisotropy, but slightly higher density than lherzolites. Elasticity data of pyroxenes show that they have significantly lower velocities of elastic waves than the common type of olivine, but almost all pyroxenes have higher densities. Similarly garnets are very dense minerals, but elastic wave velocities in garnets are approximately the same as the average velocities in olivine. Both pyroxenes and garnet can thus contribute to increase density, the increasing portion of pyroxenes causes, however, decreasing of the seismic velocities.

It is very difficult to make any conclusion about the regionally variable upper mantle structure from the study of a small number of xenoliths, which are believed to be real representatives of the mantle rocks. The following schematic structure adapted from JACKSON and WRIGHT [1970] may be proposed. The uppermost mantle

beneath the MOHOROVIČIĆ-discontinuity is probably composed of olivine-rich, highly anisotropic rocks. The horizontal scale of anisotropy in this layer depends on dimensions and homogeneity of the stress field. This might be homogeneous over vast regions below the oceanic bottom and quite variable in the continental areas. Under the assumption of increasing content of pyroxene and garnet the velocity of seismic waves and the elastic anisotropy may decrease to some depth, the density is, however, increasing.

4. Acknowledgments

I am indebted to Professor Francis Birch for the use of the facilities at Hoffman Laboratory and for his advice throughout the experimental work, and to Dr. J. Vaněk for critical reading of the manuscript. Drs. M. H. Beeson, E. D. Jackson, H. G. Wilshire, J. B. Reid, and T. R. McGetchin generously donated xenolite samples. The experimental part of the work was supported by the Committee on Experimental Geology and Geophysics, Harvard University.

References

- BABUŠKA, V.: Elasticity and fabric of ultramafic xenoliths (under preparation)
- BIRCH, F.: The velocity of compressional waves in rocks to 10 kilobars, Part 1. *J. Geophys. Res.* 65, 1083–1102, 1960
- CHRISTENSEN, N. I., and R. S. CROSSON: Seismic anisotropy in the upper mantle. *Tectonophysics* 6, 93–107, 1968
- JACKSON, E. D., and T. L. WRIGHT: Xenoliths in the Honolulu volcanic series, Hawaii. *J. Petrology* 11, 405–430, 1970
- KEEN, C. E., and C. TRAMONTINI: A seismic refraction study on the Mid – Atlantic Ridge. *Geophys. J.* 20, 473–491, 1970
- KEEN, C. E., and D. L. BARRETT: A measurement of seismic anisotropy in the northeast Pacific. *Can. J. Earth Sci.* 8, 1056–1064, 1971
- KUMAZAWA, M., and O. L. ANDERSON: Elastic moduli, pressure derivatives and temperature derivatives of single-crystal olivine and single-crystal forsterite. *J. Geophys. Res.* 74, 5961 to 5972, 1969
- MORRIS, G. B., R. W. RAITT, and G. G. SHOR, JR.: Velocity anisotropy and delay-time maps of the mantle near Hawaii. *J. Geophys. Res.* 74, 4300–4316, 1969
- RAITT, R. W., G. G. SHOR, JR., T. J. G. FRANCIS, and G. B. MORRIS: Anisotropy of the Pacific upper mantle. *J. Geophys. Res.* 74, 3095–3109, 1969

Theory of Elastic Wave Propagation in Inhomogeneous Media

V. ČERVENÝ, Prague¹⁾

Eingegangen am 22. Februar 1972

Summary: A short outline of recent theoretical methods of the investigation into the propagation of elastic body waves in inhomogeneous media is given. Above all the laterally inhomogeneous media, such as the Earth's crust and the uppermost mantle, are considered.

Zusammenfassung: Es wird eine kurze zusammenfassende Übersicht über die Theorie der Ausbreitung elastischer Raumwellen in inhomogenen Medien vorgelegt. Besondere Aufmerksamkeit wird der Theorie der Wellenausbreitung in lateral inhomogenen Medien gewidmet, welche vor allem in der Erdkruste und in den obersten Partien des Erdmantels vorausgesetzt werden müssen.

1. Introduction

The theoretical investigation of seismic body waves propagation in the Earth's crust and the uppermost mantle has progressed considerably during the last few years. Theoretical seismology, however, is not yet able to give an exhaustive answer to many problems in this field. The structure of the Earth's crust and the uppermost mantle is very complicated. The velocity of seismic waves changes in all the three coordinates, discontinuities have complicated geometrical shapes and physical properties (discontinuities of first or higher order, transition zones, laminated zones, corrugated interfaces, a.s.o.). The block structure and the presence of low velocity channels make the situation even more complicated. The properties of seismic discontinuities and low velocity channels can vary laterally. Only in deeper parts of the Earth is the structure simpler and the expressive lateral changes of velocity are unlikely. Within the Earth's crust and the uppermost mantle, however, the deviations from the one-dimensional velocity distribution considerably affect the properties of seismic body waves and it is hardly possible to neglect them.

The three main theoretical approaches to the investigation of seismic body waves propagation are as follows: a) the ray series method and its modifications, b) the wave method, c) the finite difference method. For the complicated, laterally inhomogeneous media, the formal integral solutions of the equation of motion are

¹⁾ Dr. VLASTISLAV ČERVENÝ, Geofyzikální ústav Karlovy university., Ke Karlovu 3, Praha-2, ČSSR.

not known. Therefore, the wave method can be used only for simplified models of media (e.g., in the case of one-dimensional velocity distribution). Its great value consists in the possibility to give an exact solution to certain specific problems (say, reflections from strictly horizontal transition layers), but the direct application of the wave method to the interpretation of deep seismic sounding measurements will be possible only in those regions where the structure of the Earth's crust is simple.

The finite difference methods have been applied to seismological problems only lately [ALTERMAN 1968; ALTERMAN and LOEWENTHAL 1970; ALTERMAN and KARAL 1968; ALTERMAN and ABOUDI 1971; BOORE, LARNER and AKI 1971; LONG 1971; NEDOMA 1972]. Since they are based on direct numerical solutions of equations of motion, they can be applied in general to rather complicated media. However, it will take some time to develop them for the solution of more complex problems.

The main problem in the application of the ray series method lies in the fact that it is only approximate and has a number of serious restrictions. Nevertheless, at the present time this is the only method that is able to give us an approximate answer to many problems in seismic body waves propagation in inhomogeneous media with non-plane interfaces. It can also be used as a basis for the solution of certain inverse problems in laterally inhomogeneous media. In the following, the possibilities and limitations of the ray theory will be shortly discussed. Further, the application of other methods to certain specific problems will be mentioned. No results of computations are presented; the interested reader is referred to the quoted papers where he will find many other references also. For an extensive bibliography see ČERVENÝ [1968, 1972b].

2. Ray method

While previously the ray theory was used particularly for the media with one-dimensional velocity distribution, at the present time methods have been elaborated for constructing rays, wavefronts and travel times and computing ray amplitudes of body waves propagating in media where the velocity depends on two or three coordinates and in which non-plane interfaces of first order may exist. Computational methods are mostly based on the numerical solution of systems of *ordinary* differential equations. These systems can be solved by standard numerical technique. See, e.g. BELONOSOVA et al. [1967], MARCINKOVSKAYA and KRASAVIN [1968], BELONOSOVA [1969], UGINČIUS [1969, 1970], WESSON [1970], YACOB et al. [1970], MIRI-ZADE [1970], JACOB [1970], ČERVENÝ and RAVINDRA [1971], PŠENČÍK [1972]. For inhomogeneous anisotropic media see VLAAR [1968], ČERVENÝ [1972a], ČERVENÝ and PŠENČÍK [1972a]. The possibility to calculate theoretical time-distance curves (and ray amplitudes) in laterally inhomogeneous, possibly anisotropic media, can help us to check preliminary interpretations of seismic measurements of the structure of the Earth's crust, which are usually based on the assumption of horizontal layering.

Considerable attention has been paid to the inverse kinematic problems for laterally inhomogeneous media. Results have been obtained concerning the uniqueness and stability of these problems [LAVRENTYEV and MUKHOMETOV 1969]. The WIECHERT-HERGLOTZ-method was generalized for the case of two-dimensional velocity distribution by BELONOSOVA and ALEKSEYEV [1967]. Certain methods for the velocity determination in laterally inhomogeneous media have been verified both on theoretical and real models of media [ALEKSEYEV et al. 1969, 1970, 1971; FAZYLOV 1971].

A problem which has not yet been quite satisfactorily solved is the suitable parametrization of a medium. To describe the two- or three-dimensional velocity distribution is rather complicated. It is obvious that it will be hardly possible to describe the velocity distribution over the whole region of interest by some elementary functions. Usually the velocities are given by a rectangular network. From this network the smooth velocity distribution must be constructed. The linear approximation is not quite satisfactory, as the interfaces of second order generate false irregularities on travel-time and amplitude-distance curves. Even the interfaces of third order cause certain false irregularities on the amplitude-distance curves [JANSKÝ 1969, 1970; CHAPMAN 1971]. The interfaces of higher order are acceptable when we are interested only in the zero-order ray theory. *It seems that the best way now for the approximation of velocity distribution is to use splines. They guarantee the continuity of velocity and its first and second derivatives. (However, in certain cases neither the splines are quite satisfactory as they may oscillate and generate undesirable false low velocity channels.)* The same problem arises with the analytical description of curved interfaces. They must be smooth enough not to cause singularities in time-distance and amplitude-distance curves of reflected waves. Linear and parabolic representations are inconvenient. Again, the use of splines is suitable for this purpose.

When the velocities and interfaces (of first order) are suitably parametrized, the computation of rays, arrival times and ray amplitudes of individual non-interfering waves does not cause principal difficulties, neither in very general types of media. Difficulties arise when an extremely large number of waves must be considered. In inhomogeneous media with curved interfaces an infinite number of waves can arrive at the receiver within even a narrow time window. The problem of constructing ray theoretical seismograms in general inhomogeneous media with curved interfaces has not yet been solved satisfactorily. The only situation in which the problem has been solved fully is the liquid medium composed of plane parallel homogeneous layers. (The same procedure can be, of course, applied to P-waves in a solid medium, when we do not take into account the PS and SP conversions.) The number of waves, which arrive at the receiver within a finite time window is always finite in this case. The situation is considerably simplified by the fact that the individual waves can be grouped into the families of kinematically and dynamically analogous waves. This considerably decreases the number of waves which must be considered [PETRASHEN and VAVILOVA 1968, VAVILOVA and VOLODKO 1968; HRON 1971; HRON and KANASEWICH 1971]. However, even in this case the number

of groups remains very high, mainly when the epicentral distance is large and/or when thin layers are present in the medium and/or when we are interested in a long interval of the theoretical seismogram.

The ray theory has certain serious restrictions. It is not applicable in the case of rapid changes of velocity within short distances. The most typical example is a transition zone. Further, the ray theory is not applicable when the radii of curvature of the interface of first order are of the same order of magnitude or smaller than the wavelength. An example is the corrugated interface. The ray theory can neither be used for the investigation of wave propagation in shadow zones, for the investigation of various types of inhomogeneous and diffracted waves and in the neighbourhood of singular points (caustics, critical region, grazing rays, a.s.o.). Great difficulties also arise in the case of low velocity layers.

In some of the above situations, certain modifications of the ray method can be used. Here the method of parabolic equation [see, e.g., YANOVSKAYA 1968] and the geometrical theory of diffraction [KELLER 1958; LEVY and KELLER 1959; SECKLER and KELLER 1959; MUKHINA 1971] should be mentioned. The modified ray methods are again applicable to inhomogeneous media with slightly curved interfaces, and remove certain difficulties of the ray theory (the neighbourhood of caustics and critical rays, for example). The geometrical theory of diffraction can serve as a basis for computation of diffracted rays, penetrating into the shadow zones, and their time-distance curves [ČERVENÝ and PŠENČIK 1972b].

3. Exact ray theory, wave method and other approaches

The methods mentioned in the preceding section are only approximate ones. In the frequency domain, they give the better results, the higher is the frequency. It is not simple to appreciate quantitatively the accuracy of these methods. The simplest approach is to compare the ray results with the exact ones, obtained by different methods (for the situations where they are known). In a medium composed of homogeneous planparallel layers, the exact ray theory can be used for this purpose. Also wave methods [SATO 1969] and finite difference methods can be used. Of course, these methods do not serve only to check the ray theory, but they are used generally to obtain an answer to problems which can hardly be attacked by the ray theory (transition zones, corrugated interfaces, a.s.o.).

The exact ray theory is based on the decomposition of the wave field in horizontally layered media into contributions each of which can be attributed to a special ray from the source to the receiver. Various methods are used to obtain *exact* expressions for individual contributions, suitable for numerical calculations (the methods of Cagniard-de Hoop, Smirnov-Sobolev, Garvin, Pekeris, and Bortfeld, for example). For details and numerical examples see PODYAPOLSKIY [1959], BORTFELD [1967], GARVIN [1956], SPENCER [1965], PEKERIS et al. [1965], MÜLLER [1968, 1969, 1970], ČERVENÝ [1967], HELMBERGER [1968], HELMBERGER and MORRIS [1969, 1970]. The

computation of individual ray contributions (elementary seismograms) is rather fast. Computation of theoretical seismograms with the aid of the exact ray theory, however, becomes lengthy when a large number of elementary waves must be considered (e.g., in the case of a thin layered medium). MÜLLER [1970] has studied the possibilities of the exact ray theory to the investigation of elastic wave propagation in vertically inhomogeneous media (the medium is simulated by a stack of homogeneous layers). Some approximations are necessary in this case to save the computer time as the number of elementary waves would be extremely high. Computations of theoretical seismograms can be restricted only to certain low-order multiply reflected waves. In spite of these approximations, the method of MÜLLER is very promising. The interested reader will find an excellent description of the exact ray theory and of its possibilities and limitations in papers of MÜLLER, quoted above.

The principles of the wave method have been known for a long time. They are based on formal integral solutions of equations of motion, satisfying boundary conditions relevant to the model under study. These solutions, however, are known only for simple media (for example, for vertically inhomogeneous media). The fundamental mathematical theory for vertically inhomogeneous media was presented by GILBERT and BACKUS [1966] in their paper on propagator matrices. For radially symmetric media see CHAPMAN and PHINNEY [1970]. When the equation of motion for a vertically inhomogeneous medium is suitably transformed with respect to time and epicentral distance, the ordinary differential equation for the transformed displacement-stress vector is obtained. This ordinary differential equation can be solved by standard numerical methods. It can be used to compute the reflection coefficient (reflectivity) for an arbitrary inhomogeneous layer. At high frequencies, the frequency-dependent reflection coefficient can be also calculated from the equation by asymptotic methods [RICHARDS 1971, 1972]. Also other approaches can be adopted to compute the reflection coefficient from a transition layer. Simulating the transition layer by a stack of thin homogeneous layers, THOMSON-HASKELL-matrix formalism can also be used (see KNOPOFF [1964] and DUNKIN [1965] to improve the original Thomson-Haskell-method). Details are given in FUCHS [1968a]. CHERNYSHEV [1969] has applied a finite difference method to the problem of reflection (transmission) of plane *transient* waves from (through) a transition layer. Numerical examples are given in CHERNYSHEV and MIKHAYLENKO [1971]. In the case of specific velocity variations the reflection coefficient can be calculated analytically [BREKHOVSKIKH 1960; GUPTA 1966a, 1966b; PHINNEY 1970; MERZER 1971].

The reflection coefficient being found, an integration must be performed to evaluate the wave field from a transition layer due to a *point source*. The numerical integration meets a number of difficulties (rapid oscillations of the integrand, poles and branch points along the integration contour). FUCHS [1968b, 1970] has successfully computed theoretical seismograms of reflected waves from transition layers by assuming that the integral with infinite limits with respect to the wave number can be effectively

replaced by the integral with finite limits (integration over real angles of incidence). He has also compared his results with those obtained by the exact ray theory [FUCHS and MÜLLER 1971]. The agreement is satisfactory for practical purposes. Another approach to the computation of similar integrals was proposed by PHINNEY [1965]. Phinney computes the spectra of the theoretical seismogram as viewed through the exponentially decaying time window. The exponentially decaying time window emphasizes the early arriving phases in comparison with later arrivals. The spectrum is smoother and its numerical evaluation is easier. Also asymptotic methods can be used to evaluate the integrals. For detailed mathematical treatment see TSEPELEV [1968]. FUCHS [1971] has used the method of stationary phase for this purpose. NAKAMURA [1968] and MERZER [1971] has investigated head waves from transition layers by asymptotic evaluation of branch line integrals. The first quite exact solution of the point source — linear transition layer problems has been obtained by HIRASAWA and BERRY [1971]. Exact solutions are derived by numerical integration of the contour integral in the complex wave number plane.

The theory of reflection of seismic body waves from irregular interfaces (or, wave propagation in a half-space with irregular boundary) is considerably more complicated. The difficulty is caused by the boundary conditions which must be applied on the irregular interface. When the curvature of the interface is small, the ray theory and its modifications can be often applied [GELCHINSKIY et al. 1968]. The ray theory, however, is not applicable when the curvature is large. Mostly only the incidence of plane waves has been investigated. For detailed description of various methods and for other references see ABUBAKAR [1962, 1963], ASANO [1966], McIVOR [1969], AKI and LARNER [1970], BOORE et al. [1971]. The propagation of elastic waves generated by an impulse *point source* in a half-space with a corrugated surface was investigated by ALTERMAN and ABOUDI [1971] using a combination of a perturbation theory and a finite difference method.

References

- ABUBAKAR, I.: Buried compressional line source in a half space with irregular boundary. J. Phys. Earth 10, 21–38, 1962
- ABUBAKAR, I.: Scattering of plane elastic waves at rough interfaces. I. Proc. Cambridge Phil. Soc. 58, 136–157, 1962; II. Proc. Cambridge Phil. Soc. 59, 231–248, 1963
- AKI, K., and K. L. LARNER: Surface motion of a layered medium having an irregular interface due to incident SH waves. J. Geophys. Res. 75, 933–954, 1970
- ALEKSEYEV, A. S., M. M. LAVRENTYEV, R. G. MUKHOMETOV, and V. G. ROMANOV: Numerical method for the solution of three-dimensional inverse kinematic problem of seismology (in Russian). Mathematical Problems of Geophysics 1, 179–201, Acad. of Sci. USSR, Novosibirsk 1969

- ALEKSEYEV, A. S., M. M. LAVRENTYEV, R. G. MUKHOMETOV, I. L. NERSESOV, and V. G. ROMANOV: Method for numerical investigation of lateral inhomogeneities in the earth's mantle from seismological data. 10th Gen. Ass. Europ. Seism. Comm., 26–30, Acad. of Sci. USSR, Moscow 1970
- ALEKSEYEV, A. S., M. M. LAVRENTYEV, R. G. MUKHOMETOV, I. L. NERSESOV, and V. G. ROMANOV: Numerical method for determination of the structure of the Upper Mantle of the Earth (in Russian). *Mathematical Problems of Geophysics* 2, 143–165, Acad. of Sci. USSR, Novosibirsk 1971
- ALTERMAN, Z. S.: Finite difference solution to geophysical problems. *J. Phys. Earth* 16, 113–128, 1968
- ALTERMAN, Z. S., and J. ABOUDI: Propagation of elastic waves caused by an impulsive source in a half space with a corrugated surface. *Geophys. J.* 24, 59–76, 1971
- ALTERMAN, Z. S., and F. C. KARAL: Propagation of elastic waves in layered media by finite difference methods. *Bull. Seism. Soc. Am.* 58, 367–398, 1968
- ALTERMAN, Z. S., and D. LOEWENTHAL: Seismic waves in a quarter and three-quarter plane. *Geophys. J.* 20, 101–126, 1970
- ASANO, S.: Reflection and refraction of elastic waves at a corrugated interface. *Bull. Seism. Soc. Am.* 56, 201–221, 1966
- BELONOSOVA, A. V.: On numerical realization of ray method for determination of travel-times and amplitudes of elastic waves for two-dimensional block models of media (in Russian). *Mathematical Problems of Geophysics* 1, 212–224, Acad. of Sci. USSR, Novosibirsk 1969
- BELONOSOVA, A. V., and A. S. ALEKSEYEV: On one formulation of inverse kinematic problem of seismology for a two-dimensional continuously inhomogeneous medium (in Russian). *Certain Methods and Algorithms in the Interpretation of Geophysical Data*, 137–154, Nauka, Moscow 1967
- BELONOSOVA, A. V., S. S. TADZHIMUKHAMEDOVA, and A. S. ALEKSEYEV: Computation of travel-time curves and geometrical ray spreading in inhomogeneous media (in Russian). *Certain Methods and Algorithms in the Interpretation of Geophysical Data*, 124–136, Nauka, Moscow 1967
- BOORE, D. M., K. L. LARNER, and K. AKI: Comparison of two independent methods for the solution of wave scattering problems: Response of a sedimentary basin to vertically incident SH waves. *J. Geophys. Res.* 76, 558–569, 1971
- BORTFELD, R.: Elastic waves in layered media. *Geophys. Prospect.* 15, 644–650, 1967
- BREKHOVSKIKH, L. M.: *Waves in layered media*. Academic Press, New York 1960
- ČERVENÝ, V.: The amplitude-distance curves for waves reflected at a plane interface for different frequency ranges. *Geophys. J.* 13, 187–196, 1967
- : Theory of seismic body waves. *Upper Mantle Seismological Investigations, Progress Report I*, Europ. Seism. Comm., 5–35, Soviet Geophys. Committee, Moscow 1968
- ČERVENÝ, V., and R. RAVINDRA: *Theory of seismic head waves*. University of Toronto Press, Toronto 1971

- ČERVENÝ, V.: Seismic rays and ray intensities in inhomogeneous anisotropic media. *Geophys. J.* 28, 1972a (in press)
- : Theory of seismic body wave propagation. Upper Mantle Seismological Investigation, Progress Report II, Europ. Seism. Comm., Soviet Geophysical Committee, Moscow 1972b (in press)
- ČERVENÝ, V., and I. PŠENČÍK: Rays and time-distance curves in inhomogeneous anisotropic media. *Z. Geophys.* 38, 565–577, 1972a
- : Computation of diffracted rays in inhomogeneous media with curved interfaces. *Studia geoph. et geod.* 16, 1972b (in press)
- CHAPMAN, C. H.: On the computation of seismic ray travel-times and amplitudes. *Bull. Seim. Soc. Am.* 61, 1267–1274, 1971
- CHAPMAN, C. H., and R. A. PHINNEY: Diffraction of P waves by the core and an inhomogeneous mantle. *Geophys. J.* 21, 185–206, 1970
- CHERNYSHEV, YU. C.: Numerical solution of certain direct dynamic problems of propagation of plane waves in inhomogeneous media (in Russian). *Mathematical Problems of Geophysics* 1, 284–314, Acad. of Sci. USSR, Novosibirsk 1969
- CHERNYSHEV, YU. C., and B. G. MIKHAYLENKO: Certain dynamic peculiarities of reflected and refracted plane waves in elastic transition media (in Russian). *Mathematical Problems of Geophysics* 2, 238–250, Acad. of Sci. USSR, Novosibirsk 1971
- DUNKIN, J. W.: Computation of modal solutions in layered elastic media at high frequencies. *Bull. Seism. Soc. Am.* 55, 335–358, 1965
- FAZYLOV, F. N.: Numerical solution of one inverse kinematic problem of seismology (in Russian). *Mathematical Problems of Geophysics* 2, 213–222, Acad. of Sci. USSR, Novosibirsk 1971
- FUCHS, K.: Das Reflexions- und Transmissionsvermögen eines geschichteten Mediums mit beliebiger Tiefenverteilung der elastischen Moduln und der Dichte für schräge Einfall ebener Wellen. *Z. Geophys.* 34, 389–413, 1968a
- : The reflection of spherical waves from transition zones with arbitrary depth-dependent elastic moduli and density. *J. Phys. Earth* 16, 27–41, 1968b
- : On the determination of velocity-depth distributions of elastic waves from the dynamic characteristics of the reflected wave field. *Z. Geophys.* 36, 531–548, 1970
- : The method of stationary phase applied to the reflection of spherical waves from transition zones with arbitrary depth-dependent elastic moduli and density. *Z. Geophys.* 37, 89–117, 1971
- FUCHS, K., and G. MÜLLER: Computation of synthetic seismograms with the reflectivity method and comparison with observations. *Geophys. J.* 23, 417–433, 1971
- GARVIN, W. W.: Exact transient solution of the buried line source. *Proc. Roy. Soc. London* A 234, 528–541, 1956

- GEL'CHINSKIY, B. Ya., N. A. KARAYEV, L. D. KOGAN, and O. M. PROKATOR: Theoretical and model investigation of wave fields, reflected from corrugated curved interfaces (in Russian). Problems of the Dynamic Theory of Propagation of Seismic Waves 9, 184–212, Nauka, Leningrad 1968
- GILBERT, F., and G. E. BACKUS: Propagator matrices in elastic wave and vibration problems. Geophysics 31, 326–332, 1966
- GUPTA, R. N.: Reflection of elastic waves from a linear transition layer. Bull. Seism. Soc. Am. 56, 511–526, 1966a
- : Reflection of plane elastic waves from transition layers with arbitrary variation of velocity and density. Bull. Seism. Soc. Am. 56, 633–642, 1966b
- HELMBERGER, D. V.: The crust mantle transition in the Bering Sea. Bull. Seism. Soc. Am. 58, 179–214, 1968
- HELMBERGER, D. V., and G. B. MORRIS: A travel time and amplitude interpretation of a marine refraction profile: primary waves. J. Geophys. Res. 74, 483–494, 1969
- : A travel time and amplitude interpretation of a marine refraction profile: transformed shear waves. Bull. Seism. Soc. Am. 60, 593–600, 1970
- HIRASAWA, T., and M. J. BERRY: Reflected and head waves from a linear transition layer in a fluid medium. Bull. Seism. Soc. Am. 61, 1–26, 1971
- HRON, F.: Criteria for selection of phases in synthetic seismograms for layered media. Bull. Seism. Soc. Am. 61, 765–779, 1971
- HRON, F., and E. R. KANASEWICH: Synthetic seismograms for deep seismic sounding studies using asymptotic ray theory. Bull. Seism. Soc. Am. 61, 1169–1200, 1971
- JACOB, K. H.: Three-dimensional seismic ray tracing in a laterally heterogeneous spherical earth. J. Geophys. Res. 75, 6675–6689, 1970
- JANSKÝ, J.: Refracted wave in a horizontally stratified medium with constant velocity gradients. Studia geoph. et geod. 13, 423–443, 1969
- : Refracted wave in a horizontally layered medium with continuous velocity gradients. Studia geoph. et geod. 14, 286–295, 1970
- KELLER, J. B.: A geometrical theory of diffraction. Calculus of variations and its applications, 27–52, McGraw Hill, New York 1958
- KNOPOFF, L.: A matrix method for elastic wave problems. Bull. Seism. Soc. Am. 54, 431–438, 1964
- LAVENTYEV, M. M., and R. G. MUKHOMETOV: Investigation of stability of inverse kinematic problem of seismology (in Russian). Mathematical Problems of Geophysics 1, 83–91, Acad. of Sci. USSR, Novosibirsk 1969
- LEVY, B. R., and J. B. KELLER: Diffraction by a smooth object. Comm. Pure Appl. Math. 12, 159–209, 1959
- LONG, T. L.: Finite difference propagation of waves in fluid media with a linear velocity gradient (Abstract). Earthquake Notes 42, 13, 1971

- MARCINKOVSKAYA, N. G., and V. G. KRASAVIN: Algorithm for calculation of the reflected waves field in media with curved interfaces (in Russian). *Problems of the Dynamic Theory of Propagation of Seismic Waves* 9, 135–144, Nauka, Leningrad 1968
- MCIVOR, I. K.: Two-dimensional scattering of a plane compressional wave by surface imperfections. *Bull. Seism. Soc. Am.* 59, 1349–1364, 1969
- MERZER, A. M.: Head waves from different transition layers. *Geophys. J.* 24, 77–95, 1971
- MIRI-ZADE, S. A.: Numerical method for the construction of reflecting interfaces in complicated inhomogeneous media (in Russian). *Problems of the Dynamic Theory of Propagation of Seismic Waves* 10, 103–110, Nauka, Leningrad 1970
- MUKHINA, I. V.: Geometrical theory of diffraction in inhomogeneous media separated by arbitrary smooth interface (in Russian). *Proc. V. Symp. on Diffraction and Wave Propagation*, 163–170, Nauka, Leningrad 1971
- MÜLLER, G.: Theoretical seismograms for some types of point sources in layered media. Part 1: Theory. *Z. Geophys.* 34, 15–35, 1968. Part 2: Numerical calculations. *Z. Geophys.* 34, 147–162, 1968. Part 3: Single force and dipole sources of arbitrary orientation. *Z. Geophys.* 35, 347–371, 1969
- : Exact ray theory and its applications to the reflection of elastic waves from vertically inhomogeneous media. *Geophys. J.* 21, 261–284, 1970
- NAKAMURA, Y.: Head waves from a transition layer. *Bull. Seism. Soc. Am.* 58, 963–976, 1968
- NEDOMA, J.: Investigation of linear harmonic source field of SH-waves in a stratified inhomogeneous medium using the finite difference method. *Z. Geophys.* 38, 529–542, 1972
- PEKERIS, C. L., Z. ALTERMAN, F. ABRAMOVICI, and H. JAROSCH: Propagation of a compressional pulse in a layered solid. *Rev. Geophys.* 3, 25–47, 1965
- PETRASHEN, G. I., and T. I. VAVILOVA: On the calculation of the intensity of summary multiple waves in multilayered media for arbitrary position of source and receiver (in Russian). *Problems of the Dynamic Theory of Propagation of Seismic Waves* 9, 77–96, Nauka, Leningrad 1968
- PHINNEY, R. A.: Theoretical calculations of the spectrum of first arrivals in layered elastic mediums. *J. Geophys. Res.* 70, 5107–5123, 1965
- : Reflection of acoustic waves from a continuously varying interfacial region. *Rev. Geophys.* 8, 517–532, 1970
- PODYAPOLSKIY, G. S.: The propagation of elastic waves in a layered medium, I, II. *Bull. (Izv.) Acad. Sci. USSR, Geophys. Ser.*, 788–793, 913–919, 1959
- PŠENČÍK, I.: Kinematics of refracted and reflected waves in inhomogeneous media with nonplanar interfaces. *Studia geoph. et geod.* 16, 126–152, 1972
- RICHARDS, P. G.: Elastic wave solutions in stratified media. *Geophysics* 36, 798–809, 1971
- : Seismic Waves Reflected from Velocity Gradient Anomalies within the Earth's Upper Mantle. *Z. Geophys.* 38, 517–527, 1972
- SATO, R.: Amplitude of body waves in a heterogeneous sphere. Comparison of wave theory and ray theory. *Geophys. J.* 17, 527–544, 1969

- SECKLER, B. D., and J. B. KELLER: Geometrical theory of diffraction in inhomogeneous media. *J. Acoust. Soc. Am.* 31, 192–205, 1959
- SPENCER, T. W.: Long-time response predicted by elastic ray theory. *Geophysics* 30, 363–368, 1965
- TSEPELEV, N. V.: Propagation of elastic waves in a medium with a transition layer (in Russian). *Proc. Math. Inst. Acad. Sci. of USSR* 95, 184–212, 1968
- UGINČIUS, P.: Intensity equations in ray acoustics. Part I: *J. Acoust. Soc. Am.* 45, 193–205, 1969. Part II: *J. Acoust. Soc. Am.* 45, 206–209, 1969. Part III: Exact two-dimensional formulation. *J. Acoust. Soc. Am.* 47, 339–341, 1970
- VAVILOVA, T. I., and L. V. VOLODKO: Algorithm and programme for the calculation of the intensity of summary multiple reflections propagating without conversions in axially symmetric inhomogeneous layered media (in Russian). *Problems of the Dynamic Theory of Propagation of Seismic Waves* 9, 174–183, Nauka, Leningrad 1968
- VLAAR, N. J.: Ray theory for an anisotropic inhomogeneous elastic medium. *Bull. Seism. Soc. Am.* 58, 2053–2072, 1968
- WESSON, R. L.: A time integration method for computation of the intensities of seismic rays. *Bull. Seism. Soc. Am.* 60, 307–316, 1970
- YACOB, N. K., J. H. SCOTT, and F. A. McKEOWN: Computer ray tracing through complex geological models for ground motion studies. *Geophysics* 35, 586–602, 1970
- YANOVSKAYA, T. B.: Approximate methods in elastic wave theory. Notes of lectures, Dept. of Appl. Math. and Theoret. Physics, Cambridge University, 1968

Interpretation of Discontinuities by Seismic Imaging

J. BEHRENS¹), R. BORTFELD²), G. GOMMLICH¹) and K. KÖHLER²), Clausthal and Hannover

Eingegangen am 16. Februar 1972

Summary: We discuss a method that yields the true geometry of complex seismic interfaces. It is a computer program known under the headings of migration, seismic holography, or seismic imaging.

The method has been successfully applied to model records from sine-shaped discontinuities. On comparing the result of seismic imaging with the known geometry of the model, it is possible to check directly the usability of the procedure.

Zusammenfassung: Im Folgenden wird über eine Methode berichtet, die die wirkliche Geometrie einer komplizierten seismischen Grenzfläche wiedergibt. Es handelt sich dabei um ein Rechenprogramm, das sich auf Verfahren stützt, die unter den Bezeichnungen Migration, seismische Holographie oder seismisches Abbilden bekannt sind.

Diese Methode wurde erfolgreich auf Seismogramme angewendet, die mit Hilfe modellseismischer Messungen an einer sinusförmigen Grenzfläche gewonnen wurden. Die Brauchbarkeit der Rechenprozedur konnte mit dem Vergleich zwischen der bekannten Geometrie des Modells und dem Ergebnis des seismischen Abbildens direkt überprüft werden.

1. Introduction

The paper "Model Investigations with Respect to the Interpretation of Complicated Seismic Discontinuities" [BEHRENS and GOMMLICH, 1972] deals with complex interfaces and shows how complex interfaces might be characterized.

The said paper states that it is possible, by using both kinematic and dynamic parameters of the recorded signals, to discriminate between the individual interfaces, if traveltimes, amplitude and phase spectra, and the phenomena of amplitude variations, can be properly interpreted. This interpretation, i. e. the interrelation between the measured values and the geometry of the interface, is however the crux of the problem.

¹) Prof. Dr. JÖRN BEHRENS und Dipl.-Geophys. GÖTZ GOMMLICH, Institut für Geophysik der Technischen Universität Clausthal, 3392 Clausthal-Zellerfeld, Adolf-Römer-Str. 2A, BRD.

²) Dr. R. BORTFELD und Dipl.-Geophys. K. KÖHLER, PRAKLA-SEISMOS GMBH, 3 Hannover, Haarstr. 5, BRD.

2. Model Investigations

At the meeting of the ESC¹⁾ in Luxembourg, September 1970, it was suggested that special model measurements near the shotpoint should be carried out, i. e. that deep seismic soundings should be modelled. Figs. 1 and 2 were prepared according to this suggestion. The lower part of Fig. 1 shows one of the models investigated.

The two-dimensional model consists of a layer of Plexiglas and a halfspace of Aluminium. Source and receiver are placed on the free surface of the model. The radiation pattern of the source corresponds nearly to the theoretical characteristic of an impact on the free surface of the halfspace. The receiver records the vertical component of acceleration.

The amplitude of the corrugation, ξ_w , is 2.4 cm; the wavelength of the corrugation, λ_w , is 9.6 cm. The wavelength of the incident wave is $\lambda_1 = 3$ cm. The ratio of ξ_w to λ_1 is 0.8, the ratio of λ_w to λ_1 is 3.2. The distance between the shotpoints is $2.25 \lambda_w$, that means the shotpoints are located above different "phases" of the sine-shaped interface.

In the upper part of Fig. 1 are shown the record section for a straight interface, the record section for the corrugated interface, and the computed travel-time curves for the corrugated interface.

The positions of the receivers run from 1 to 43. There is no overlapping. The comparison with records for the straight interface shows the well-known characteristics of deep seismic sounding: a sequence of events, the amplitudes and shapes of which change laterally and timewise; it gives the impression of a series of discrete reflecting elements.

1) „European Seismological Commission.“

Fig. 1: Seismograms and travel-time curves of the investigated model. The positions of the receivers run from 1 to 43 for each shotpoint. Spacing of shotpoints is $2.25 \lambda_w$.

- a) Record section of the reflections (P_1P_1) from a model with a straight interface of first order.
- b) Record section of the reflections (P_1P_1) from a model with a corrugated interface.
- c) Computed travel-time curves for the reflections (P_1P_1) of the corrugated interface model.
- d) Model section with the parameters of the corrugated model and the positions of the shotpoints (SP).
 - λ_1 = predominant wavelength of the incident signal
 - λ_w = wavelength of the corrugation
 - ξ_w = amplitude of the corrugation
 - V_p = P -wave velocity
 - h_1 = thickness of the Plexiglas-layer (from the surface to the central-line of corrugation).

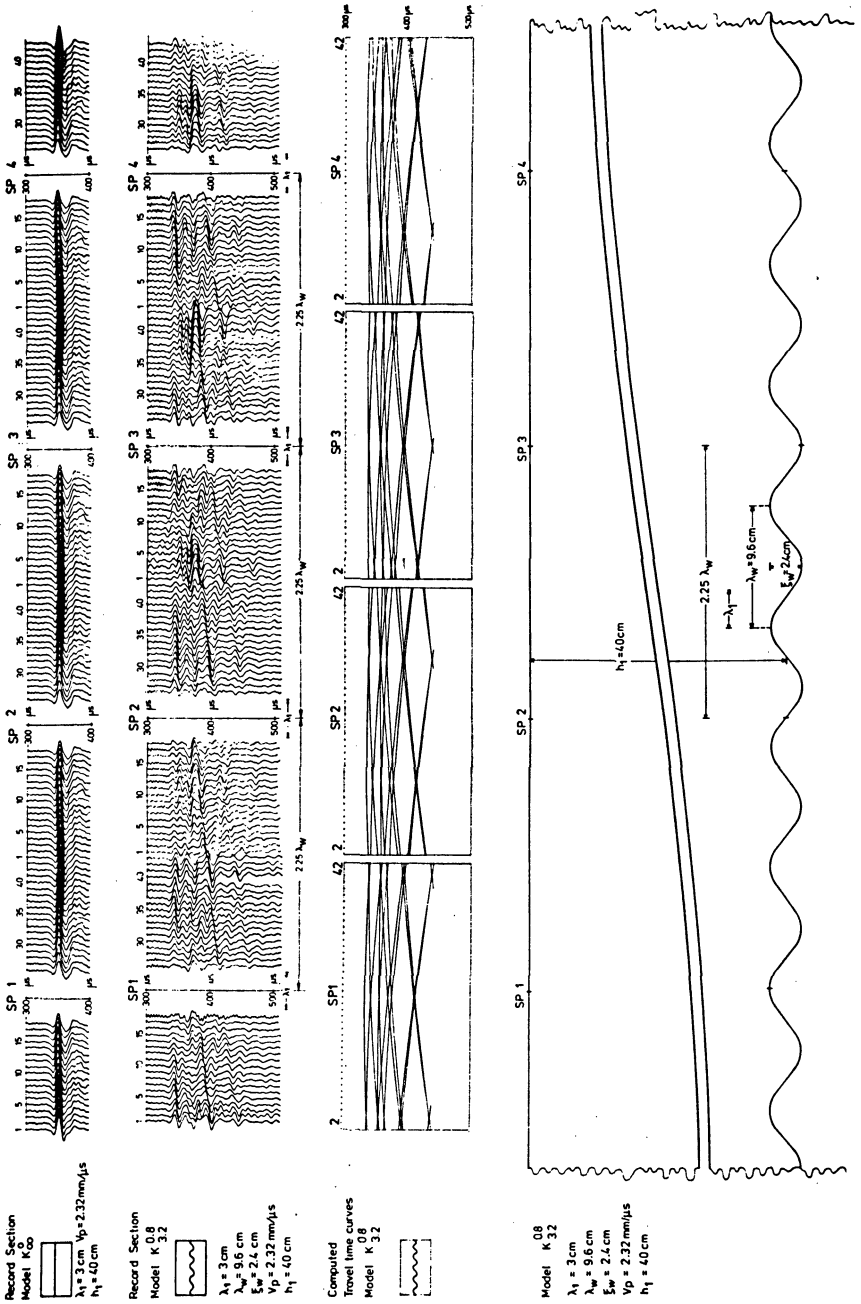


Fig. 2 demonstrates this assertion. The upper part shows once more the seismograms, the lower part the model with the geometry of the interface.

The onsets in the records have been used to construct the apparent reflection elements by the mirror-image-method. The result shows a structure of single reflection-elements one below the other, with different dips above and below the true interface.

Thus, an interpretation according to the usual seismic procedures results in a complex interface structure, but not in the true geometric structure of the interface.

In the following chapters we shall discuss the result of applying seismic imaging.

3. Preprocessing of the model records

Fig. 3 shows the subsurface coverage of the records. The individual traces were dynamically corrected and represented half way between the receiver and the shot.

At first, instead of the meager subsurface coverage of the recorded seismograms, multiple coverage has been simulated. We may assume that the same seismograms would have been recorded if the shotpoints and geophone spreads had been shifted by 9.6 cm (the period of corrugation) along the line. Thus, we assumed further shotpoints, and obtained a spacing of 2.4 cm instead of a shotpoint spacing of 21.6 cm. This yields a 3.75-fold coverage.

Fig. 4 shows the result of stacking of the simulated multiple coverage. Compared with the preceding figure, the present result shows a considerable improvement. The noise level is lower. Further, we can easily recognize the repetition period of 9.6 cm. Although the depth of the highest points of the interface can be recognized, the true shape of the interface cannot yet be seen.

4. Seismic imaging

For a detail-discussion of seismic imaging we refer to the bibliography.

Seismic imaging is an application of Huygens' principle. If any point in space is a diffracting point, we may compute the travel-time curve for the diffracted wave. Seismic imaging basically consists of summing seismic events along these travel-time curves.

For identical positions of shot and receiver, travel-times of the diffracted events are obtained by

$$t = \sqrt{t_0^2 + \left(\frac{2x}{\bar{v}}\right)^2}$$

where

t_0 = two-way travel-time for the vertex of the diffraction curve;

x = horizontal distance from the vertex of the diffraction curve;

\bar{v} = root mean square velocity.

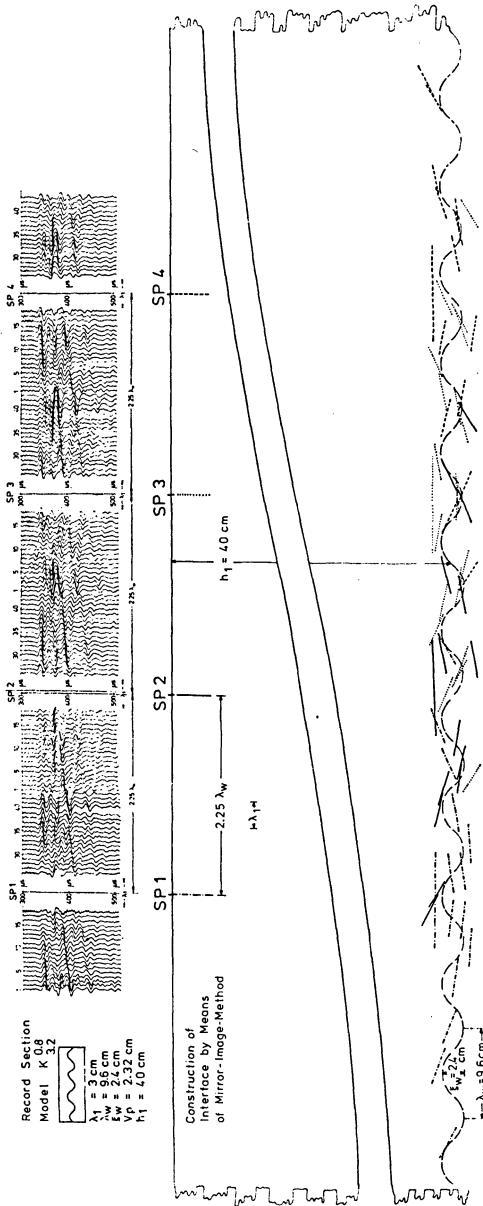
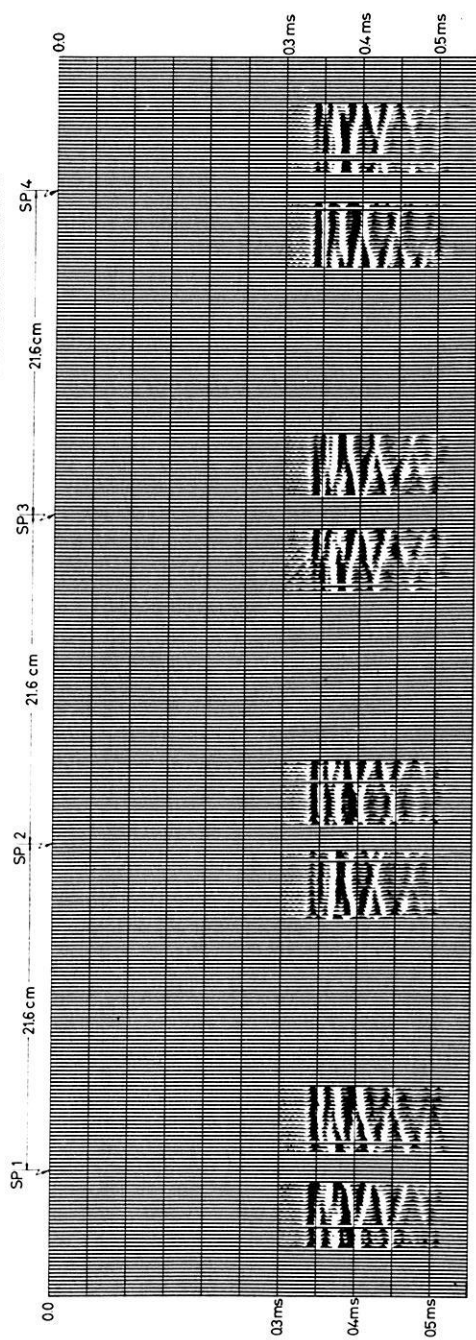


Fig. 2: Interpretation of the record section obtained from the corrugated interface by means of the mirror-image-method.

SEISMOGRAMS REGISTERED ON THE TWO-DIMENSIONAL MODEL BELOW, AFTER DYNAMIC CORRECTION
THE TRACES ARE PLACED IN THE MIDDLE BETWEEN THE RESPECTIVE SHOT POINT AND THE PLACE OF THE RESPECTIVE RECEIVER



CONTOUR OF THE SEISMIC STRUCTURE IN THE MODEL

THE STRUCTURE CONTINUES IN THE SHOWN PERIODICAL WAY IN HORIZONTAL DIRECTION TO BOTH SIDES

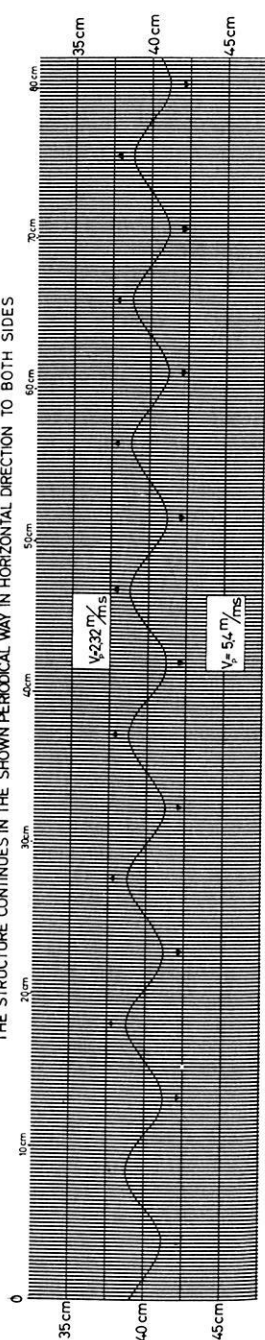
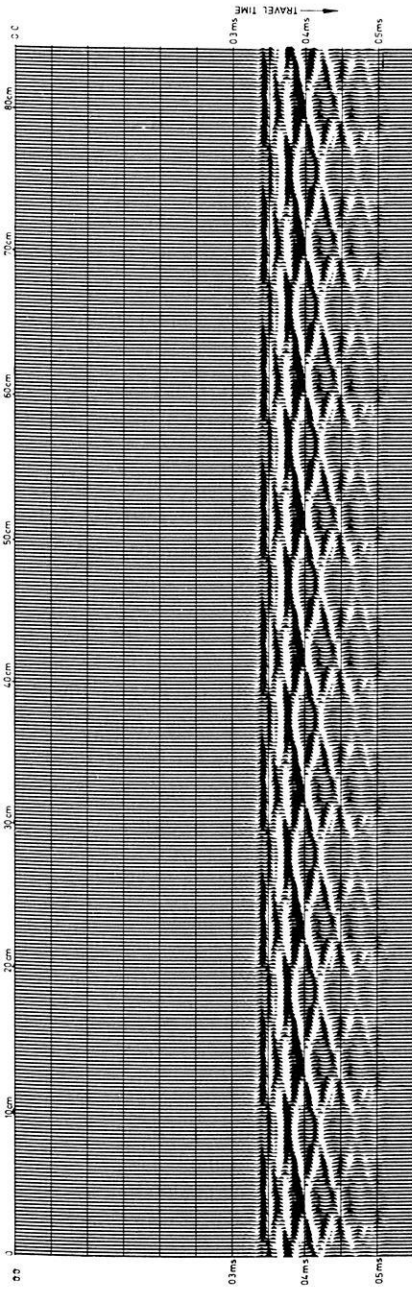


Fig. 3: Corrected seismograms from a two-dimensional model (top). The model is shown at the bottom.

STACKED SECTION FROM SEISMOGRAMS REGISTERED ON A TWO-DIMENSIONAL MODEL
 SPLIT SPREAD SHOOTING, OFFSET: 2cm; RECEIVER SPACING: 0.502cm; NUMBER OF RECEIVERS PER SHOT: 2 x 18; SHOT SPACING: 2.4cm; COVERAGE: 3.75 FOLD



CONTOUR OF THE SEISMIC STRUCTURE IN THE MODEL

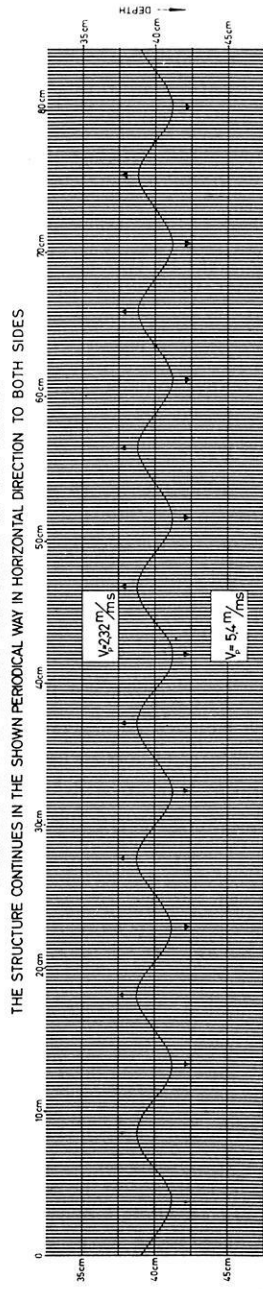


Fig. 4: Stacked section for a two-dimensional model (top). The model is shown at the bottom.

Fig. 5 shows some diffraction travel-time curves for this assumption.

We also assume that stacked traces correspond to a geometry of identical shot and receiver positions. This, however, is an approximation. It is possible to avoid such an approximation by omitting the stacking process. At first, we make use of this approximation and treat the stacked traces as traces without offset.

Seismic imaging means interpreting a seismic section as a superposition of elementary diffracted waves. The superposition will destroy by destructive interference many elementary waves, and the envelope will yield the wave front.

An example of such a stacking of travel-time hyperbolae is presented in Fig. 6. The greater the number of superimposed travel-time hyperbolae the smaller the 'noise' at the respective interface. The limiting case for a great number of elementary waves is shown in Fig. 7.

Fig. 8 shows the stacked section of the model again. The poorly defined hyperbola which is drawn across the section defines the travel-time function of one possible diffracted wave.

Seismic imaging means adding the amplitudes of the seismic traces along such travel-time curves. The sum is the result of imaging for the vertex of the curve. The procedure must be repeated for all samples of the result-trace, and for all traces of the migrated section.

4.1 Seismic imaging of the stacked data

By applying seismic imaging to the stacked model records in Fig. 4, we get the section in Fig. 9. It is represented as a time section. In order to get the corresponding depth section, one has to multiply the vertical scale by the factor $V_p/2$.

The undulating structure of the interface can clearly be seen. The amplitude of the corrugation is exact. The quality of the image is satisfactory.

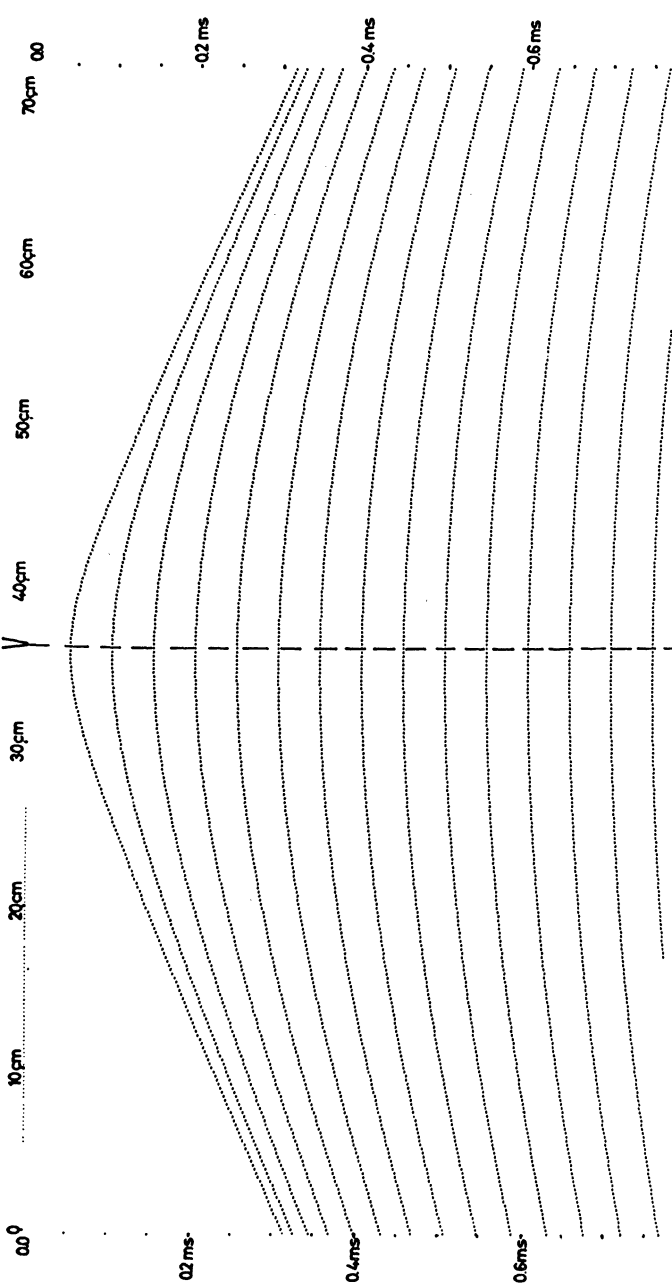
Fig. 5: Diffraction travel-time curves for identical positions of shot and receiver.

- t = travel-time for a point on a hyperbola of diffraction
- t_0 = travel-time in the vertex of the hyperbola of diffraction in question
- x = horizontal distance from the vertex of the hyperbola of diffraction in question
- \tilde{v} = root mean square velocity
- = vertical line with diffracting points ($x=0$)

POSSIBLE CURVES OF DIFFRACTION IN A SEISMIC SECTION.

THE TRAVEL PATHS FORTH AND BACK ARE IDENTICAL. SEISMIC VELOCITY: $V_p = 2,32 \text{ m/ms}$

$X=0$



THE TRAVEL-TIMES CORRESPOND TO THE FORMULA:

$$t = \sqrt{t_0^2 + \left(\frac{2X}{V}\right)^2}$$

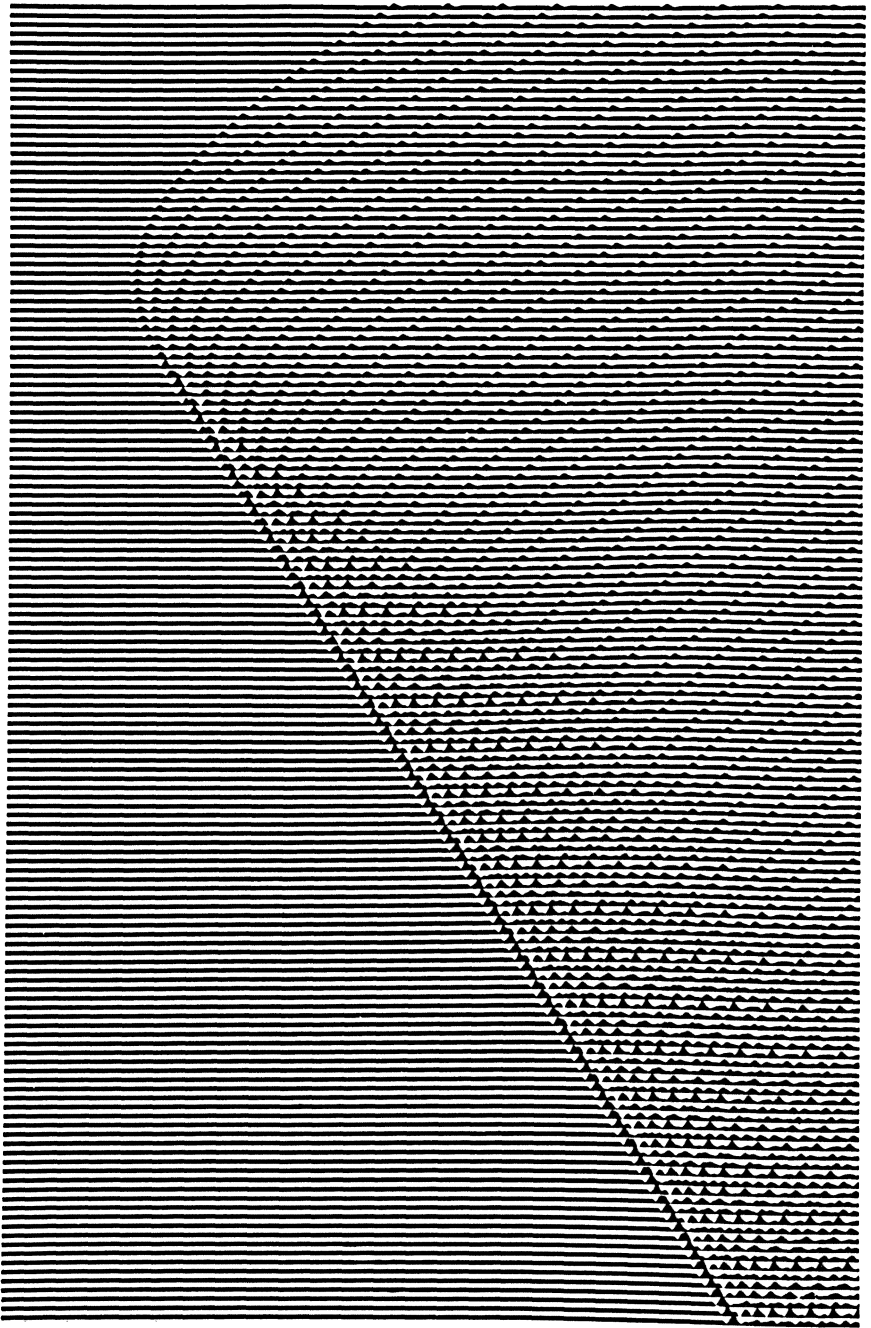


Fig. 6: Diffraction hyperbolae for discrete points on an inclined, truncated interface.

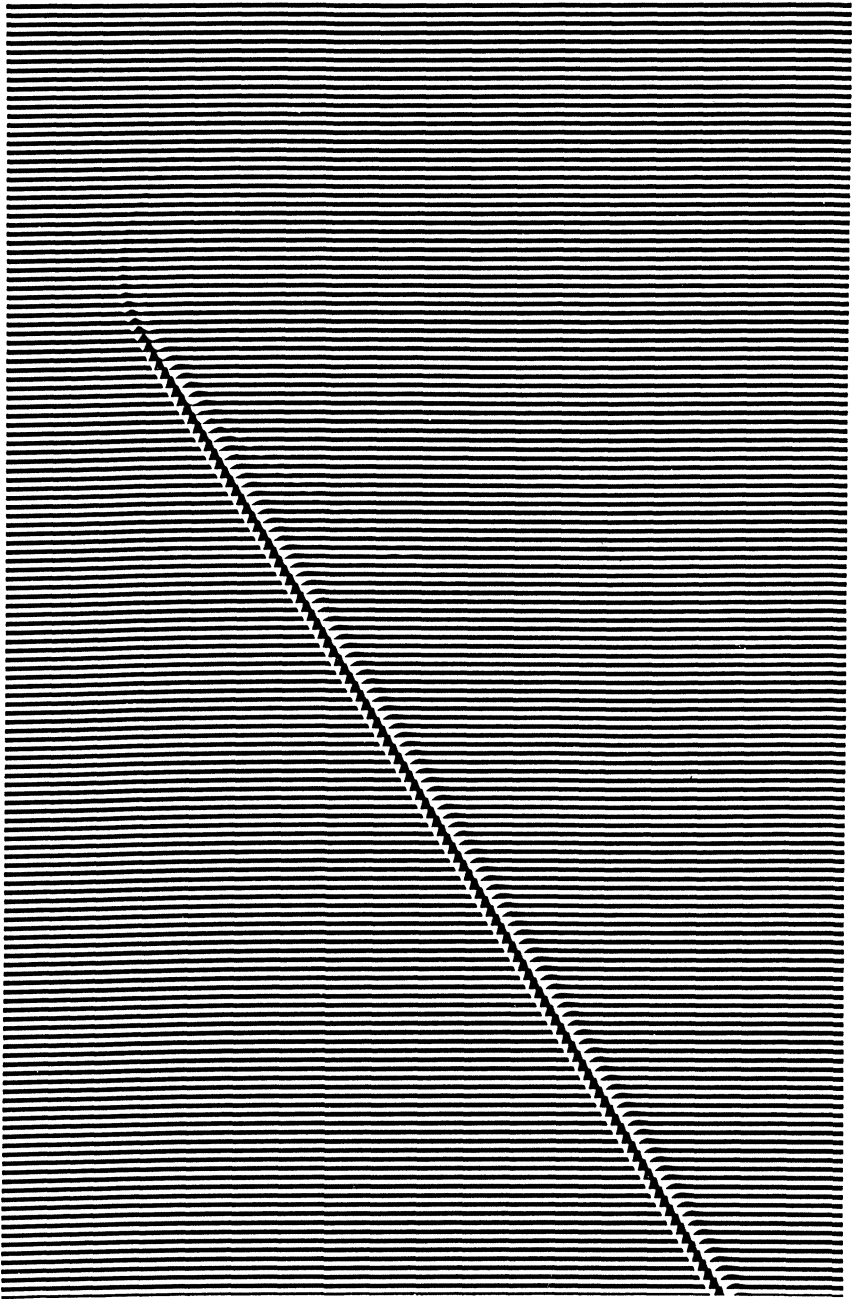
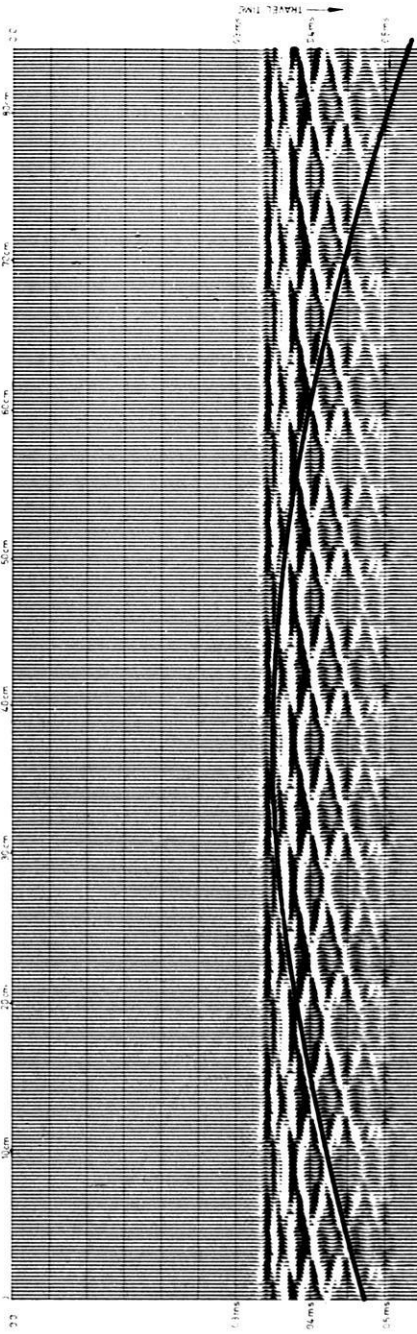


Fig. 7: Limiting case of Fig. 6 with an infinite number of diffracting points.

STACKED SECTION FROM SEISMOGRAMS REGISTERED ON A TWO-DIMENSIONAL MODEL

SPLIT SPREAD SHOOTING, OFFSET: 2 cm, RECEIVER SPACING: 0.502 cm, NUMBER OF RECEIVERS PER SHOT: 2 * 18, SHOT SPACING: 2.4 cm, COVERAGE: 3.75 FOLD



CONTOUR OF THE SEISMIC STRUCTURE IN THE MODEL

THE STRUCTURE CONTINUES IN THE SHOWN PERIODICAL WAY IN HORIZONTAL DIRECTION TO BOTH SIDES

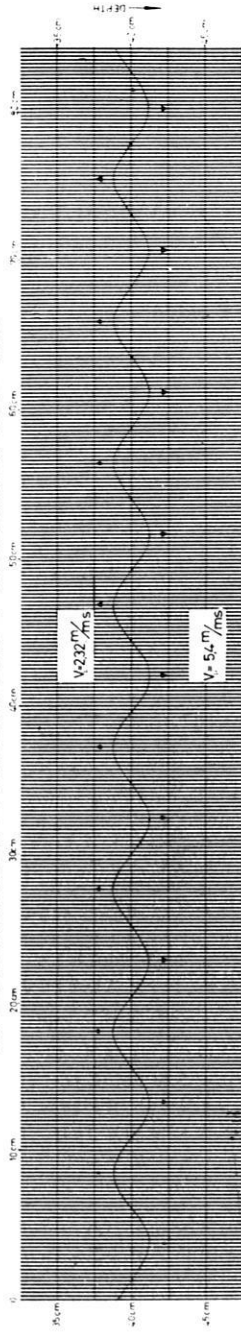


Fig. 8: Stacked section with one diffraction travel-time curve (poorly defined).

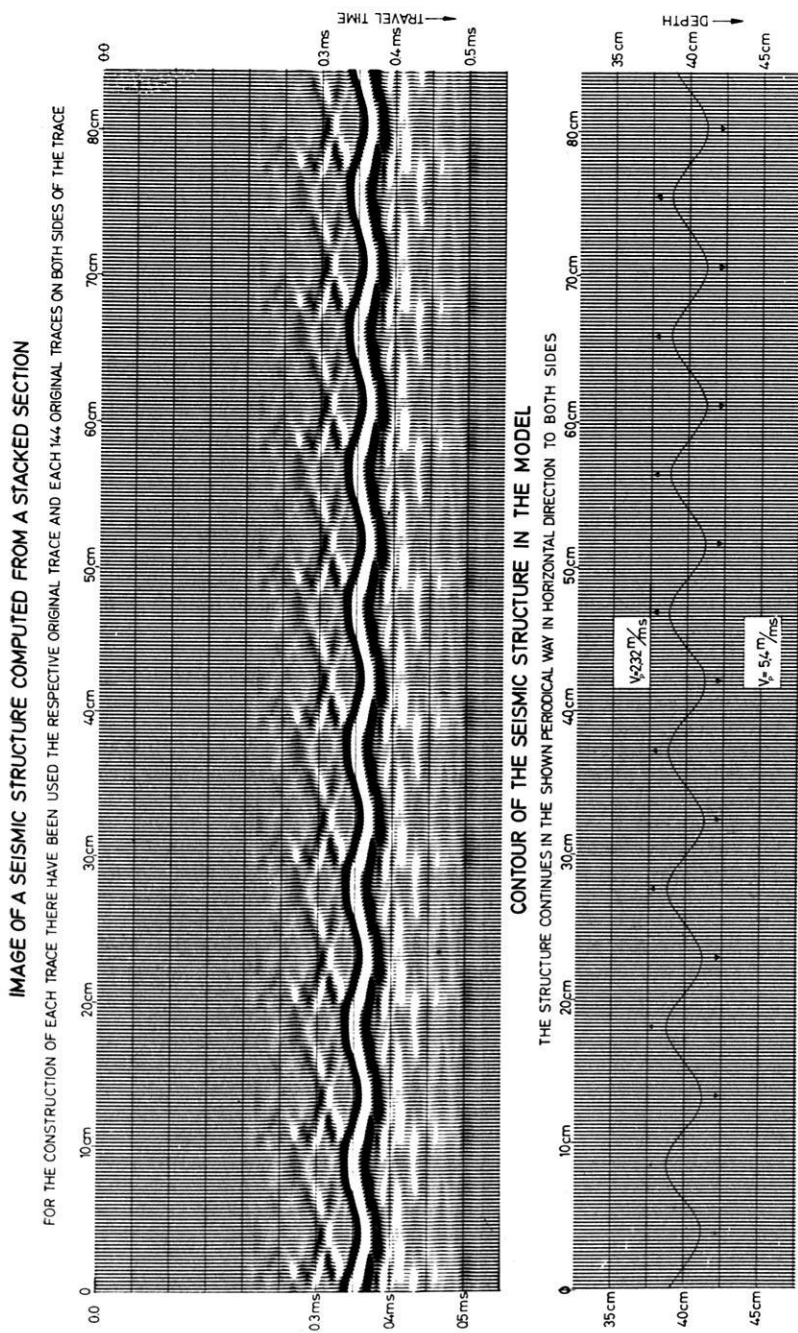


Fig. 9: Seismic imaging of the records in Fig. 4.

4.2 Seismic imaging of the unstacked data

Seismic imaging of unstacked data works with the original traces, before any dynamic correction. Assuming any subsurface point to be a diffracting point, one may compute, for a given geometry of shot and receiver, the travel-time curve for the diffracted event. The original seismic trace is sampled at this travel-time. The sum of these samples, for a sufficiently large number of traces, is the result for this particular subsurface point. The procedure is repeated for every sample and for every trace of the output section.

Naturally, this type of imaging takes more computer time.

The result of seismic imaging of the unstacked model records is shown on the right hand side of Fig. 10. As compared with Fig. 9, the result has been improved. There is less noise. The region of maximum dip at the zero crossings of the sine is a little clearer.

5. A note on the number of traces used for imaging

According to Huygens' principle, the diffraction travel-time curve, along which we sample and sum the seismic traces, has to be extended to infinity. This, of course, is not feasible. We must cut the curves somewhere.

We reworked the imaging of the stacked data with various extensions of the diffraction curves. The result is shown in Fig. 11.

We extended the diffraction curves over 3, 49, 145, 241, and 337 traces, respectively. That means that any output sample was obtained by adding samples from 3, 49, 145, 241, or 337 traces, respectively.

It is obvious that about 300 traces must be used. That means one must record, and finally use with the imaging procedure, seismic traces from at least 80 cm of the model.

On transforming the scale of our model to the search for the *M*-discontinuity, we must multiply by roughly 100000. Thus, as a result of the model investigations, at least 80 km must be used for recording and for computing.

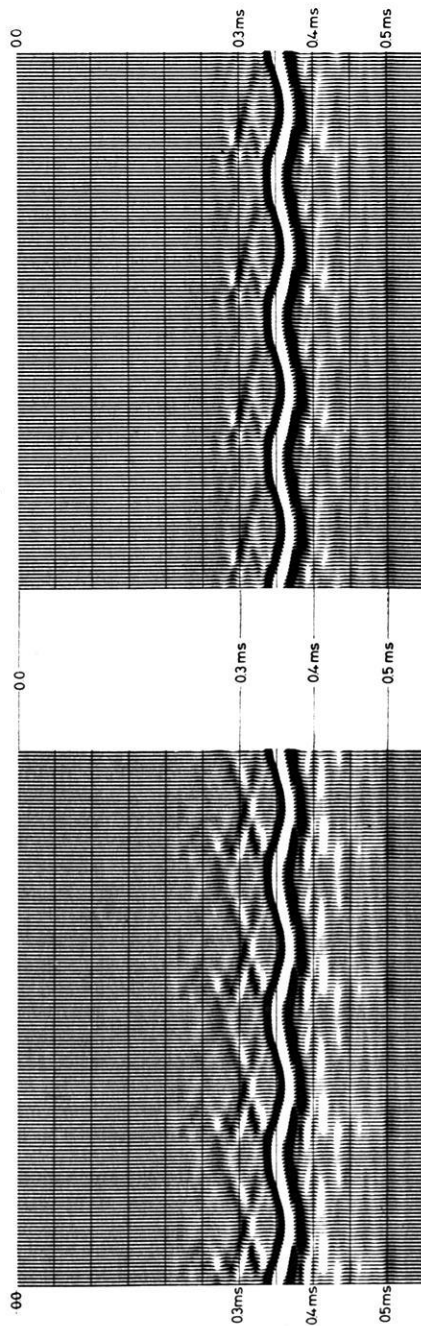
Fig. 10: Comparison of seismic imaging of stacked records (left) with seismic imaging of unstacked uncorrected records (right).

COMPARISON OF TWO IMAGES OF A SEISMIC STRUCTURE GENERATED BY DIFFERENT METHODS

LEFT: IMAGING FROM STACKED SECTION

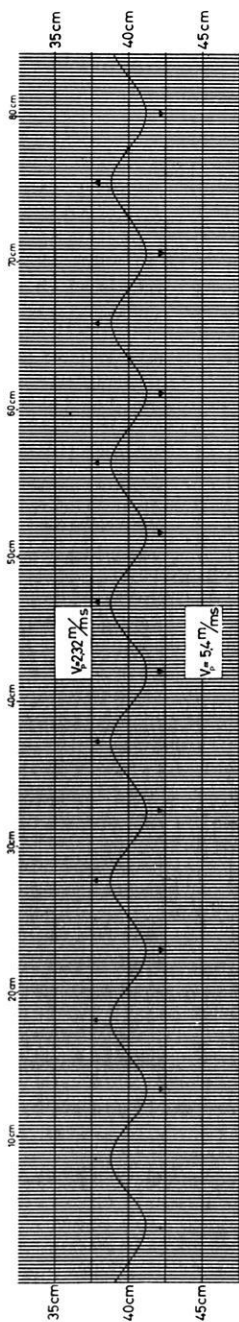
RIGHT: DIRECT IMAGING FROM DYNAMICALLY NOT CORRECTED SEISMOGRAMS

IN BOTH CASES FOR THE CONSTRUCTION OF A TRACE THERE HAVE BEEN USED ALL ORIGINAL TRACES UP TO 144 TRACES DISTANT FROM THE NEW TRACE
 SPLIT SPREAD SHOOTING, OFFSET: 2cm RECEIVER SPACING: 0.502cm, NUMBER OF RECEIVERS PER SHOT: 2+18, SHOT SPACING: 24cm, COVERAGE: 3.75 FOLD



CONTOUR OF THE SEISMIC STRUCTURE IN THE MODEL

THE STRUCTURE CONTINUES IN THE SHOWN PERIODICAL WAY IN HORIZONTAL DIRECTION TO BOTH SIDES



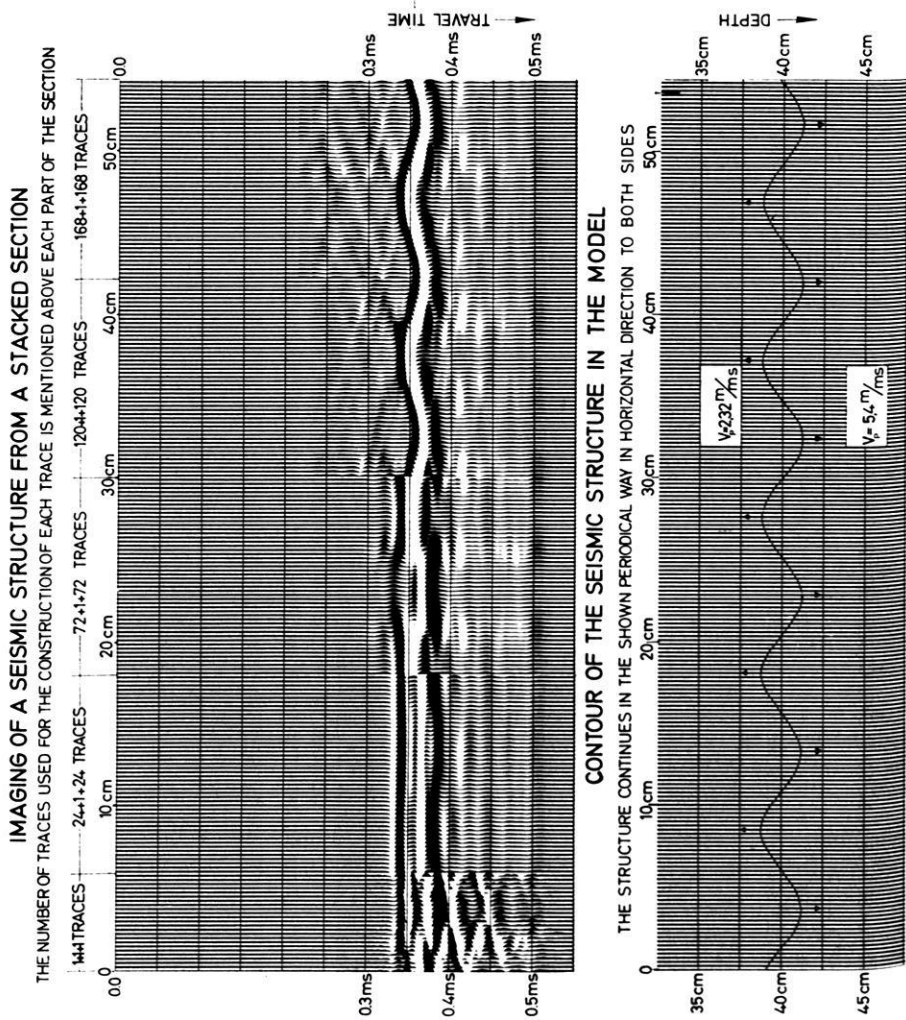


Fig. 11: Comparison of seismic imaging using different numbers of traces.

6. Conclusions

The described application of seismic imaging to seismic model measurements demonstrates the usefulness of seismic imaging for the characterization of complicated boundary structures.

The limited validity of the general evaluation methods for deep seismic sounding becomes obvious.

The dimension of the survey and the large number of data which are required for a real characterization of discontinuities in the Earth's crust and upper mantle lead to a new aspect of field investigations.

7. Acknowledgements

The model investigations were sponsored by the Deutsche Forschungsgemeinschaft.

References

- ABUBAKAR, J.: Scattering of plane elastic waves at rough surfaces I. *Proc. Cambridge Phil. Soc.* 58, 136–157, 1962
- ASANO, S.: Reflection and refraction of elastic waves at a corrugated interface. *Bull. Seism. Soc. Am.*, 56, 201–221, 1966
- BEHRENS, J.: Die Charakterisierung seismischer Grenzflächen mit Hilfe modellseismischer Verfahren im Hinblick auf Deutungsmöglichkeiten des Krustenaufbaus. *Habilitationschrift, Technische Universität Clausthal*, 1969
- BEHRENS, J.: Model investigations on the boundary structure Earth's crust/mantle. *Proceedings of the 12th General Assembly of the European Seismological Commission, Luxembourg*, 1971
- BEHRENS, J., and G. GOMMLICH: Model investigations with respect to the interpretation of complicated seismic discontinuities. *Z. Geophys.* 38, 659–673, 1972
- BEHRENS, J., J. KOZÁK, and L. WANIEK: Investigation of wave phenomena on corrugated interfaces by means of the Schlieren-method. *Proceedings of the 12th General Assembly of the European Seismological Commission, Luxembourg*, 1971
- BORN, M., and E. WOLF: *Principles of Optics*. Pergamon Press, 1959
- BORTFELD, R.: Seismic and optical imaging. Paper presented at the 33rd Meeting of the European Association of Exploration Geophysicists (EAEG), Hannover, 1971
- BORTFELD, R.: Seismische Abbildungen. Paper presented at the 16th Geophysical Symposium in Siófók, Hungary, 1971
- FARR, J. B.: Earth holography, a potential new seismic method. Paper presented at the 38th Meeting of the Society of Exploration Geophysicists (SEG), Denver, 1968
- FONTANEL, A.: *Holosismique*, Dissertation, Paris, 1971

- FONTANEL, A., and G. GRAU: Principe de l'holographie sismique. Paper presented at the 31st Meeting of the European Association of Exploration Geophysicists (EAEG), Venice, 1969
- FONTANEL, A., and G. GRAU: Application of impulse seismic holography. Paper presented at the 39th Meeting of the Society of Exploration Geophysicists (SEG), Calgary, 1969
- FONTANEL, A., G. GRAU, and CH. HEMON: Holosismique impulsionelle. Paper presented at the 32nd Meeting of the European Association of Exploration Geophysicists (EAEG), Edinburgh, 1970
- GOMMLICH, G., and E. KITTER: Modellseismische Untersuchungen über den Entstehungs- und Ausbreitungsmechanismus reflektierter Wellen an welligen Grenzflächen. Paper presented at the 31st Meeting of the Deutsche Geophysikalische Gesellschaft (DGG), Karlsruhe, 1971
- HEMON, CH.: Restitution automatique en profondeur. Proceedings of the 8th World Petroleum Congress, Panel Discussion, 6, 1971
- KITTER, E.: Modellseismische Untersuchungen über den Ausbreitungsmechanismus reflektierter Wellen an welligen Grenzflächen. Diplomarbeit, Technische Universität Clausthal, 1971
- LERWILL, W. R.: Holography at seismic frequencies. Paper presented at the 31st Meeting of the European Association of Exploration Geophysicists (EAEG), Venice, 1969
- LEVY, A., and H. DERESIEWICZ: Reflection and transmission of elastic waves in a system of corrugated layers. Bull. Seism. Soc. Am., 57, 393–419, 1967
- LINDSEY, J. P.: Direct migration of seismic data. Paper presented at the 40th Meeting of the Society of Exploration Geophysicists (SEG), New Orleans, 1970
- POHL, R. W.: Einführung in die Mechanik, Akustik und Wärmelehre. 10th and 11th edition, fig. 381, Berlin und Göttingen, 1947
- ROCKWELL, D. W.: Migration stack aids interpretation. The Oil and Gas Journal, April, 1971
- SCHNEIDER, W. A., and A. ALAM: Migration stack process. Paper presented at the 40th Meeting of the Society of Exploration Geophysicists (SEG), New Orleans, 1970

Amplitude-Distance Curves of Seismic Body Waves in the Neighbourhood of Critical Points and Caustics — A Comparison

V. ČERVENÝ and J. ZAHRADNÍK, Prague¹⁾

Eingegangen am 7. Februar 1972

Summary: The amplitude-distance curves of refracted waves in the neighbourhood of the caustic are compared with those of reflected waves in the critical region. When the caustic is connected with the left reversal (cusp) of the travel-time curve, the behaviour of both amplitude-distance curves is very similar. The maximum amplitude does not occur just at the caustic (or at the critical point) as would follow from the ray theory, but is shifted to larger epicentral distances. The position of the maximum is frequency dependent. The higher the frequency, the smaller the shift. Certain quantitative differences are found and discussed in detail. For the caustic connected with the right reversal of the travel-time curve, the shift is opposite — to smaller epicentral distances.

Zusammenfassung: Die Amplitudenkurven von Refraktionswellen in der Nähe der Kaustik und von Reflexionswellen im kritischen Bereich werden verglichen. Falls die Kaustik dem linken Wendepunkt der Laufzeitkurve entspricht, haben beide Amplitudenkurven einen sehr ähnlichen Verlauf. Die maximale Amplitude liegt nicht genau in der Kaustik (oder im kritischen Punkt) — wie aus der Strahlentheorie folgt —, sondern sie ist in Richtung größerer Epizentralentfernungen verschoben. Die Lage des Maximums ist frequenzabhängig. Je höher die Frequenz, um so kleiner ist die Verschiebung. Es wurden einige quantitative Unterschiede gefunden, die in der Arbeit ausführlich diskutiert werden. Für die Kaustik, die dem rechten Wendepunkt entspricht, entstehen Verschiebungen in umgekehrter Richtung, d. h. zu kleineren Epizentralentfernungen.

1. Introduction

The most important seismic body waves propagating in the Earth's crust are waves reflected from various discontinuities and refracted (diving) waves. Refracted waves are usually used to find the velocity-depth distribution, the reflected waves give information about seismic discontinuities.

The interpretation based on travel-times only is not unique. The travel-time curve of refracted waves is not simple and has very often two, three or more branches. Some of these branches can be similar to the travel-time curves of reflected waves

¹⁾ Dr. VLASTISLAV ČERVENÝ and Dr. JIŘÍ ZAHRADNÍK, Geofyzikální ústav Karlovy university, Ke Karlovu 3, Praha-2, ČSSR.

in certain regions of epicentral distances. These facts, together with others, can lead to serious errors in the interpretation.

To avoid mistakes in the solution of an inverse problem, a comparison of theoretical and experimental amplitude-distance curves corresponding to individual waves can be very useful. Such epicentral distances, in which strong waves are recorded, are the most informative. This applies, for example, to the critical region in the case of reflected waves. Similarly, the neighbourhood of the caustic is very important in the case of refracted waves.

In both these cases, the travel-time curves of recorded waves are very similar. Two branches of the travel-time curve are tangent one to another at a critical point as well as at a caustic. However, the physical mechanism of the concentration of the seismic energy is rather different. Unlike a critical point, the caustic need not be connected with any discontinuity of first order in the medium.

It is well known that the ray theory fails in the neighbourhood of critical points and caustics, other methods must be used for the theoretical investigation. The basic theoretical problems connected with caustics have been solved by BREKHOVSKIKH [1960], YANOVSKAYA [1964, 1968], GAZARYAN [1961], LUDWIG [1966], SATO [1969], and others. The neighbourhood of critical points was studied in detail, e.g. by SMIRNOVA [1959], MÜLLER [1968a, 1968b, 1969], and ČERVENÝ [1965, 1971].

The aim of this paper is to discuss the amplitude-distance curves in the neighbourhood of caustics and to compare them with those in the neighbourhood of critical points. Some similarities, as well as differences are found.

2. Theoretical considerations

To find theoretically the most characteristic properties of body seismic waves in the neighbourhood of critical points and caustics, simple models of media will be used in this paper. The investigation of more realistic models of the earth's crust will be easier after this preliminary study.

Theoretical travel-times and amplitudes of seismic body waves can be approximately calculated using the ray methods [ALEKSEYEV, BABICH, and GEL'CHINSKIY 1961]. It was mentioned in the introduction that the ray theory fails in the neighbourhood of critical points and caustics. Certain modifications of the ray theory or the wave methods must be used. Modified asymptotic wave methods [ČERVENÝ 1965, BREKHOVSKIKH 1960] that remove some difficulties connected with the above singularities (e.g., the infinite values of amplitudes) are used. These methods are also only asymptotic with respect to frequency. They become more accurate when the frequency increases.

2.1 Description of a medium

Let us suppose that the isotropic perfectly elastic medium is composed of a system of planparallel layers (thick as regards the wavelength), located on a half-space. The velocities of seismic body waves depend on the depth only. The ratio of P - and S -

velocities is constant ($=\sqrt{3}$) through the whole medium as well as the density. The point source is located near the surface. A spherical harmonic P -wave is emitted from the source. The frequency of the source is assumed to be so high that the changes of the velocity on the wavelength within the layers are small.

The following notation will be used: a denotes the P -wave velocity, z the depth, r the epicentral distance, f the frequency, λ the wavelength.

Two types of models will be considered:

(i) The models composed of homogeneous layers separated by discontinuities of first order. The most important waves propagating in these models of media are waves reflected from various discontinuities of first order and head waves. To simplify the discussion, we shall deal only with models with one homogeneous layer located on a homogeneous half-space. The thickness of the layer is denoted by H , the P -velocity in the layer by a_1 , the P -velocity in the half-space by a_2 , the refractive index by n ($n = a_1/a_2$). It is assumed that $n < 1$. Wave reflected from the sharp boundary and the corresponding head wave will be of interest. Both these waves interfere in the critical region ($r \sim 2Hn/(1 - n^2)^{\pm}$).

(ii) The models composed of generally inhomogeneous layers without any boundary of first order in the medium. The most important waves propagating in these models are refracted waves (also known as diving waves or internally reflected waves). In the ray conceptions, the rays of refracted waves are those with a smooth minimum inside the medium. The caustic can be formed by the rays of refracted waves. Models with one second order discontinuity will mainly be dealt with. The velocity in individual layers varies linearly with the depth. The gradient of velocity in the lower layer (half-space) is higher than that in the upper layer. Also more complicated models, without any boundary of second order, will be considered [JANSKÝ 1969, 1970].

2.2 Wave field in the neighbourhood of the caustic

By the definition, the caustic points are those at which the cross-sectional area of an elementary ray tube equals zero. Thus, at a caustic and its immediate neighbourhood, the seismic energy is concentrated.

By the equivalent definition, a caustic is an envelope of rays. It separates the shadow from the illuminated (lit) region. There are no rays in the shadow but two rays are passing through each point of the lit region. These rays form two branches of the travel-time curve in the lit region.

Note that the term "caustic" is used here to denote not only the envelope of rays (as defined above) but also the point at which the envelope intersects the surface.

It should be mentioned that the refracted wave can have more than two branches and that the rays corresponding to other branches can penetrate into the "shadow" zone described above. In the following, we shall invariably consider those two

branches which form the caustic separately from the (possible) other branches. Sometimes the other branches are not considered at all.

Simple examples of time-distance curves are given in Fig. 1. Three models are considered, all with the interface of second order at a depth of 15 km. The travel-time curve corresponding to the first model (with homogeneous upper layer) has only one cusp point at the epicentral distance of $r^* = 120$ km, at which the caustic intersects the surface. (The direct wave propagating in a homogeneous layer is not taken into account.) In the case of models 2 and 3, the time-distance curve has two cusp points; a loop is formed. Only the cusp point I at smaller epicentral distance corresponds to the caustic. The turning point II is caused by the interface of second order. In other words, the caustic is formed only by rays having the smooth minimum in the lower layer. The lower branch of the travel-time curve (which is not connected with the caustic at I) corresponds to the rays with the minimum in the upper layer. This wave will be treated separately.

As has been shown in Fig. 1, not every cusp point of the travel-time curve is connected with the caustic (with the concentration of energy). For example, the reversals due to the discontinuity of second order (they are denoted by II in Fig. 1) are not connected with caustics. However, the more complicated models without any discontinuity of first or second order, will be considered in which both two cusp points correspond to caustic (Fig. 10). In such a case, the wave field of refracted wave between both caustics can be very complicated, particularly when the distance between them is small. In this paper, both these caustics are formally treated separately.

2.3 Theoretical amplitudes in the neighbourhood of caustics

For the calculation of the *P*-wave amplitudes, the wave method has been used starting from the wave equation. However, for the inhomogeneous elastic medium, the system of the wave equations for *P*- and *S*-waves is not equivalent to the equation of motion. The conditions at which this simplification is permitted in the vicinity of a caustic are briefly discussed in [ZAHRADNÍK 1970] where the method used is described in greater detail.

The method is based on the asymptotic approximation of the formal (integral) expression of the *P*-wave potential. In the neighbourhood of a caustic, there are two saddle points close to each other, but also another saddle points can exist. The high-frequency contributions of individual saddle points are identical with the zero approximation of the ray theory. In the high-frequency ray conceptions, the saddle points close to each other correspond to the rays forming the caustic. Their asymptotic contributions are infinite at a caustic. Other saddle points correspond to other branches of the travel-time curve. They usually give smooth contributions across the epicentral distance corresponding to the caustic. As an example, see the lower branch of the travel-time curve in models 2 and 3, Fig. 1, corresponding to the rays with the minimum in the upper layer.

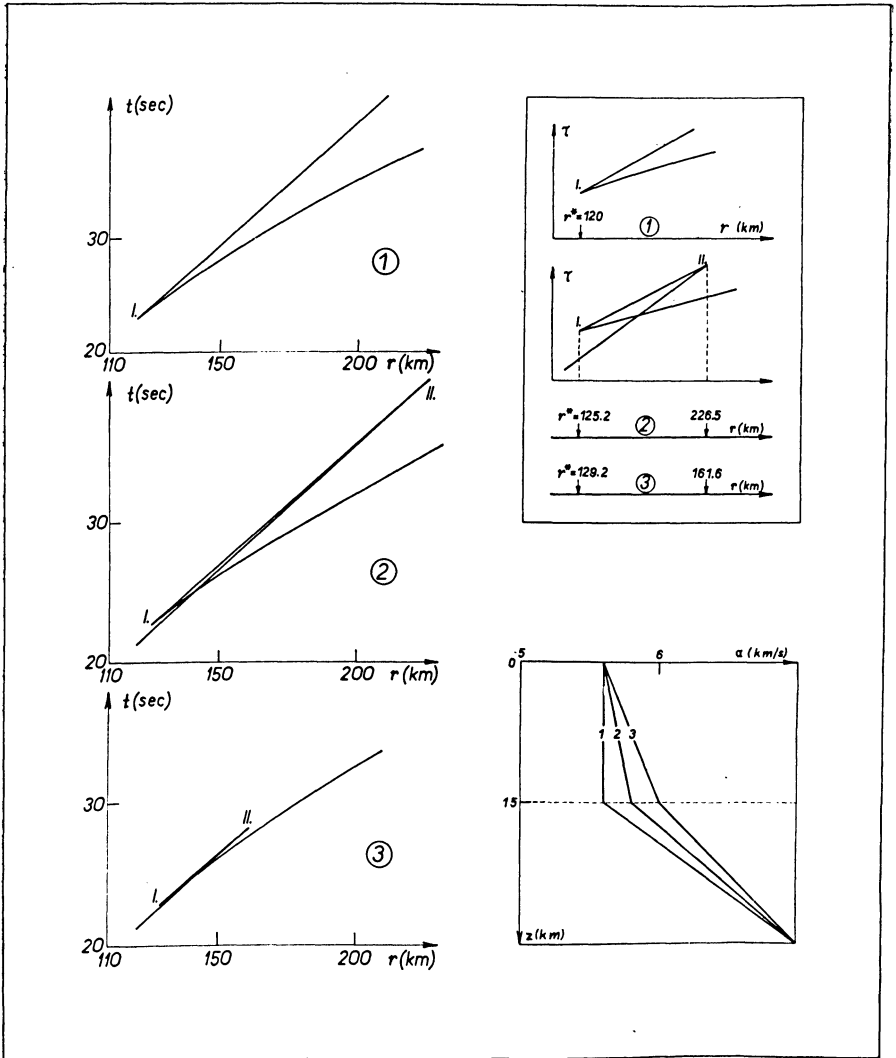


Fig. 1: Travel-time curves (on the left) and their schematic presentations for three given velocity-depth graphs. The reversal points denoted by I are connected with the caustics (r^*).

The modified asymptotic formulae have been derived for the interference wave field corresponding to the saddle points close to each other using the so-called integral approximation of third order [BREKHOVSKIKH 1960]. The phase function of the integral solution has been approximately expressed by the Taylor series up to the third order; the Airy function has been used. Not only the wave field in the "lit region" but also in the "shadow" have been approximately obtained. We must bear in mind that such formulae fail if more than two saddle points are close one to another. This applies, e.g. to the region between two caustics which are close to each other.

The example of the amplitude-distance curve in the neighbourhood of a caustic is given in Fig. 2. The amplitude curves of refracted waves found by different formulae for a simple model of medium are presented. The curve \bar{V} computed by ray formulae has two branches (1 and 2) corresponding to the two branches of the travel-time curve. It reaches infinity at the caustic. \bar{V}_i denotes the amplitude curve of the interference refracted wave, formed by the superposition of both above branches. As both branches are infinite at the caustic, \bar{V}_i is also infinite there. The curve \tilde{V} was

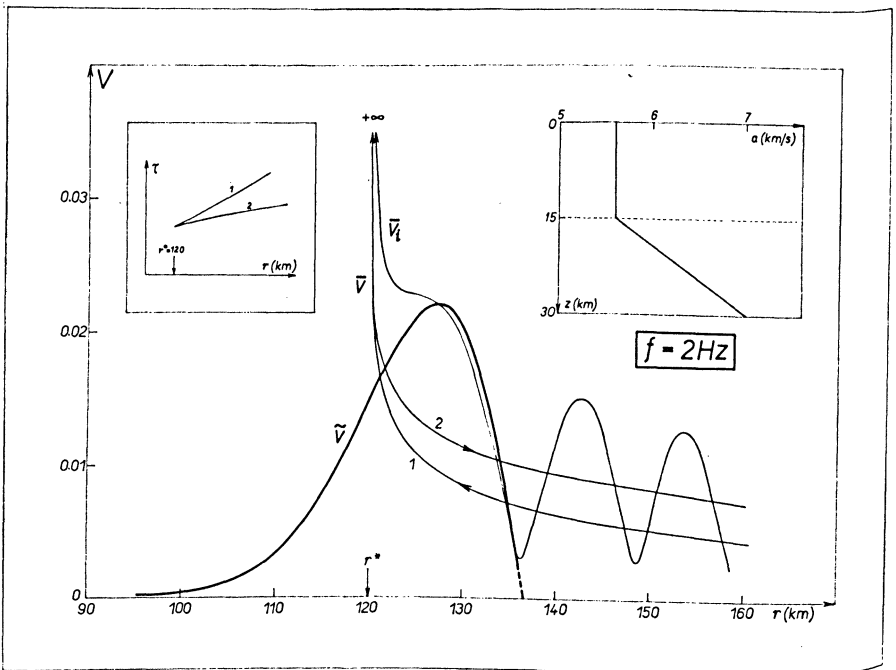


Fig. 2: Amplitude-distance curve of refracted waves in the neighbourhood of the caustic (r^*) found by different methods. The schematic presentation of the travel-time curve and the velocity-depth graph are given in the small frames. For details, see text.

found by modified asymptotic formulae [ZÁHRADNÍK 1970]. It increases from very small values in the shadow, is finite at the caustic, and reaches its maximum beyond the caustic. The modified asymptotic formulae give the better approximation of the wave field of refracted wave in the region of the caustic than the ray ones (compare \tilde{V} and V_i). At larger epicentral distances beyond the caustic, modified asymptotic formulae cannot be used; the ray formulae are, however, applicable. Note that both methods give practically the same amplitudes in some range of epicentral distances beyond the caustic.

2.4 Theoretical amplitudes in the neighbourhood of critical points

The methods for the investigation of the wave field in the critical regions are well known. Exact ray theory or various modifications of the ray theory can be used. For details see ČERVENÝ and RAVINDRA [1971] where other references are given.

An example of the amplitude-distance curves in the neighbourhood of the critical point is given in Fig. 3. The parameters of the medium are as follows: $a_1 = 6.4$ km/

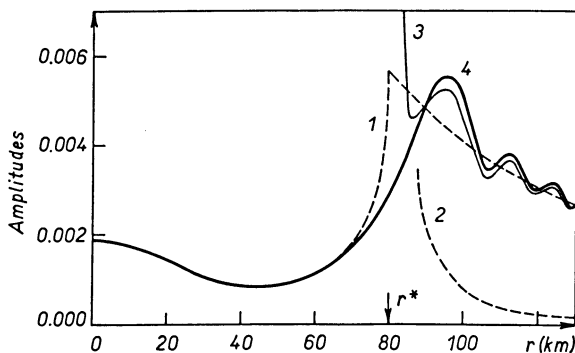


Fig. 3: Amplitude-distance curve of reflected waves in the neighbourhood of the critical point (r^*) found by different methods. For details, see text.

sec, $a_2 = 8$ km/sec, $n = a_1/a_2 = 0.8$, $H = 30$ km, $f = 6.4$ Hz (cps.). The amplitudes of reflected wave (1), head wave (2), and interference reflected-head wave (3) were computed by the ray formulae. The ray amplitudes of head waves and interference reflected-head waves reach infinity at the critical point. In contrast to the ray theory, the amplitude curve (4) of the reflected wave found by modified asymptotic formulae is finite and smooth at the critical point. It reaches its maximum beyond the critical point.

3. Amplitude-distance curves

The amplitude-distance curves depend on the parameters of medium as well as on the frequency. The dependence on frequency is particularly expressive in the neighbourhood of critical points and caustics.

3.1 The influence of frequency

The amplitude-curves of refracted waves in the immediate neighbourhood of the caustic for different values of the frequency are given in Fig. 4. The modified asymptotic formulae were used to compute these curves. The amplitude curves for finite frequencies are quite smooth and continuous in the neighbourhood of the caustic and have a maximum value at a certain distance beyond the caustic. When the frequency increases, the amplitude curve is narrower and has a more pronounced maximum, closer to the caustic.

The situation in the neighbourhood of a critical point is similar. In Fig. 5, the amplitude curves of reflected waves for different values of the frequency are plotted.

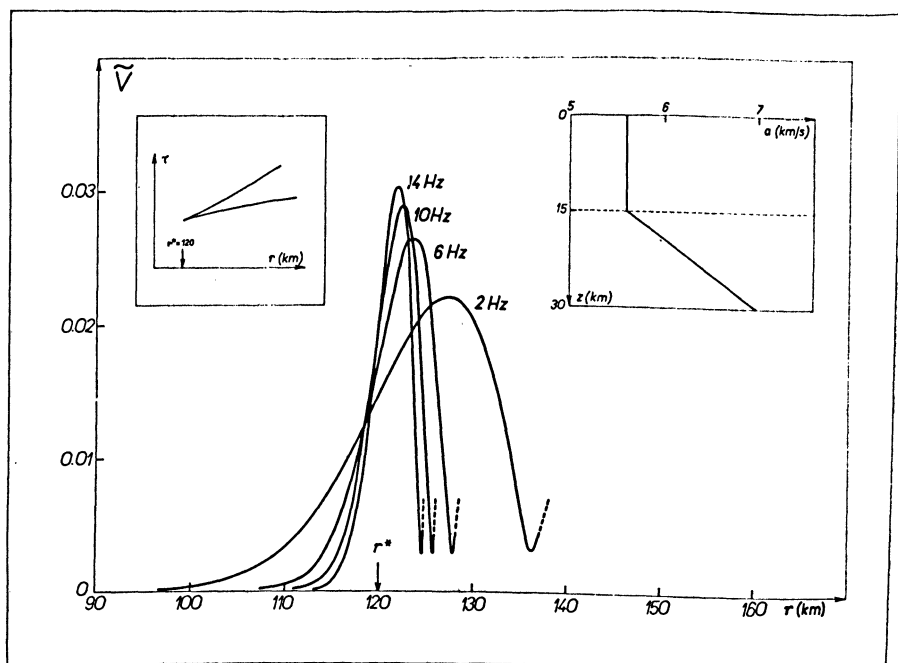


Fig. 4: Amplitude-distance curves of refracted waves in the immediate neighbourhood of the caustic (r^*) for different frequencies ($f = 2, 6, 10, 14$ Hz). The schematic presentations of the travel-time curve and the velocity-depth graph are given in small frames.

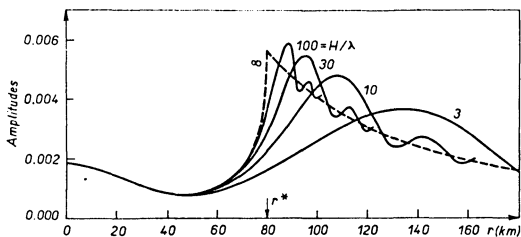


Fig. 5: Amplitude-distance curves of reflected waves in the neighbourhood of the critical point (r^*) for different frequencies, $f = 0.64, 2.13, 6.4, 21.3,$ and ∞ Hz ($H/\lambda = 3, 10, 30, 100,$ and ∞).

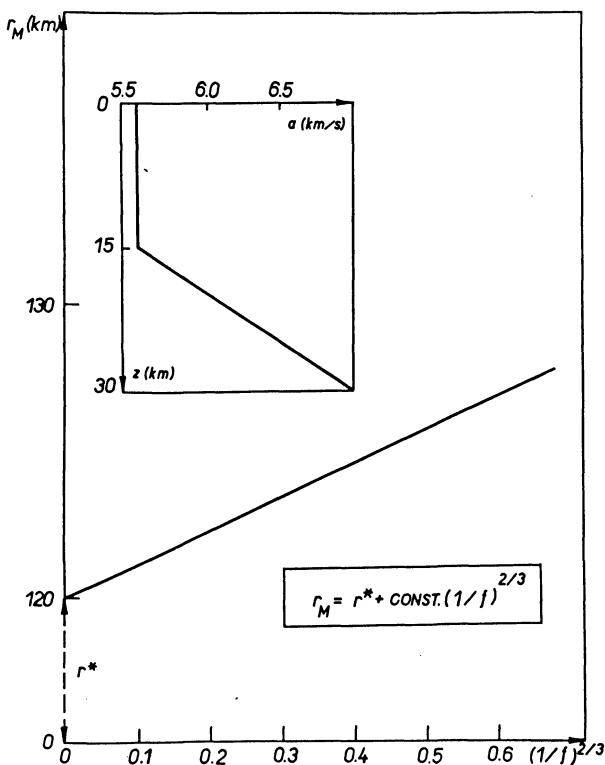


Fig. 6: Frequency dependence of the epicentral distance of maximum amplitude (r_M) in the case of the caustic. The epicentral distance of the caustic is denoted by r^* . The approximate formula for $r_M = r_M(f)$ is also presented.

The model of the medium is the same as in section 2.4. The values of H/λ (viz., 3, 10, 30, and 100) correspond to the frequencies $f = 0.64, 2.13, 6.4,$ and 21.3 Hz, respectively. The ray amplitude curve is also given for comparison ($H/\lambda = f = \infty$). Conclusions similar to those for the caustic can be made.

As has been shown, the position of maximum (r_M) of the amplitude curve is frequency dependent. Such dependence for the simple model producing the caustic is demonstrated in Fig. 6. The approximate analytical expression is generally valid for the interference wave field corresponding to the rays forming a caustic. The constant in the expression depends on the parameters of the medium [ZAHRADNÍK 1970].

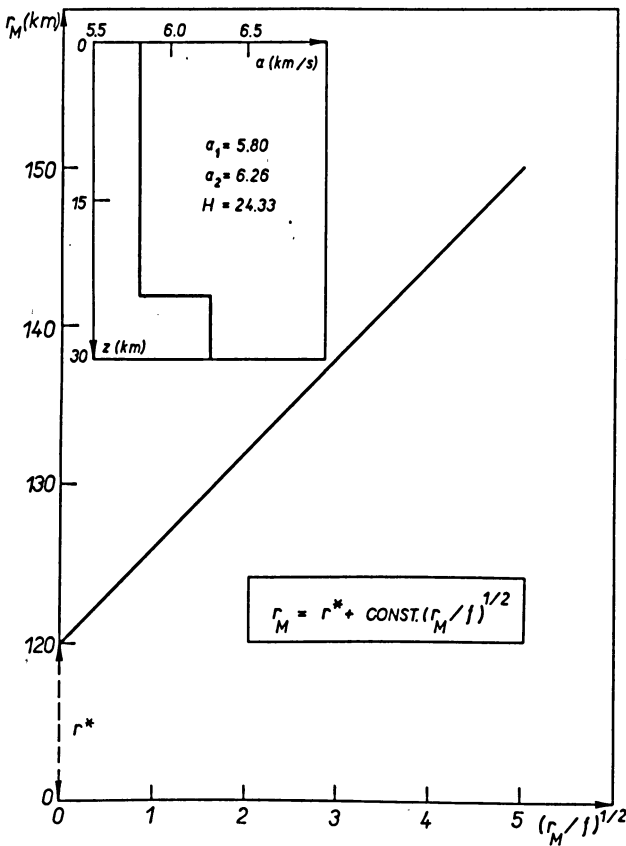


Fig. 7: Frequency dependence of the epicentral distance of maximum amplitude (r_M) in the case of the critical point. The approximate formula for $r_M = r_M(f)$ is also presented.

Similar dependence for the case of a critical point is given in Fig. 7. This is also very simple. The differences between both two dependences will be discussed later. The approximate formula for $r_M = r_M(f)$ presented above can be used to compute the position of critical points and caustics from seismic measurements. The experimental amplitude curves for different frequency ranges must be known.

3.2 The influence of parameters of medium

The amplitude curves have been computed for many models of the medium. Some typical examples will be presented.

In Fig. 8, three simple models of medium (cf. section 2.2.) and three corresponding amplitude curves of refracted waves for $f = 2$ Hz are given. The positions of the caustic are denoted by arrows. The modified asymptotic formulae have been used to compute the interference wave field in the immediate neighbourhood of the caustic.

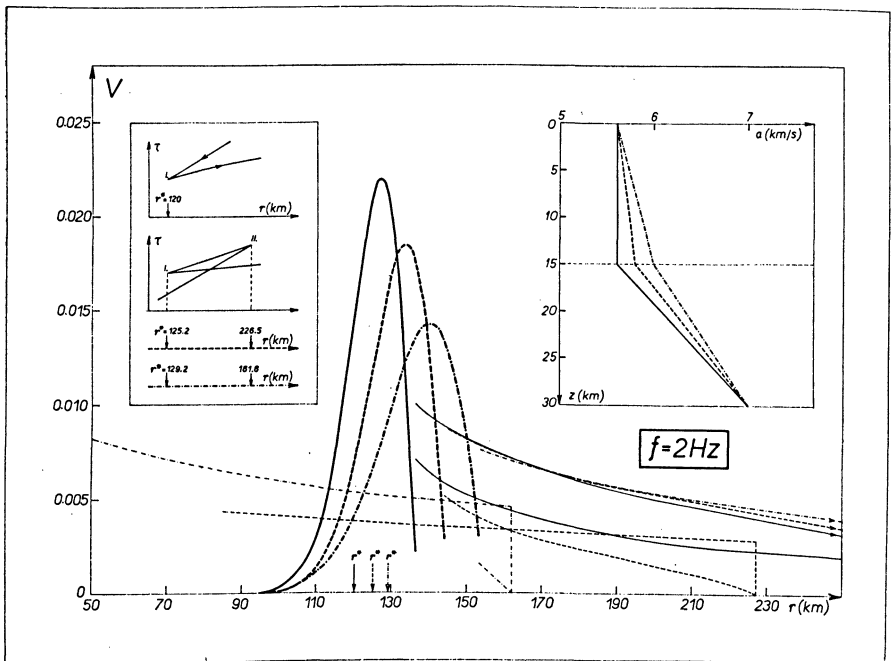


Fig. 8: Amplitude-distance curves of refracted waves in the neighbourhood of the caustic (r^*) for three given velocity-depth distributions. The travel-time curves are given schematically.

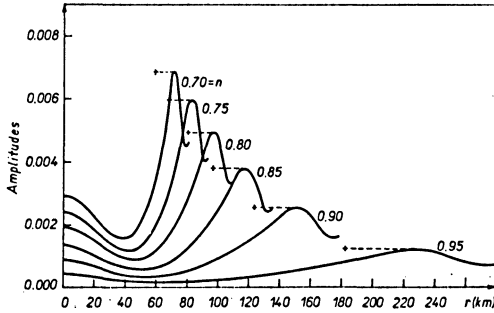


Fig. 9: Amplitude-distance curves of reflected waves in the neighbourhood of critical points for six models of media ($H = 30$ km, $a_2 = 8$ km/sec, $f = 6$ Hz). The values of the refractive index n are shown at the corresponding amplitude-distance curves.

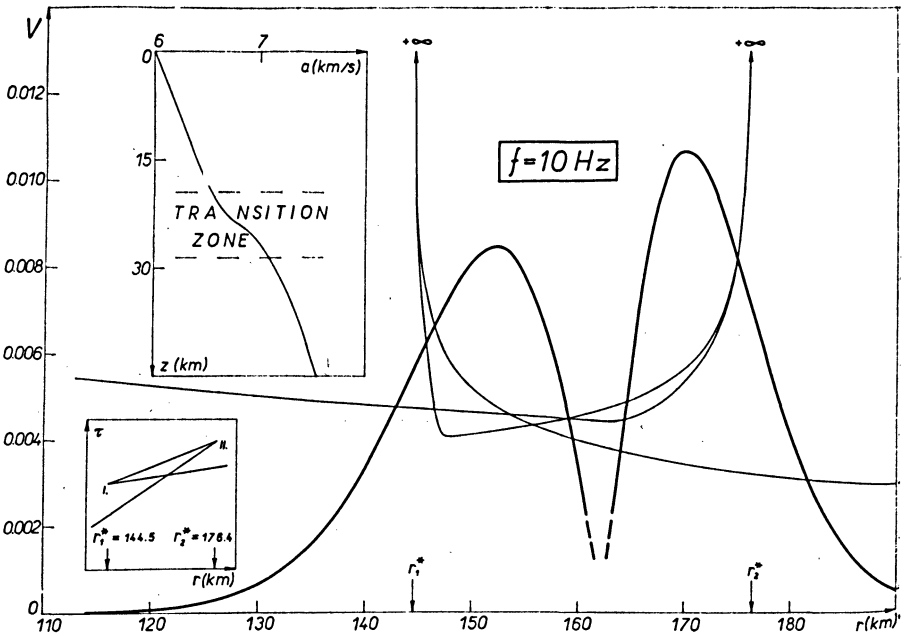


Fig. 10: Amplitude-distance curves of refracted waves for the given velocity-depth distribution with continuous velocity gradients. The travel-time curve is given schematically. Both cusp points (I and II) are connected with the caustics (r_1^* and r_2^*).

Other parts of the wave field have been computed separately by the ray formulae. See also Fig. 2 for a comparison of the modified and ray formulae.

The influence of parameters of the medium (the refractive index n) on the amplitude curve of reflected wave in the neighbourhood of the critical point is demonstrated in Fig. 9. The models of the first type (see section 2.1.) are studied, with $H = 30$ km, $a_2 = 8$ km/sec, $f = 6$ Hz. The positions of critical points are denoted by crosses.

The models considered above are very simple. The amplitude curve of refracted wave for the more realistic model is given in Fig. 10. It is clear from the velocity-depth graph that there is no discontinuity of first or second order inside the medium. The travel-time curve has two cusp points at epicentral distances denoted by arrows. At both these points, the caustics (r^*_1 and r^*_2) intersect the surface and the seismic energy is concentrated there. The amplitude curve computed by the ray formulae is denoted by a thin line. In the neighbourhood of caustics, two of the three branches of the ray amplitude curve reach infinity. Those parts of the wave field corresponding to these two branches have been computed also by the modified asymptotic formulae for $f = 10$ Hz (see the heavy lines). In other words, the heavy lines do not represent the resulting amplitude curve of the whole field of refracted wave but only the more suitable (with respect to the ray theory) approximation of its parts. Combining the ray and modified formulae, the amplitude curve corresponding to the total wave field could be obtained provided that the caustics are not very close to each other. In the latter case, the higher modifications (see e.g. [BREKHOVSKIKH 1960]) must be used. Note that similar difficulties arise also in the case of low frequencies.

4. A comparison of the amplitude curves in neighbourhood of critical points and caustics

There is no doubt now that the amplitude curves in neighbourhood of critical points and caustics are quite similar to each other. There is a similar shape of curves, the frequency dependence of the position of the maximum etc. In this section, we shall compare them quantitatively.

Such models may be compared, which are equivalent to each other in some sense of word. From the point of view of the seismological interpretation, the analogy of travel-time curves and/or amplitude-distance curves of seismic body waves is especially interesting.

4.1 *Similar travel-time curves*

For the given model producing the caustic, an equivalent model with the discontinuity of first order can be found so that the travel-time curves are, to a certain extent, analogous. The examples of velocity-depth graphs and corresponding travel-time curves of such models are given in Fig. 11. The model with a sharp discontinuity has been found analytically in such a way that (i) a position of the critical point is the same as that of the caustic, (ii) the arrival time and (iii) the slope of the travel-time curve at the critical point are the same as those at the caustic.

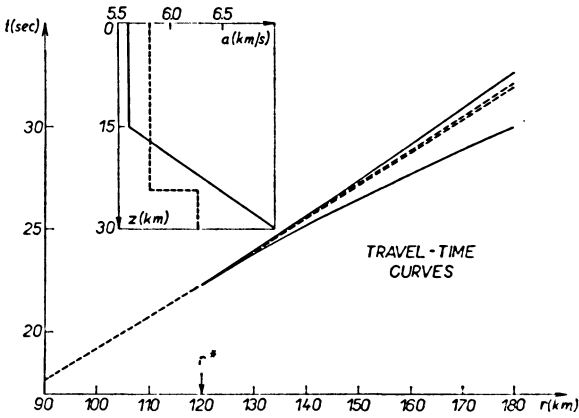


Fig. 11: Velocity-depth graphs and corresponding travel-time curves. For details, see text.

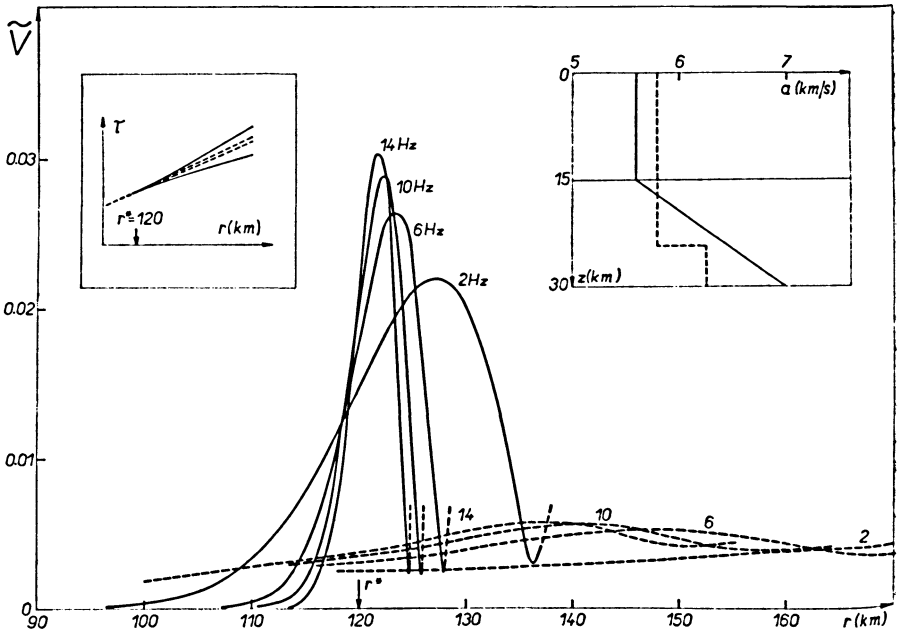


Fig. 12: Amplitude-distance curves of refracted waves in the neighbourhood of caustic (full lines) and of reflected waves near to the critical point (dashed lines) for given velocity-depth distributions. The values of frequency are shown at individual curves. The travel-time curves are given schematically (cf. Fig. 11). For details, see text.

The amplitude curves corresponding to both models described above are given in Fig. 12. (The arrow denotes the position of the caustic or the critical point.) They were computed for the system of frequencies. It is quite clear that both systems of curves are different. The very pronounced maxima correspond to the caustic. The amplitude curves are very high and narrow. On the other hand, the equivalent model does not produce such pronounced maxima. The amplitude curves of reflected waves are substantially lower and broader. They are very inexpressive. Similar comparisons have been made for other pairs of models, too. For example, the gradient in the lower layer was chosen somewhat smaller to reduce amplitudes in the neighbourhood of the caustic. However, with the gradient decreasing, the refractive index of equivalent model increases; then the amplitudes of reflected wave decrease in such a way that for the studied range of gradient, the amplitude contrast remains the same.

Not only the shape of amplitude curves but also the frequency dependence of position of maximum differs for critical points and caustics. This fact can be clearly verified in Fig. 12. For a given range of frequencies, the maxima lie in a much smaller range of epicentral distances for the case of caustic than for the case of critical point. The comparison of such frequency dependencies for five pairs of equivalent models (denoted by the numbers) is demonstrated in Fig. 13. Each pair of curves corresponds to one pair of equivalent models. The curves denoted by the heavy lines correspond to the pair of equivalent models discussed above (see Figs. 11 and 12). The slope of

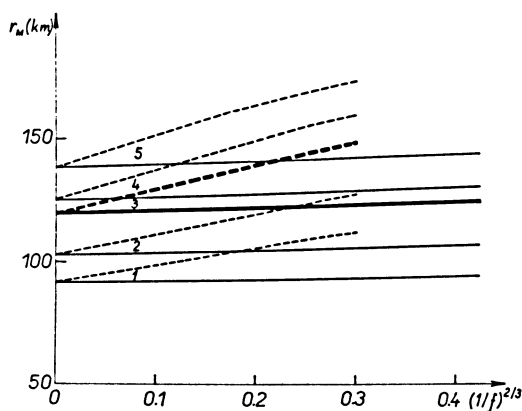


Fig. 13: Frequency dependence of the epicentral distance of maximum amplitude (r_M) for five pairs of equivalent models. The curves with a bigger slope correspond to the case of critical points.

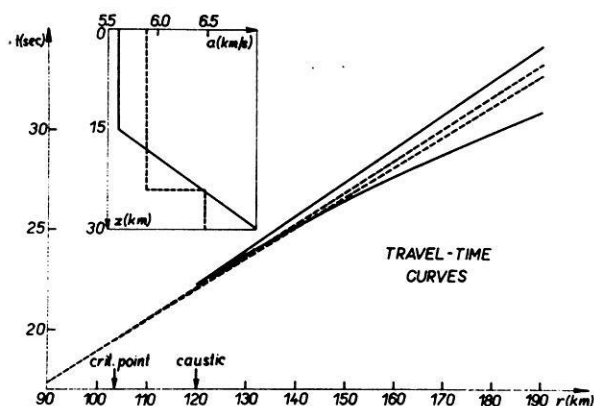


Fig. 14: Velocity-depth distributions and corresponding travel-time curves of two models with the same position of maxima of the amplitude curves (cf. Fig. 15).

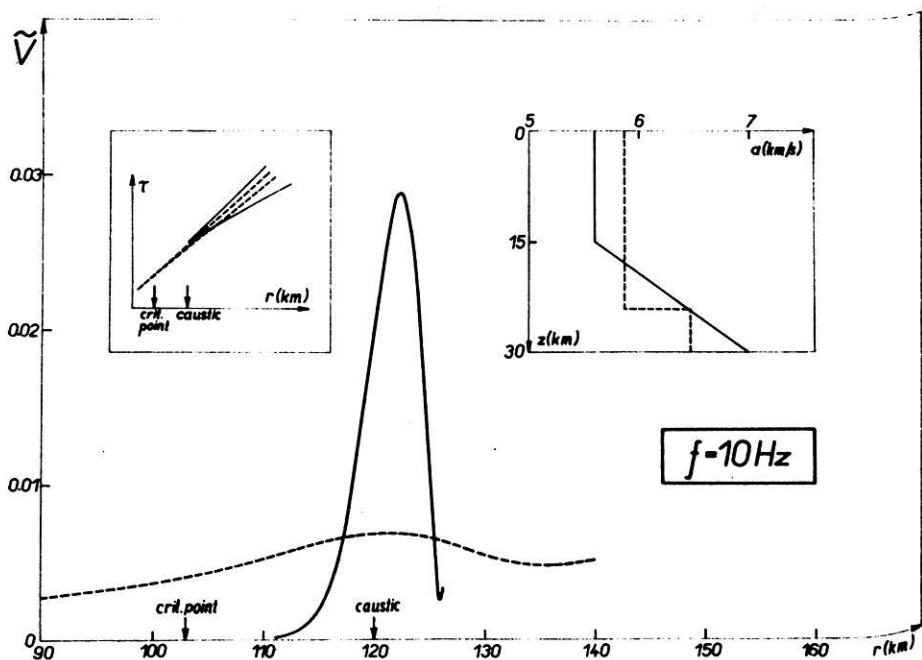


Fig. 15: Amplitude-distance curves of refracted waves in the neighbourhood of caustic (full line) and of reflected waves near to critical point (dashed line) for given velocity-depth distributions. The frequency is 10 Hz. The travel-time curves are given schematically (cf. Fig. 14).

curves for critical points is higher than that for caustics. In other words, with the frequency decreasing the maximum shifts more quickly from a geometrical critical point than from a caustic. Moreover, there is another difference which cannot be seen in Fig. 13. In the case of critical point, the maximum always shifts to greater epicentral distances. On the other hand, in the case of caustic, it can shift to smaller epicentral distances, too. This is valid for the maximum connected with the right-hand caustic in Fig. 10, for example. With the frequency decreasing, it shifts to smaller epicentral distances.

4.2 *The models with the same position of the maximum*

Let us now consider the pair of models with practically the same positions of maxima of the amplitude curves for a given frequency.

The travel-time curves for two models are given in Fig. 14. The positions of the critical point and of the caustic are not identical, but those of maxima of amplitude curves are practically the same (Fig. 15). The shape of both amplitude curves (only the first maxima are plotted) differs substantially. There is a very sharp maximum produced by the caustic. On the contrary, the amplitude curve of a reflected wave is very broad and inexpressive. Let us note, that similar conclusions have been obtained for other pairs of models, too.

5. Conclusion

A comparison of the amplitude-distance curves of refracted waves in the neighbourhood of the caustic with those of reflected waves in critical region shows that they are similar to each other. Moreover, the travel-time curves of both waves are also similar. Two branches of the travel-time curve are tangent to each other at a critical point as well as at a caustic.

The results of a computation for simple mathematical models of media indicate that very pronounced maxima and oscillations of the amplitude curves are connected rather with caustics than with critical points.

References

- ALEKSEYEV, A. S., V. M. BABICH, and B. Y. GEL'CHINSKIY: Ray method for the computation of the intensity of wave fronts. In: Problems in the dynamic theory of propagation of seismic waves (Ed. G. I. PETRASHEN) 5, 3–24, Leningrad University Press, Leningrad 1961 (in Russian)
- BREKHOVSKIKH, L. M.: Waves in layered media. Academic Press, New York 1960
- ČERVENÝ, V.: The dynamic properties of reflected and head waves around the critical point. Travaux Inst. Géophys. Acad. Tchécosl. Sci. No. 221, Geofysikální Sborník 13, 135–245, 1965

- ČERVENÝ, V., and R. RAVINDRA: Theory of seismic head waves. University of Toronto Press, Toronto 1971
- GAZARYAN, YU. L.: Geometrical-acoustical wave approximation in the neighbourhood of the non-regular part of the caustic. In: Problems in the dynamic theory of propagation of seismic waves (Ed. G. I. PETRASHEN) 5, 73–89, Leningrad University Press, Leningrad 1961 (in Russian)
- JANSKÝ, J.: Refracted wave in a horizontally stratified medium with constant velocity gradients. *Studia geoph. et geod.* 13, 423–443, 1969
- : Refracted wave in a horizontally layered medium with continuous velocity gradients. *Studia geoph. et geod.* 14, 286–295, 1970
- LUDWIG, D.: Uniform asymptotic expansions at a caustic. *Comm. Pure Appl. Math.* 19, 215–250, 1966
- MÜLLER, G.: Theoretical seismograms for some types of point-sources in layered media.
Part I: Theory. *Z. Geophys.* 34, 15–35, 1968a
Part II: Numerical calculations. *Z. Geophys.* 34, 147–162, 1968b
Part III: Single force and dipole sources of arbitrary orientation. *Z. Geophys.* 35, 347–371, 1969
- SATO, R.: Amplitude of body waves in a heterogeneous sphere. Comparison of wave theory and ray theory. *Geophys. J.* 17, 527–544, 1969
- SMIRNOVA, N. S., and N. I. YERMILOVA: On the construction of theoretical seismograms in the neighbourhood of critical points. In: Problems in the dynamic theory of propagation of seismic waves (Ed. G. I. PETRASHEN) 3, 161–213, Leningrad University Press, Leningrad 1959 (in Russian)
- YANOVSKAYA, T. B.: Investigation of dynamic theory of elasticity solutions in the neighbourhood of the caustic. In: Problems in the dynamic theory of propagation of seismic waves (Ed. G. I. PETRASHEN) 7, 61–76, Leningrad University Press, Leningrad 1964 (in Russian)
- : Approximate methods in elastic wave theory. Notes of lectures, Dept. of Applied Math. and Theoret. Physics, Cambridge University, 1968
- ZAHRADNÍK, J.: The kinematic and dynamic properties of seismic waves in the neighbourhood of caustics. *Acta Univ. Carol., Math. et Phys.* 11, 77–106, 1970

Seismic Waves Reflected from Velocity Gradient Anomalies within the Earth's Upper Mantle¹⁾

P. G. RICHARDS, Palisades²⁾

Eingegangen am 7. Februar 1972

Summary: Classical THOMSON-HASKELL methods have recently been extended, to obtain the asymptotic wave solution in a stratified elastic medium which has both first and second order discontinuities in the elastic parameters. These methods are used here in a discussion of the observed precursors to seismic waves $P'P'$. The frequency-dependent reflection coefficient R (= reflected/incident displacement amplitudes) is calculated for several models of transition regions in the Earth's mantle. To generate observable precursors to $P'P'$, by reflection from horizontal layering within the mantle, the thickness L of the region of transition is shown to be much smaller than has generally been supposed. This result follows from the rapid decrease in R as the transition thickness increases from zero to one wavelength. For example, R (1 second) $> 2\frac{1}{2}\%$ only if $L < 4$ km., even in cases of 10% total changes in velocity.

Zusammenfassung: Die klassischen THOMSON-HASKELL-Methoden wurden vor kurzem vom Autor um asymptotische Lösungen erweitert, die die Wellenausbreitung in geschichteten elastischen Medien mit Diskontinuitäten erster und zweiter Ordnung in den elastischen Parametern beschreiben. Diese Methoden werden in dieser Arbeit zur Diskussion der beobachteten Vorläufer der seismischen Kernphase $P'P'$ benutzt. Der frequenzabhängige Reflexionskoeffizient R (= Verhältnis von reflektierter zu einfallender Verschiebungsamplitude) wird für mehrere Modelle von Übergangszonen im Erdmantel berechnet. Um beobachtbare $P'P'$ -Vorläufer durch Reflexion an horizontal geschichteten Inhomogenitäten im Mantel zu erzeugen, muß die Dicke L dieser Übergangszonen viel kleiner sein als bisher im allgemeinen angenommen wurde. Dieses Resultat folgt aus der schnellen Abnahme von R , wenn die Dicke der Übergangzone von 0 bis zu einer Wellenlänge zunimmt. Beispielsweise ist für Perioden von 1 Sekunde $R > 2,5\%$ nur dann, wenn $L < 4$ km ist. Das gilt selbst dann, wenn die Änderung in der Geschwindigkeit 10% beträgt.

1. Introduction

Modern geophysical studies have done remarkably little to change the gross features of Earth models suggested more than thirty years ago by GUTENBERG and JEFFREYS. In particular, recent modelling of the Earth's compressional-wave velocity-profile stresses details in the velocity gradient, and does little to change the average velocity

¹⁾ Lamont-Doherty Geological Observatory contribution 1784.

²⁾ Prof. PAUL G. RICHARDS, Lamont-Doherty Geological Observatory, Columbia University, Palisades, New York 10964, U.S.A.

over scales of, say, a hundred vertical kilometres. But, of course, it is just these details which are important for the development of compositional Earth models.

The most recent evidence for anomalies in the velocity gradient is the observation [GUTENBERG 1960, ADAMS 1968, BOLT, O'NEILL and QAMAR 1968, ENGDahl and FLINN 1969 a, b, HUSEBYE and MADARIAGA 1970, WHITCOMB and ANDERSON 1970] of body waves which appear to be reflected from some depth within the mantle itself. In this paper, it is concluded that the reflection interpretation requires highly localised anomalies to yield the published observations, and that, at some depths within the mantle, the P-wave velocity may change by several per cent over only three or four kilometres depth. Such an Earth model is at odds with most petrological interpretations of simple transition zones. For example, AKIMOTO and FUJISAWA [1968] find that the two-phase region between olivine and spinel in the mantle would be spread over 50 to 80 kilometres.

It is hoped that some of the methods used here, for calculating the properties of elastic waves reflected by second order discontinuities within the Earth, will provide useful estimates of velocity gradient anomalies within the upper mantle. This paper contains a brief summary of relevant seismic observations, and outlines several methods for obtaining the reflection coefficient of a given transition zone. It also attempts to describe the future work needed, to provide convincing evidence that the reflection interpretation of the seismic data (and its consequent strong implications for the velocity gradient anomaly) is indeed correct.

2. Summary of Seismic Observations

In a study of waves which have been multiply reflected from the surface of the Earth, GUTENBERG [1960] noted some "small waves, some of which emerge by as much as 20 seconds before the main phase". He concluded that these precursors were due to waves reflected "at the MOHORoviČIĆ-discontinuity or other discontinuities below the surface." ADAMS [1968] has given an extended discussion of early arrivals of the phase $P'P'$ (often denoted $PKPPKP$), finding precursors up to nearly 70 seconds before the main phase. This main phase has travelled through the Earth's core, has been reflected at the Earth's free surface (or at the bottom of the crust or the ocean) and has travelled back through the Earth's core again, before being recorded. The main advantage of working with precursors to this phase, in a study of possible reflections from transitions within the upper mantle, is precisely that the arrivals occur in a clear portion of a seismogram, and not in the coda of the main phase. ADAMS notes that "At times there are clear, pulselike early arrivals, of period comparable with that of the main phase, but more often there is a gradual build up of energy with no definite beginning. This emergent forerunner is usually of short period (one sec. or less). ... Amplitudes observed for the clearer reflections ranged from a few per cent up to 20 per cent and in one case 40 per cent of the main phase." We find below that it is short period data such as these which lead to the strongest con-

straints on acceptable transition regions in the mantle. ADAMS [1968] concludes from his survey that there is "fair evidence for a reflecting surface at a depth of about 70 km", and indications of regional deeper reflectors.

BOLT, O'NEILL and QAMAR [1968] found short-period phases, arriving near 110° , up to 90 seconds before PP . They suggested a reflection interpretation, with a number of discrete shells of different elastic properties in the Earth's upper mantle above 400 km. ENGDAHL and FLINN [1969a] have found a phase arriving nearly $2\frac{1}{2}$ minutes before $P'P'$, their data coming from two earthquakes recorded on shortperiod instruments at stations throughout the world. They were also able to determine the slowness as 2.9 sec./degree at a distance $\Delta=72.2^\circ$ —thus showing that the phase has both the correct travel time and correct angle of arrival for a reflection from 650 km depth. ENGDAHL and FLINN [1969b] also found an arrival occurring 30–40 seconds before the normal $P'P'$, but with slowness 4.4 sec./degree. They identified it as $SKKKP$, and suggested that several of ADAMS' observations should be interpreted by this phase. HUSEBYE and MADARIAGA [1970] investigated the origin of precursors to core waves, and paid particular attention to arrivals following P (diffracted). Their conclusion, that these phenomena were reflections or multiple paths in the upper mantle, was obtained by elimination of other alternatives.

Results of perhaps the most extensive survey, on precursors to $P'P'$, have been published by WHITCOMB and ANDERSON [1970], who found the strongest evidence was for a reflector at depth 630 km, with other reflectors at depths 280, 520, 940, and possibly also at 50, 130, 410, and 1250 km. They have furthermore associated a particular compositional feature with each reflector. The ratio of precursor amplitude to main phase amplitude, from their records, ranges from 30% to 50% for depths above 100 km., and about 10% for deeper reflectors: no systematic difference in period is noted between the main branches of $P'P'$ and the early arrivals, and their data is for periods of about 1 or 2 seconds. They have given a model of the upper mantle with six first order discontinuities, and we now turn to an examination of the reflection coefficient of theoretical transition zones, finding that a model like a first order discontinuity does indeed seem to be required, if the precursors are due to reflection from horizontal layering. The seismic observations of amplitude ratios are for a main phase which has travelled a somewhat different path than the supposed reflection. The main phase may thus have suffered further degradation by scattering and attenuation in the low velocity zone. A conservative allowance for these effects has been made by WHITCOMB and ANDERSON, and in what follows we shall try to explain the seismic observations in terms of a transition region which reflects about 5% of the incident shortperiod energy.

3. The Theory: Calculations and Comparisons

In this section is obtained the reflection coefficient, R , for four different models of the transition zone at 650 km depth. The data summarised above presents evidence

which is strongest for a reflector at this depth, and it is assumed that the lower medium has a density (ρ) about 5% larger, a longitudinal velocity (α) about 10% larger, and a shear velocity (β) about 20% larger than corresponding parameters in the upper medium. A P' -wave is presumed to be incident from below at an angle i (say) of 16° to the vertical, this value being chosen to fit the slowness observations of the precursors. An S -wave with the same slowness has at this depth an angle j (say) of about 9° to the vertical.

3.1 *Transition Model I:*

This is a simple model, which serves as a basic reference, and consists of the first order discontinuity between two slightly different welded homogeneous half-spaces. The exact solution for the reflection coefficient can be obtained, but a convenient and accurate approximation, correct to first order in the fractional change of elastic properties, is

$$R = (\Delta\rho/\rho)(\cos 2j - \frac{1}{2}) + \frac{1}{2}(\Delta\alpha/\alpha) \sec^2 i - 4(\Delta\beta/\beta) \sin^2 j \tag{1}$$

(see BORTFELD [1961, page 489]), where $\Delta\rho$ is the difference between the two densities, ρ is the average density and $\Delta\alpha, \Delta\beta, \alpha, \beta$ are similarly defined for the seismic velocities.

With values $(\Delta\rho/\rho, \Delta\alpha/\alpha, \Delta\beta/\beta) = (0.05, 0.1, 0.2)$, and $i = 16^\circ, j = 9^\circ$, formula (1) returns a value $R = 5.7\%$. This coefficient may be large enough to explain the observed precursors. Note that it is independent of frequency. It would be the limiting value for very low frequencies, in a transition with some finite thickness, since, for a length scale based on wavelength, the transition would appear arbitrarily thin, and hence like a first order discontinuity. Before passing to a study of extended transitions, it is of interest to note that the conversion coefficient C , giving the downward reflected SV -displacement corresponding to upward unit P -displacement, is given accurately by

$$C = \frac{1}{2} \sec j [(\Delta\rho/\rho) \sin(i + 2j) + 4(\Delta\beta/\beta) \sin j \cos(i + j)]$$

This formula correctly gives the limit $C \rightarrow 0$ as i (and hence j) $\rightarrow 0$, but, in our case of $i = 16^\circ$, the reflected SV displacement turns out to be nearly twice as large as the reflected P . This type of scattered energy is, however, difficult to identify on seismic records, because the S -wave energy typically is attenuated much more than P , during the subsequent propagation.

3.2 *Transition Model II:*

BREKHOVSKIKH [1960] presents an extended account of the EPSTEIN [1930] method of studying wave propagation in inhomogeneous media, and describes the calculation of reflection coefficients (for different angles of incidence) for a transition given as a

function of depth z by

$$\alpha(z)/\alpha(\infty) = [1 - N \exp\{-m(z - z_0)\} / (1 + \exp\{-m(z - z_0)\})]^{-\frac{1}{2}}$$

where N and m are real constants. This profile is a smooth transition between the two values

$$\alpha(\infty) \quad \text{and} \quad \alpha(-\infty) = \alpha(\infty)(1 - N)^{-\frac{1}{2}}$$

and, for this study of the 650 km ($=z_0$) transition in the Earth, a 10% change in velocity is attained with the choice $N = -0.21$. The constant m is related to the effective thickness l (say) of the transition, and we take $m = 3.52/l$, since then the velocity difference

$$\alpha(z_0 + \frac{1}{2}l) - \alpha(z_0 - \frac{1}{2}l)$$

is three-quarters of the total difference $\alpha(\infty) - \alpha(-\infty)$. With these definitions, an alternative formula for the profile is given at the top right of Figure 1, and the velocities are shown graphically at the left of Figure 1.

BREKHOVSKIKH gives for the modulus of the reflection coefficient the exact formula

$$R = \sinh\{2\pi^2 [\cos i - (\cos^2 i - N)^{\frac{1}{2}}] / \lambda m\} / \sinh\{2\pi^2 [\cos i + (\cos^2 i - N)^{\frac{1}{2}}] / \lambda m\} \tag{2}$$

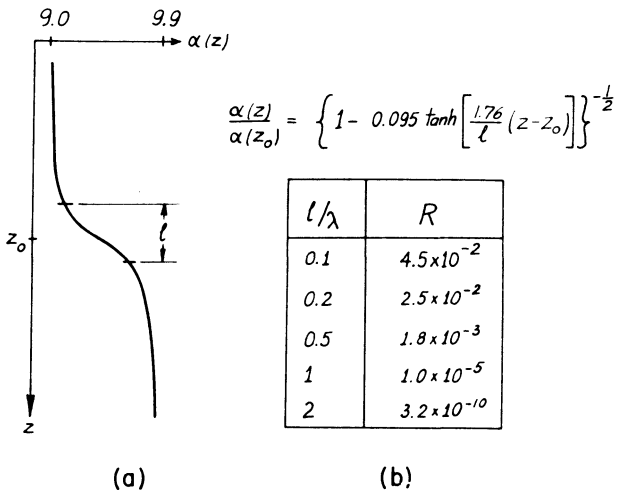


Fig. 1: a) The velocity profile α (km/sec) for a particular EPSTEIN layer, shown as a function of depth z .

b) The specific equation of the profile, and a table of values for the reflection coefficient R , calculated as a function of the ratio l/λ .

where i is the angle of incidence at $z = +\infty$ (taken as 16° in our application) and λ is the incident wavelength. The Table insert of Figure 1 shows some values of R , calculated for this smooth transition at different values of the ratio l/λ . Note that the special case $R = 5.7 \times 10^{-2}$, obtained above for Model I in the case $l/\lambda = 0$ (a first order discontinuity) fits in well with the sequence of values in Figure 1. The most important quality of the R values tabulated is their extremely rapid fall-off as l is increased beyond about a fifth of a wavelength.

The method of EPSTEIN is not strictly applicable to transitions in the solid Earth, since it is essentially a theory for scalar waves in a fluid of varying bulk modulus. Although PHINNEY [1970] has shown how to allow for a varying density, the exact effects of a varying shear velocity are unknown. However, a justification for accepting the results of formula (2) as accurate can be based on the results of RICHARDS (1971a), who showed how the elastic equation of motion can be separated, at high frequencies, into two decoupled equations for P - and S -waves, these equations being in just the canonical form needed to apply EPSTEIN's method.

It follows from the Table in Figure 1 that a wave with the predominant period of two seconds (say), and wavelength 20 km., incident upon the transition from below, is reflected back down with more than 2.5% of its incident amplitude only if the transition thickness is less than about 4 km. And a one second wave, reflected back down with more than 4% of its incident amplitude, implies a thickness of less than about 1 km. In order to check whether these thicknesses are really implied by the given values of the reflection coefficient, it is clearly necessary to see if other transition models can in some sense be more efficient reflectors.

3.3 Transition Model III:

In RAYLEIGH's [1880] account of waves propagating in media of varying refractive index, a reflection solution is given which also solves the seismological problem of vertical reflection from the profile displayed at the left of Figure 2, that is, a linear transition in velocity between two homogeneous half-spaces. Taking α_1 as the velocity of the half-space in which the wave is incident, and α_2 as the other half-space velocity, with transition thickness L and radian frequency ω , the reflection coefficient is

$$R = S / \{S^2 + 4m^2\}^{\frac{1}{2}}, \quad (3)$$

where

$$S = |\sin [m \log (\alpha_1 / \alpha_2)]| \quad \text{and} \quad m = \{(\omega L)^2 (\alpha_1 - \alpha_2)^{-2} - \frac{1}{4}\}^{\frac{1}{2}}.$$

The formula (3) shows that $R = 0$ for certain specific values of L/λ , where λ is the incident wavelength. And, for high frequencies, a useful approximation for an upper bound to R is

$$R < \frac{1}{2} m^{-1} \approx (\alpha_1 - \alpha_2) (\lambda / L) / 4\pi.$$

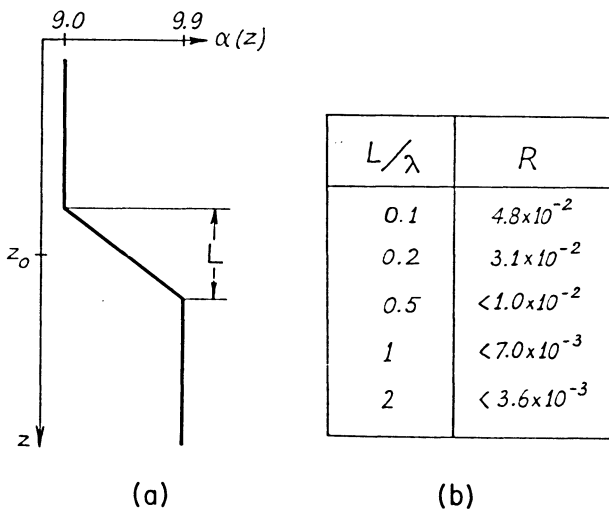


Fig. 2: The velocity profile α (km/sec) for a linear transition between two half-spaces.

b) A table of values for the reflection coefficient R , calculated as a function of the ratio L/λ .

This upper limit is almost reached when reflections from the upper and lower second order discontinuities are in phase—reflection from a single such discontinuity having approximate magnitude $\frac{1}{4}m^{-1}$.

The formula (3) is used to obtain the Table insert of values in Figure 2. By comparing with Figure 1, it is seen that the pair of second order discontinuities is indeed a more efficient reflector than the completely smooth profile, particularly for the very short wavelengths. However, if the data indicate that the reflection coefficient is more than 3%, then $L/\lambda < 0.2$ is required by the model. And for a two second period, the thickness must be less than about 4 km.

The present model may be criticised on the grounds that it, like Model II, does not allow for variations in density and shear velocity. And it is for vertical incidence only. The main feature it displays is a difference from Model II in the way that R decreases at short wavelengths (see SCHELKUNOFF [1951] for discussion of this phenomenon).

3.4 Transition Model IV:

A recent paper of RICHARDS [1971] has shown how the effects of simultaneous variation of ρ , α , and β may be calculated, in plane stratified media with both first and second order discontinuities. The method is an extension of classical THOMSON-HASKELL methods, to include the system of boundary conditions arising from the

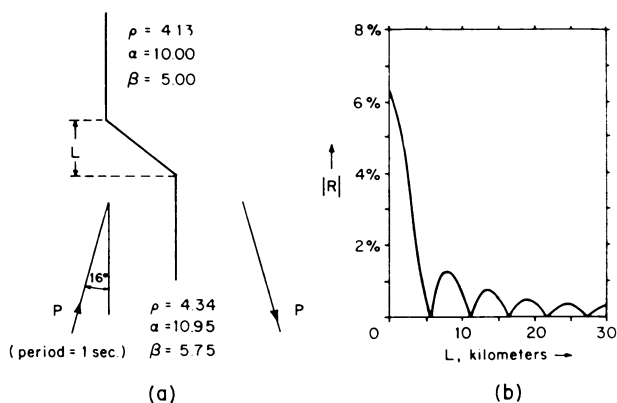


Fig. 3: a) The profile of ρ (gm./c. c.), α , and β (km/sec), for a model of the transition at depth 650 km.

b) A graph of the corresponding reflection coefficient R , plotted against thickness L , for a one second P -wave incident on the transition from below at an angle of 16° to the vertical.

asymptotic wave solution in each single inhomogeneous elastic layer, and it is particularly suited to the examination of reflection, transmission and conversion coefficients for relatively high frequencies. This method has been used for the transition model depicted at the left of Figure 3, with a one second P -wave incident from below at 16° to the vertical. The resulting reflection coefficient (for downgoing P -waves) is shown to the right of the Figure.

In common with Model III, it is seen from Figure 3 that a system of destructive interference gaps occurs. But even the intervening maxima (which are due to constructive interference) are very low in value. If the data indicate that the reflection coefficient is more than 2.5% for a one second wave, then a thickness L less than 4 km is required by the model. For a two second wave, this value of L may be doubled. At the other end of the scale, Figure 3 shows a reflection coefficient of somewhat less than $\frac{1}{2}\%$ for a thickness of 25 km (and period one second).

4. Discussion

We have examined four models of transition zones in the upper mantle, and showed how three simple models have a simple formula for the reflection coefficient. These imply a very localised transition zone, if precursors to the seismic phase $P'P'$ are indeed due to reflection from a horizontal transition. The fourth model, which allowed for a transition in density and the two seismic velocities at 650 km depth (the depth most strongly suggested as a reflector by published seismic data), also implies a transition of thickness less than 4 km.

This value appears to be much smaller than has generally been supposed from experimental and theoretical studies of solid-solid phase changes. Before insisting that it is a correct value, we must therefore check carefully if the seismic observations do require such thin transitions. In particular, we must critically examine the hypothesis of a horizontal reflector. The following remarks are intended both to suggest alternative explanations of the observations, and to suggest ways in which they may be verified or rejected.

DAVIES and FRASIER [1971], page 18] have pointed out the importance of a small amount of curvature in the reflector. The consequent focussing and defocussing would presumably lead to reflection amplitudes ranging between large and non-observable. Analysis of this effect is difficult, and must rely heavily on the statistics of absence of expected phases. VINNIK and DASHKOV [1970] have found this procedure productive for observations of *PcP*. However, the evidence given by WHITCOMB and ANDERSON [1970] for a reflector at 650 km shows that the expected precursor is almost always present.

In several other fields of wave propagation, the problem has arisen of constructing an acceptable transition to explain an observed reflection. (For example, radar reflections from atmospheric layering.) The solution often adopted has involved some measure of turbulence in the medium of propagation. Our seismological problem may somewhat similarly be resolved if the reflector consists of a layered region in which there are interleaved high and low velocities. CLOWES and KANASEWICH [1970] have used this model, for reflections within the crust. Such transitions still contain very high velocity gradients, and present even more puzzles to the geochemist. Their existence can be verified only after analysis of the pulse shapes or frequencies present in the reflections.

A feature often overlooked in the analysis of *P'P'* and its precursors is that these ray paths are true *maximum* time paths. JEFFREYS and LAPWOOD [1957] have shown how there is a cancellation, of energy arriving (before the true ray arrival time) from the vicinity of the ray reflection point. In this sense, it may be said that the pulse shape of *P'P'* arrives *after* its coda. It is to be hoped that further theoretical studies of this problem will reveal what happens if some slight perturbation of elastic parameters, in the vicinity of the reflection point, destroys the cancellation for times much before the ray arrival time. Presumably there would be precursors to the main *P'P'* phases. However, it appears unlikely that these could arrive with the large $2\frac{1}{2}$ minute lead time associated with a deep reflector.

In final conclusion, a strong case can be made for a 4 km thick transition region, in the upper mantle at a depth of 650 km. The evidence comes from short-period seismic phases which appear to have been reflected from this level at near vertical incidence. It appears that no other type of seismic observation can confirm the localised nature of this transition, since neither long-period waves nor $dt/d\Delta$ measurements (and HERGLOTZ-WIECHERT inversion) can provide the necessary vertical resolution. The seismological evidence for thin transitions at other depths is perhaps not yet

so strong, but it is hoped that further geochemical research will be stimulated, to indicate what kinds of abrupt transitions are acceptable. A discussion of this problem is given by GARLICK [1969], who examines the consequences of chemical equilibrium across phase changes within the mantle.

5. Acknowledgments

The author appreciates discussions with many colleagues during the course of this investigation. They include Drs. D. L. ANDERSON, C. B. ARCHAMBEAU, J. N. BRUNE, C. W. FRASIER, R. A. PHINNEY, and J. H. WHITCOMB. He also thanks Drs. J. DORMAN and H. KUTSCHALE for their critical reading of the manuscript.

This research was supported by the *Advanced Research Projects Agency of the Department of Defense*, and was monitored by the *Air Force Cambridge Research Laboratories* under Contract No. F 19628-71-C-0245.

References

- ADAMS, R. D.: Early reflections of $P'P'$ as an indication of upper mantle structure. *Bull. Seism. Soc. Am.* 58, 1933–1947, 1968
- AKIMOTO, S., and H. FUJISAWA: Olivine-spinel solid solution equilibria in the system Mg_2SiO_4 - Fe_2SiO_4 . *J. Geophys. Res.* 73, 1467–1479, 1968
- BOLT, B. A., M. O'NEILL, and A. QAMAR: Seismic waves near 110° : is structure in core or upper mantle responsible? *Geophys. J.* 16, 475–487, 1968
- BORTFELD, R.: Approximations to the reflection and transmission coefficients of plane longitudinal and transverse waves. *Geophys. Prospect.* 9, 485–502, 1961
- BREKHOVSKIKH, L. M.: *Waves in layered media*. Academic Press, London, 1960
- CLOWES, R. M., and E. R. KANASEWICH: Seismic attenuation and the nature of reflecting horizons within the crust. *J. Geophys. Res.* 75, 6693–6705, 1970
- DAVIES, D., and C. W. FRASIER: Seismic discrimination, semiannual technical summary report, 1 July–31 December 1970, Lincoln Laboratory, Massachusetts Inst. of Tech., pp. 17–19, issued 4 February 1971
- ENGDAHL, E. R., and E. A. FLINN: Seismic waves reflected from discontinuities within Earth's upper mantle. *Science* 163, 177–179, 1969a
- ENGDAHL, E. R., and E. A. FLINN: Remarks on the paper "Early reflections of $P'P'$ as an indication of upper mantle structure." by R. D. Adams. *Bull. Seism. Soc. Am.* 59, 1415 to 1417, 1969b
- EPSTEIN, P. S.: Reflection of waves in an inhomogeneous absorbing medium. *Proc. Natl. Acad. Sci. U.S.A.* 16, 627–637, 1930

- GARLICK, G. D.: Consequences of chemical equilibrium across phase changes in the mantle. *Lithos* 2, 325–331, 1969
- GUTENBERG, B.: Waves reflected at the “surface” of the Earth: $P'P'P'P'$. *Bull. Seism. Soc. Am.* 50, 71–79, 1960
- HUSEBYE, E., and R. MADARIAGA: The origin of precursors to core waves. *Bull. Seism. Soc. Am.* 60, 939–952, 1970
- JEFFREYS, H., and E. R. LAPWOOD: The reflexion of a pulse within a sphere. *Proc. Roy. Soc. London, Series A* 241, 455–479, 1957
- PHINNEY, R. A.: Reflection of acoustic waves from a continuously varying interfacial region. *Rev. Geophys. Sp. Sci.* 8, 517–532, 1970
- RAYLEIGH (LORD): On reflection of vibrations at the confines of two media between which the transition is gradual. *Proc. Lond. Math. Soc.* 11, 51–56, 1880
- RICHARDS, P. G.: Potentials for elastic displacement in spherically symmetric media. *J. Acoust. Soc. Am.* 50, 188–197, 1971a
- RICHARDS, P. G.: Elastic wave solutions in stratified media. *Geophysics* 36, 798–809, 1971b
- SCHELKUNOFF, S. A.: Remarks concerning wave propagation in stratified media. *Communs. Pure and Appl. Math.* 4, 117–128, 1951
- VINNIK, L. P., and G. G. DASHKOV: PcP waves from atomic explosions and the nature of the core-mantle boundary. *Izvestiya, Phys. Sol. Earth (Eng. trans.)*, 4–9, Jan. 1970
- WHITCOMB, J. H., and D. L. ANDERSON: Reflection of $P'P'$ seismic waves from discontinuities within the mantle. *J. Geophys. Res.* 75, 5713–5728, 1970

Investigation of Linear Harmonic Field of SH-Waves in a Stratified Inhomogeneous Medium Using the Finite Difference Method

J. NEDOMA, Prague¹⁾

Eingegangen am 12. Februar 1972

Summary: The propagation of seismic waves through the inhomogeneous medium is studied by the finite difference method. The possibility of solving this problem is studied on several models, whose parameters of elasticity are variable with the depth.

Zusammenfassung: In der Arbeit wird das Problem der Ausbreitung seismischer Wellen in inhomogenen Medien mittels des Differenzverfahrens studiert. Das Problem wird für einige Modelle, in denen die Elastizitätsparameter als Funktionen der Tiefe auftreten, untersucht.

1. Introduction

The propagation of seismic waves through the Earth characterized by an inhomogeneous medium with the elastic parameters, which are functions of the depth, was studied theoretically by means of simplified models in several papers using wave method [PEKERIS 1946, BREKHOVSKIKH 1962, SATO 1969]. The solution could only be found in closed form for several special cases varying the wave velocity with depth. But if the discontinuity surfaces of the velocity of seismic waves are generally non-planar, the solutions are more complicated.

With the development of computers also methods of numerical analysis of solving partial differential equations evolved and these methods were also applied to the solution of the problem of propagation of seismic waves in the stratified homogeneous medium in the time domain (hyperbolic equations) [ALTERMAN, KARAL 1968, ALTERMAN, ROTENBERG 1969] and in media with generally nonplanar or corrugated interfaces of arbitrary shapes in the frequency domain (elliptic equations) [NEDOMA, PĚČ 1971] and [NEDOMA 1972].

In this contribution we should like to discuss the possibility of solving this problem using the finite difference method. The elastic parameters are assumed to be arbitrary, generally discontinuous functions of the depth. The wave field will be described, as we know, by a complex vector of displacement, which represents the solution of a partial differential equation with complex coefficients for the displacement in the

¹⁾ Ing. Jiří NEDOMA, Geofyzikální ústav ČSAV, Praha 4 – Spořilov, Boční II, ČSSR.

studied region. The solution of a differential equation is reduced to a solution of a system of linear algebraic equations for the value of the displacement in all the mesh points in the studied region.

2. Theory

Let us consider an inhomogeneous medium composed of inhomogeneous layers with parameters $\mu_j(z)$, $\rho_j(z)$, $c_j(z)$, $\kappa_j(z)$ i. e. rigidity, density, velocity, wave number in the j -th layer, which are continuous or discontinuous functions of the variable z i. e. of the depth, lying on an inhomogeneous half-space with parameters $\mu(z)$, $\rho(z)$, $c(z)$, $\kappa(z)$. We assume that the linear source radiates harmonic cylindrical SH waves. The problem can be studied as a two dimensional problem. The origin of Cartesian system of co-ordinates (x, z) will be placed on the surface of the first layer and z -axis pointed into it. The harmonic cylindrical source of SH -waves with an angular frequency ω will be located at the z -axis at a distance of z_0 from the origin of the coordinate system in the l -th layer. The interfaces between the layers represent arbitrary functions, continuous in parts, under the assumption that the rays reflected from them do not return back to the vicinity of the source. In our case we shall also consider a medium with non-zero absorption $\alpha = \alpha(x, z, \lambda)$, i. e. α is a function of place and wavelength λ . The problem is described by the following equation

$$L[u] \equiv \frac{\partial}{\partial x} \left(\mu(z) \frac{\partial u}{\partial x} \right) + \frac{\partial}{\partial z} \left(\mu(z) \frac{\partial u}{\partial z} \right) + (\rho(z)\omega^2 - i\omega\alpha)u = 0. \tag{1}$$

Generally the problem is formulated for a stratified inhomogeneous half-space. As the finite difference method can be also applied in a finite region G with boundary $\partial G = \partial G_1 \cup \dots \cup \partial G_5$, we shall transform our problem into a finite region (see fig. 1). This fact is given by the boundary conditions, which can be written in the form:

On the boundary ∂G_2 and ∂G_3 we have the condition

$$u|_{\partial G_2 \cup \partial G_3} = 0, \tag{2a}$$

i. e. the inhomogeneous absorption $\alpha(x, z, \lambda)$ of the near boundary $\partial G_2 \cup \partial G_3$ will increase to damp the wave so that the displacement may be considered zero. Physically this requirement can be met by preventing the waves reflected from boundaries $\partial G_2 \cup \partial G_3$ from penetrating into the region G .

On the boundary ∂G_1 , i. e. on the free surfaces, we have

$$\left. \frac{\partial u}{\partial n} \right|_{\partial G_1} = 0, \tag{2b}$$

i. e. the elastic stress at the free surfaces is zero.

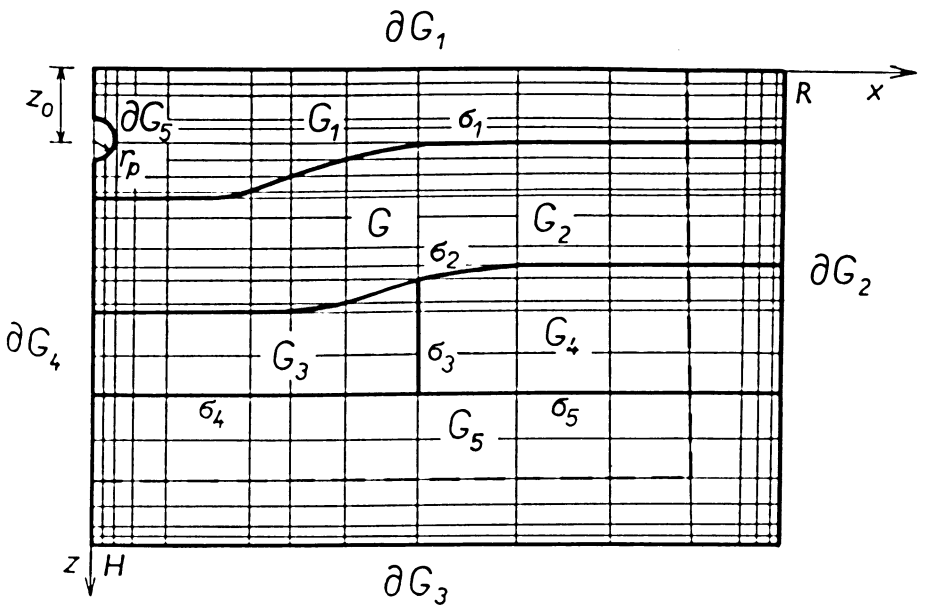
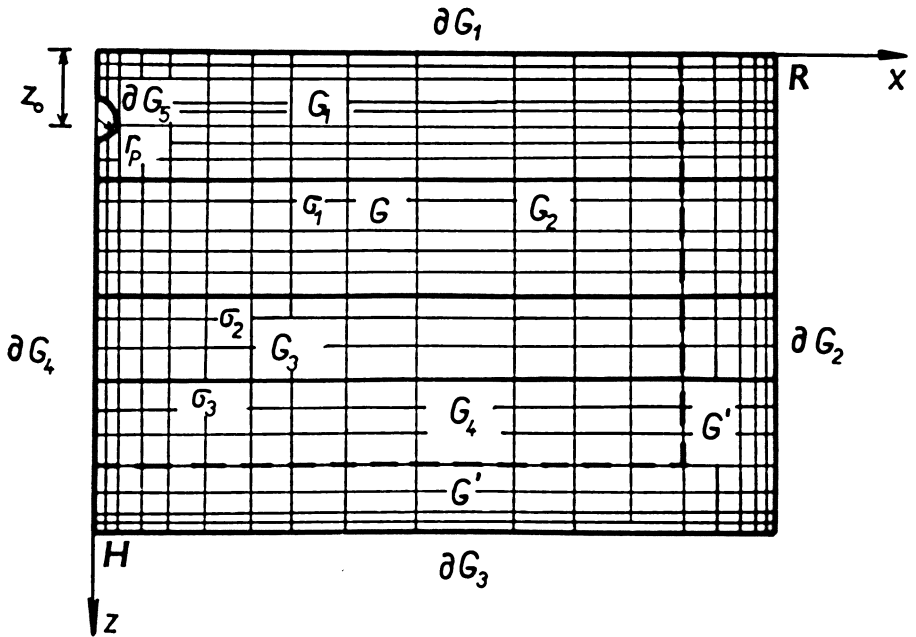


Fig. 1a, b: General schemes of computation fields.

On the boundary ∂G_4 we have

$$\left. \frac{\partial u}{\partial x} \right|_{\partial G_4} = 0, \quad (2c)$$

this condition is a condition of symmetry.

Singularity in the source is of the type $r^{-\frac{1}{2}}$. We shall describe a cylindrical surface around the source with a sufficiently small radius r_p so that we can neglect the non-singular component of the field and consider a singular part of the field only, i. e.

$$u|_{\partial G_5} = \exp(i\kappa_l r_p) \cdot r_p^{-\frac{1}{2}} \quad (2d)$$

At the interfaces σ_j , between the inhomogeneous layers, the elastic displacements and stresses are continuous functions

$$u_j = u_m; \quad \mu_j(z) \frac{\partial u_j}{\partial n} = \mu_m(z) \frac{\partial u_m}{\partial n}. \quad (2e)$$

For solving this problem by finite difference method, we define the mesh region G_h , generally with non-uniform spatial mesh and we shall replace region G by region G_h . In all mesh points we shall find elastic displacement. The differential operator is approximated by the difference operator in the form

$$\begin{aligned} L_h[u] &\equiv P_{i,j} u_{i+1,j} + Q_{i,j} u_{i-1,j} + R_{i,j} u_{i,j+1} + S_{i,j} u_{i,j-1} - (T_{i,j} + iV_{i,j}) u_{i,j} = \\ &= \frac{1}{4} \tau_{i,j} (h_{i-1} + h_i) (k_{j-1} + k_j), \end{aligned} \quad (3)$$

where $\tau_{i,j}$ is an approximation error and

$$\begin{aligned} P_{i,j} &= \frac{k_{j-1} + k_j}{2h_i} \mu_{i+\frac{1}{2},j}; & Q_{i,j} &= \frac{k_{j-1} + k_j}{2h_{i-1}} \mu_{i-\frac{1}{2},j}; \\ R_{i,j} &= \frac{h_{i-1} + h_i}{2k_j} \mu_{i,j+\frac{1}{2}}; & S_{i,j} &= \frac{h_{i-1} + h_i}{2k_{j-1}} \mu_{i,j-\frac{1}{2}}; \end{aligned} \quad (4)$$

$$T_{i,j} = P_{i,j} + Q_{i,j} + R_{i,j} + S_{i,j} - \frac{1}{4} \varrho_{i,j} \omega^2 (h_{i-1} + h_i) (k_{j-1} + k_j);$$

$$V_{i,j} = \frac{1}{4} \omega \alpha_{i,j} (h_{i-1} + h_i) (k_{j-1} + k_j); \quad u_{i,j} = u_{i,j}^{(1)} + iu_{i,j}^{(2)}; \quad u_{i,j} = u(x_i, z_j), \quad \text{e.t.c.};$$

where h_i, k_j are spacings of the mesh, and the operator of the boundary conditions are approximated with best accuracy.

The approximation of conditions on the interfaces σ_j between the inhomogeneous layer, i. e. on the surfaces of discontinuity of the velocity of seismic waves, can be made in several ways. Conditions on the interfaces σ_j (2e) can be approximated by centring differences or using the integration method to derive the difference equation for the mesh points of the interfaces σ_j . We obtain the equation in the form (3)–(4), where

$$\mu = \mu\left(z_j + \frac{1}{2}k_j\right) \quad \text{or} \quad \mu\left(z_j - \frac{1}{2}k_{j-1}\right)$$

or

$$\frac{1}{2}\left[\mu\left(z_j + \frac{1}{2}k_j\right) + \mu\left(z_j - \frac{1}{2}k_{j-1}\right)\right]$$

in the coefficients of Eq. (4), according to the place of the mesh points of a five-point pattern at the interfaces σ_j and in their neighbourhood.

Then it may be shown that

$$\begin{aligned} \|L[u] - L_h[u]\| &\rightarrow 0, \\ \|l_i[u] - l_{hi}[u]\| &\rightarrow 0 \quad (i = 1, \dots, 5), \end{aligned}$$

for

$$h = \max_G(h_i, h_{i-1}, k_j, k_{j-1}) \rightarrow 0,$$

i. e. that our problem of the propagation of *SH* waves may be solved for $h \rightarrow 0$ by finite difference method.

Now equations (3)–(4) and equations of approximation of the boundary conditions can be divided into the real and the imaginary parts. In this way we arrive at a system of algebraic equations

$$A\mathbf{u} = \mathbf{b} \tag{5}$$

where \mathbf{u} is the displacement vector in inhomogeneous medium, \mathbf{b} is the vector of the right size obtained from the boundary conditions and $A = (A_k, l)$ is the block matrix of the form

$$A = \begin{bmatrix} A_{1,1} & A_{1,2} & 0 & \dots & 0 & A_{1,p} & 0 & \dots & \dots & \dots & 0 \\ A_{2,1} & A_{2,2} & A_{2,3} & 0 & \dots & 0 & A_{2,p+1} & 0 & \dots & \dots & 0 \\ 0 & \cdot & \cdot & \cdot & \cdot & \cdot & \cdot & \cdot & \cdot & \cdot & \cdot \\ \vdots & \cdot & \cdot & \cdot & \cdot & \cdot & \cdot & \cdot & \cdot & \cdot & \cdot \\ \vdots & \cdot & \cdot & \cdot & \cdot & \cdot & \cdot & \cdot & \cdot & \cdot & \cdot \\ \vdots & \cdot & \cdot & \cdot & \cdot & \cdot & \cdot & \cdot & \cdot & \cdot & \cdot \\ 0 & \cdot & \cdot & \cdot & \cdot & \cdot & \cdot & \cdot & \cdot & \cdot & A_{p,N} \\ A_{p+1,1} & \cdot & \cdot & \cdot & \cdot & \cdot & \cdot & \cdot & \cdot & \cdot & \cdot \\ 0 & \cdot & \cdot & \cdot & \cdot & \cdot & \cdot & \cdot & \cdot & \cdot & \cdot \\ \vdots & \cdot & \cdot & \cdot & \cdot & \cdot & \cdot & \cdot & \cdot & \cdot & \cdot \\ \vdots & \cdot & \cdot & \cdot & \cdot & \cdot & \cdot & \cdot & \cdot & \cdot & \cdot \\ 0 & \dots & \dots & \dots & 0 & A_{N,p-1} & 0 & \dots & \dots & 0 & A_{N,N-1} & A_{N,N} \end{bmatrix},$$

where $A=(A_{k,l}), k=1, \dots, N, l=1, \dots, N$, is five block diagonal matrix and where non-zero 2×2 order matrix are formed by coefficients (4), i. e.

$$A_{k,k} = \begin{bmatrix} T_{i,j} & -V_{i,j} \\ V_{i,j} & T_{i,j} \end{bmatrix}, \quad A_{k,k+1} = \begin{bmatrix} P_{i,j} & 0 \\ 0 & P_{i,j} \end{bmatrix}, \quad A_{k+1,k} = \begin{bmatrix} Q_{i,j} & 0 \\ 0 & Q_{i,j} \end{bmatrix},$$

$$A_{k,k+p} = \begin{bmatrix} R_{i,j} & 0 \\ 0 & R_{i,j} \end{bmatrix}, \quad A_{k+p,k} = \begin{bmatrix} S_{i,j} & 0 \\ 0 & S_{i,j} \end{bmatrix}.$$

It may be shown that this matrix is regular and spectral radius $\rho(B)$ of JACOBI-matrix $B=I-A$ is less than unity. Then the system of algebraic equations (5) can be solved by iterative method of relaxation.

It may be also shown that for the guarantee of the convergence of this iterative process we have to reckon with a certain minimum number of mesh points per wave length, which is given by the estimation for the mesh spacing in dependence on elastic parameters of the medium, i. e.

$$k < \min_{\downarrow G} \left\{ \min \left[\mu \left(z_j + \frac{1}{2} k_j \right), \mu \left(z_j - \frac{1}{2} k_{j-1} \right) \right] \cdot \omega^{-2} \rho^{-1} (z_j) \right\}^{\frac{1}{2}}$$

The last estimation also gives a criterion for the extent of the studied models according to the parameters of computing technique. These restrictions either lead to a study of waves of intermediate and long wave lengths only, propagating in more extensive regions, or to the study of short-period waves in small regions i. e. in the domain of a high frequency we can study models, where the wavelengths λ are around 7 to 10 km and the dimensions of this studied regions are around 10 or 12 λ .

3. Discussion

In this section we should like to present some models of propagation of SH-waves in stratified inhomogeneous medium. The linear harmonic source is situated in a different depth in inhomogeneous medium. In the present figures of the studied

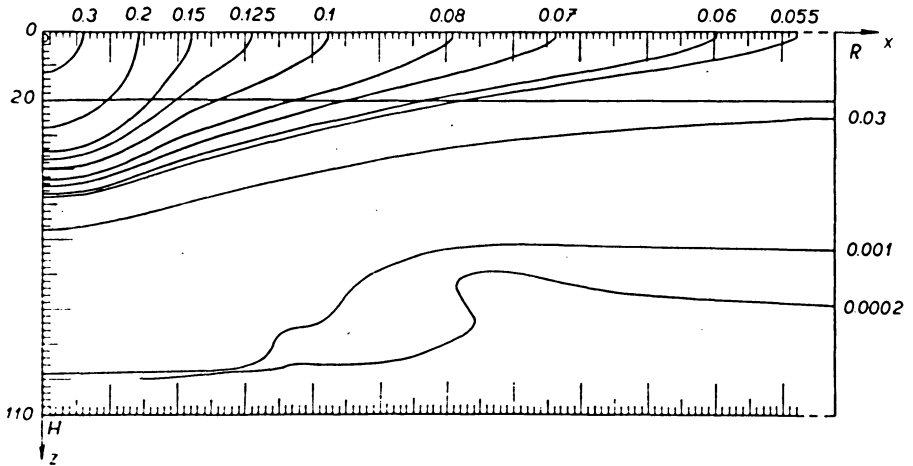


Fig. 2a: The surfaces of the same amplitudes.

Dimension of the model: $R = 280$ km, $H = 110$ km.
 Angular frequency $\omega = 0.39$ sec $^{-1}$.
 Coef. of the absorption
 in the working region $\alpha_0 = 0.00005$ g cm $^{-3}$ sec $^{-1}$.
 Position of the source $z_0 = 2.0$ km.

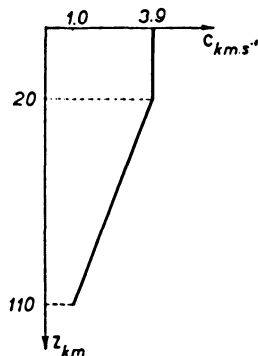


Fig. 2b: Velocity of seismic waves as a function of the depth.

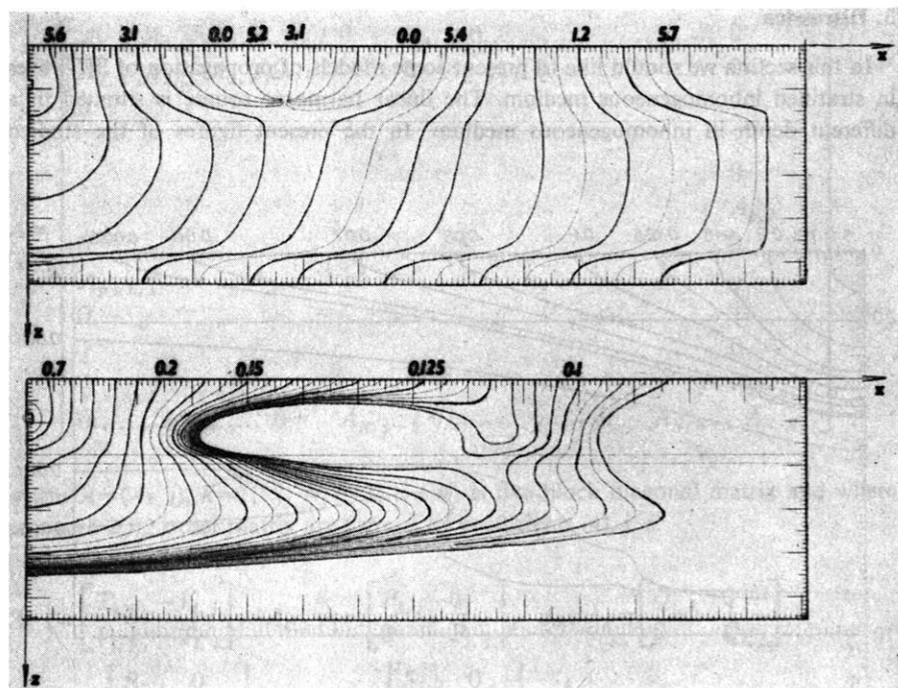


Fig. 3a: The surfaces of the same phases and amplitudes.

Dimension of the model: $R = 100$ km, $H = 30$ km.

Angular frequency $\omega = 0.78$ sec $^{-1}$.

Coef. of the absorption

in the working region $\alpha_0 = 0.00005$ g cm $^{-3}$ sec $^{-1}$.

Position of the source $z_0 = 4.91$ km.

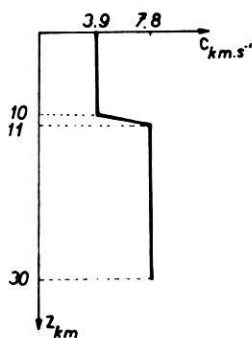


Fig. 3b: Velocity of seismic waves as a function of the depth.

models denoted by a), we can see the surfaces of the same phases and the same amplitudes of the displacement, and those denoted by b)—give the velocity of seismic waves as a function of depth. In Fig. 2a we can see the surfaces of the same amplitudes only.

The first model (Fig. 2a) shows the propagation of SH-waves in inhomogeneous medium with negative gradient of velocity. The elastic parameters are linear function in a part with respect to the depth, see fig. 2b. Occurrence of the shadow region is in good agreement with the known physical knowledge.

In the next figures (Fig. 3a and Fig. 4a) the models with a transition layer with high gradient of velocity (see fig. 3b and fig. 4b) are studied. While the thickness of this transition layer is about 1 km with the first model and it converges to the planar surfaces, with the second model, the thickness of the transition layer is about 4 km. The changes in the form of the surfaces of the same amplitudes (it is probably interference effect) and the shifts of the synphase surfaces are evident from the comparison of these models.

In the figures 5a and 6a, the propagation of SH-waves in medium with channel of the low or high velocity are studied. In the first figure (Fig. 5a), the layer of a negative gradient of velocity is represented, which in the depth of about 15 km passes into a medium with a positive gradient of velocity, and this one is situated under a homogeneous layer (see Fig. 5b). The second figure (Fig. 6a) shows the layer with positive gradient of velocity lying under homogeneous layer in the depth of about 10 km and which in the depth of about 20 km passes into the medium of negative gradient of velocity (see Fig. 6b).

In the end, we should like to discuss the possibility of numerical analysis for solving several cases of the problem of propagation of seismic waves in stratified generally inhomogeneous medium. It has proved that for the assumption of the existence of strongly absorptive medium, which absorbs the energy of the seismic waves, the region can be defined from the unlimited half-space, in which these properties of this wave field can be studied. It is evident that the formerly introduced strongly absorptive medium has the required properties. In the figures given above, i. e. in the case of the negative linear gradient of velocity it has been shown that the wave field in this working part of the medium is practically undisturbed. Analogous results were obtained for the models of homogeneous stratified medium given by one layer lying on the half-space, in which the SH-waves were generated by the harmonic spherically symmetrical source. Several cases of stratified medium with constant and varying thickness of the layer have been studied. Also the first experiment was carried out to compile the dispersive curves in several distances from the source.

In the case shown in Fig. 3a, b, the velocities of seismic waves are also continuous functions of the depth, but the transition layer converges to the planar surface, i. e. to the case, where the velocities of seismic waves are discontinuous functions of the depth. The obtained results are in good agreement with known physical facts, but there is much more to be explained about the shadow zone (see Fig. 3a). For a higher

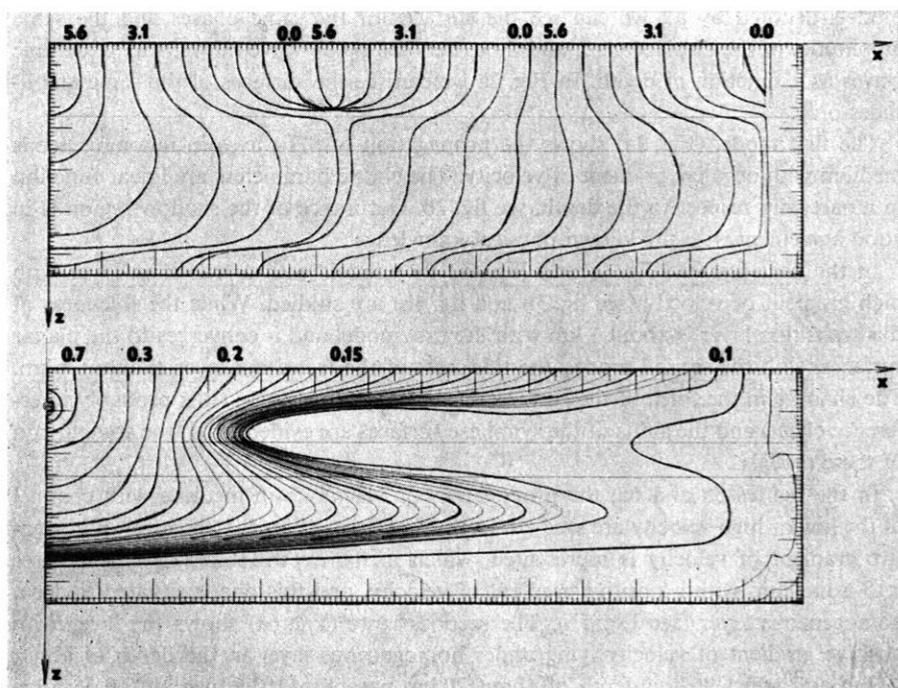


Fig. 4a: The surfaces of the same phases and amplitudes.

Dimension of the model: $R = 100$ km, $H = 30$ km.

Angular frequency $\omega = 0.78 \text{ sec}^{-1}$.

Coef. of the absorption
in the working region $\alpha_0 = 0.00005 \text{ g cm}^{-3} \text{ sec}^{-1}$.

Position of the source $z_0 = 4.91$ km.

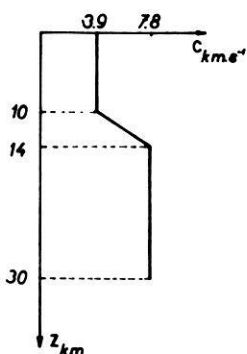


Fig. 4b: Velocity of seismic waves as a function of the depth.

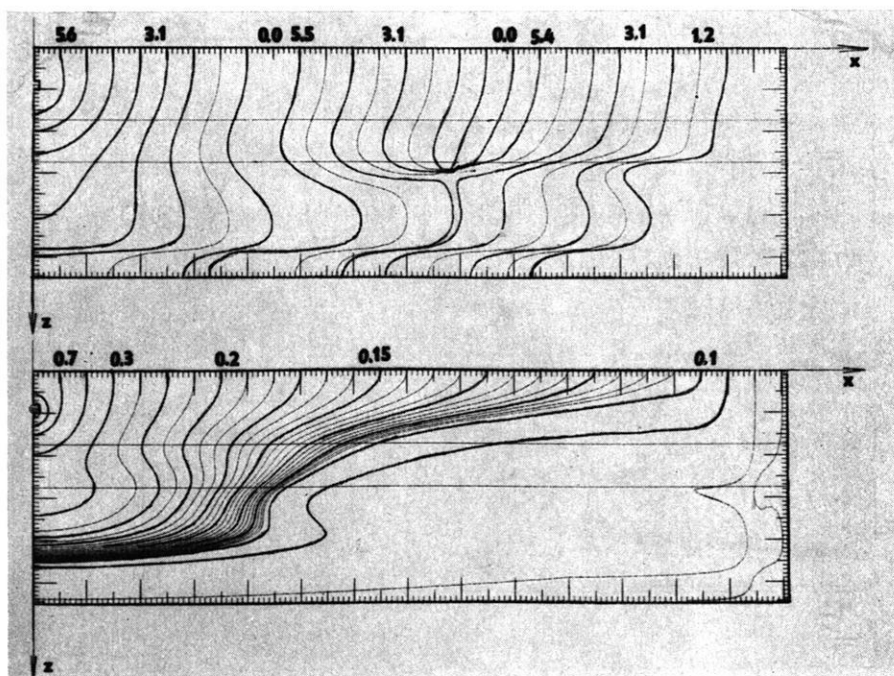


Fig. 5a: The surfaces of the same phases and amplitudes.

Dimension of the model: $R = 100$ km, $H = 30$ km.

Angular frequency $\omega = 0.78$ sec $^{-1}$.

Coef. of the absorption $\alpha_0 = 0.00005$ g cm $^{-3}$ sec $^{-1}$.
in the working region

Position of the source $z_0 = 4.91$ km.

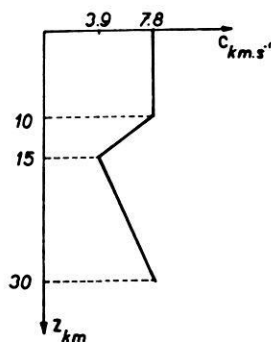


Fig. 5b: Velocity of seismic waves as a function of the depth.

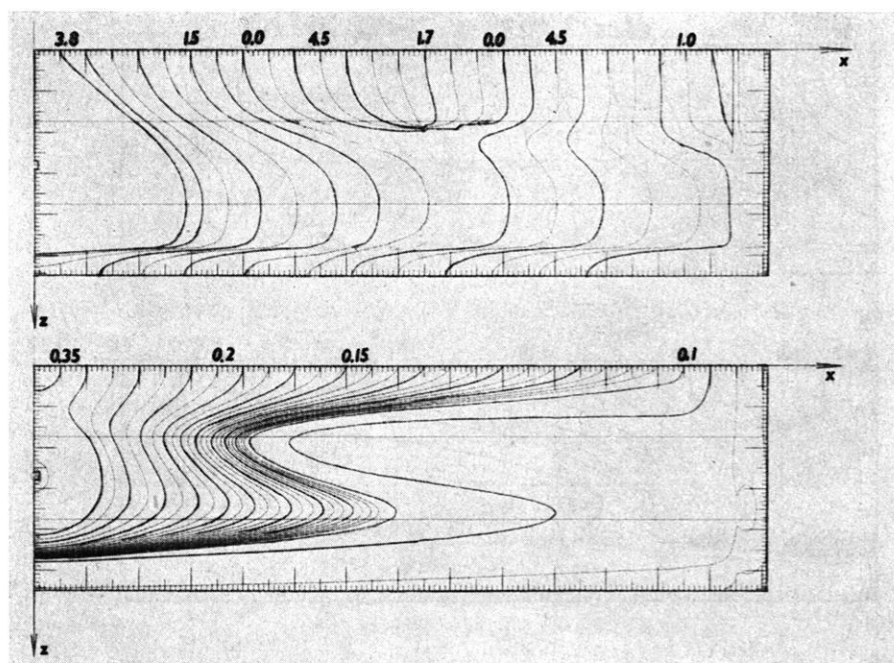


Fig. 6a: The surfaces of the same phases and amplitudes.

Dimension of the model: $R = 100$ km, $H = 30$ km.

Angular frequency $\omega = 0.78$ sec $^{-1}$.

Coef. of the absorption
in the working region $\alpha_0 = 0.00005$ g cm $^{-3}$ sec $^{-1}$.

Position of the source $z_0 = 14.73$ km.

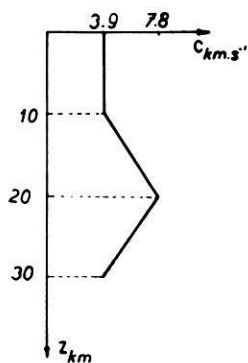


Fig. 6b: Velocity of seismic waves as a function of the depth.

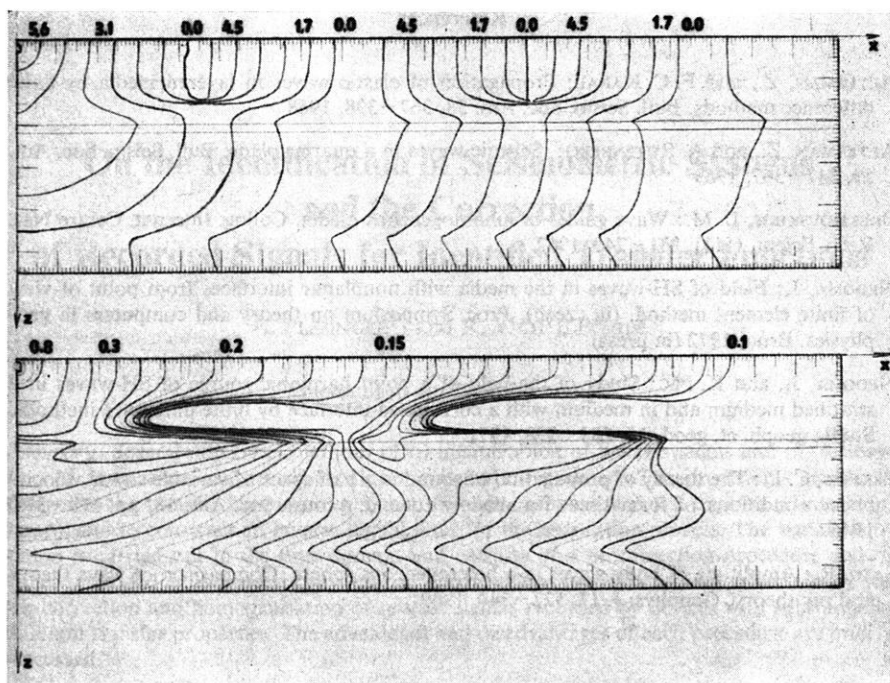


Fig. 7: The surfaces of the same phases and amplitudes.

Dimension of the model: $R = 100$ km, $H = 27.5$ km.

Angular frequency $\omega = 1.17$ sec $^{-1}$.

Coef. of the absorption
in the working region $\alpha_0 = 0.00005$ g cm $^{-3}$ sec $^{-1}$.

Position of the source $z_0 = 1$ km.

Situation of the layers $z_{\text{layer}} = 0, 10, 11, 27.5$ km.

Velocity in the depth

z_{layer} $c = 3.9, 3.9, 7.8, 7.8$ km sec $^{-1}$.

frequency the shadow zone is shifted to the vicinity of the source and as it can be seen from Fig. 7, the shadow zones regularly occur in conformity with some properties of SH-waves. From the preliminary results we are able to conclude that we are dealing with an interference feature, to which a further investigation has to be devoted.

4. Conclusion

In this paper the formal solution of the propagation of SH-waves in a stratified inhomogeneous medium using the finite difference method is presented. Several models are discussed there, the velocities are supposed to be continuous functions of the depth.

References

- ALTERMAN, Z., and F. C. KARAL: Propagation of elastic waves in layered media by finite difference methods. *Bull. Seism. Soc. Am.* 58, 367–398, 1968
- ALTERMAN, Z., and A. ROTENBERG: Seismic waves in a quarter plane. *Bull. Seism. Soc. Am.* 59, 347–367, 1969
- BREKHOVSKIKH, L. M.: Wave guides in inhomogeneous media. *Collog. Internat. Centre Nat. Rech. Scient.* (111), 231–240, 1962
- NEDOMA, J.: Field of SH-waves in the media with nonplanar interfaces from point of view of finite element method. (in czech). *Proc. Symposium on theory and computers in geophysics, Brno, 1972* (in press)
- NEDOMA, J., and K. PĚČ: Study of the field of a point harmonic source of SH-waves in a stratified medium and in medium with a corrugated interface by finite difference methods. *Studia geoph. et. geod.* 15, 288–298, 1971
- PEKERIS, C. L.: The theory of propagation of sound in a half space of variable sound velocity under conditions of formation of a shadow zone. *J. Acoust. Soc. Am.* 18, pp. 295–315, 1946
- SATO, R.: Amplitude of body waves in a heterogeneous sphere. Comparison of wave theory and ray theory. *Geophys. J.* 17, 527–544, 1969

On the Identification of Seismometric Systems and the Correction of Recorded Signals for Identified Transfer Functions

A. PLEŠINGER¹⁾ and R. VÍCH²⁾, Prague

Eingegangen am 22. Februar 1972

Summary: Several numerical methods of (i) identification of linear systems and (ii) restoration of input signals distorted by linear systems are outlined. The procedures enable to determine the transfer function of a system from its response to a test-impulse (Dirac, step, ramp), and to construct an inverse digital filter for the restoration process. The signal restoration is carried out in the time domain and consists of a precorrection procedure and of either one-sided or two-sided convolution. The described methods proved to be suitable for the correction and homogenisation of seismic signals recorded by devices with substantially different transfer properties. The advantages and disadvantages of each procedure are briefly discussed.

Zusammenfassung: Die Grundlagen einiger numerischer Verfahren zur (a) Identifizierung linearer Übertragungssysteme und (b) Wiederherstellung von durch lineare Systeme verzerrten Eingangssignalen werden beschrieben. Die Verfahren ermöglichen es, die Übertragungsfunktion eines Systems aus dessen Testimpulsantwort (Dirac, Sprung, Rampe) zu bestimmen und ein inverses Digitalfilter für die Signalwiederherstellung zu konstruieren. Die Signalverzerrung wird im Zeitbereich durchgeführt und besteht aus einer Vorkorrektionsprozedur und entweder einseitiger oder zweiseitiger Konvolution. Die beschriebenen Verfahren eignen sich zur Korrektur und Homogenisierung von Ausgangssignalen seismischer Meßgeräte mit wesentlich unterschiedlichen Übertragungseigenschaften. Die Vorteile und Nachteile der einzelnen Verfahren werden kurz diskutiert.

1. Introduction

The precise interpretation of seismic discontinuities requires exact knowledge of kinematic and dynamic characteristics of seismic waves covering a broad frequency range. Standard class seismograph systems and numerous devices used in laboratory investigations of seismic structures, however, in many cases give rise to linear distortions of the seismic information. Usually the distortions are caused by an insufficient pass-band of the system in comparison with the spectrum of the investigated pheno-

¹⁾ Dr. AXEL PLEŠINGER, Geofyzikální ústav ČSAV, Praha 4–Spořilov, Boční II, ČSSR.

²⁾ Dr. ROBERT VÍCH, Ústav pro radiotechniku a elektroniku ČSAV, Lumumbova 1, Praha-8-Kobylisy, ČSSR.

menon and/or by a non-linear course of the phase response of the system within its pass-band. In such a case the direct interpretation of the recording can lead to erroneous conclusions. Thus it is often unavoidable to correct the recorded signal for the transfer properties of the system before interpreting it.

For this purpose we need a complete description of the system, i. e. the general form and the coefficients of its transfer function. The exact determination of the transfer function and the system parameters by analytical methods and direct measurements is, however, either a very laborious and tedious business or—in the case of relatively complicated systems—even impracticable. The transfer properties of seismometric devices are therefore mostly established and checked by test-signal methods, i. e. by measuring the response of the system in either the frequency domain or the time domain to a certain input signal (or to a set of known input signals). From the response, the transfer function of the system must then be determined by an identification method.

The process of restoration usually consists of (i) the synthesis of a stable digital filter that approximates in a certain frequency range the inverse transfer function of the system and (ii) the convolution of the selected portion of the seismic recording with the impulse response of this filter; alternatively, the restoration can be carried out in the frequency domain by (i) correcting the complex spectrum of the signal for the frequency response of the system and (ii) inverse Fourier transformation of the corrected spectrum [RICE 1962, BOGERT 1962, SAVARENSKI, FEDOROV and GOKIKAISHVILI 1963, HON-YIM KO and SCOTT 1967, VÍCH 1970a, PLEŠINGER, SCHICK and ZÜRN 1971].

In this contribution we briefly report on the principles and basic properties of generally applicable identification and restoration procedures which proved to be suitable for homogenizing data recorded by seismometric devices with quite different transfer functions.

2. Identification procedures

The methods described below enable to determine the impulse invariant transfer function of a linear system from its measured response to various test signals (Dirac, step, ramp). The procedures require no knowledge of the general form of the transfer function of the investigated system. In principle, they can be also used for the direct construction of an inverse digital filter for the restoration process.

2.1 Identification by approximation of the system response.

This method is based on the facts that responses of the mentioned type can be closely approximated by a sum of damped cosine functions

$$f(t) = \sum_{i=1}^k C_i e^{-\alpha_i t} \cos(\beta_i t + \gamma_i),$$

where $C_i, \alpha_i, \beta_i, \gamma_i$ are positive real numbers, and that the Z -transform of a sequence f_n obtained by equidistant sampling of such a function ($f_n=f(nT); n=0, 1, 2, \dots, s; T$ =sampling interval) has the form of a discrete transfer function

$$F^*(z) = \frac{A_0 z^r + A_1 z^{r-1} + \dots + A_{r-1}}{z^r + B_1 z^{r-1} + \dots + B_r},$$

where r is the so-called "approximation degree" [VÍCH 1968]. For the coefficients A_0, A_1, \dots and B_1, B_2, \dots of the transfer function $F^*(z)$ hold recurrent relations which can be presented in matrix form as

$$\begin{aligned} A_0 &= f_0, \\ [P] \cdot [X] &= [f], \end{aligned} \quad (1)$$

where

$$[P] = \left[\begin{array}{ccc|ccc} 1 & 0 \dots 0 & -f_0 & 0 & \dots & 0 \\ 0 & 1 \dots 0 & -f_1 & -f_0 & \dots & 0 \\ \vdots & \vdots & \vdots & \vdots & \vdots & \vdots \\ 0 & 0 \dots 1 & -f_{r-2} & -f_{r-3} \dots & 0 & \\ 0 & 0 \dots 0 & -f_{r-1} & -f_{r-2} \dots -f_0 & & \\ 0 & 0 \dots 0 & -f_r & -f_{r-1} \dots -f_1 & & \\ 0 & 0 \dots 0 & -f_{r+1} & -f_r & \dots -f_2 & \\ \vdots & \vdots & \vdots & \vdots & \vdots & \vdots \\ 0 & 0 \dots 0 & -f_{s-1} & -f_{s-2} \dots -f_{s-r} & & \end{array} \right],$$

$$[X] = \begin{bmatrix} A_1 \\ A_2 \\ \vdots \\ A_{r-1} \\ B_1 \\ B_2 \\ \vdots \\ B_r \end{bmatrix}, \quad [f] = \begin{bmatrix} f_1 \\ f_2 \\ \vdots \\ f_{r-1} \\ f_r \\ f_{r+1} \\ \vdots \\ f_s \end{bmatrix}.$$

Let us denote the response of the system which we want to identify $h(t)$. Setting in the recurrent relations for $f_n = h_n - \varepsilon_n$, where h_n are equidistant samples of $h(t)$ and $\varepsilon_n = h_n - f_n$ approximation errors, we obtain a modified system of Eqs. (1). This system can now be solved by the method of least squares.

A description of this considerably laborious process is given in a previous paper [PLEŠINGER and VÍCH 1971]. The result is a system of normal equations of $2r-1$

unknowns, which, expressed in matrix notation, has the form

$$\begin{aligned} A_0 &= h_0, \\ [T] \cdot [Q] \cdot [X] &= [0], \end{aligned} \quad (2)$$

where $[T]$ is the transposed matrix $[P]$ in the modified system (1), $[Q]$ is the matrix $[P]$ completed by the column of the right sides of this system and $[0]$ is a zero matrix. The solution of the system (2) yields the coefficients A_i, B_i ($i=1, 2, \dots, r$) of a transfer function $H^*(z)$ the impulse response of which approximates the sequence h_n in the sense of least squares.

Because the number of unknowns is $2r-1$, the number of given samples h_n must be $s+1 \geq 2r$. When digitizing the response $h(t)$ we get a sequence h_n the values of which are beginning from a certain $n > N$ smaller than the reading (or quantization) errors. Thus equations beginning with $N+r+1$ lose their sense. Therefore must hold $N+r \geq s$ and, together with the foregoing condition,

$$2r-1 \leq s \leq N+r. \quad (3)$$

By solving the system of Eqs. (2) for a set of gradually increasing values of r fulfilling condition (3) we obtain a set of transfer functions corresponding to the given response. If noise components contained in the digitized response are smaller than $\sim 0.1\%$ of its maximal amplitude, some zeros and poles of the transfer functions are —beginning from a certain value $r > R$ —practically identical so that their influence is cancelled. The value of R depends on the complexity of the tested system. In “over-approximated” cases, i. e. if $r > R$, the number of cancelling zero/pole pairs is $R-r$ so that the degree of the identified transfer function can be decreased to the “optimal” value R . If the identified transfer function has no zeros outside the unit circle $|z|=1$, the inversion of $H^*(z)$ yields directly the transfer function of a stable inverse digital filter.

The last step, completing the identification procedure, is the determination of the continuous transfer function $H(p)$ corresponding to $H^*(z)$. In our case no discrete system is investigated but only the discrete simulation of a continuous system is sought. Thus the main requirement is that both systems are impulse invariant. A procedure which performs the conversion of $H^*(z)$ into $H(p)$ with respect to this requirement is described in par. 2.3.

In accordance with the test-signal applied to the system the resulting expression for $H(p)$ must be, finally, completed by the respective number of zeros in the origin of the p -plane. The final expression for the continuous transfer function of the system is thus $S(p)=H(p) \cdot p^m$, where m is the number of additive zeros at $p=0$ (in the case of an electromagnetic pendulum type seismograph, for instance, tested by a current step in its calibration coil, $m=3$).

2.2 Identification by expansion of the system response into a continued fraction.

Contrary to the method outlined in par. 2.1 this procedure is a purely algebraic one. It takes advantage of the properties of continued fractions and proved to be suitable for an exact determination of transfer functions from relatively noise-free responses.

Let h_n ($n=0, 1, 2, \dots, s$) be again a sequence obtained by appropriate equidistant sampling of the system response $h(t)$. By Z-transforming this sequence we get the transfer function

$$H^*(z) = \sum_{n=0}^s h_n z^{-n} = h_0 + h_1 z^{-1} + \dots + h_s z^{-s} \quad (4)$$

of an impulse invariant system. Applying the method described by KHOVANSKI [1956] we may expand the polynomial (4) into a continued fraction, i. e. into the form

$$H^*(z) = \frac{a_1}{b_1 + \frac{a_2 z^{-1}}{b_2 + \frac{a_3 z^{-1}}{b_3 + \dots}}} \quad (5)$$

where a_1, a_2, \dots and b_1, b_2, \dots are real numbers. The approximants of the continued fraction are rational fractions in the variable z^{-1} [KHOVANSKI 1956]. If we use i members of the continued fraction, the respective approximant is given as

$$H_i^*(z) = \frac{\alpha_0 + \alpha_1 z^{-1} + \dots + \alpha_j z^{-j}}{\beta_0 + \beta_1 z^{-1} + \dots + \beta_k z^{-k}} \quad (6)$$

where $\alpha_0, \alpha_1, \dots$ and β_0, β_1, \dots are again real numbers and where $j=k=(i-1)/2$ or $k=i/2, j=k-1$ if i is an odd or an even number, respectively. The expression (6) can now be arranged into the form of a function in the variable z .

As result we obtain the transfer function

$$H_i^*(z) = \frac{A_1 z^m + A_2 z^{m-1} + \dots + A_j}{B_1 z^n + B_2 z^{n-1} + \dots + B_k} \quad (7)$$

of a discrete system the impulse response of which approximates the given sequence h_n with a zero-error in the points h_0, h_1, \dots, h_i . The index i (=number of used members of the continued fraction (5)) states simultaneously the total number of the coefficients A_1, A_2, \dots and B_1, B_2, \dots , i. e. $j+k=i$. Furthermore, for the degree of the

polynomial in the numerator of the expression (7) holds $m=n-1$ if $h_0=0$ and $m=n$ if $h_0 \neq 0$.

This procedure evidently enables to construct a set of recursive transfer functions which approximate with a gradually increasing accuracy an arbitrarily "long" discrete transfer function given in the non-recursive form (4). The fact that the index i gives the number of samples of the response $h(t)$ for which the approximation error equals zero is a very favourable property: together with the estimated degree of the continuous transfer function of the investigated system it yields a practical criterion for an optimal choice of the sampling interval T which should be used when digitizing the response $h(t)$.

If noise components contained in the sequence h_n are negligible ($\leq 0.1\%$ of the maximal amplitude of the response), in the identified transfer functions $H_i^*(z)$ appear—beginning from a certain $i > i_{opt}$ —some equal zeros and poles which can be omitted so that the degree of the respective transfer function is decreased.

From the resulting expression for $H_i^*(z)$ the continuous transfer function $S(p)$ of the system can then be determined in the same way as described in par. 2.1.

2.3 Conversion of identified discrete transfer functions.

The requirement that the continuous system and its discrete simulation have to be impulse invariant means that both systems must have for $t=nT$ ($n=0, 1, \dots$; T =sampling interval) the same impulse response. This condition is fulfilled if the conversion of $H^*(z)$ into $H(p)$ is performed in the following way.

We expand the given function $H^*(z)$ which can be expressed in the form

$$H^*(z) = H \frac{\prod_{i=1}^{r-1} (z - \alpha_i)}{\prod_{i=1}^r (z - \beta_i)}$$

(where H is a real constant and α_i, β_i are generally complex zeros and poles), into partial fractions. That means we express it as

$$H^*(z) = \sum_{i=1}^r C_i z / (z - \beta_i).$$

Now we find for a given T the respective component of the analogous decomposition of the sought \mathcal{L} -transform

$$H(p) = \sum_{i=1}^r K_i / (p - p_i) \quad (8)$$

via the known relations

$$\beta_i > 0, \text{ real: } \Rightarrow p_i = \frac{1}{T} \ln \beta_i,$$

$$\beta_i < 0, \text{ real: } \Rightarrow p_i = \frac{1}{T} \ln |\beta_i| + j \frac{\pi}{T}, \quad (j = \sqrt{-1}),$$

$$\beta_i \text{ complex: } \Rightarrow p_i = \frac{1}{T} \ln |\beta_i| + j \frac{1}{T} \arg \beta_i,$$

$$\beta_i = 0: \quad \text{cannot occur for physical reasons.}$$

(In the case that any β_i are complex they will always occur only in complex conjugate pairs.) After having obtained the transfer function $H(p)$ in form (8) we arrange it to the usual form of the ratio of two polynomials $M(p)/N(p)$ by mechanical summation of the partial fractions. The poles of the resulting function are given directly by (8), the zeros are obtained as the solution of the equation $M(p)=0$.

In order to avoid oscillations of the response $h(t) = \mathcal{L}^{-1}\{H(p)\}$ between the points $t = nT$ it is necessary to choose the main branch of $\arg \beta_i$ in the conversion of β_i into p_i .

3. Restoration procedures

Before coming to the description of the methods, it is desirable to point out the fundamental problems of practical restoration.

Let $S(p)$ be the identified transfer function of a linear system and $x(t)$, $y(t)$ its input and its output signal, respectively. For the sought input signal then holds

$$x(t) = y(t) * \mathcal{L}^{-1}\{1/S(p)\}, \quad (9)$$

i. e. it can be restored by convolving the given output $y(t)$ and the impulse response of the inverse system.

Here we meet the first problem caused by the fact that inverse transfer functions of physical systems are generally unstable. The inverse transfer function of a standard class seismograph systems, for instance, has the form

$$S^{-1}(p) = (p^4 + a_1 p^3 + a_2 p^2 + a_3 p + a_4) / K p^3, \quad (10)$$

where K, a_1, \dots, a_4 are positive real constants. It is obvious that $|S^{-1}(j\omega)| = S^{-1}(\omega) \rightarrow \infty$ with the slope ω^3 or ω if $\omega \rightarrow 0$ or $\omega \rightarrow \infty$, respectively. Irrespective of this instability the restoration could easily be performed if we knew the system response $y(t)$ to the actual input signal exactly. However, as no physical system is totally noise-free,

the output function $y(t)$ always contains components which have no relation to $x(t)$. Moreover, the generally infinite-length function $y(t)$ is usually obtained by analogue registration and must be appropriately truncated and digitized beforehand. Even if this is done carefully, error components of up to several percent can appear in the respective sequence y_n .

Due to these noise components and to the instability of the deconvolution operator the process of direct numerical restoration can become unstable. For instance, if the operator has the form (10), the error components rapidly cumulate (the process contains a triple integration) so that the "restored" signal often grows without limit with increasing time.

To overcome these difficulties it is evidently unavoidable to use a "stabilized" method of numerical restoration. That is to say, for the purpose of practical restoration we must design a stable digital filter the transfer function of which approximates not only the continuous inverse transfer function $S^{-1}(p)$ but moreover cuts off error spectral components of the discrete signal y_n .

3.1 Noncausal deconvolution

The convolution (9) can be performed numerically in various ways. One of the simplest possibilities consists in dividing the Z -transform $Y^*(z) = Z\{y_n\}$ by the polynomial $S^*(z) = Z\{s_n\}$ where s_n ($n=0, 1, \dots, N$) is the digitized impulse response of the system (from the identified transfer function $S(p)$ the sequence s_n can be determined by numerical inverse Laplace transformation). However, this direct method is very sensitive to instability.

One way how to avoid the instability is the procedure of TREITEL and ROBINSON [1964] who treat the inverse function $1/S^*(z)$ as a general two-sided impulse response. The procedure consists of the following steps:

1. the solution of the polynomial equation $z^N S^*(z) = 0$;
2. the decomposition of the polynomial into two parts: $S_1^*(z)$ with roots $|z_i| < 1$ (minimum-delay polynomial) and $S_2^*(z)$ with roots $|z_i| > 1$ (maximum-delay polynomial);
3. the inversion of $S_1^*(z)$ and $S_2^*(z)$; this inversion yields a stable "memory" and a stable "anticipation" function;
4. the convolution of these two functions; the result is a two-sided stable deconvolution operator s_n^{-1} ($n = -N_1, -N_1 + 1, \dots, -1, 0, 1, \dots, N_2$) composed of N_1 delay and N_2 advance members.

The restoration procedure itself can then be carried out by convolving y_n with s_n^{-1} , where y_n must have as many "past" (delay) members as s_n^{-1} . In practice it is more convenient to evaluate this convolution with the aid of the Z -transforms of the two sequences. The samples \tilde{x}_n of the restored input signal $\tilde{x}(t)$ (=approximation of the actual $x(t)$) are then given by the coefficients at the respective powers of z in the

resulting polynomial $\tilde{X}^*(z) = Y^*(z) \cdot S^{*-1}(z)$, where $Y^*(z) = Z\{y_n\}$ and $S^{*-1}(z) = Z\{s_n^{-1}\}$.

In comparison with the procedure described in par. 3.2 this method gives better results in the case of non-zero initial conditions of the processed signal, i. e. the method enables to correct the signal $y(t)$ "per partes" (for instance only a selected wave group of a complete seismogram). A disadvantage of the method is that it requires a very exact solution of a polynomial equation of a very high degree (the lengths of sequences approximating "well" impulse responses of physical systems currently reach values of $N = 50 \div 200$) which must be carried out in multiple arithmetics. For this reason and because of the double convolution the noncausal method is very time consuming. Moreover, in practical cases it often happens that some roots of the polynomial $S^{*-1}(z)$ lie in the close vicinity of the boundary of stability so that even small error components in the sequence y_n can significantly influence the result.

3.2 Approximate inverse digital filtering.

Due to the contents of noise components in the discrete signal y_n the restored input function can become unstable even if a stable deconvolution operator is used. It is obvious that to stabilize the process we must in some way suppress such noise components which constitute the main source of the instability. In the following procedure this is done with the aid of a filter that limits the frequency band in which the deconvolution is carried out.

The method is based on the assumption that the energy of the input signal to be restored is concentrated within a limited frequency band. If this assumption is not fulfilled, we must be satisfied with a more or less imperfect approximation of the actual input signal. The applicability of the method is limited to minimum-phase systems (i. e. to systems the transfer function of which has no zeros in the right half of the p -plane).

A suitable filter for a given case can be constructed in various ways. The method described below proved to be favourable especially for processing output signals of conventional seismograph systems.

First we compute by current numerical methods the amplitude spectrum $a(\omega)$ of the signal to be convolved and the amplitude curve $A^{-1}(\omega)$ of the inverse system. By multiplying the two functions we obtain a "corrected" amplitude spectrum which usually has a reasonable course only in a limited frequency band $\langle \omega_1, \omega_2 \rangle$ and rapidly grows without limit outside this band. This effect is caused by the spectral noise components contained in $a(\omega)$. Thus the frequencies ω_1, ω_2 and the slope of the course of $A^{-1}(\omega)$ outside the frequency band $\langle \omega_1, \omega_2 \rangle$ yield appropriate criteria for the design of an "optimal" band-pass filter for the given case. It can be shown that the transfer function of such a filter will have the general form

$$H(p) = \frac{p^m}{(p^m + a_{m-1}p^{m-1} + \dots + a_0) \cdot (p^n + b_{n-1}p^{n-1} + \dots + b_0)}. \quad (11)$$

The necessary degree of the numerator and of the denominator can be determined from the slopes of the course of $A^{-1}(\omega)$ in the frequency bands $\omega < \omega_1$ and $\omega > \omega_2$. Let q, r be integers which give the slopes in multiples of 6 db/octave; for m and n then must hold $m > q$ and $n > r$. The higher the degrees are chosen, the more efficiently the noise components will be suppressed. From the known values of the cut-off frequencies ω_1, ω_2 the respective filter can now be constructed by current methods of network synthesis [BALABANIAN 1958]. To avoid undesirable resonance effects we mostly use the Thompson (maximally flat group delay) approximation.

In practice the cut-off frequency ω_2 is frequently pre-determined by the used sampling frequency $\omega_N = \pi/T$. In such a case a high-pass filter (i. e. a function of the type (11) with $n=0$) is sufficient for the stabilization.

After having designed the filter we construct—using one of the methods described in a previous paper [VÍCH 1970b]—a discrete transfer function $\tilde{S}^{*-1}(z)$ which simulates the frequency properties of the “stabilized” continuous transfer function $\tilde{S}^{-1}(p) = H(p)/S(p)$.

The approximation $\tilde{x}(t)$ of the actual input signal $x(t)$ is then gained in the same way as described in par. 3.1, i. e. the samples \tilde{x}_n are obtained from the polynomial $\tilde{X}^*(z) = Y^*(z) \cdot \tilde{S}^{*-1}(z)$ which results from the process of digital filtering.

3.3 Pre-correction of digitized portions of analogue recordings.

Hand or automatically digitized portions of analogue seismic recordings frequently contain a predominant noise component in the form of a non-zero mean value and a linear trend. To eliminate this destabilizing component from the signal to be deconvolved we use a method of additive pre-correction which is based on the same principle as that applied to the integration of accelerograms [SCHIFF and BOGDANOFF 1967]. The method differs from others in the detail that we do not correct the digitized signal $y(t)$ itself but its first integral.

The process consists of the following steps (for simplification the discrete signals are noted as continuous time functions):

1. simple and double numerical integration of $y(t)$ by the trapezoidal rule and evaluation of the definite integrals (Simpson rule)

$$B_i = \int_0^L v(t) t^{i+1} dt \quad \text{where } i=0, 1, 2,$$

$L = (N-1)T$ is the length of $y(t)$ (N =number of samples, T =sampling interval) and

$$v(t) = \int \int y(t) dt;$$

2. solution of the system of equations

$$\begin{bmatrix} L^3/3 & L^4/8 & L^5/15 \\ L^4/4 & L^5/10 & L^6/18 \\ L^5/5 & L^6/12 & L^7/21 \end{bmatrix} \cdot \begin{bmatrix} c_0 \\ c_1 \\ c_2 \end{bmatrix} = \begin{bmatrix} B_0 \\ B_1 \\ B_2 \end{bmatrix};$$

as a result we obtain the values of the constants c_0 , c_1 , c_2 that minimize the definite integral

$$\int_0^L v_c^2(t) dt$$

in which

$$v_c(t) = \int [a(t) - (c_0 + c_1 t + c_2 t^2)] dt \quad \text{and} \quad a(t) = \int y(t) dt;$$

3. determination of the pre-corrected first integral $a_c(t)$ of the signal $y(t)$:

$$a_c(t) = a(t) - (c_0 + c_1 t + c_2 t^2).$$

The main advantage of this modified method is that its application enables to avoid one integration in processes of deconvolution which contain a multiple integration (i. e. in cases of transfer functions $S(p)$ which have zeros in the origin of the p -plane). That means that one pole $p_t=0$ of the inverse transfer function $1/S(p)$ —from which the deconvolution operator is derived—can be left out. It was experienced that this simplification significantly contributes to the stabilization of the process of deconvolution.

4. Conclusion

The properties of the individual procedures were verified by processing analytical signals with modelled error components, shake table data, and semiautomatically digitized actual seismograms and test-signal responses.

For the identification of selective systems the procedure 2.1 proved to be superior to that described in par. 2.2. The results of the identification of conventional seismograph systems by both methods were comparable.

In comparison with the procedure 3.2, the method of noncausal deconvolution can be said to be more convenient for processing pre-corrected signals containing no instrumental noise. This method is also more generally applicable and less sensitive to truncation errors. The procedure 3.2, eventually combined with 3.3, is favourable for processing relatively "noisy" signals. However, the result always represents only a compromise solution of the restoration problem.

Results of the practical application of the methods given in this informative paper will be presented and discussed in detail at the "Seminar on Deconvolution of Seismograms" which will be held in March 1972 in Prague.

References

- BALABANIAN, N.: *Network Synthesis*. Prentice-Hall Inc., New York 1958
- BOGERT, B. P.: Correction of Seismograms for the Transfer Function of the Seismometer. *Bull. Seism. Soc. Am.* 52, 781–792, 1962
- HON-YIM KO, R. F. SCOTT: Deconvolution Techniques for Linear Systems. *Bull. Seism. Soc. Am.* 57, 1393–1408, 1967
- KHOVANSKI, A. N.: Application of Continued Fractions and of their Generalizations to Approximate Analysis (in Russian). Gosudarstv. Isdatelstvo Tekhniko-Teoret. Literaturny, Moscow 1956
- PLEŠINGER, A., R. SCHICK, W. ZÜRN: Stability Problems in the Approximation of True Ground Motion. Proc. of the XII. Gen. Ass. of the ESC (Luxembourg 1970), Inst. Météorologique de Belgique, 253–256, Bruxelles 1971
- PLEŠINGER, A., R. VÍCH: Two Identification Methods and their Application to Seismograph System Calibration. PÚRE No. 47 (Proc. of the Inst. of Radio Engin. and Electr.), Praha 1971
- RICE, R. B.: Inverse Convolution Filters. *Geophysics* 27, 4–18, 1962
- SAVARENSKI, E. F., S. A. FEDOROV, B. V. GOKIKAISHVILI: Determination of the True Ground Motion and of its Spectrum from Seismograms (in Russian). *Izvestia Acad. of Sciences USSR, seria geofisicheskaja*, No. 9, 1340–1346, 1963
- SCHIFF, A., J. L. BOGDANOFF: Analysis of Current Methods of Interpreting Strong-motion Accelerograms. *Bull. Seism. Soc. Am.* 57, 857–874, 1967
- TREITEL, S., E. A. ROBINSON: The Stability of Digital Filters. *IEEE Transact. on Geosci. Electr.*, GE-2, 6–18, 1964
- VÍCH, R.: About Some Problems of Seismic Signal Processing. Proc. of the I. FORMATOR Symposium on Mathematical Methods for the Analysis of Large Scale Systems (Liblice 1970), Inst. of Information Theory and Automation, Praha 1970a
- VÍCH, R.: Some Approximation Methods for Digital Simulation of Continuous Systems. PÚRE No. 45 (Proc. of the Inst. of Radio Engin. and Electr.), Praha 1970b

The Influence of the Low Velocity Zone on Phase Velocities and Amplitudes of Love Waves

K. PĚČ and O. NOVOTNÝ, Prague¹⁾

Eingegangen am 12. Februar 1972

Summary: The model CANSD of the Canadian Shield has been used to study the influence of shear velocities on Love wave phase velocities. The fundamental and the first two higher modes have been considered. Compared with the fundamental mode, the higher modes are more convenient to structure studies of low velocity zones since they are more sensitive to shear velocities. It has been shown on our particular model that the amplitudes of higher modes are comparable with the amplitudes of the fundamental mode if the source is situated in the low velocity zone or below it.

Zusammenfassung: Zur Untersuchung des Einflusses der Scherwellengeschwindigkeit auf die Phasengeschwindigkeit der Love-Wellen wurde die Tiefenstruktur des Kanadischen Schildes, wie sie im Modell CANSD vorausgesetzt wird, angewendet. Die charakteristischen Parameter der Grundmode und der höheren Moden der Love-Wellen wurden theoretisch behandelt. Im Vergleich zur Grundmode sind die höheren Moden bei der Festlegung seismischer Strukturen mit Zonen niedrigerer Geschwindigkeit vorteilhafter, da sie gegenüber der Scherwellengeschwindigkeit empfindlicher sind. Für den Fall der Herdlage innerhalb oder unterhalb der Zone mit niedrigerer Geschwindigkeit konnte gezeigt werden, daß die Amplituden höherer Moden vergleichbar mit den Amplituden der Grundmode sind.

1. Introduction

The low velocity zones are very important regions of the Earth, but the investigation of their detailed structure meets great difficulties, especially when body wave methods are applied. The contemporary knowledge on low velocity zones has been mostly obtained using surface wave dispersion. Mainly, the fundamental mode has been made use of. The recent studies with reference to the higher modes properties [ANDERSON 1967; KOVACH 1965] have shown the possibility of utilizing them to the low velocity structure determination for following reasons:

1. A good deal of surface wave energy propagates in a certain period range within the low velocity zone (as it follows e. g. from the study of the surface wave displacement distribution with depth [KOVACH 1965; KOVACH and ANDERSON 1964]) and under suitable circumstances the share of the higher mode energy may be considerable.

¹⁾ Prof. Dr. KAREL PĚČ and Dr. OLDŘICH NOVOTNÝ, Geofyzikální ústav Karlovy university, Ke Karlovu 3, Praha-2, ČSSR.

2. There is not a period range for the fundamental mode where the influence of low velocity layers would be predominant. The influence of the layers situated close to the Earth's surface keeps to be comparatively large within the whole period range [BRUNE and DORMAN 1963; NOVOTNÝ 1970]. On the other hand, it will be shown by means of partial derivatives of higher mode dispersion curves that an interval of periods does exist where the low velocity zone layers affect more the behaviour of the dispersion curve than the surface layers.

The present contribution deals with partial derivatives of dispersion curves of the fundamental and the first two higher modes of Love waves for the examination of their sensitivity to layer parameters variation. Further, the theoretical seismograms of separate Love wave modes have been calculated in order to estimate the mutual amplitude relationship of the individual modes.

All conclusions made in this paper are, strictly speaking, restricted to the considered model CANSD, but their validity may be very probably extended to other models including a low velocity zone.

2. Partial derivatives of the fundamental, first and second higher modes of Love waves

The BRUNE'S DORMAN'S model CANSD [1963] chosen for the purpose of the present study consists of 8 layers. The first three are crustal layers, then follows one high velocity layer, next come two low velocity layers (numbers 5 and 6) as shown in Table 1.

The dispersion curves belonging to the model CANSD are drawn in Fig. 1. The slope of the higher mode curves varies fastly in the vicinity of the period of 9 sec. At that point the dispersion curves c_1 and c_2 approach very closely to each other. A similar

Table 1: Parameters of the model CANSD [BRUNE and DORMAN, 1963]. Letter i is layer number, b_i shear wave velocity in km/sec, ρ_i density in g/cm³, and d_i thickness of the layer in km.

i	b_i	ρ_i	d_i
1	3.47	2.70	6
2	3.64	2.80	10.5
3	3.85	2.85	18.7
4	4.72	3.30	80
5	4.54	3.44	100
6	4.51	3.53	100
7	4.76	3.60	80
8	5.12	3.76	

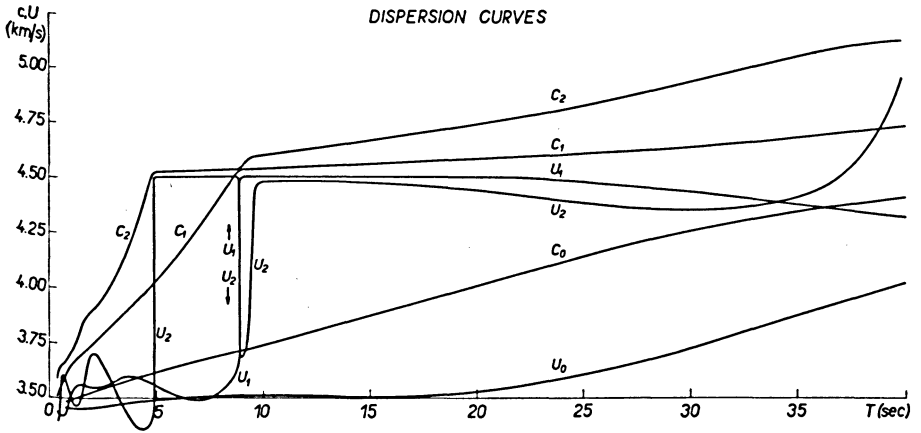


Fig. 1: The Love wave dispersion curves of the model CANSD. The curves c_0 and U_0 mean the phase and the group velocities of the fundamental mode, c_1 (c_2) and U_1 (U_2) correspond to the first (second) higher mode.

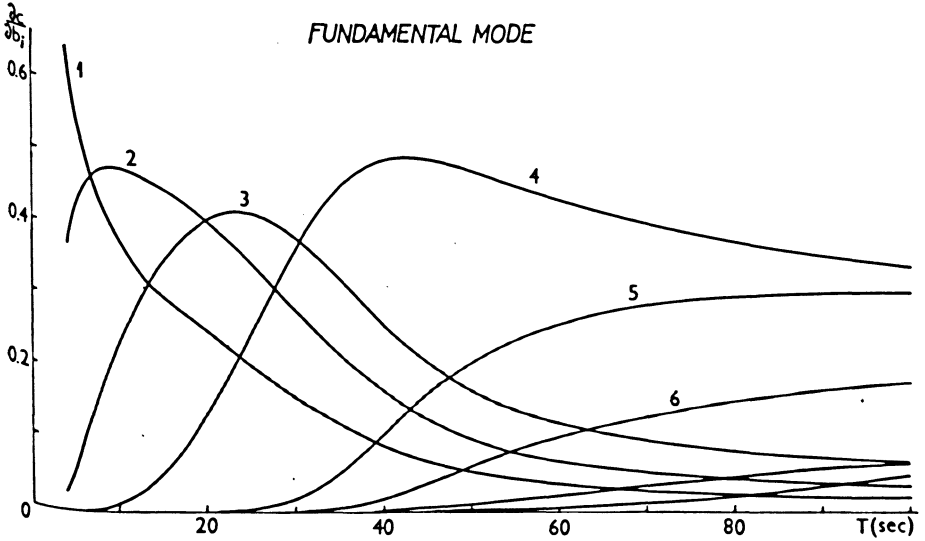


Fig. 2: The partial derivatives of the fundamental mode of Love waves with respect to shear wave velocities (model CANSD). The numbers with the curves represent the layer numbers given in Tab. 1.

behaviour of the dispersion curve can be seen in the neighbourhood of the period of 5 sec.

The sensitivity of the dispersion curves to the variation of layer parameters and consequently the possibility to use them to the structure determination is expressed by partial derivatives of the dispersion curves with respect to the layer parameters. The partial derivatives of the fundamental mode with respect to the shear velocities are given in Fig. 2. The curves have been calculated analytically by means of the algorithm described in the paper [NOVOTNÝ, 1970]. Fig. 3 shows the partial derivatives of the first higher mode of Love waves with respect to the shear velocities. The period of 9 sec. divides the pattern in two separate ranges, a short period and a long period range. In each of them the curves behave in a quite different way. Within the short period range the highest values of partial derivatives reach the curves associated with the shear wave velocities of the crustal layers 1, 2, 3. In the long period range there is practically nothing but two curves corresponding to the low velocity layers 5, 6.

It follows that the first higher mode discriminates fairly between low velocity layers and crustal layers. The fundamental mode has not the described property (compare Figs. 2, 3), which is the essential difference between the fundamental and the higher modes.

The physical reason for the described behaviour of the partial derivatives is following. Love waves propagate in a relatively thin surface layer for very short periods. The periods getting greater, the depth of penetration increases reaching the critical value, in this particular case 9 sec, the energy flux penetrates suddenly from the sur-

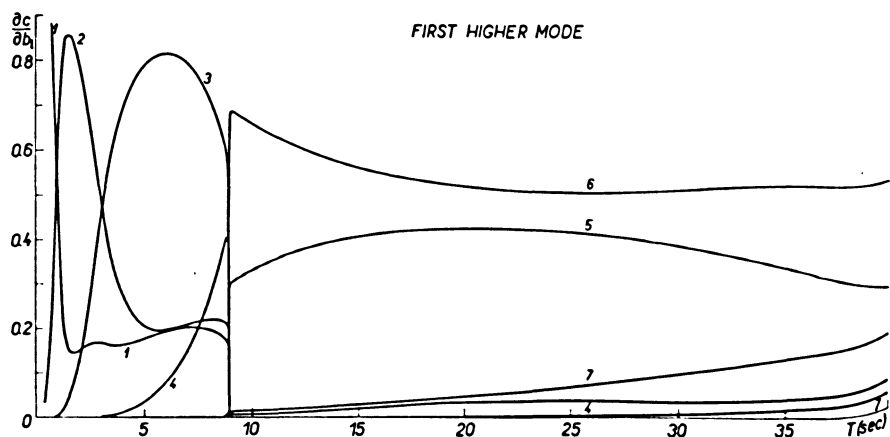


Fig. 3: The partial derivatives of the first higher mode with respect to the shear wave velocities. (For notation see Fig. 2).

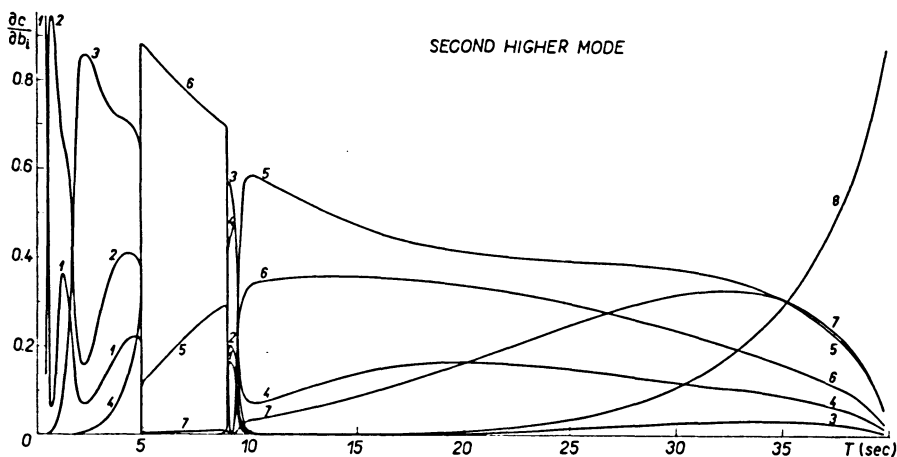


Fig. 4: The partial derivatives of the second higher mode with respect to the shear wave velocities.

face layers into the low velocity channel. Consequently the behaviour of dispersion curves is influenced in the short period range mainly by the crustal layers, less by the high velocity layer and in the long period range it is affected chiefly by the low velocity zone layers.

The behaviour of the partial derivatives of the second higher mode is much more complex, as seen in Fig. 4, but generally speaking, it has the same features.

In order to be able to successfully explore these favourable properties of higher modes of Love waves, it is essential to know the possibilities of observing them, i. e. to know the amplitude ratio of the higher modes to the fundamental one. Theoretical seismograms have been calculated for this purpose.

3. Theoretical seismograms of the fundamental, first and second higher modes of Love waves

The spectral component of the Love wave displacement for a particular angular frequency ω in the epicentral distance ϱ (on the surface) may be expressed as $v(\omega, \varrho) = V_1 \cdot V_2 \cdot V_3$, where the expressions V_i have the following meaning:

$$V_1 = -8 \pi \mu_j r_j H_0^{(1)}(k \varrho), \quad (\text{for a torque source})$$

$$V_2 = \mu_n r_n G_{12} + G_{22},$$

$$V_3 = -1/(dF/dk)_{k=k_\omega}.$$

The symbol μ_m is the rigidity of the m -th layer,

$$r_m = (c^2/b_m^2 - 1)^{\frac{1}{2}},$$

c being the phase velocity of Love wave, b_m the shear wave velocity in the m -th layer, $k = \omega/c$ is the wave number. The subscript j refers to the source layer and n to the halfspace. The G_{12} and G_{22} are the elements of a matrix $G = a_n \cdot a_{n-1} \dots a_j$. The matrix a_j is in THOMSON-HASKELL notation

$$a_m = \begin{pmatrix} \cos Q_m, i\mu_m^{-1} \cdot r_m^{-1} \cdot \sin Q_m \\ i\mu_m \cdot r_m \cdot \sin Q_m, \cos Q_m \end{pmatrix}$$

where $Q_m = k \cdot r_m \cdot d_m$, d_m being the thickness of the m -th layer.

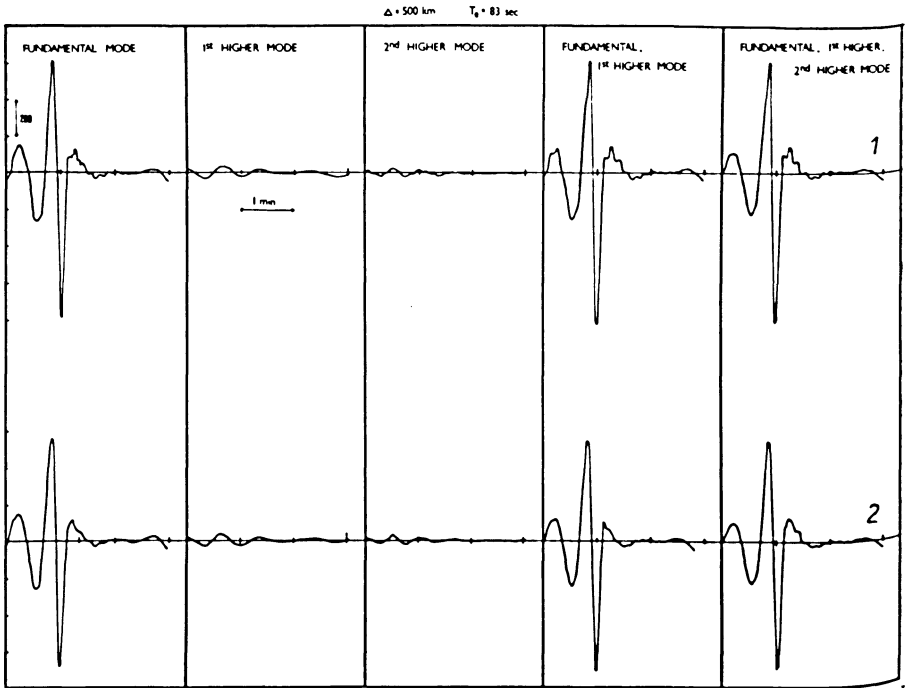


Fig. 5: Theoretical seismograms. The numbers on the right hand side of the figure are numbers of the layer, on the top of which the source is situated.

The function V_1 expresses the influence of the source mechanism, in our case of a simple torque source and involves the Hankel function $H_0^{(1)}(k\rho)$. The expression V_2 depends on the properties of the layers below the source layer. The frequency equation, as matter of fact its partial derivative with respect to the wave number is involved in the expression V_3 . The details concerning the method of calculation will be described in a special paper.

Since the low velocity layers affect the long period range, as we have seen from the partial derivatives of dispersion curves, such a source function has been chosen, which has a box-shape spectrum with rounded edges within the interval 9–60 sec. A pulse corresponding to this spectrum is not very different from the sine function.

Fig. 5 shows theoretical seismograms calculated for the distance of 500 km. The seismograms start with the reference time $T_0=83$ sec. In the first row are given seismograms calculated for the source situated on the top of the first layer, the second row corresponds to the position of the source on the top of the second layer. Fig. 6 is a continuation of Fig. 5 for source positions on the top of the third layer a. s. o. The scale of both figures is the same.

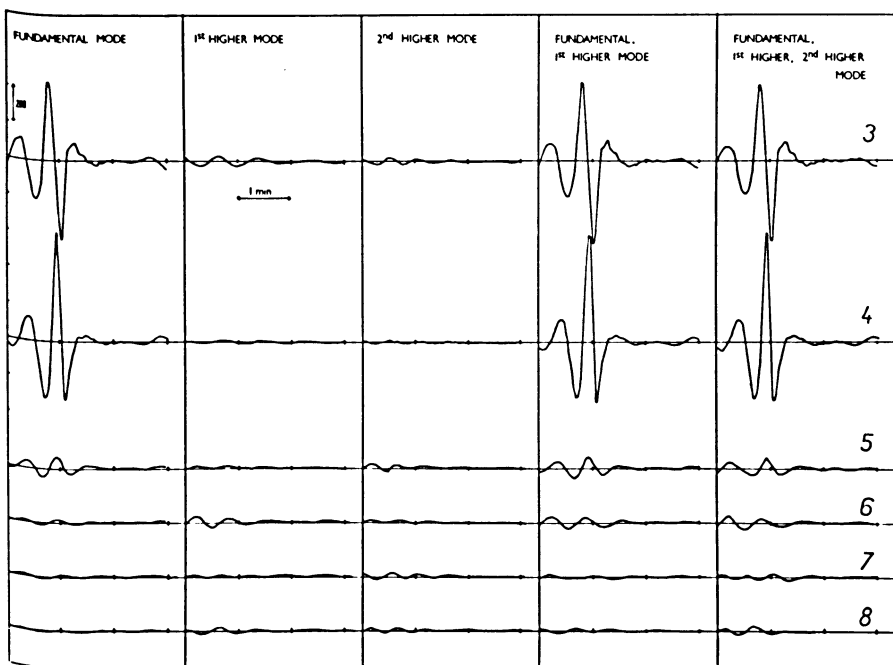


Fig. 6: Continuation of Fig. 5.

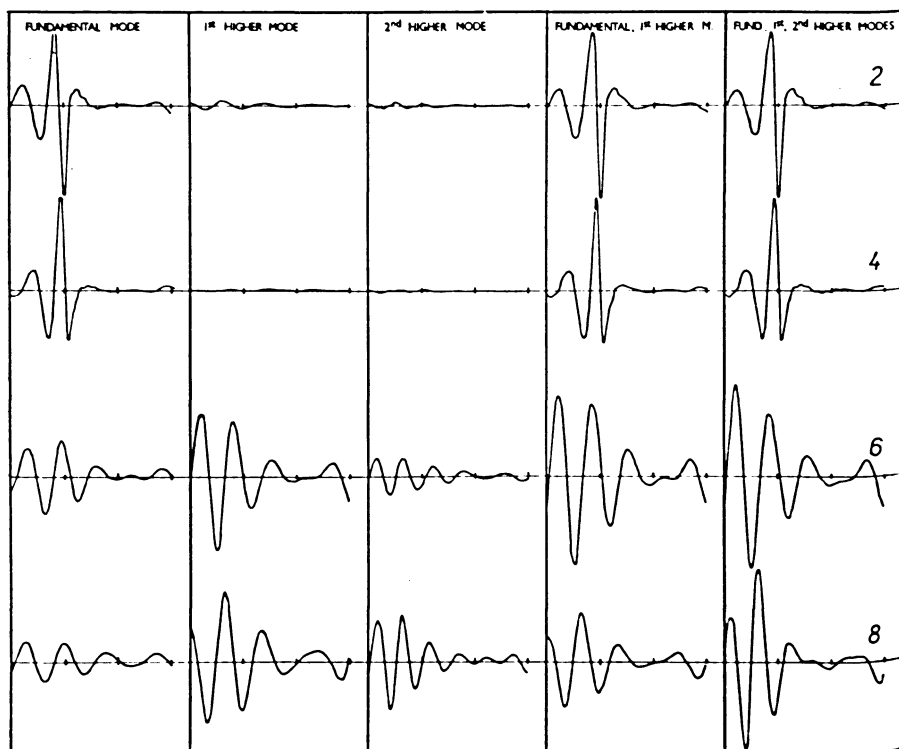


Fig. 7: Normalized seismograms.

The seismograms normalized to the maximum amplitude of the composite seismograms in the last columns in Figs. 5, 6 are given in Fig. 7.

We can see that the seismograms corresponding to crustal foci contain negligible portion of higher modes, the mutual separation of the individual modes seems to be practically excluded. If the seismic focus is situated in the low velocity zone or below it, the higher modes have the amplitudes comparable with the amplitudes of the fundamental mode.

4. Conclusion

Two questions have been examined. First, the ability of discrimination between layers with normally increasing velocity and layers of the low velocity zone by means of the fundamental mode and higher modes of Love wave. The partial derivatives of dispersion curves with respect to shear wave velocities have been calculated for

this objective. It has been shown that the overburden of the low velocity zone has a screening effect through the whole period range in the case of the fundamental mode. In a quite different way behave higher mode dispersion curves. There exists a period range where the course of the curves depends on the velocities of shear waves of low velocity zone layers and does not depend practically at all upon velocities in the overburden of the low velocity channel.

In order to be able to successfully explore these favourable properties of higher modes of Love wave we have to know the possibilities of observing them, i. e. the amplitude ratio of higher modes to the fundamental one. This was the second examined question.

In studying theoretical seismograms of CANS model, we have shown that the contents of higher modes in the surface wave portion of the seismogram is relatively high, if the seismic focus is located either directly in the low velocity zone or below it. In the opposite case amplitudes of higher modes are negligibly small with respect to the amplitudes of the fundamental mode and consequently it is practically impossible to observe them.

References

- ALTERMAN, Z.: Higher-mode surface waves. Geoph. Monogr. No. 13, The Earth's Crust and Upper Mantle, edited by P. J. Hart, Am. Geoph. Union, Washington, 265–272, 1969
- ANDERSON, D. L.: Latest information from seismic observations. The Earth's Mantle, edited by T. F. Gaskell, Academic Press, 355–420, 1967
- BRUNE, J., and J. DORMAN: Seismic waves and Earth structure in the Canadian Shield. Bull. Seism. Soc. Am. 53, 167–209, 1963
- HARKRIDER, D. G.: Surface waves in multilayered elastic media, 1, Rayleigh and Love waves from buried sources in a multilayered elastic half-space. Bull. Seism. Soc. Am. 54, 627 to 679, 1964
- HARKRIDER, D. G., and D. L. ANDERSON: Surface wave energy from point sources plane layered earth models. J. Geophys. Res. 71, 2967–2980, 1966
- KOVACH, R. L.: Seismic surface waves: Some observations and recent developments. Phys. Chem. Earth 6, 251–314, 1965
- KOVACH, R. L., and D. L. ANDERSON: Higher mode surface waves and their bearing on the structure of the Earth's mantle. Bull. Seism. Soc. Am. 54, 161–182, 1964
- NOVOTNÝ, O.: Partial derivatives of dispersion curves of Love waves in a layered medium. Studia geoph. et geod. 14, 36–50, 1970

Rays and Travel-Time Curves in Inhomogeneous Anisotropic Media

V. ČERVENÝ¹⁾ and I. PŠENČÍK²⁾, Prague

Eingegangen am 7. Februar 1972

Summary: Systems of ordinary differential equations of first order for seismic rays in inhomogeneous anisotropic media are presented. The systems are used to compute ray diagrams and travel-time curves of quasi-compressional waves in a simple mathematical model of inhomogeneous anisotropic earth's crust.

Zusammenfassung: Es werden die Systeme gewöhnlicher Differentialgleichungen erster Ordnung für seismische Strahlen in inhomogenen, anisotropen Medien angegeben. Die Systeme werden zur Berechnung der Strahlendiagramme und der Laufzeitkurven von quasikompressionellen Wellen in einem einfachen mathematischen Modell einer inhomogenen und anisotropen Erdkruste benutzt.

1. Introduction

Methods for the computation of seismic rays and travel-time curves in inhomogeneous *isotropic* media in which the velocity is an arbitrary function of two or all three coordinates are well known. Seismic rays in inhomogeneous isotropic media are described by a system of ordinary differential equations which can be solved by standard numerical procedures. The rapid development of these methods has been closely connected with the investigation of lateral inhomogeneities of the earth's crust and the upper mantle.

A similar system of ordinary differential equations for seismic rays in inhomogeneous *anisotropic* media was proposed by ČERVENÝ [1972]. The system can be used to compute rays, wavefronts, travel-time curves and other important quantities in a general anisotropic medium in which the elastic parameters are arbitrary continuous functions of all three coordinates (see eq. (3) in this paper). For simpler situations, the proposed system can be considerably simplified.

In this paper, a simpler anisotropic medium is considered. The medium is described by nine independent elastic parameters which depend on two coordinates only.

¹⁾ Dr. VLASTISLAV ČERVENÝ, Geofyzikální ústav Karlovy university, Ke Karlovu 3, Praha-2, ČSSR.

²⁾ Dr. IVAN PŠENČÍK, Geofyzikální ústav ČSAV, Praha-4–Spofilov, Boční II, ČSSR.

Simplifying initial conditions are also chosen. They guarantee that the rays of quasi-compressional and quasi-shear waves are plane curves. The systems of ordinary differential equations for these rays are presented. The derived ray-trace systems have been used to compute ray diagrams and travel-time curves of various waves propagating in certain simple mathematical models of inhomogeneous anisotropic earth's crust. One example for quasi-compressional waves is presented.

Note that the ray theory was also used for the investigation of seismic body waves propagation in inhomogeneous anisotropic media by BABICH [1961], GASSMANN [1964], HELBIG [1966] and VLAAR [1968].

2. Theory

In general inhomogeneous anisotropic media in which the elastic parameters c_{ijkl} and the density ρ are arbitrary continuous functions of all three coordinates, three independent wavefronts can propagate. One of them corresponds to the quasi-compressional wave, the other two wavefronts to two different quasi-shear waves. The wavefronts are described by the equation $t = \tau(x_i)$, where t is the time and x_i rectangular Cartesian coordinates. The function $\tau(x_i)$ is a solution of the non-linear partial differential equation of first order

$$G_m(p_i, x_i) = 1, \quad (1)$$

where $m = 1, 2$ or 3 , depending on the type of wave. G_m ($m = 1, 2, 3$) denote the eigenvalues of the matrix Γ_{jk} , which is given by the formula

$$\Gamma_{jk} = p_i p_l a_{ijkl}. \quad (2)$$

Here $p_i = \partial\tau/\partial x_i$ are the components of the slowness vector, $a_{ijkl} = c_{ijkl}/\rho$. The partial differential equation (1) is analogous to the well-known eiconal equation for isotropic media.

The seismic rays are the characteristics of the non-linear partial differential equation (1). The system of ordinary differential equations of first order for the characteristics of (1) can be written in the following form

$$\begin{aligned} \frac{dx_i}{d\tau} &= a_{ijkl} p_l D_{jk}/D, \\ \frac{dp_i}{d\tau} &= -\frac{1}{2} \frac{\partial a_{l j k s}}{\partial x_i} p_l p_s D_{jk}/D, \end{aligned} \quad (3)$$

$i = 1, 2, 3$. The system (3) can be used for numerical computation of seismic rays in inhomogeneous anisotropic media. It will be called here the ray-trace system. The

values of D_{jk} and D are given by formulae

$$\begin{aligned}
 D_{11} &= (\Gamma_{22} - 1)(\Gamma_{33} - 1) - \Gamma_{23}^2, \\
 D_{22} &= (\Gamma_{11} - 1)(\Gamma_{33} - 1) - \Gamma_{13}^2, \\
 D_{33} &= (\Gamma_{11} - 1)(\Gamma_{22} - 1) - \Gamma_{12}^2, \\
 D_{12} &= D_{21} = \Gamma_{13}\Gamma_{23} - \Gamma_{12}(\Gamma_{33} - 1), \\
 D_{13} &= D_{31} = \Gamma_{12}\Gamma_{23} - \Gamma_{13}(\Gamma_{22} - 1), \\
 D_{23} &= D_{32} = \Gamma_{12}\Gamma_{13} - \Gamma_{23}(\Gamma_{11} - 1), \\
 D &= D_{11} + D_{22} + D_{33}.
 \end{aligned} \tag{4}$$

To solve the system (3), initial conditions must be known. Each seismic ray is specified by initial conditions:

$$\text{for } \tau = t_0 \quad x_i = (x_i)_0, \quad p_i = (p_i)_0. \tag{5}$$

The values of $(p_i)_0$ at the point $(x_i)_0$ are not arbitrary, they must satisfy the condition

$$G_m((x_i)_0, (p_i)_0) = 1. \tag{5'}$$

The initial conditions (5) specify the coordinates of the point on the ray at the initial time $\tau = t_0$ and also the components of the slowness vector at that point. The condition (5') specifies the type of a wave whose ray is to be calculated, as we can insert $m = 1, 2$ or 3 . When $G_1 \neq G_2 \neq G_3$, the ray-trace system (3) is the same for all three types of waves (the quasi-compressional wave and the two quasi-shear waves). The type of the wave is specified by (5') only. It is easy to show that $G_m(x_i, p_i) = 1$ along the whole ray. The ray-trace system can be solved by standard numerical techniques, such as RUNGE-KUTTA's method or HAMMING's predictor-corrector method. As a result, the coordinates of the points of the ray $x_i(\tau)$ and the components of the slowness vector $p_i(\tau)$ are obtained along the whole ray. The parameter along a ray is the time ($t = \tau$).

The presented ray-trace system (3) can be used to compute rays in a general inhomogeneous medium, in which all 21 elastic parameters are continuous functions of all three coordinates. In simpler anisotropic media, the system can be considerably simplified.

In the following, the elastic parameters A_{ij} (with two indices) instead of the elastic parameters a_{ijkl} (with four indices) will be used. This notation is common in the literature dealing with anisotropic media. The elastic parameters A_{ij} form a sym-

metric matrix of the dimension 6×6

$$\begin{pmatrix} A_{11} & A_{12} & A_{13} & A_{14} & A_{15} & A_{16} \\ & A_{22} & A_{23} & A_{24} & A_{25} & A_{26} \\ & & A_{33} & A_{34} & A_{35} & A_{36} \\ & & & A_{44} & A_{45} & A_{46} \\ & & & & A_{55} & A_{56} \\ & & & & & A_{66} \end{pmatrix}.$$

In fact, A_{ij} denote elastic parameters divided by density. For the sake of brevity, A_{ij} are called elastic parameters.

We have not yet used the general ray-trace system (3) for the computation of rays in media in which all 21 elastic parameters are non-zero. The knowledge of elastic parameters A_{ij} in the earth's interior is very poor and it is not so simple to choose a suitable mathematical model for computation. Moreover, it is necessary to start with the investigation of simpler situations. In the following, the anisotropic medium which is described by nine non-zero elastic parameters will be considered. The matrix of elastic parameters is as follows

$$\begin{pmatrix} A_{11} & A_{12} & A_{13} & 0 & 0 & 0 \\ & A_{22} & A_{23} & 0 & 0 & 0 \\ & & A_{33} & 0 & 0 & 0 \\ & & & A_{44} & 0 & 0 \\ & & & & A_{55} & 0 \\ & & & & & A_{66} \end{pmatrix}.$$

It is well known that this case includes the transversely isotropic medium, for which $A_{11} = A_{22}$, $A_{44} = A_{55}$, $A_{23} = A_{13}$, $A_{12} = A_{11} - 2A_{66}$.

To further simplify the computations and the discussion of the results, two important assumptions are made:

1. The elastic parameters do not depend on one coordinate, e. g. on x_2 .
2. It is assumed that $(x_2)_0 = 0$, $(p_2)_0 = 0$.

In other words, we assume that the source lies in the plane (x_1, x_3) and that the normal to the wavefront at the source, corresponding to the ray under study, lies also in that plane. It is easy to show that under these assumptions the whole ray will be a plane curve and will lie in the plane (x_1, x_3) . For simplicity, a new notation is introduced:

$$x_1 = x, \quad x_3 = z, \quad p_1 = p, \quad p_3 = q.$$

Under x the epicentral distance is understood, under z the depth.

The ray-trace system (3) can be divided into two systems in our situation. One of these systems describes the rays of quasi-compressional and quasi-shear SV waves, the other the rays of quasi-shear SH waves. Both systems are formed by four ordinary differential equations for x, z, p and q .

2.1 Ray-trace system for quasi-compressional and quasi-shear SV waves.

After some mathematics, we obtain from (3)

$$\begin{aligned} \frac{dx}{d\tau} &= p(A_{11} + A_{55} - 2A_{11}A_{55}p^2 + Aq^2)/D, \\ \frac{dz}{d\tau} &= q(A_{33} + A_{55} - 2A_{33}A_{55}q^2 + Ap^2)/D, \\ \frac{dp}{d\tau} &= -\left[\frac{\partial A_{11}}{\partial x} p^2 D_2 + \frac{\partial A_{33}}{\partial x} q^2 D_1 + \frac{\partial A_{55}}{\partial x} F + 2 \frac{\partial A_{13}}{\partial x} p^2 q^2 (A_{13} + A_{55}) \right] / 2D, \\ \frac{dq}{d\tau} &= -\left[\frac{\partial A_{11}}{\partial z} p^2 D_2 + \frac{\partial A_{33}}{\partial z} q^2 D_1 + \frac{\partial A_{55}}{\partial z} F + 2 \frac{\partial A_{13}}{\partial z} p^2 q^2 (A_{13} + A_{55}) \right] / 2D, \end{aligned} \tag{6}$$

where

$$\begin{aligned} D_1 &= 1 - A_{11}p^2 - A_{55}q^2, \\ D_2 &= 1 - A_{55}p^2 - A_{33}q^2, \\ D &= D_1 + D_2, \\ A &= A_{13}^2 + 2A_{13}A_{55} - A_{11}A_{33}, \\ F &= p^2 + q^2 - A_{11}p^4 - A_{33}q^4 + 2p^2q^2A_{13}. \end{aligned} \tag{6'}$$

The system is simple and does not need any comment. The initial conditions are given as follows

$$\text{for } \tau = t_0, \quad x = x_0, \quad z = z_0, \quad p = p_0, \quad q = q_0. \tag{7}$$

The values of p_0 and q_0 are not arbitrary, they must satisfy the condition $G_m = 1$ ($m = 1, 2$ for quasi-compressional and quasi-shear SV waves). In our case we have

$$\frac{1}{2} [P_0 + \sqrt{P_0^2 - 4Q_0}] = 1 \tag{8}$$

for quasi-compressional waves,

$$\frac{1}{2} [P_0 - \sqrt{P_0^2 - 4Q_0}] = 1 \tag{8'}$$

for quasi-shear SV waves, where

$$P_0 = (A_{11} + A_{55})p_0^2 + (A_{33} + A_{55})q_0^2,$$

$$Q_0 = (A_{11}p_0^2 + A_{55}q_0^2)(A_{55}p_0^2 + A_{33}q_0^2) - (A_{13} + A_{55})^2 p_0^2 q_0^2.$$

To fulfil the above conditions, it is useful to parametrize the ray by φ_0 , the angle between the x -axis and the normal to the wavefront corresponding to the ray under study at the point $[x_0, z_0]$. Then the initial values are given by x_0, z_0 and φ_0 , instead of (7) and (8) or (8'). If φ_0 is known, the normal velocities V_P (quasi-compressional wave) and V_{SV} (quasi-shear SV wave) at the point $[x_0, z_0]$ can be determined by well-known methods. Then

$$p_0 = \cos \varphi_0 / V_P, \quad q_0 = \sin \varphi_0 / V_P \quad (7')$$

for quasi-compressional waves,

$$p_0 = \cos \varphi_0 / V_{SV}, \quad q_0 = \sin \varphi_0 / V_{SV} \quad (7'')$$

for quasi-shear SV waves. It can be proved that these values of p_0 and q_0 satisfy (8) and (8'). Thus, when determining p_0 and q_0 we can decide which type of wave we wish to calculate.

The ray-trace system (6) is the same for both waves. It is not difficult to show that the following equations will be valid along the whole ray (see (1))

$$2 A_{33} A_{55} q^2 = B - \sqrt{B^2 - 4 A_{33} A_{55} C} \quad (9)$$

for quasi-compressional waves,

$$2 A_{33} A_{55} q^2 = B + \sqrt{B^2 - 4 A_{33} A_{55} C} \quad (9')$$

for quasi-shear SV waves, where

$$B = A_{33} + A_{55} + A p^2,$$

$$C = 1 - (A_{11} + A_{55}) p^2 + A_{11} A_{55} p^4,$$

A is given by (6').

From (9) and (9'), the values of q can be computed when p is known, and vice versa. Therefore, we can omit one differential equation from the ray-trace system (6), either the equation for $dq/d\tau$ or for $dp/d\tau$, and to compute the value of q or p directly from (9) or (9').

Thus, finally we have three ordinary differential equations for the ray, similarly as in isotropic media. When the elastic parameters depend on one coordinate only, e. g. on depth, the ray-trace system can be solved in closed-form integrals. This fact is well known from the theory of elastic waves propagation in isotropic media; similar integrals can be also written for anisotropic media. VLAAR [1968] was the first who obtained these integrals for transversely isotropic media.

2.2 Ray-trace system for quasi-shear *SH* waves.

The system of differential equations for the ray of quasi-shear *SH* waves is simpler than that for quasi-compressional and quasi-shear *SV* waves. From (3) we obtain

$$\begin{aligned}\frac{dx}{d\tau} &= pA_{66}, \\ \frac{dz}{d\tau} &= qA_{44}, \\ \frac{dp}{d\tau} &= -\frac{1}{2}\left(\frac{\partial A_{66}}{\partial x}p^2 + \frac{\partial A_{44}}{\partial x}q^2\right), \\ \frac{dq}{d\tau} &= -\frac{1}{2}\left(\frac{\partial A_{66}}{\partial z}p^2 + \frac{\partial A_{44}}{\partial z}q^2\right).\end{aligned}\tag{10}$$

The initial conditions are again given by (7). The values of p_0 and q_0 must satisfy the condition

$$A_{66}p_0^2 + A_{44}q_0^2 = 1.\tag{11}$$

If the ray is parametrized by φ_0 , we obtain

$$p_0 = \cos \varphi_0 / V_{SH}, \quad q_0 = \sin \varphi_0 / V_{SH},\tag{11'}$$

where

$$V_{SH} = \sqrt{A_{66} \cos^2 \varphi_0 + A_{44} \sin^2 \varphi_0}.$$

V_{SH} is the normal velocity of quasi-shear *SH* waves. The values of x , z , p and q will satisfy the equation

$$A_{66}p^2 + A_{44}q^2 = 1\tag{12}$$

along the whole ray. Therefore, one differential equation in (10) can be replaced by (12), either the equation for $dp/d\tau$ or for $dq/d\tau$.

The ray-trace systems (6) and (10) can be used when the elastic parameters are continuous functions of coordinates. If the ray impinges on an interface of first order,

additional conditions must be taken into account. These conditions are given, e. g., in FEDOROV [1965]; they will not be presented here.

A computer program based on the above presented ray-trace systems (6) and (10) has been written. The RUNGE-KUTTA's method was chosen to solve the systems. The program computes rays, wavefronts and travel-time curves of quasi-compressional, quasi-shear SV and quasi-shear SH waves. Interfaces of first order may exist in the medium. At any point of the ray, a number of physical parameters is computed: ray velocity and normal velocity, the components of the slowness vector, the direction of the ray, the direction of the normal to the wavefront, the direction of the displacement vector (zeroth order approximation), a. s. o.

It should be noted that the ray-trace system for the quasi-compressional and quasi-shear SV waves (6) contains only four elastic parameters, A_{11} , A_{33} , A_{55} and A_{13} . Similarly, the ray-trace system for the quasi-shear SH waves (10) contains only A_{44} and A_{66} . The elastic parameters A_{22} , A_{12} and A_{23} do not appear in (6) and (10). This fact is caused by the assumptions that were made earlier. If we assume that A_{ij} do not depend on x_1 and that $(x_1)_0=0$, $(p_1)_0=0$, the ray will again be a plane curve, but it will lie in the plane (x_2, x_3) . The ray-trace systems will not contain the elastic parameters A_{11} , A_{12} , A_{13} in this case. For the general case of $(p_i)_0 \neq 0$ ($i=1, 2, 3$), the ray-trace system (3) must be used, even if A_{ij} do not depend on one or two coordinates. There are certain exceptions. For a transversely isotropic medium, in which A_{ij} depend on the depth only, the systems (6) and (10) can be used for arbitrary $(p_i)_0 \neq 0$. We must, of course, insert $A_{55}=A_{44}$ and understand x to be the distance from the z -axis. In this case we can also use the integral expressions as was mentioned above.

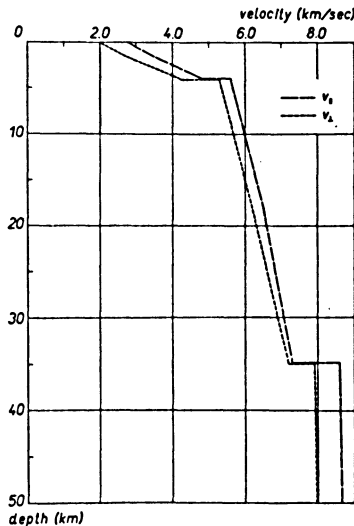
3. Numerical example

The ray diagrams and travel-time curves for certain simpler mathematical models of the anisotropic earth's crust have been computed using the programs mentioned above. The results of numerical computation for one model of transversely isotropic earth's crust will be presented here. The elastic parameters are assumed to depend only on depth. It should be again emphasized that the mentioned programs enable us to compute considerably more complicated models than the model presented here. Attention will be paid only to the quasi-compressional waves which are of greatest importance in seismology. The kinematics of a quasi-compressional wave in our model depends only on four elastic parameters, A_{11} , A_{33} , A_{44} ($=A_{55}$) and A_{13} , as was mentioned earlier (see also the ray-trace system (6)). The numerical values of elastic parameters used for the calculation are listed in Table 1. There is a discontinuity of first order at a depth of 4 km, Mohorovičić-discontinuity lies at a depth of 35 km. Discontinuities of second order are at depths of 1.5 km and 18 km. The dependence of A_{ij} on depth is linear between the interfaces. From the given A_{ij} we can compute v_{\parallel} and v_{\perp} , where v_{\parallel} denotes the velocity of propagation in the direction of

Table 1: Values of A_{11} , A_{33} , A_{44} and A_{13} (in $(\text{km/s})^2$) for a numerical example.

depth (km)	A_{11}	A_{33}	A_{44}	A_{13}
0	7.84	4.00	1.33	2.61
1.5	12.25	7.29	2.43	4.08
4 (above)	23.04	17.64	5.88	7.68
4 (below)	31.36	28.09	9.36	10.45
18	42.25	38.44	12.81	14.08
35 (above)	53.29	51.84	17.28	17.76
35 (below)	73.96	62.41	20.80	24.65
50	74.82	63.20	21.06	24.94

the x -axis, v_{\perp} in the direction of z -axis. Figure 1 shows velocity-depth curves for v_{\parallel} and v_{\perp} . It can be seen from the figure that the chosen anisotropy of velocities is not too great and that it decreases with depth in the earth's crust. It is a little greater only within the surface layer of 4 km and under the Mohorovičić-discontinuity; but at depths from 4 km to 35 km the ratio $(v_{\parallel} - v_{\perp})/v_{\parallel}$ does not exceed 5.4% anywhere. At the bottom of the earth's crust the ratio is only about 1.3%. The value of v_{\parallel} is higher than v_{\perp} throughout the chosen model. The source of seismic waves lies close to the earth's surface. Figure 2 shows the travel-time curves of the refracted wave


 Fig. 1: Horizontal and vertical velocities, v_{\parallel} and v_{\perp} , versus depth.

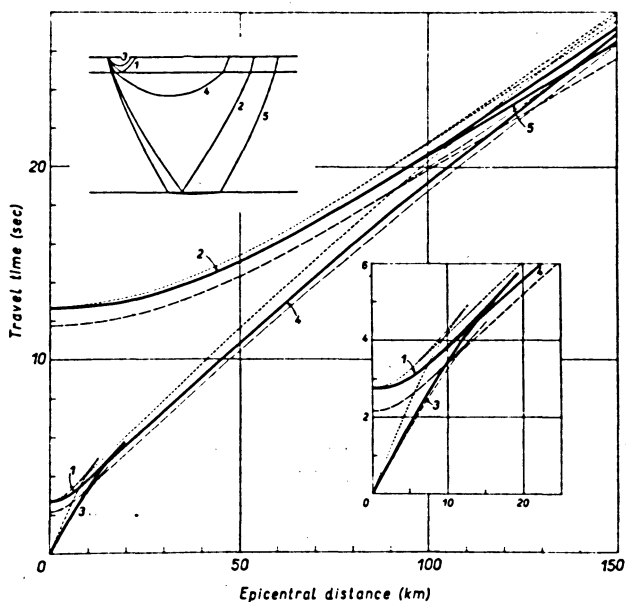


Fig. 2: Travel-time curves of various quasi-compressional waves propagating in the model of transversely isotropic earth's crust, described in the text. In the upper left corner the rays of individual waves are given schematically. For comparison, travel-time curves of the same waves propagating in the isotropic earth's crust described by velocities v_{\parallel} and v_{\perp} are also presented (see dashed and dotted curves). Details of travel-time curves at small epicentral distances are given in the right lower corner.

and of waves reflected from the interfaces at depths of 4 km and 35 km, respectively. Note that the travel-time curve of a refracted wave has three branches. The first branch (from 0 to 19 km) corresponds to rays with a minimum in the surface layer, the second branch (from 9 to 199 km) corresponds to rays with a minimum in the earth's crust below the surface layer, and the third branch (from 81 km) corresponds to rays with a minimum below the earth's crust. Simultaneously, travel-time curves calculated for the isotropic medium described by the velocities v_{\parallel} and v_{\perp} are drawn.

The time differences between the arrival times of individual waves in the anisotropic medium and corresponding isotropic media attain values close to 1 second at some epicentral distances. The anisotropy has also a considerable influence on regions of existence of individual waves. For example, in the anisotropic model the wave reflected from the interface at 4 km can be observed up to the epicentral distances of 19 km. In the isotropic models, these epicentral distances are 15 and 13 km. The same applies to refracted waves. Thus, the anisotropy will have a considerable influence on the

behaviour of waves in the transition zone between the lit and shadow regions. The shadow region for isotropic medium can change into the lit region, when the medium is slightly anisotropic (and vice versa).

To appreciate properly the influence of anisotropy on the travel-time curves, the following numerical experiment has been performed. We have calculated velocity-depth distribution from theoretical travel-time curves obtained for anisotropic media under the assumption that the medium is isotropic. This numerical experiment is very close to seismic practice. All interpretation programs in seismology and seismic prospecting are based on the assumption that the medium is isotropic. When the medium is anisotropic, the interpretation will not be correct. The question is: How large are the errors caused by this fact?

Standard programs for the interpretation of travel-time curves have been used. A certain modification of WIECHERT-HERGLOTZ-method was used to determine the velocity-depth distribution, another program was used to compute the depths of interfaces from travel-time curves of reflected waves. Results are given in the following figures. The determined velocity-depth distribution in the upper part of the earth's

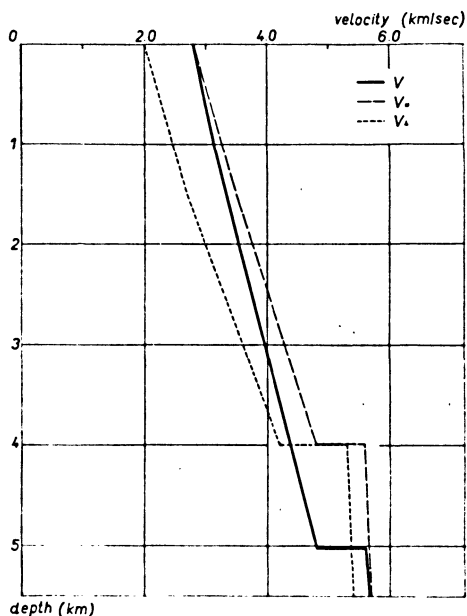


Fig. 3: Velocity-depth distribution in the upper part of the earth's crust as obtained from travel-time curves given in Figure 2 (heavy line). Values of $v_{||}$ and v_{\perp} are given for comparison. For details see the text.

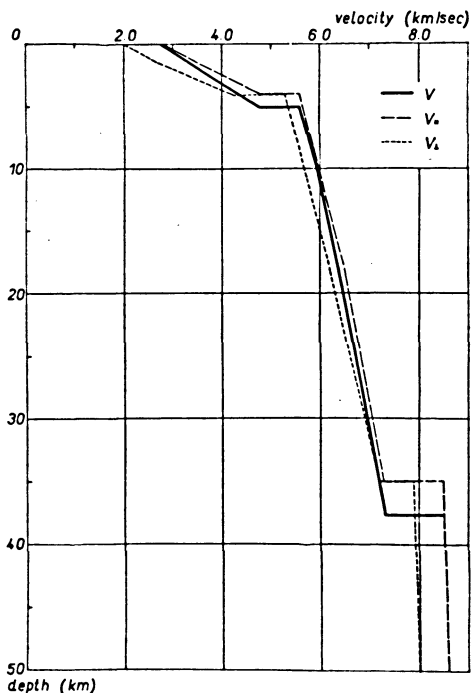


Fig. 4: Velocity-depth distribution in the whole earth's crust as obtained from travel-time curves given in Figure 2 (heavy line). Values of $v_{||}$ and v_{\perp} are given for comparison. For details see the text.

crust is given in Figure 3. In this part of the earth's crust the anisotropy was relatively strong. Therefore the differences are remarkable. The most substantial difference is in the depth of the interface, which lies in fact at a depth of 4 km. The interface was found at a depth of 5.1 km. This means that the anisotropy has caused an error larger than 25% in the determination of the depth of the interface. The determined velocity-depth distribution for the whole earth's crust is presented in Figure 4. The Mohorovičić-discontinuity was found at a depth of 37.6 km. In fact, it lies at a depth of 35 km. The error in the determination of the depth is almost 3 km. If we do not take into account the neighbourhood of interfaces of first order, the determined velocity always lies between $v_{||}$ and v_{\perp} .

The discussed differences are fully caused by the anisotropy of the medium. In any case they cannot be caused by the inaccuracy of interpretation programs. The results were checked by direct computations.

4. Conclusions

The systems of ordinary differential equations of first order, presented in the paper, can be used to compute ray diagrams and travel-time curves in general inhomogeneous anisotropic media, in which the elastic parameters and the density are arbitrary continuous functions of all three coordinates.

Numerical computations for a simple model of the anisotropic inhomogeneous earth's crust were performed. The results indicate that even slight anisotropy can cause serious errors in the interpretation of the materials of deep seismic sounding of the earth's crust.

5. Acknowledgments

The authors wish to express their cordial thanks to Dr. V. BABUŠKA and Dr. K. KLÍMA (Geophys. Inst., Czechosl. Acad. Sci.) for helpful discussions, valuable comments and suggestions.

References

- BABICH, V. M.: Ray method for the computation of the intensity of wavefronts in elastic inhomogeneous anisotropic medium. *Problems in the Dynamic Theory of Propagation of Seismic Waves* 5, 36–46, Leningrad Univ. Press, Leningrad 1961 (in Russian)
- ČERVENÝ, V.: Seismic rays and ray intensities in inhomogeneous anisotropic media. *Geophys. J.*, 29, 1–13, 1972
- FEDOROV, F. I.: *Theory of elastic waves in crystals*. Nauka, Moscow 1965 (in Russian)
- GASSMANN, F.: Introduction to seismic travel-time methods in anisotropic media. *Pure and Appl. Geophys.* 58, 63–112, 1964
- HELBIG, K.: A graphical method for the construction of rays and travel-times in spherically layered media, Part 2: Anisotropic case, theoretical consideration. *Bull. Seism. Soc. Am.* 56, 527–559, 1966
- VLAAR, N. J.: Ray theory for an anisotropic inhomogeneous medium. *Bull. Seism. Soc. Am.* 58, 2053–2072, 1968

Interpretation of Discontinuities by Seismic Modelling Methods

J. BEHRENS, Clausthal¹⁾, O. G. SHAMINA, Moscow²⁾
and L. WANIEK, Prague³⁾

Eingegangen am 7. Februar 1972

Summary: In the present paper a brief review on model investigations will be given, which have been carried out for a better and more correct interpretation of seismic discontinuities and intermediate layers.

Zusammenfassung: In der vorliegenden Übersicht sind in kurzer Form die modellseismischen Untersuchungen beschrieben worden, deren Ergebnisse zu einer besseren und sicheren Interpretation seismischer Diskontinuitäten und Zwischenschichten führen können.

1. Introduction

In the recent stage seismic model measurements represent in most cases the bridge between theory and field measurements. Therefore also in the history model investigations were stimulated by the development of theory and by new seismological data simultaneously. In dependence of new ideas of a possible velocity-depth function in the Earth's interior and of the development of new model techniques, seismic model measurements at all times helped to explain the complexity of the structure of the Earth.

Seismic modelling as one of the methods for studying the Earth's structure was begun to be systematically used about twenty years ago. Solid-liquid and solid two- and three-dimensional models of homogeneous layered media were used in seismic modelling up to 1956. The first step in the direction of modelling of a more complicated medium was made by OLIVER [1956].

In 1960 the idea to control the elastic properties of materials by varying the temperature of the model was proposed by a group of Soviet seismologists [RYKUNOV, KHOROSHEVA, SEDOV 1960]. They investigated the first solid two-dimensional model of a wave-guide with nonsharp boundaries.

In the same year GILBERSHTEJN, GURVICH and POCHOTOVIK [1966] suggested a method of modelling of gradient media by means of two-dimensional perforated models.

¹⁾ Prof. Dr. JÖRN BEHRENS, Institut für Geophysik der Technischen Universität Clausthal, 3392 Clausthal-Zellerfeld, Adolf-Römer-Straße 2 A, BRD.

²⁾ Dr. OLGA G. SHAMINA, Institut Fiziki Zemli ANSSSR, Moskva, Bolshaja Gruzinskaya 10, UdSSR.

³⁾ Dr. LUDVÍK WANIEK, Geofyzikální ústav ČSAV, Praha 4 – Spořilov, Boční II, ČSSR.

The next step in modelling of gradient media was made by VANĚK, WANIEK, PROS and KLÍMA [1966]. They proposed a method of fabricating three-dimensional gel models by means of a great number of thin layers with practically continuously varying properties as a function of depth.

In 1965 SHAMINA elaborated a method for the construction of a three-dimensional solid model. The method was based on the regulation of the sedimentation of a solid filler in epoxid resin during its polymerization.

In the present paper we shall try to give a brief review on model investigations which have been carried out for a better and more correct interpretation of discontinuities.

First of all we have to discuss what is the meaning of interpretation of a discontinuity in general. It seems that three groups of problems are included:

1. Characterization of discontinuity structure.
2. Investigation and good knowledge of the propagation of elastic waves on different types of discontinuities or series of discontinuities.
3. Comparison of model results with computed or evaluated models of the Earth's structure.

Respecting these facts complete characteristics of a discontinuity can be given by:

1. The geometric structure (plane interface, interface with periodic geometry, interface with blockstructure etc.)
2. The ratio of the elastic parameters of the media above and below the discontinuity.
3. The depth-distribution of elastic parameters within a transition-layer between two homogeneous media (continuous or in single steps or in the form of a channel).
4. Velocity-depth function in two inhomogeneous media above and below a discontinuity.
5. The estimation of the geological and petrological properties of the considered interfaces. This point, however, cannot be solved by seismic modelling methods.

The existing modelling methods can be used for detailed measurements and evaluation of the nearly complete seismic wave field. As a result of these efforts following dependences can be given: Travel-time curves of phase- and group-velocities, amplitude-distance curves, amplitude-depth curves, amplitude spectra, phase spectra, predominant frequency-distance curves etc. All these results compared with field measurements and theoretical computations and their correct interpretation are the key to find out the actual properties of a discontinuity.

The description of the model investigations on interpretation of seismic discontinuities can be divided into two groups. The first group includes investigations of *seismic boundaries*, the second group includes investigations of *intermediate layers* especially of transition layers and wave guides.

2. Interpretation of discontinuities

Comprehensive model investigations have been carried out on *plane interfaces* of the first order in comparison and in good agreement with theoretical work. These investigations on plane interfaces were carried out in the vicinity of the critical points by investigating the subcritical and overcritical reflection, because in the region of the critical point we observe the greatest changes of kinematic and dynamic parameters of the registered seismic signals.

These investigations indicated very characteristic features of kinematic and dynamic parameters of the observed waves [SHAMINA 1961, 1965; EPINATEVA 1957, 1961; POLEY 1964; BEHRENS, DRESEN, HINZ 1969]. Besides the kinematic parameters the amplitude-distance curves and amplitude- and phase-spectra of sub- and overcritical reflections as well as of the headwave have been studied. Important information about the principles of wave propagation for this most simple type of discontinuity and its influence on the seismogram is the amplitude increase of reflections in the vicinity of the critical points and its importance for the evaluation of field-observations, the relatively small amplitude of the head-wave, the very characteristic behaviour of the amplitude- and phase-spectra of reflected waves and head-waves (also especially in the neighbourhood of the critical point).

Studies of *discontinuities of first order with a periodic geometry* confirmed that a characterization or identification of this type of structure is not possible only by evaluating the kinematic parameters of the signals. This result has been obtained by investigations on 2-dimensional models with corrugated sinusoidal interface structures [BEHRENS 1969, 1971; BEHRENS, KOZÁK, WANIEK 1971]. These studies were stimulated by the first results of the theory suggested by ASANO [1966] and ABUBAKAR [1962] so far valid only for normal incidence or very small angles of incidence.

Model studies presented detailed information about the amplitude of *reflected waves* from normal incidence to supercritical angles and the amplitude of *head-wave* in dependence of the parameters of the interface structure i.e. amplitude and wave length of corrugation (Fig. 1).

The form of amplitude-distance curves—quite different from those of models with a plane interface—the amplitudes of head-waves, the quite special structure of amplitude- and phase-spectra in the neighbourhood of the critical distance—all these effects point to possibilities of characterization, identification or distinction of interface structures.

With respect to the work of interpretation of seismic discontinuities or interface structures, the amplitudes of *head-waves* or the ratio of the head-wave amplitudes to the amplitudes of the direct or reflected *P*-waves play a special role.

The model investigations on corrugated interfaces show, that the amplitude of head wave increases, if the amplitude of corrugation in relation to the wave length of the incident wave increases (Fig. 2). That means, with respect to the predominant wave length of the incident signal, the discontinuity becomes more complicated and

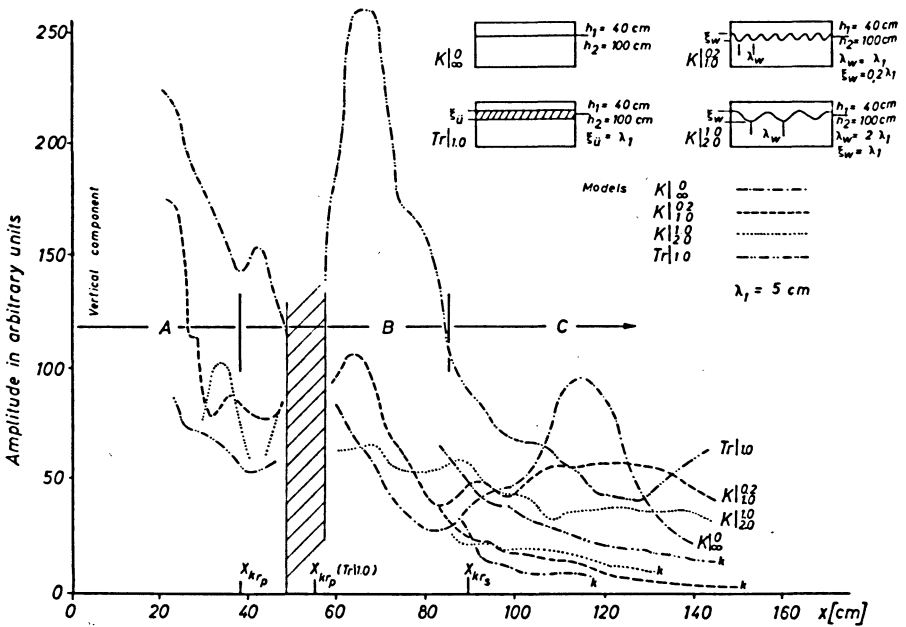


Fig. 1: Amplitude-distance curves of the vertical component of reflected P -waves and head-waves (k) on plane and corrugated interfaces of first order and on a transition layer.

K_1^i = symbol denoting the corrugated boundary

i = amplitude; j = wavelength of corrugation expressed by the wavelength λ_1 of the incident wave

$Tr \xi_u/\lambda_1$ = symbol denoting the transition layer

ξ_u = thickness of the transition layer

A = subcritical region, B = interference-zone of reflected wave and head-wave, C = zone of separation of the reflected wave and head-wave

x_{crp} , x_{crs} = 1st and 2nd critical distance

[BEHRENS 1969]

less and less sharp. This behaviour of the head-wave amplitude could be observed on other complicated, poorly defined boundaries (transition layers, low velocity layers, layers with laminated structure).

With respect on the interpretation of *higher order discontinuities*, we can say in general that only scarce results can be given. It is the aim of the project of "test models", recommended by the *European Seismological Commission* in Copenhagen 1967, to support these investigations.

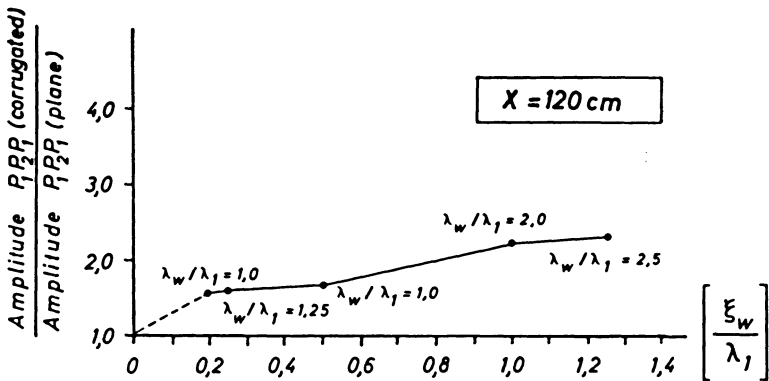


Fig. 2: Ratio of amplitudes of head-waves on corrugated and plane interfaces in dependence of the amplitude of corrugation.

Model: Plexiglas – Aluminium

ξ_w = amplitude of corrugation

λ_w = wavelength of corrugation (compare Fig. 1)

x = distance from shotpoint

λ_1 = wavelength of incident wave

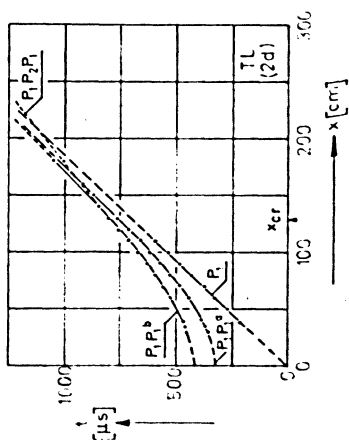
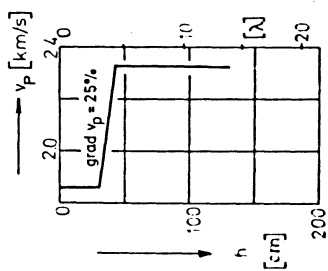
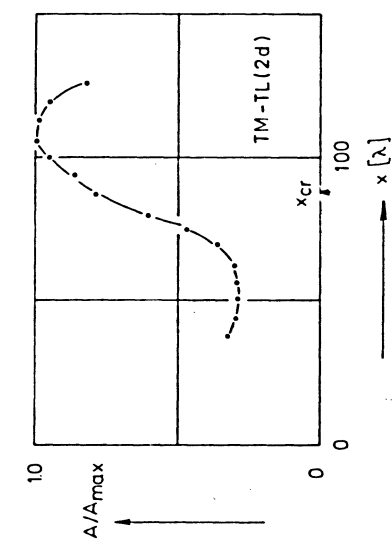
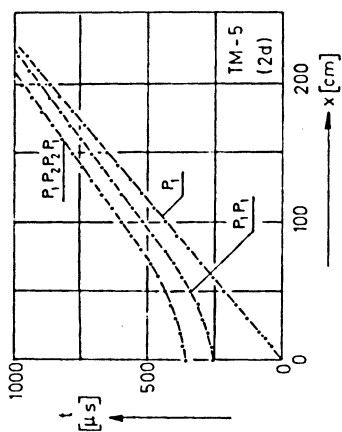
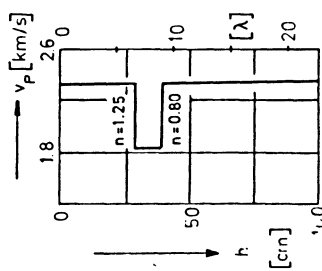
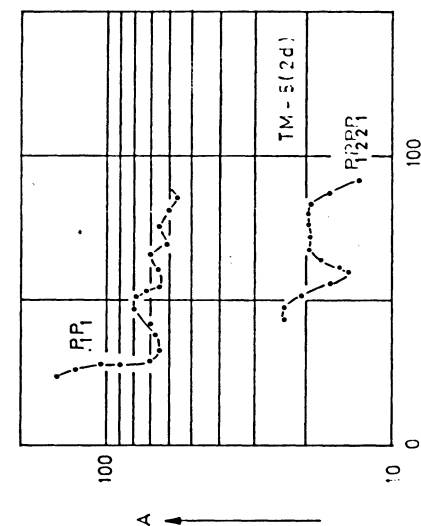
[BEHRENS 1969]

3. Interpretation of intermediate layers

Systematical model studies on the interpretation of intermediate layers had been carried out by means of the 2- and 3-dimensional model techniques [BEHRENS, DRESEN, WANIEK 1971 a, b; BEHRENS, SIEBELS 1972] and by means of the schlieren-method [KOZÁK, WANIEK 1970; WANIEK 1972]. The results of investigations of the *reflected* waves indicated in the same way as described in the foregoing chapter, that only the combined evaluation of the kinematic and dynamic parameters of the considered signals may lead to a true interpretation of the interface structure.

Particularly the results of 2- and 3-dimensional investigations on the previous mentioned “test-models” clearly showed, that the structures can be distinguished very often with the aid of amplitude-distance curves only [BEHRENS, DRESEN, WANIEK 1971 a, b]. This is valid for geometric structures als well as for a special velocity depth distribution—for instance a transition layer or a low velocity channel (Fig. 3).

Besides these investigations of the kinematic and dynamic parameters of *reflected* waves from intermediate layers the propagation of *head-waves* within such layers was the subject of detailed model studies in the last time. NAKAMURA [1968], BEHRENS [1969, 1971] and SIEBELS [1971] studied especially the properties of head-waves in *transition layers*.



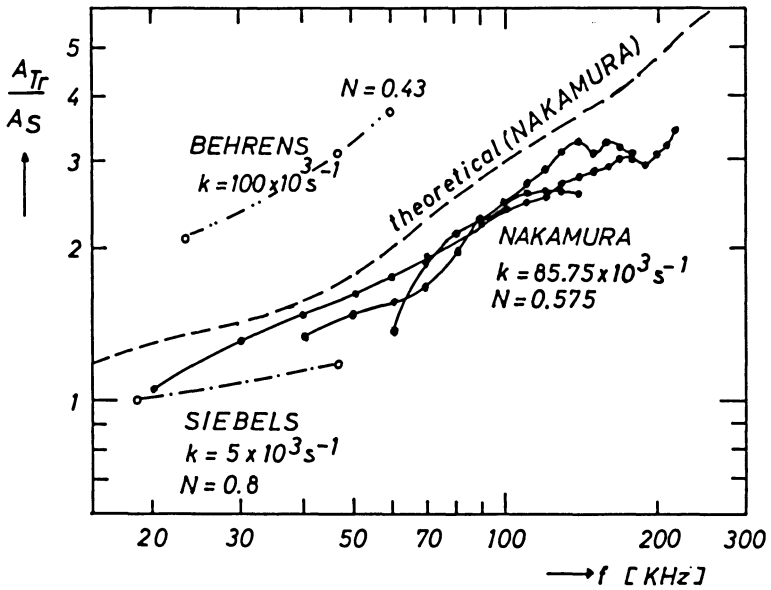


Fig. 4: Ratio of head-wave amplitudes A_{Tr}/A_S in dependence of the main frequency f of the incident wave for various refraction indices N . After NAKAMURA 1968.

Tr = Transition layer

S = Sharp discontinuity of I. order

$$N = V_{p1}/V_{p2}; \quad R = \frac{V_{p1} - V_{p2}}{\xi_{\ddot{u}}}$$

$\xi_{\ddot{u}}$ = Thickness of the transition layer.

Fig. 3: Travel-time curves and amplitude-distance curves of reflected P -waves on a low velocity layer (Test model No. 5) and a transition layer (Test model Nr. TM-TL) observed by two-dimensional model technique.

[BEHRENS, DRESEN, WANIEK 1971 b]

NAKAMURA [1964, 1968] showed by model experiments that the amplitude of the refraction arrival approaches zero at distances, where the refraction arrival is expected from pure geometry, when the frequency of the wave motion is much higher than the velocity gradient of the investigated transition layer. Further, it could be pointed out, that over a frequency range (or wave length) comparable with the velocity gradient (or thickness) of the transition layer, the amplitude of the refraction arrival changes with frequency, showing finite amplitude at low frequencies and disappearing at high frequencies. Thus the "cutoff-frequency", where the amplitude starts decreasing might be a measure for the thickness of a surmised transition layer (Fig. 4). In field experiments NAKAMURA and HOWELL [1964] observed losses of high-frequency energy in seismograms at a cutoff frequency of 7 cps. This would correspond to a thickness of 1 km or more for the M-discontinuity.

It is fair to point out that this way of interpretation or characterization of seismic structures involves some difficulties. NAKAMURA and HOWELL [1964], SISKIND and HOWELL [1967] and HOWELL and BAYBROOK [1967] obtained from model experiments, that the influence of a thin intermediate-velocity transition layer on the seismogram of the head-wave cannot be distinguished from the effect of a transition layer consisting of a linear increase in velocity without any jump in velocity or from an irregular boundary with saw-toothed structure. These results could be confirmed by the studies of the dynamic parameters of the head-wave on corrugated interfaces, mentioned in this paper [BEHRENS 1971].

In comparison with the theoretical and experimental results of NAKAMURA [1968], BEHRENS [1969] and SIEBELS [1971] showed by model studies, that the previously described *increase* of the head-wave amplitude in dependence of the degree of sharpness of the poorly defined interface structure becomes *smaller*, if the index of refraction decreases (Fig. 4).

A second group of important intermediate layers investigated in detail by seismic modelling methods is represented by the *low velocity layers* (channels or wave guides).

Up to now a great number of wave guide models has been examined. It is possible to classify the wave guide models as follows:

1. Wave guide with sharp boundaries. Two-dimensional models of homogeneous layered medium have been used [RYKUNOV, KHOROSHEVA, SEDOV 1960; CHOWDHURY, DEHLINGER 1963].
2. Wave guide with non-sharp boundaries. Two-dimensional bimorphic models [RIZNICHENKO, SHAMINA 1963a, b; 1964; 1965], three-dimensional gelmodels [VANĚK, WANIEK, PROS, KLÍMA 1966] and solid models [SHAMINA 1966, 1967], two-dimensional perforated models [KAPCAN, KISLOVSKAJA 1966, GILBERSHTEJN, GURVICH, POCHTOVIK 1966] have been applied.
3. Wave guide with internal inhomogeneities. Two-dimensional perforated model has been used [IVAKIN, KAPCAN 1968].
4. Dipping wave guide. A solid three-dimensional model has been employed [SHAMINA 1970].

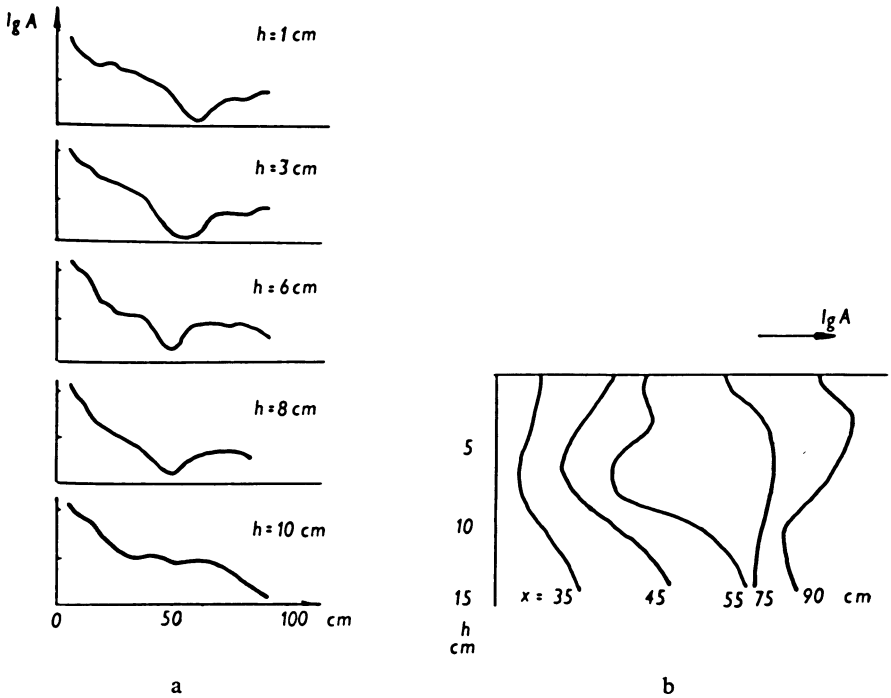


Fig. 5: a) Amplitude-distance curves for P -waves in a wave guide model, h – source depth (depth of the wave guide axis 7,5 cm).
 b) Amplitude-depth curves for P -waves in a wave guide model, x – epicentral distance
 c) Amplitude distance curves for P -waves in a wave guide model, d – thickness of the wave guide, λ – wave-length of the incident wave.
 [RIZNICHENKO, SHAMINA 1964]

The investigations were carried out mainly along two directions: research of the first arrivals on the surface of the model (simulating the Earth's surface) and research of wave pattern for channel waves P_a and S_a . Some general characteristics of the behaviour of the examined waves can be selected. In spite of the difference in methods of model fabrication and the character of a wave guide, the following general conclusions can be drawn:

A. The first arrivals recorded on the surface of models, containing homogeneous, non-sharp, horizontal wave guides, have following typical features:

For the P -wave on the amplitude-distance curves a minimum can be observed, well known as "shadow zone". This minimum shifts towards the epicenter and disappears when the source is submerged (Fig. 5a).

The minimum on the amplitude-depth curve for the P -wave, observed in the region of the shadow-zone has the same depth as the wave guide axis (Fig. 5b).

Both minimum on amplitude-distance curve and minimum on amplitude-depth curve disappear, if the period of recorded waves increases (Fig. 5c).

If the wave guide is submerging (or rising) the above mentioned peculiarities can not be observed. In this case the most expressive characteristic of the wave pattern is a minimum on the amplitude-depth curve when the source is situated at the depth

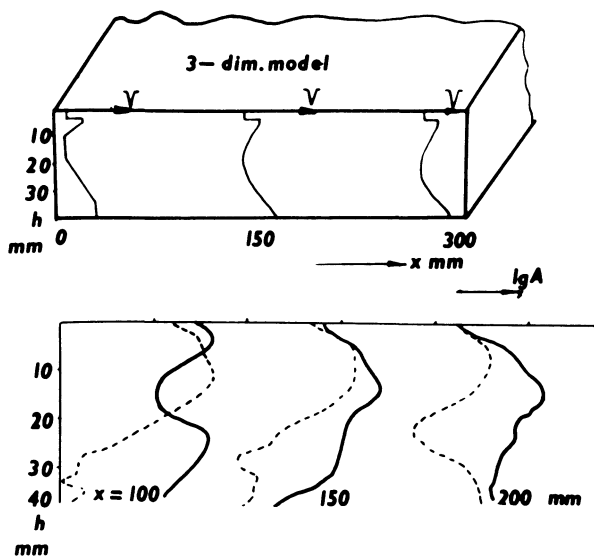


Fig. 6: Amplitude-depth curves if wave guide is submerging (full lines) or rising (dashed lines).

[SHAMINA 1970]

of the wave guide axis. The epicentral distance at which the minimum on the amplitude-depth curves exists increases, when the wave guide is submerged (Fig. 6).

B. The first arrivals recorded at internal points of the model have following specific characteristics:

The velocity of wave propagation in wave guides with sharp boundaries decreases when the period of recorded waves decreases.

If the source is situated within the wave guide, a phenomenon of energy concentration is observed regardless of the sharpness of boundaries. The maximum of the amplitude can be observed in the inner part of the wave guide.

C. The channel wave has the following features, when the source is located within a wave guide:

The channel-wave is observed inside and outside of the wave guide at distances about one wave length (Fig. 7).

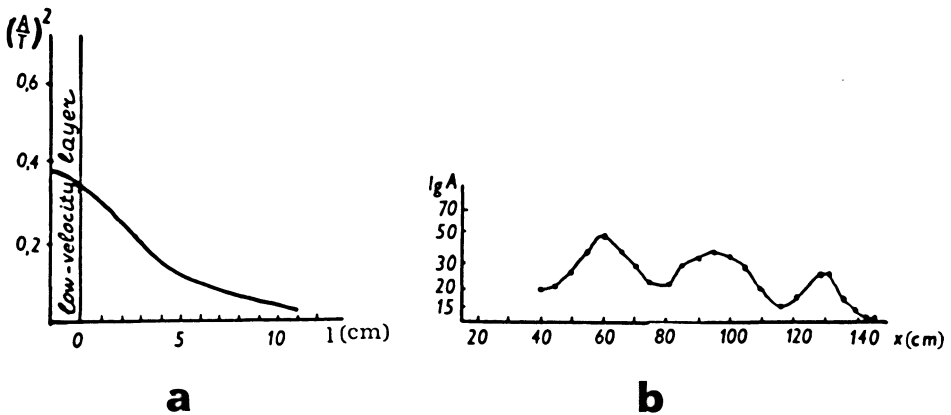


Fig. 7: a) Dependence of the channel wave P_α on distance from the boundary of the low velocity layer [CHOROSHEVA 1962].

b) Amplitude distance curve of P -waves along the wave guide axis [KAPCAN, KISLOVSKAYA 1966].

The channel-wave shows normal dispersion, the group velocity increases when the period of wave increases.

An interchange of maxima and minima can be observed, when the source (or the receiver) moves along the axis of a wave guide (Fig. 7b).

The kinematic and dynamic properties of elastic waves on seismic models with wave guides were applied by seismologists for the purpose of interpretation of seismo-

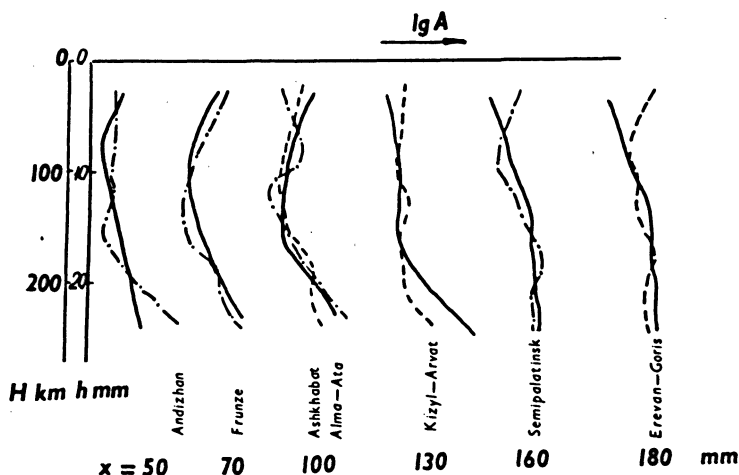


Fig. 8: Amplitude-depth curves in a wave guide model (solid lines) and in nature (dashed lines) [SHAMINA 1967].

logical data [VANĚK, WANIEK, PROS, KLÍMA 1966]. Velocity-depth function for the upper mantle in the region of south-eastern Europe could be derived by treating three-dimensional gel models. The results are based on the comparison of the amplitude-distance curves of seismic body waves with corresponding curves observed on seismic models. The existence of a wave guide in the upper mantle for the region of Middle Asia was confirmed by the observations of SHAMINA [1967] (Fig. 8).

KAPCAN and KISLOVSKAJA [1966] compared seismological amplitude data and model amplitude-distance curves of channel-waves. They established non-sharp boundaries of the low velocity channel in the upper mantle and determined the thickness of this layer to equal 156 km.

This short review shows, that model investigations on wave guides have already made some contributions to the problem of studying the Earth's structure. It is interesting to note that the conclusions of the existence of a wave guide in the upper mantle have been obtained by means of three different methods, namely, by means of comparison of seismological and model amplitude-distance curves, by evaluation of the amplitude-depth functions for *P*-waves and by estimation of amplitude-distance functions for channel waves. Seismological data have been obtained for different regions but every time only one of the methods has been used. That is why none of all investigations proves that the obtained solution is the only one. It would be very useful to carry out seismological observations of different kinds in the same region to conclude the structure of the upper mantle with more confidence.

Thin layers with higher velocity form another group of intermediate layers. They were closely investigated for the purposes of seismic prospecting. Since high velocity contrasts were particularly studied, the obtained results do not fit the scope of this article focused on deeper structures of the Earth. However, a detailed review can be found in [BEHRENS, WANIEK 1972].

4. Conclusion

The presented paper indicates the difficulties of interpreting seismic interface structures. The consideration of only a part of the profile (subcritical reflection, overcritical reflection, head-wave) or only a part of parameters of the observed seismic signals will never provide information on the real structure of the interface. Thus the situation calls for some more systematic model experiments stimulated by field experiments and theoretical studies. This would be the only way of obtaining complete information on the discontinuity structure on the one hand and on the other hand it may be a step towards improving seismic observations.

References

- ABUBAKAR, J.: Scattering of plane elastic waves at rough surfaces. Proc. Cambr. Phil. Soc. 58, 136–157, 1962
- ASANO, S.: Reflection and refraction of elastic waves at a corrugated interface. Bull. Seism. Soc. Am. 56, 201–221, 1966
- BEHRENS, J.: Die Charakterisierung seismischer Grenzflächen mit Hilfe modellseismischer Verfahren im Hinblick auf Deutungsmöglichkeiten des Krustenaufbaues. Habilitationsschrift, Technische Universität Clausthal, 1969
- : Model investigations on the boundary structure Earth's crust/mantle, Proc. 12th Assembly ESC, Luxembourg, 1971
- BEHRENS, J., L. DRESEN und E. HINZ: Modellseismische Untersuchungen der dynamischen Parameter von Kopfwelle und Reflexion im überkritischen Bereich. Z. Geophys. 35, 43–68, 1969
- BEHRENS, J., L. DRESEN und L. WANIEK: Modellseismische Untersuchungen an 2- und 3-dimensionalen Testmodellen, Teil 1. Studia geoph. et geod. 15, 147–160, 1971 a
- BEHRENS, J., L. DRESEN, and L. WANIEK: Investigation on two- and three-dimensional test-models. Proc. 12th Assembly ESC, Luxembourg, 1971 b
- BEHRENS, J., J. KOZÁK, and L. WANIEK: Investigation of wave phenomena on corrugated interfaces by mean of the schlierenmethod. Proc. 12th Assembly ESC, Luxembourg, 1971
- BEHRENS, J., und L. WANIEK: Modellseismik (Übersichtsartikel) Z. Geophys. 38, 1–44, 1972

- BEHRENS, J., and J. SIEBELS: Model investigations on low velocity layers. *Z. Geophys.* 38, 627–646, 1972
- CHOWDHURY, D. K., and P. DEHLINGER: Elastic wave propagation along layers in two-dimensional models. *Bull. Seism. Soc. Am.* 53, 593–618, 1963
- EPINATEVA, A. M.: Reflected waves produced at angles of incidence greater than critical. *Bull. (Izv.) Acad. Sci. USSR, Geophys. Ser.*, 16–40, 1957
- : On dynamic relations of reflected and head waves beyond initial points. *Publ. Bur. Cent. Sism. Int., Ser. A, Travaux Sci.*, No. 21, 23–27, 1961
- GILBERSHTEJN, P. G., I. I. GURVICH, and V. S. POCHTOVIK: Model investigations of two-dimensional wave guides with sharp boundaries. *Bull. (Izv.) Acad. Sci. USSR, Geophys. Ser.* 12, 11–27, 1966
- HOWELL, JR., B. F., and Z. G. BAYBROOK: Scale-model study of refraction along an irregular interface. *Bull. Seism. Soc. Am.* 57, 443–446, 1967
- IVAKIN, B. N., and A. V. KAPCAN: Modelling of an astenospheric low velocity layer with internal inhomogeneities. *Bull. (Izv.) Acad. Sci. USSR, Geophys. Ser.* 4, 39–47, 1968
- KAPCAN, A. D., and V. V. KISLOVSKAJA: Investigation of a wave guide with weak boundaries in two-dimensional perforated models. *Studia geoph. et geod.* 10, 360–369, 1966
- KOZÁK, J., und L. WANIEK: Schlierenoptische Untersuchungen an seismischen Gelmodellen mit photometrischer Auswertung des Wellenfeldes. *Z. Geophys.* 36, 175–192, 1970
- NAKAMURA, Y., and B. F. HOWELL: Maine seismic experiment: frequency spectra of refraction arrivals and the nature of the MOHOROVIČIĆ-discontinuity. *Bull. Seism. Soc. Am.* 54, 9–18, 1964
- NAKAMURA, Y.: Model experiments on refraction arrivals from a linear transition layer. *Bull. Seism. Soc. Am.* 54, 1–8, 1964
- : Head-waves from a transition layer. *Bull. Seism. Soc. Am.* 58, 963–976, 1968
- OLIVER, J.: Body waves in layered seismic models. *Earthquake Notes Seism. Soc. Am.* 27, 29–38, 1956
- OLIVER, J., F. PRESS, and M. EWING: Two-dimensional model Seismology. *Geophysics* 19, 202–219, 1954
- POLEY, J. P.: Critical angle effects in seismic exploration. *Geophys. Prospect.* 12, 397–421, 1964
- RIZNICHENKO, JU. V., and O. G. SHAMINA: Modelling of longitudinal waves in the Earth's upper mantle. *Bull. (Izv.) Acad. Sci. USSR, Geophys. Ser.* 2, 134–148, 1963a
- : Investigation of the shadow zone on models of the Earth's crust and upper mantle. *Bjull. sov. po. sejsmologii ANSSSR* 15, 11–24, 1963b
- : A comparison of amplitude curves obtained on a wave guide model of the mantle with seismic data. *Bull. (Izv.) Acad. Sci. USSR, Geophys. Ser.* 8, 1129–1141, 1964
- : Model study of the upper mantle shadow zone. *Tectonophysics* 1, 439–448, 1965

- RYKUNOV, L. N., V. V. CHOROSHEVA, and V. V. SEDOV: A two-dimensional model of a seismic wave guide with soft boundaries. *Bull. (Izv.) Acad. Sci. USSR, Geophys. Ser.* 11, 1069 to 1071, 1960
- SHAMINA, O. G.: Modelluntersuchungen von Kopf- und Reflexionswellen außerhalb des kritischen Winkels. *Freiberger Forschungshefte, C 116, Geophysik*, 1961
- Attenuation of head-waves from thin beds for rigid and sliding contact. *Bull. (Izv.) Acad. Sci. USSR, Geophys. Ser.* 3, 11–21, 1965a
 - A method of three-dimensional modelling of a wave guide layer with solid media. *Bull. (Izv.) Acad. Sci. USSR, Earth Physics* 7, 484–486, 1965b
 - Experimental investigation of necessary and sufficient characteristics of a wave guide. *Studia geoph. et geod.* 10, 341–350, 1966
 - Dependence of the amplitudes of longitudinal waves on the depth of focus. *Bull. (Izv.) Acad. Sci. USSR, Geophys. Ser.* 9, 23–44, 1967
 - Model investigations of a submerging wave guide in the upper mantle (in Russian). *Proc. 10th Assembly ESC, Moscow* 1970
- SIEBELS, J.: Modellseismische Untersuchungen der kinematischen und dynamischen Parameter von Reflexion und Kopfwelle an einfachen Erdkrustenmodellen. *Diplomarbeit, Technische Universität Clausthal*, 1971
- SISKIND, D.E., and B. F. HOWELL, JR.: Scale-model study of refraction arrivals in a three-layered structure. *Bull. Seism. Soc. Am.* 57, 437–442, 1967
- VANĚK, J.: Amplitude curves of longitudinal waves for several three-dimensional models of the upper mantle. *Studia geoph. et geod.* 10, 350–359, 1966
- VANĚK, J., L. WANIEK, Z. PROS and K. KLÍMA: Modellseismische Untersuchungen an dreidimensionalen Modellen des oberen Erdmantels. *Travaux Inst. Geophys. Acad. Tschécosl. Sci., Geofysikální sborník* 14, 247–289, 1966
- WANIEK, L.: The system water-glycerol-gelatine as a medium for three-dimensional seismic models. *Studia geoph. et geod.* 10, 273–281, 1966a
- Fabrication and properties of three-dimensional seismic models of the upper mantle. *Studia geophys. et geod.* 10, 290–299, 1966b

Contemporary Possibilities of the Schlieren-Method in the Study of Seismic Boundary Phenomena

J. KOZÁK, Prague¹⁾

Eingegangen am 12. Februar 1972

Summary: In the first part of the contribution basic principles of the schlieren-method and a characteristic of chosen methodics of schlieren measurements, which make the desired quantitative analysis of schlieren records possible, are mentioned. In the second part some results of schlieren measurements on selected seismic structures are presented.

Zusammenfassung: Im ersten Teil des Beitrages wird kurz über die Grundeigenschaften der Schlierenmethode und über die Charakteristiken der angewandten Meß- und Auswertungsmethodik berichtet. Die angegebene Methodik ermöglicht eine quantitative Analyse von Schlierenregistrierungen. Im zweiten Teil werden einige Ergebnisse von Schlierenmessungen an ausgewählten seismischen Strukturen präsentiert.

1. Introduction

The schlieren-method is an optical method by means of which optical inhomogeneities in transparent media can be made visible. Optical inhomogeneities correspond

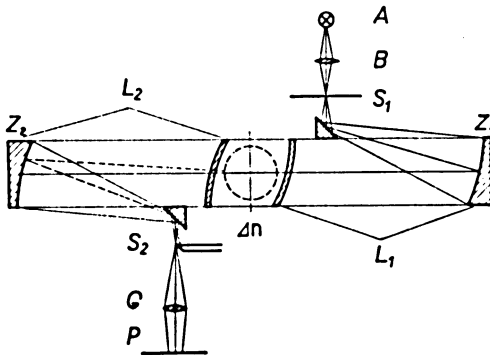


Fig. 1: Ray trajectory in the schlieren device. *A* light source, *B* condenser lens, *S₁* aperture (slit), *L₁* collimating system, *L₂* focusing system, *S₂* knife edge, *G* projection lens, *P* image plane, Δn schlieren element.

¹⁾ Dr. JAN KOZÁK, Geofyzikální ústav ČSAV, Praha 4 – Spořilov, Boční II, ČSSR.

to the regions where the refractive index is not constant. The principle of schlieren representation is evident from the analysis of the diagram of the most frequently used schlieren device working with a beam of parallel rays (Fig. 1).

Schlieren device can be used for the study not only of static inhomogeneities; when suitable registration technique is applied, also pulse phenomena where refractive index gradients arise, can be properly investigated by the method. Longitudinal elastic waves in schlieren pictures are usually represented as lighter and darker strips on gray background corresponding to compressional and tensional regions in the medium. For an example see Fig. 2, where an elastic wave field in a one-layer gel model is shown.

Before applying the schlieren-method to model measurements of seismic structures a long set of methodic measurements was performed. The object of this work was to find a way of schlieren measurements and evaluation of schlieren records enabling an unambiguous quantitative analysis of registered waves. A quantitative expression of schlieren records was obtained by densitometric measuring of these records in selected profiles; obtained densitograms characterize space distribution of refractive index gradients at a given time.

After methodic measurements the principles and conditions of the measurement were settled; in the obtained schlieren records a different degree of optical density correspond to different values of pressure in appertaining regions of the model. This analysis made it possible to use schlieren records not only for kinematic but also for dynamic analysis i.e. for the study of wavelengths and amplitudes of registered waves. Detailed results are given in Kozák [1971].

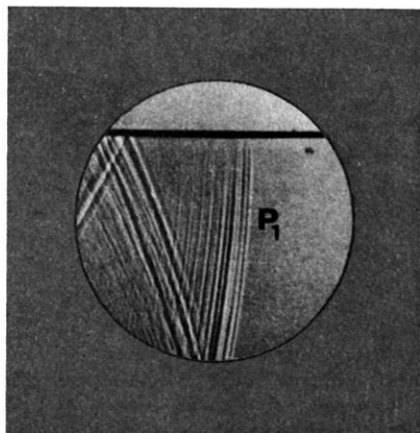


Fig. 2: Schlieren picture of elastic waves in one-layer gel model (high-speed camera record).
 P_1 direct wave.

Model measurements on seismic structures were performed using schlieren measuring arrangement the block diagram of which is shown in Fig. 3.

Before the measurements special attention was paid to the selection of model media and to the design of the model vessel. After numerous experiments it has been found that the most suitable media for seismic models are some selected liquids,

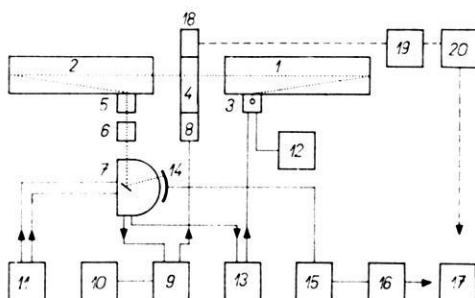


Fig. 3: Block diagram of schlieren measurements. 1 collimating system, 2 focusing system, 3 light source, 4 seismic model, 5 knife edge, 6 supplementary lenses, 7 high-speed camera, 8 wave source, 9 discharge circuit with the power supply, 10, 11 high-speed camera control panel, 12 light source power supply, 13 delay circuit, 14 high-speed camera film record, 15 automatic recording microdensitometer, 16 computer evaluation, 17 final quantitative result of schlieren measurements, 18, 19 and 20 independent piezoelectric circuit for calibration of schlieren records.

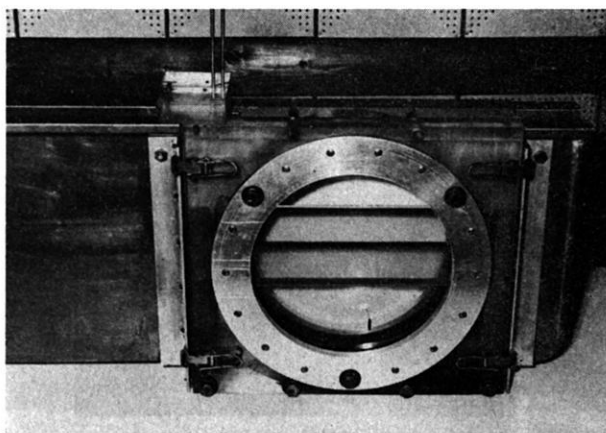


Fig. 4: Model vessel for schlieren measurements with a three-layer gel model. Dimensions of the vessel: length = 1200 mm, height = 320 mm, thickness (of the inside) = 25 mm. Windows of the vessel have the diameter of 260 mm.

three-component gels water-glycerol-gelatine, and plexiglas. For liquid and gel models it was necessary to build a suitable model vessel (Fig. 4).

Both the set of selected model media and the way of seismic models fabrication in the model vessel made it possible to design, construct and investigate layered models having velocity boundaries of 1st and 2nd order, models of velocity boundary of special geometry (curved boundaries, corrugated boundaries) and models of special structures. In the following some results of schlieren measurements on different seismic models will be briefly presented.

2. Schlieren measurements on selected structures

2.1 Models of low-velocity channels

Attention has been concentrated lately on the properties of low-velocity channels. Several liquid and gel models of symmetric and unsymmetric low-velocity channels were studied. The wave field of longitudinal waves in unsymmetric gel channel is shown in Fig. 5.

The first results indicate that the schlieren method is quite suitable for a study of properties of channel structures, especially if it is the question of energy transition along channel boundaries. Investigation of the so called channel wave and other features of low-velocity layers are analysed in [WANIEK 1972].

Some special properties of channel structures namely their ability to conduct inhomogeneous waves are mentioned by ČERVENÝ and KOZÁK [1972].

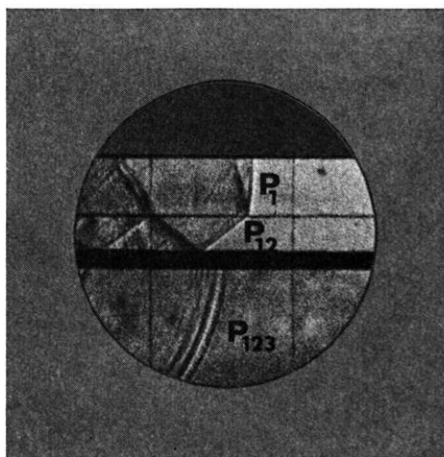


Fig. 5: Schlieren records of wave-field in three-layer gel model of unsymmetric low-velocity channel. The source is on the model surface. P_1 direct wave, P_{12} (direct) wave refracted into the low-velocity layer, P_{123} wave refracted into the third layer after passage through the low-velocity layer.

2.2 Models of corrugated 1st order discontinuities

The aim of rather comprehensive work consisting of measurements on two-layer liquid/plexiglas models with corrugated velocity boundary was to study the influence of corrugation parameters on parameters of reflected wave P_1P_1 .

In the course of measurements different models of corrugations were investigated—see Fig. 6.

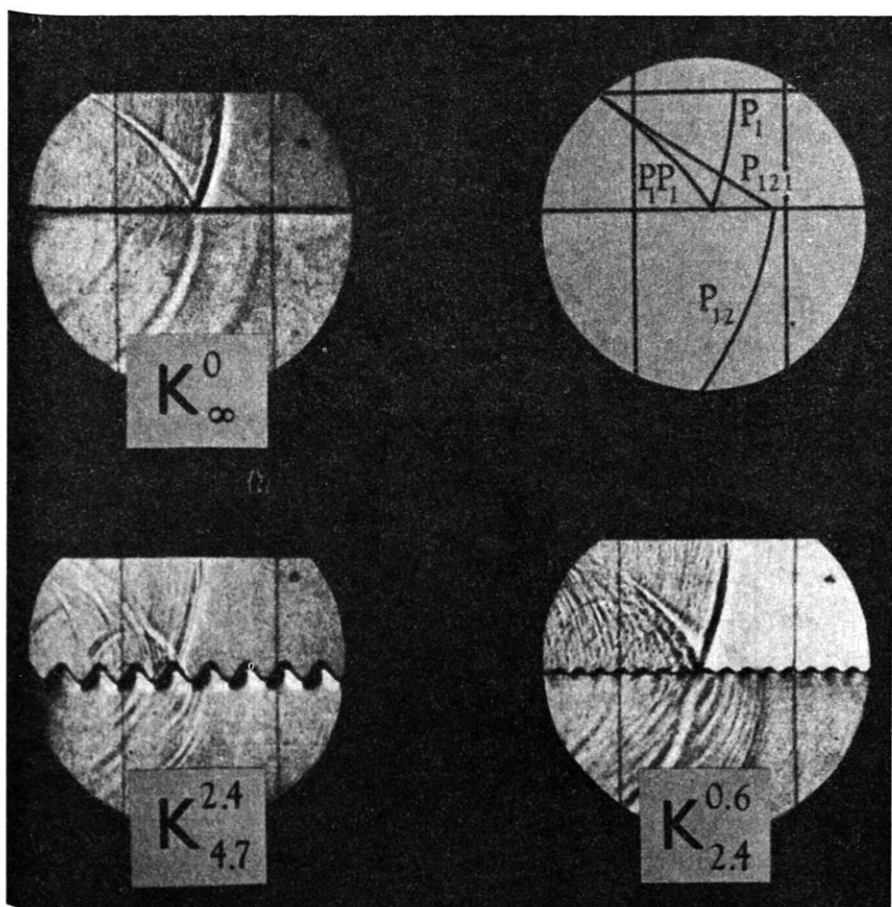


Fig. 6: Schlieren records of the wave field in a two-layer model with corrugated boundary. Interpretation of the wave groups registered is given in the upper right corner. The source is on the surface of the model. K_{ij} models investigated, i, j geometrical parameters of corrugations expressed in wave length of the incident wave.

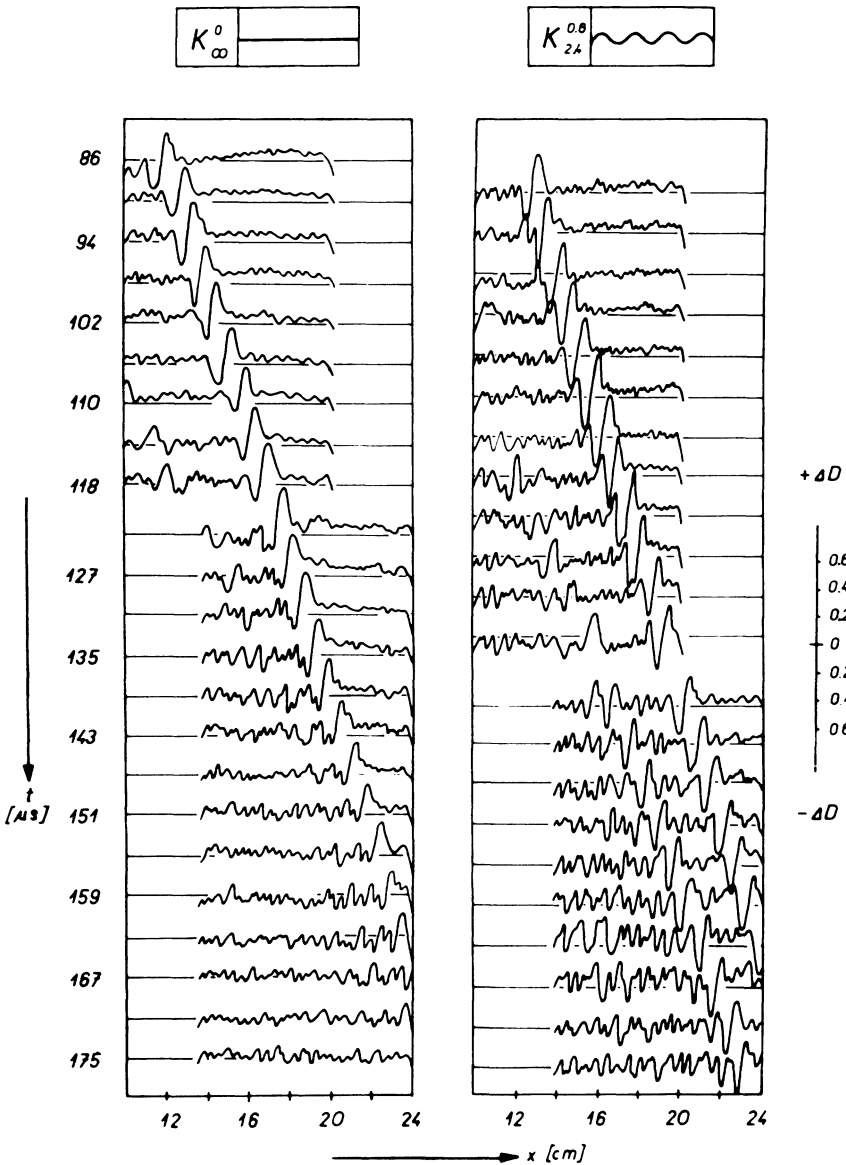


Fig. 7: Wave propagation of direct and reflected waves in microphotometric representation. Densitograms are taken close under the surface. K^j , models investigated, t registration time of separate schlieren frames, x epicentral distance, D difference between the optical density of the wave and the optical density of undisturbed field.

Records of schlieren measurements were for reflected wave P_1P_1 evaluated densitometrically and compared with results of ultrasonic measurements on similar models. In Fig. 7 densitograms characterizing the time development of direct P_1 and reflected P_1P_1 waves in models with plane and corrugated boundary are given. Note a complicated structure of the wave refracted on corrugated boundary [BEHRENS, KOZÁK, WANIEK 1971].

2.3 Models of curved boundary

The work was carried out on the basis of convex and concave curved velocity boundaries of two-layer models. Attention was paid to the study of changes of intensity of the refracted wave P_{12} after passage through curved velocity boundary. By theoretical conclusions convex curved boundary amplifies a refracted wave (and also a head-wave), whilst concave curving of the boundary diminishes and attenuates these waves.

Schlieren pictures of wave field propagating along both types of boundary are shown in Fig. 8.

Schlieren records obtained were densitometrically evaluated. In Fig. 9 a typical amplitude pattern of P_{12} waves measured just under the boundary is given. In the diagram quite different attenuation and amplitude values of amplitude curves of P_{12} wave in both models are evident; theoretical predictions are fully satisfied here.

In the diagram also the amplitude pattern of P_{12} wave measured under plane boundary in the same conditions (curve 2) is given. The first half of this curve lies between both amplitude curves, just as it was estimated. The rapid decrease of the curve 2 from the triple marker is caused by the inhomogeneity inserted into the second medium: for details – see next paragraph.

2.4 Model with a round opening

Here a two-layer liquid/plexiglas model was investigated. In the second (plexiglas) layer of the model a round opening was made. The opening was filled with the first medium. Records obtained are shown in Fig. 10.

The aim of these measurements was to find an influence of the opening on amplitude pattern of refracted P_{12} wave along two paths: in the direction close under velocity boundary parallel to it, and in the direction which goes through the openings. Results of the densitometric evaluation of all schlieren records had the same character which can be demonstrated in a typical diagram shown in Fig. 11.

It seems that the opening is concentrating and cumulating the energy of the refracted wave; an attenuation of the schlieren expression of this wave along the rays that did not enter the opening indicates that the energy of the wave is focused in the opening. At present this conclusion is experimentally verified.

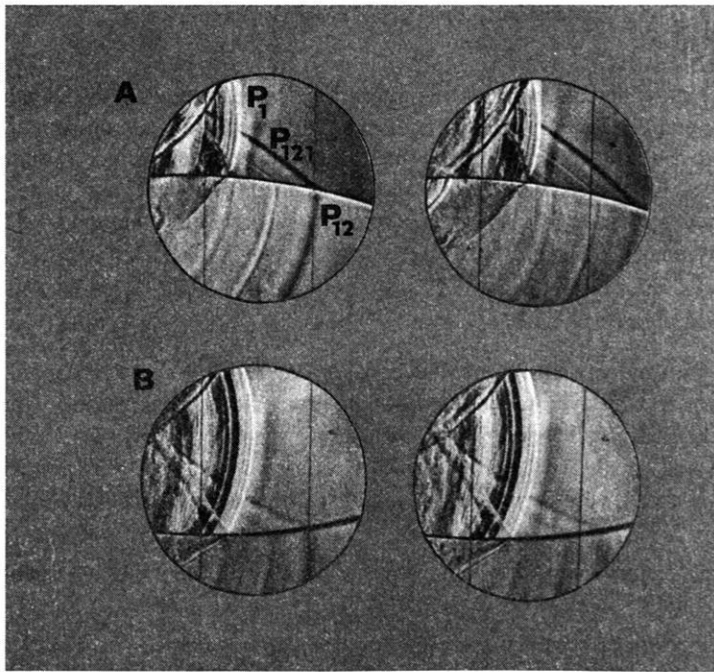


Fig. 8: Schlieren records of wave-field in two-layer turpentine/plexiglas model with curved boundary. The source is located in the upper layer 70 mm above the boundary. P_1 direct wave, P_{12} refracted wave, P_{121} head wave. *A* model with convex curved boundary, *B* model with concave curved boundary.

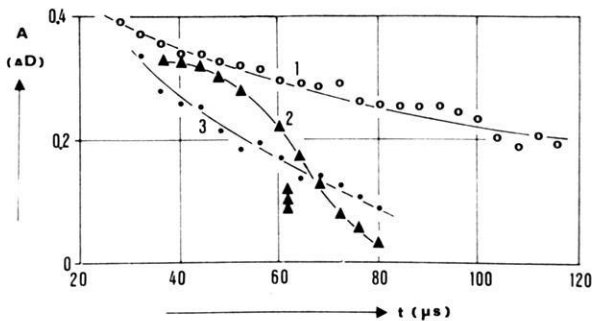


Fig. 9: Attenuation of refracted P_{12} wave in two-layer models with plane and curved velocity boundaries (microdensitometric measurements). A amplitudes of P_{12} wave in grades of optical density D , t -time,

1. model with convex boundary
2. model with plain boundary and an opening in the lower layer (see Fig. 10)
3. model with concave boundary

The time in which P_{12} wave reaches the opening (model 2) is denoted by triple marker.

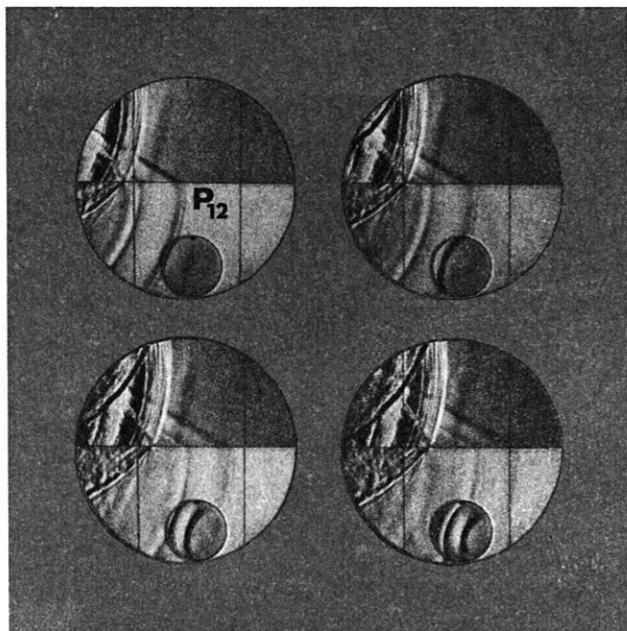


Fig. 10: Schlieren records of wave field in two-layer turpentine/plexiglas model with plain velocity boundary and an opening in the lower layer. The opening 60 mm in diameter is filled with turpentine. The source is located in the upper layer. P_{12} refracted wave. Time delay between individual frames is $8 \mu\text{s}$.

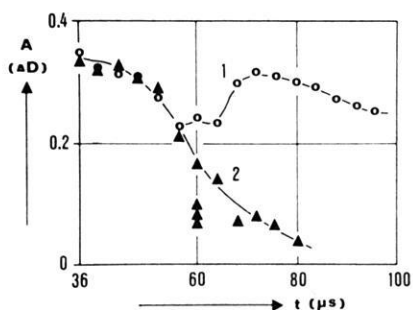


Fig. 11: Attenuation of refracted waves P_{12} in a two-layer model with an opening measured in two directions (microdensitometric measurements). A amplitude of P_{12} wave in degrees of optical density D , t -time. The triple marker has the same meaning as in Fig. 9.

1. densitometric profile measured along the ray crossing the centre of the opening,
2. densitometric profile measured close below the velocity boundary.

2.5 Models containing special structures

In model measurements described here special round structures important in seismic engineering were investigated. The structures were made of plexiglas and submerged into a gel medium. The source—an exploding wire—was gradually placed into different depths under the model surface in a wide range of epicentral distances. The wave field can be seen in Fig. 12.

Our attention was focused to direct P_1 -wave which entered the structure. For this wave kinematic and dynamic analysis was made. The pattern of amplitude curves in these models was similar to that in the model with the opening described above, only the loss of energy was greater due to reflections on outer and inner surfaces of the structure. Intensity change of the wave after passage through the structure was also well apparent in frequency spectra where the predominant frequency was shifted to lower frequencies.

2.6 Phase changes of head wave

Dynamic investigation of schlieren pictures is not limited to the study of amplitudes and wave lengths—also phase changes can be easily analysed. In some schlieren

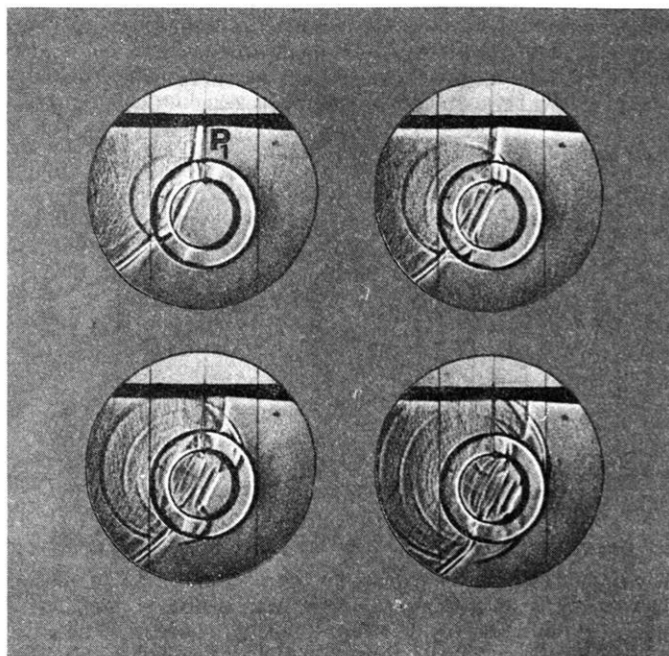


Fig. 12: Schlieren records of wave field in one-layer model with round structure 100 mm in diameter. P_1 direct wave. Time delay between individual frames is 8 μ s.

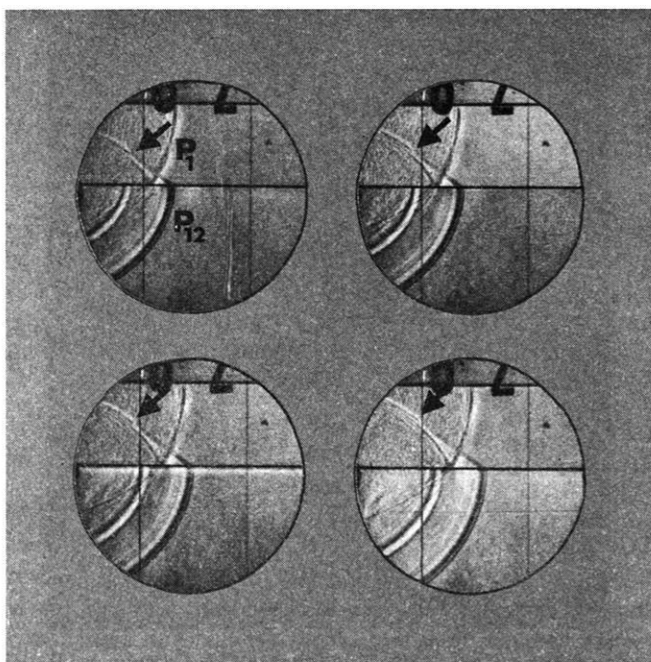


Fig. 13: Schlieren records of wave field in a two-layer water/plexiglas model. Phase change of the head-wave is denoted by arrows. P_1 direct wave, P_{12} refracted wave. Time delay of the individual frames is $4 \mu s$.

records of the wave field in two-layer liquid/solid model a change of phase of the head wave was observed—see Fig. 13.

At present the problem is solved theoretically in the Geophysical Institute of Charles University. Partial results obtained as yet show that namely the consistence of both parts of the model plays the most important role in the phase changes in question. After the computations have been completed we intend to verify the results by means of model schlieren measurements.

2.7 Model study of surface waves

Solid models can be investigated in schlieren device without any cuvette or model vessel. In the work which was carried out in our laboratory on plexiglas plates in this way, surface waves or better said the longitudinal component of surface wave was explored. This component is shown in the schlieren pictures presented in Fig. 14.

Schlieren records obtained were evaluated densitometrically from the viewpoint of kinematics and dynamics of surface waves [MOSLER, WANIEK 1971].

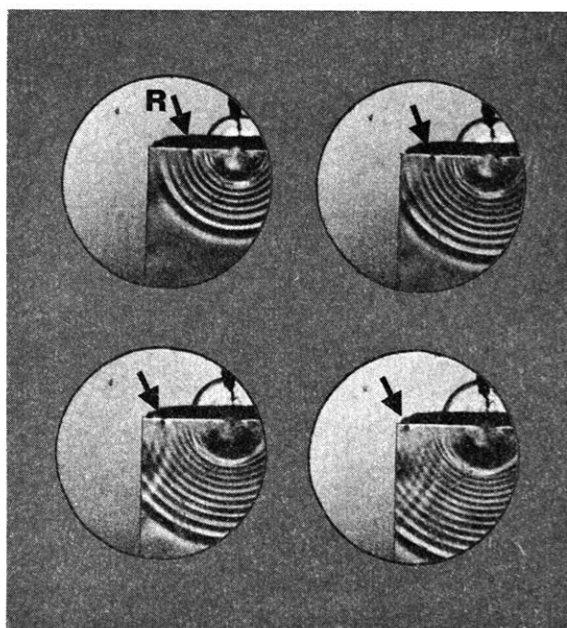


Fig. 14.

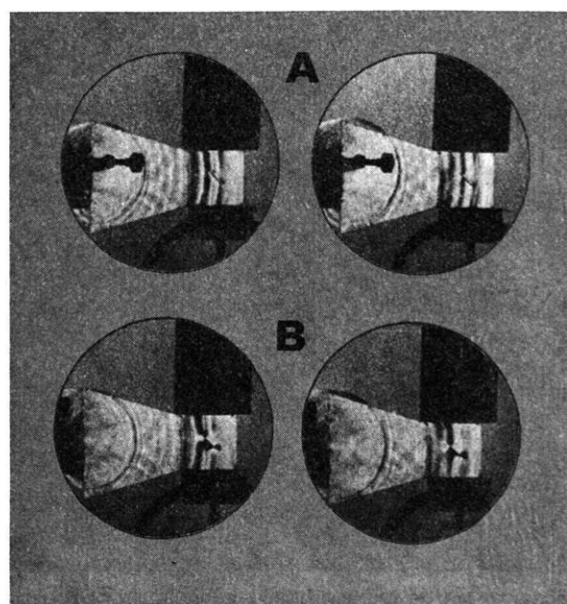


Fig. 15.

2.8 Schlieren study of seismic source

An attempt was made to use schlieren method for both static and dynamic investigation of the model of seismic source area. The model was represented by a square plexiglas plate in which a diagonal slit was made. The slit served as a model of defect in medium. The model plate was stressed by axial static load in a wide range.

The main aim of the measurement was to reach the fracture of the model and to registrate the generated "seismic" waves. This result has not been obtained yet. On the other hand the records obtained demonstrate well the deformations of the elastic waves passing through the stressed model—see Fig. 15. This work is in the very beginning and we intend to continue in it.

3. Conclusion

The results presented characterize the contemporary possibilities of the schlieren method in laboratory seismology. In the future work in two directions will be followed in our laboratory: firstly, the study of general problems connected with wave propagation and secondly model investigation of seismic source. For these reasons we plan to complement and improve the methodics of schlieren measurements and the way of evaluation of schlieren records in order to extend the range of solved problems and to improve the accuracy and reliability of model measurements.

Fig. 14: Schlieren records of longitudinal component of surface wave R . The component is registered on the edge of plexiglas plate (thickness 3 mm) and is denoted by arrows. Time delay between individual frames is 8 μ s.

Fig. 15: Schlieren records of elastic waves passing through square plexiglas plate 50×50 mm in size with diagonal slit (thickness 0.1 mm) 20 mm in length.

A unstressed model (plate)

B prestressed model (200 kp cm^{-2}).

References

- BEHRENS, J., J. KOZÁK, and L. WANIEK: Investigation of Wave Phenomena on Corrugated Interfaces by means of the Schlieren Method. Proc. 11th Ass. ESC, Obs. Royal Belg. 1971
- ČERVENÝ, V., and J. KOZÁK: Experimental Evidence and Investigation of Pseudospherical Waves. Z. Geophys. 38, 617–626, 1972
- KOZÁK, J.: Kinematic and Dynamic Properties of Elastic Waves Investigated on Seismic Models by means of the Schlieren Method. Travaux Inst. Géophys. Acad. Tchécosl. Sci., No 354. Geofyzikální sborník 1971, Academia, Praha (in press)
- MOSLER, J., and L. WANIEK: Schlierenoptische Untersuchungen der kinematischen und dynamischen Parameter von Oberflächenwellen. Studia Geoph. et Geod. 15, 424–428, 1971
- WANIEK, L.: Model Studies on Wave Propagation in Low Velocity Layers. Z. Geophys. 38, 647–658, 1972

Model Investigations of Inclusions in Medium

O. G. SHAMINA, Moscow¹⁾

Eingegangen am 6. April 1972

Summary: The wave pattern on the surface of a three-dimensional ultrasonic model with small solid inclusions has been studied. It has been found that solid inclusions with sharp boundaries lead to changes of the amplitude-distance curves, if the size of the inclusion is more than on a half of the wavelength of the incident elastic wave. No remarkable difference between amplitude-distance curves for various material of inclusions has been observed.

Zusammenfassung: Untersuchungen der *P*-Wellenamplituden an einem dreidimensionalen Modell mit eingelegten festen Inhomogenitäten wurden durchgeführt. Die Versuche zeigten, daß der Einfluß einer Inhomogenität mit scharfen Grenzflächen sich erst dann auf die Amplitudentfernungskurven auswirkt, wenn die Dimension der Inhomogenität größer als die Hälfte der Wellenlänge der einfallenden seismischen Welle ist.

1. Introduction

Model investigations of small inclusions in medium have been carried out in connection with the development of investigations of a presumed future focal region by repeated seismic sounding [KONDRATENKO, NERSESOV 1962; FEDOTOV, DOLBILKINA, MOROZOV, MYACHKIN, PREOBRAZHENSKY, SOBOLEV 1970]. The focal region of the preparing earthquake is the region of the stress concentration which will eventually lead to a fracture. This region may be considered as an inclusion and can be detected by repeated seismic sounding, if its properties distinctly differ from those of the surrounding medium and if a suitable wavelength is chosen.

Wave pattern variations before the earthquake have been observed by FEDOTOV, GUSEV, BOLDIREV, SOBOLEV, MOROZOV, MYACHKIN, PREOBRAZHENSKY, DOLBILKINA [1971] in Kamchatka. They have used seismic waves generated by explosion. Their wavelengths are of the same order as the assumed dimension of the region. Therefore the changes in the arrival times and in the wave pattern, if they are connected with the region, can be explained by diffraction.

It is known that theoretical calculations of diffraction can be performed if the wavelength λ is far smaller or far greater than the dimension d of an inclusion [NUSSEN-ZWEIG 1965; TENG, RICHARDS 1969; PHINNEY, CATHLERS 1969]. If λ is of the order of d , calculations are rather complicated, if not impossible in a general case.

¹⁾ Dr. O. G. SHAMINA, Institut Fiziki Zemli ANSSSR, B. Gruzinskaya 10, Moskva, USSR.

Experimental quantitative investigations have been performed in connection with the problem of diffraction of seismic waves by Earth's core or magmatic inclusion [RYKUNOV 1959; TENG, WU 1968; AVERKO, BALESTA 1970]. In this case the lengths of elastic waves are much smaller than the dimension of the inclusion. The diffraction of elastic waves by inclusions whose size is of the order of λ have not been practically investigated. It would be interesting to make an experiment with a model of real medium containing a small inclusion and to investigate by means of ultrasonic measurements its influence on the wave pattern observed at the surface. The first attempt to construct a model of such a kind was made by KLÍMA [1966 — not published].

2. Arrangement of experiments

The three-dimensional solid model for our investigations was made from epoxide resin, mixed with quartz sand. Conditions of the polymerization were chosen with the aim to get the velocity-depth distribution similar to that for the crust.

In Fig. 1 velocity-depth distributions in the model and in the subcontinental crust according to KOSMINSKAYA [1968] are given. Fig. 1 also shows the experimental set-up. The source may be placed on the vertical side of the model too. The predominating

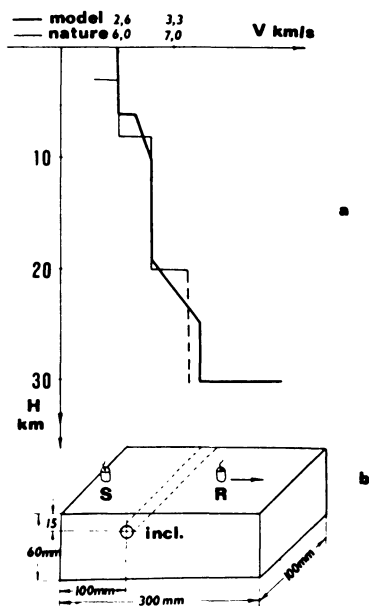


Fig. 1: *a* Velocity-depth distribution of *P*-waves in subcontinental Earth's crust (after KOSMINSKAYA 1968) and *b* corresponding three-dimensional model, *S* source, *R* receiver.

period of the generated pulses corresponds to the wave length in the model of about 5—6 mm.

In Fig. 1 the place and the shape of an inclusion are also represented. The inclusion is a cylindrical hole, which was made at the very place of a caustic according to calculations of the ray paths. The hole was filled with some material, the choice of the filler properties was made as follows.

In the focal region inevitably two stages of the preparation of an earthquake can be considered. The initial stage, when stresses increase in it and elasticity and density of the medium increase, too. Posterior stage, when stresses are strong enough to stimulate chaotic appearance of local cracks, which make the medium more ductile and loose. Accordingly, in the initial stage the focal region may be considered as a rigid inclusion and in the following stage as a soft inclusion.

The rigid inclusion was modelled with steel, the soft inclusion with paraffin. Cracks were modelled by splinters of the model material spilled into paraffin.

3. Results

On model seismograms the amplitude of the first onset and the maximum amplitude in the *P*-wave group were measured. The arrival times were examined, too, but no changes connected with the existence of an inclusion were observed.

Fig. 2 shows amplitude-distance curves obtained in a model without and with an inclusion, whose diameter is λ . The upper curves are maximum amplitudes and the lower curves are amplitudes A_{12} . All the curves were constructed up to a distance where the first onset is formed by the head wave connected with the 1st order discontinuity in the model.

It is apparent that the behaviour of the amplitude in a model with an inclusion differs from that in a model without an inclusion. The level of curves decreases with distance more rapidly, a trend to oscillations appear in these curves. It is interesting that these variations exist already before the point just over the inclusion.

No marked difference between the curves for various inclusions is observed. Nevertheless, an analysis of seismograms shows that the inner structure of the *P*-wave group is different at distances both before the inclusion and behind it.

Fig. 3 can illustrate this conclusion, for example, by comparing the relation of amplitudes A_{12} and A_{34} at a distance of 85 mm.

If the diameter of the inclusion is 2λ the shape of the *P*-wave differs more appreciably for various inclusions as seen from the comparison of records at a distance of 110 mm. Amplitude-distance curves for this case are given in Fig. 4. It can be seen that the difference between the curves in a model without and with an inclusion is much more marked than in the previous case. The oscillatory character of the curve for a model with an inclusion is more pronounced. The level of this curve in general is twice as below as the one in the model without an inclusion, but in some points the difference is 4 times.

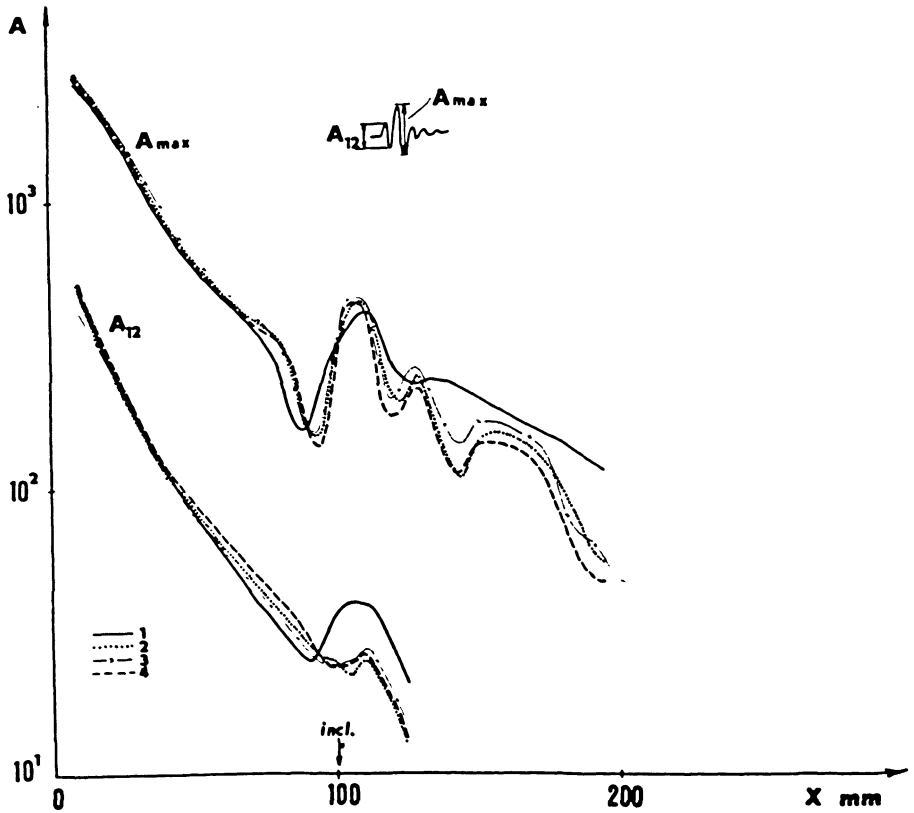


Fig. 2: Amplitude-distance curves observed on models: 1 without an inclusion and with inclusions; 2 $qv_{incl.} > qv_{mod.}$, 3 $qv_{incl.} \approx qv_{mod.}$, 4 $qv_{incl.} < qv_{mod.}$. Diameter of inclusion $d = \lambda$, depth of source 8 mm.

As concerns the difference between the amplitude-distance curves for various inclusions, it increases far less and do not exceed the average of 10–15%.

On the basis of the obtained results it may be suggested that further extension of the inclusion will lead to more changes of the shape and the amplitude of the *P*-wave. On the contrary the inclusion, whose dimension is λ , will affect the wave pattern far less.

To estimate the minimum size of an inclusion affecting the amplitude of the *P*-wave another model was used. It was the model of a homogeneous medium where the velocity is constant. The size and material of the model and the situation of the inclusion from paraffin are the same as in the considered model. The diameter of the inclusion was varied from one half λ to 2λ .

The constructed amplitude curves are presented in Fig. 5. As it was the case in an inhomogeneous model, the inclusion leads to the appearance of oscillations and to a

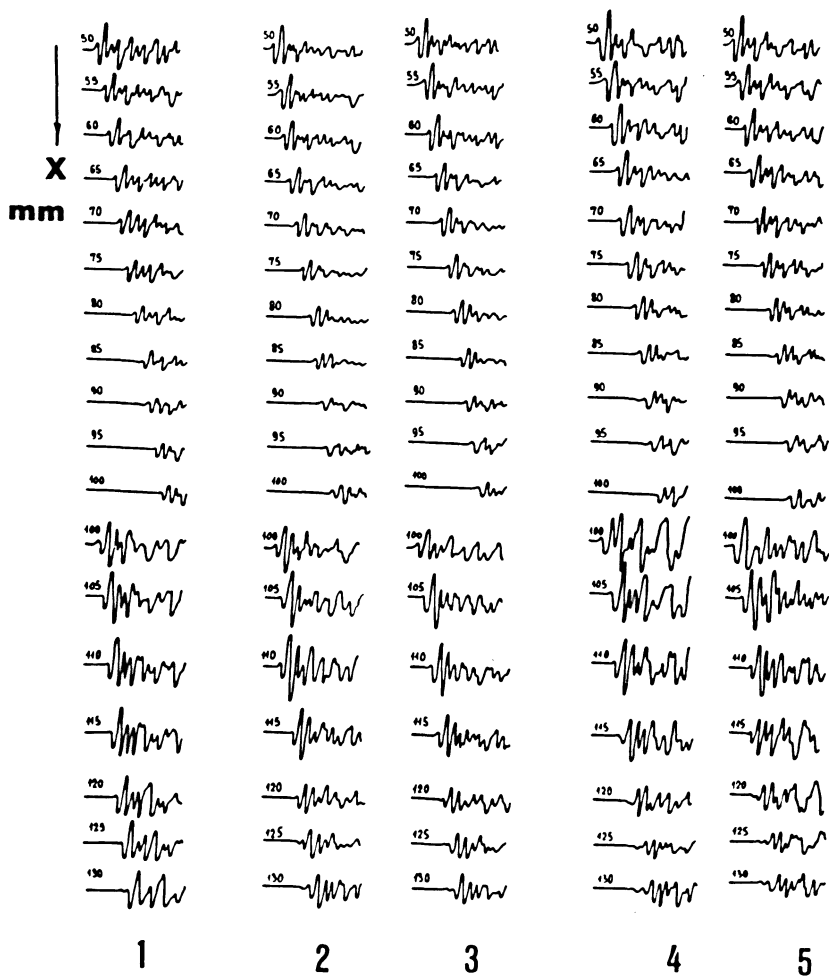


Fig. 3: Model seismograms. 1 without inclusion, 2 with inclusion $d = \lambda$, $\rho v_{incl.} > \rho v_{mod.}$, 3 with inclusion $d = \lambda$, $\rho v_{incl.} < \rho v_{mod.}$, 4 with inclusion $d = 2\lambda$, $\rho v_{incl.} > \rho v_{mod.}$, 5 with inclusion $d = 2\lambda$, $\rho v_{incl.} < \rho v_{mod.}$

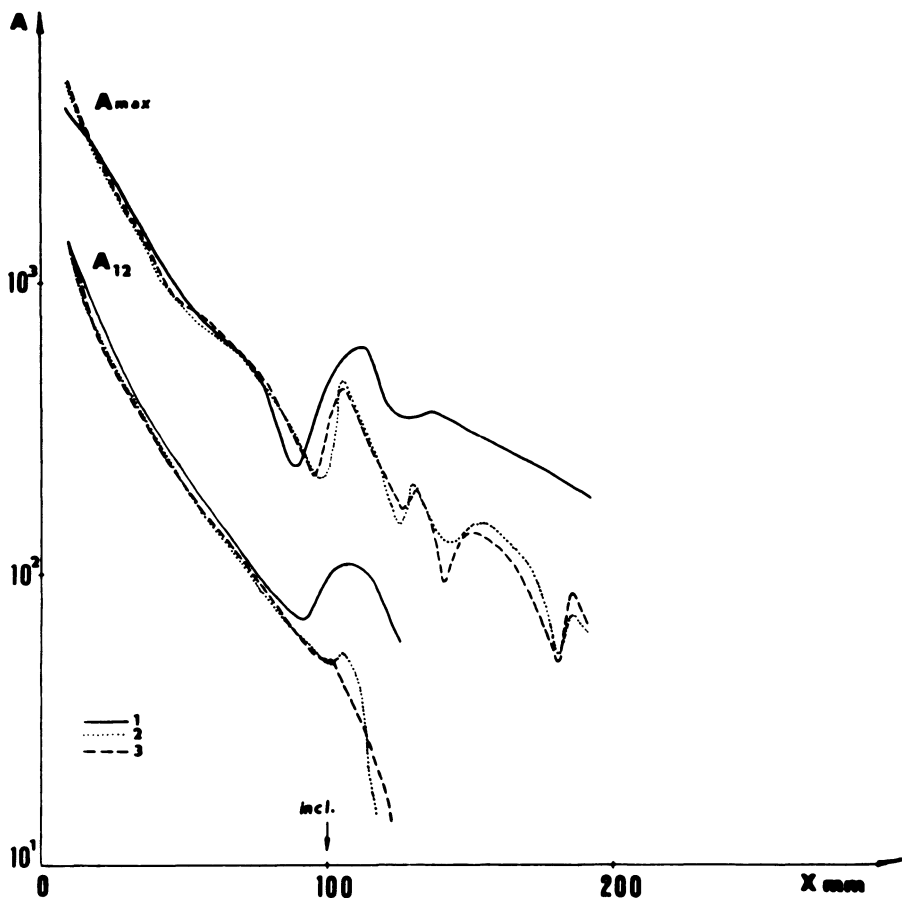


Fig. 4: Amplitude-distance curves observed on models: 1 without an inclusion, and with inclusions: 2 $\rho_{incl.} > \rho_{mod.}$, 3 $\rho_{incl.} < \rho_{mod.}$. Diameter of inclusion $d = 2\lambda$, depth of source 8 mm.

change of the level of the curve. The level increases in the vicinity of the inclusion about 30% independently on its size and then decreases. The drop of the curve is only 10% for the inclusion of the size of half λ and twice for the inclusion of the size of 2λ .

The maximum amplitude begins to change before the point just above the inclusion. The amplitude A_{12} changes only behind this point, the changes arising farther the point the lesser the inclusion.

4. Discussion of results

On the basis of these investigations the following conclusions can be drawn:
 A solid inclusion with sharp boundaries whose size is more than half of λ leads to oscillations of the amplitudes and changes the level of the amplitude-distance curve.

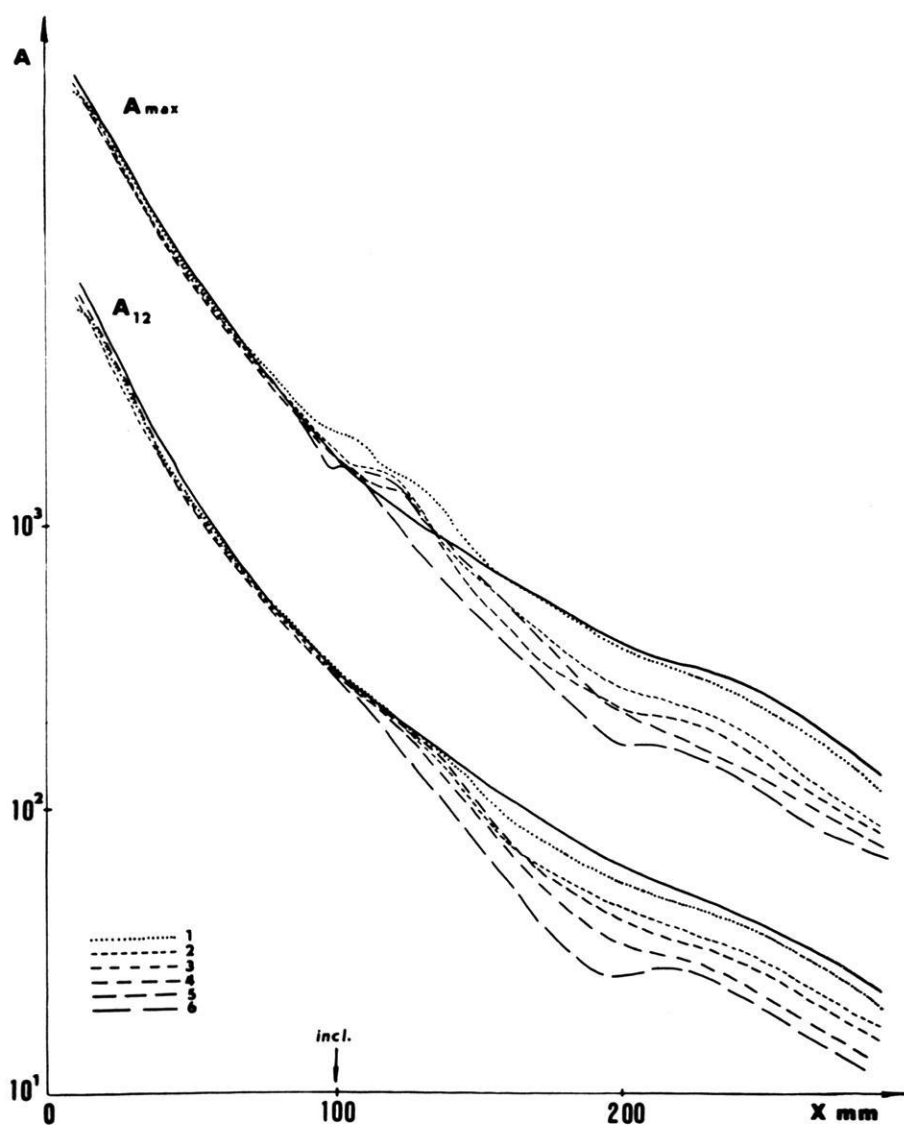


Fig. 5: Amplitude-distance curves for a homogeneous model without an inclusion (solid line) and with inclusions (dashed lines): 1 $d/\lambda = 0.5$, 2 $d/\lambda = 0.7$, 3 $d/\lambda = 0.8$, 4 $d/\lambda = 1.0$, 5 $d/\lambda = 1.5$, 6 $d/\lambda = 2.0$, depth of source 15 mm.

The change of the amplitude curve trend begins before the point just above the inclusion and continues up to a distance more than 30λ .

The difference between the amplitude in a model with and without an inclusion may be 30% for one half λ inclusion and may reach 2–4 times for 2λ inclusion. The difference between the amplitude in a model with various inclusions averages 10–15% for inclusion $(1-2)\lambda$.

Apparently the difference in properties of a focal region and of a surrounding medium is less contrasting than that in a model. Moreover, the boundaries of a focal region are certainly not sharp. Under these circumstances the obtained evaluations must be considered as limiting. Thus, the focal region can be detected if it is not less than $\lambda/2$ and the variations of a wave pattern can be looked for if the focal region is not less than 2λ .

References

- AVERKO, E. M., and S. T. BALESTA: Formulation of problem and investigation of a magmatic volcanic focus by seismic modelling method (in Russian). *Geol. i Geofizika*, No. 3, 81–88, 1970
- FEDOTOV, S. A., N. A. DOLBILKINA, V. N. MOROZOV, V. I. MYACHKIN, V. B. PREOBRAZHENSKY, and G. A. SOBOLEV: Investigation on earthquake prediction in Kamchatka. *Tectonophysics* 9, 249–258, 1970
- FEDOTOV, S. A., A. A. GUSEV, S. A. BOLDIREV, G. A. SOBOLEV, A. N. MOROZOV, V. I. MYACHKIN, V. B. PREOBRAZHENSKY, and N. A. DOLBILKINA: Progress of the earthquake prediction in Kamchatka (in Russian). Report 15th general Assembly IUGG, Moscow 1971
- KONDRATENKO, A. M., and I. L. NERSESOV: Results of investigations on *P*-wave velocities and relations of *P*- and *S*-velocities in the focal region (in Russian). *Proc. Inst. Earth Physics Acad. Sci. USSR*, 25 (192), 130–150, 1962
- KOSMINSKAYA, I. P.: Deep seismic sounding of the Earth's crust and upper mantle (in Russian). Izd. "Nauka", Moskva 1968
- NUSSENZWEIG, H. M.: High frequency scattering by an impenetrable sphere. *Ann. Phys.* 34, 29–95, 1965
- PHINNEY, R. A., and L. M. CATHLERS: Diffraction of *P* by the core. *J. Geophys. Res.* 74, 6, 1556–1574, 1969
- RYKUNOV, L. N.: On the Earth's core diffracted *P*-waves and rigidity of the core. *Bull. (zv.) Acad. Sci. USSR, Ser. Geophys.* 7, 956–964, 1959
- TENG, T. L., and P. G. RICHARDS: Diffracted *P*, *SV* and *SH* waves and their shadow boundary shifts. *J. Geophys. Res.* 74, 6, 1537–1555, 1969
- TENG, T. L., and F. T. WU: A two-dimensional ultrasonic model study of compressional and shear wave diffraction patterns produced by a circular cavity. *Bull. Seism. Soc. Am.* 58, 171–178, 1968

Experimental Evidence and Investigation of Pseudospherical Waves

V. ČERVENÝ¹⁾ and J. KOZÁK²⁾, Prague

Eingegangen am 22. Februar 1972

Summary: An inhomogeneous wave—here called pseudospherical—is investigated. The wave generated in a two-layer transparent model is made visible by means of the schlieren-method: obtained schlieren records are evaluated from the point of view of kinematics and dynamic properties of the wave. Results of the measurements are compared with the results of theoretical works in which the existence and basic properties of pseudospherical wave were predicted. Possibilities of seismic registration of the wave are briefly discussed.

Zusammenfassung: Eine inhomogene, sog. „pseudosphärische“ Welle wird untersucht. Die in einem zweischichtigen, transparenten Modell erzeugte Welle wird mittels der Schlierenmethode sichtbar gemacht. Die gewonnenen Schlierenregistrierungen werden vom Gesichtspunkt der Kinematik und der dynamischen Eigenschaften der Welle aus verarbeitet. Die so erhaltenen Daten werden mit Ergebnissen von theoretischen Arbeiten verglichen, in denen die Existenz und grundlegenden Eigenschaften von pseudosphärischen Wellen vorhergesagt wurden. Die Möglichkeiten der Registrierung von solchen Wellen an der Erdoberfläche werden angedeutet.

1. Introduction

The research into seismic wave propagation through complicated structures of the Earth has yielded significant results in recent years. Nevertheless, there are still numerous not quite explained phenomena in this field. That is why we decided—when realizing laboratory model investigation of seismic structures—to begin the work with the most simple models.

In the schlieren laboratory of the Geophysical Institute of Czech. Acad. Sci. a set of simple two-layer gel models and liquid-solid models with plane boundary of the 1st order has been studied. The model measuring equipment, technology of building of the models, experimental way of schlieren measurements and schlieren records photometric evaluation have been the same as described by KOZÁK [1972].

The very first results of these experiments indicated that even the wave field of longitudinal waves in these simple structures does not quite correspond to the ray-

¹⁾ Prof. Dr. VLASTISLAV ČERVENÝ, Geofyzikální ústav Karlovy university, Ke Karlovu 3, Praha-2, ČSSR.

²⁾ Dr. JAN KOZÁK, Geofyzikální ústav ČSAV, Praha 4- Spořilov, Boční II, ČSSR.

theory and is more complicated. Besides ordinary waves corresponding to the ray theory also different types of inhomogeneous waves can exist in these media.

Pseudospherical waves were predicted in theoretical works based on wave methods published in the forties [OTT 1942] and later [ČERVENÝ 1956, BREKHOVSKIKH 1960]. Thus, to theoreticians, these waves are not unknown; on the other hand, we have not succeeded in finding any paper dealing with experimental evidence of pseudospherical waves.

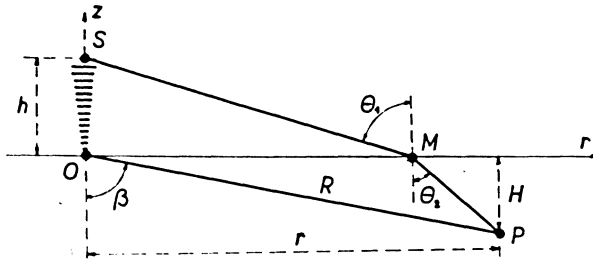
The results of theoretical works mentioned above led us to the conclusion that pseudospherical waves should be of distinct seismic importance in some cases. For instance, if the seismic source is located under the MOHORoviČIĆ-discontinuity not far from it, a pseudospherical wave should appear on the surface of the Earth.

The waves in question also propagate in a low-velocity channel if the source is outside the channel. In the model with a low-velocity layer, pseudospherical waves were first experimentally observed two years ago in our laboratory. For these reasons we performed experimental studies the aim of which was to find out basic features of the wave and we estimated the possibilities of seismic registration of this wave.

2. Theoretical considerations

If a spherical wave incidents upon the boundary at which the velocity decreases discontinuously, reflected waves (in the first medium) and refracted waves (in the second medium) originate. In the second medium one regular and one irregular wave arrive to the receiver which does not lie too far from the boundary:

- a) Regular wave corresponding to the ray theory. It will be called a regular refracted wave in this paper. The energy of this wave is transferred along the ray SMP (see Fig. 1). The angle of incidence of the ray θ_1 , and the angle of refraction θ_2 are connected by SNELL'S law. At great distances from the source, $\sin \theta_2$ will change only slightly. Therefore, the wave front of a regular refracted wave will be approximately conical in the neighbourhood of the boundary and it will form an angle with the boundary the sine of which will be close to v_2/v_1 . Here v_1 (v_2) denotes a P -wave velocity in the first (second) medium.
- b) Irregular wave (here called pseudospherical). It does not exist in the ray approximation. The energy of a pseudospherical wave is transferred along a path which does not correspond to the ray conception. A physical explanation of the existence of a pseudospherical wave is based on the fact that in the decomposition of a spherical wave into plane waves, inhomogeneous plane waves also exist. Refraction of a spherical wave into the medium of lower velocity and the origin of the pseudospherical wave are presented in Fig. 1.



Refraction of a spherical wave into the medium of lower velocity.

SMP-ray of a regular refracted wave

SOP-path along which the energy of a pseudospherical wave is transferred

S - source, P - receiver

The potential $\bar{\Phi}$ of a pseudospherical wave is given by an approximate formula :

$$\bar{\Phi} = \frac{2n}{R} e^{i\omega(R/\alpha_1 - t)} e^{-kh\sqrt{n^2 \sin^2 \beta - 1}} \left(\frac{\rho \cos \beta}{n \rho \cos \beta + i\sqrt{n^2 \sin^2 \beta - 1}} + \frac{i\rho}{(1-n^2)kR} \right)$$

Fig. 1: Pseudospherical wave—explanation of various symbols. The other symbols in the formula for $\bar{\Phi}$: n refractive index ($n = \alpha_1/\alpha_2$), α_1 (α_2) P wave velocity in the upper (lower) layer, ω frequency, k wave number ($k = \omega/\alpha_1$), ρ density ratio ($\rho = \rho_2/\rho_1$), t time.

From the approximate formula shown in Fig. 1 some properties of a pseudospherical wave can be obtained:

1. The wave front of a pseudospherical wave is spherical, with the centre in the projection of the source at the boundary. It makes an angle $\pi/2$ with the boundary.
2. The travel-time curve of a pseudospherical wave along the boundary is a straight line, $t = R/\alpha_2$.
3. Amplitudes of a pseudospherical wave decrease exponentially with increasing frequency as distinct from a refracted wave which has a finite amplitude even at an infinite frequency.
4. Amplitudes of a pseudospherical wave decrease exponentially with increasing h (i.e., with increasing distance of the source from the boundary). Consequently, it will be possible to record them only when the distance of the source from the boundary is small.

3. Laboratory investigations

For the experimental study of pseudospherical waves in two-layer models ($x_1 > x_2$) the schlieren-method was chosen since it enables the study of wave fields inside the model investigated. The photograph of the schlieren modelling device used is shown in Fig. 2.

Model measurements were carried out on two-layer models built up of two kinds of transparent gels with different velocities of compressional waves. The models were placed in a model vessel for schlieren measurements.

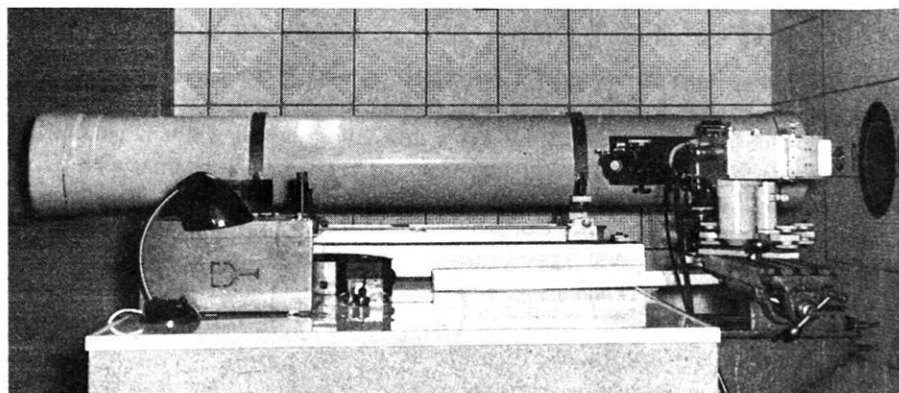


Fig. 2: Focusing system of the schlieren device IAB-451 coupled with high-speed camera SFR-2 (operating rate up to 2.5 millions frames/s). The focus length of the schlieren system is 1917 mm.

Elastic waves were generated by an exploding wire submerged gradually into the model up to the depth of the velocity boundary and below it. The exploding wire was discharged at the wide range of epicentral distances. Frequency analysis has shown that the amplitude spectrum of generated pulses was very sharp, with the dominant frequency of 27.5 kcps and corresponding wavelengths between 5.5 and 9.6 mm for different model media.

The arrangement of the experiment did not correspond fully to the theoretical assumptions under which formula in Fig. 1 was derived but this fact did not change the physics of the phenomenon investigated. The differences between the experiment and theoretical assumptions are discussed in the paper by ČERVENÝ, KOZÁK, and PŠENČÍK [1972]. Two typical sets of frames obtained during the measurements are reproduced in Fig. 3. Both frames correspond to the measurements performed for $x_0 = 250$ mm (i.e., the horizontal distance of the source from the first reference distance line in the field of vision was 250 mm). In the first case the source was

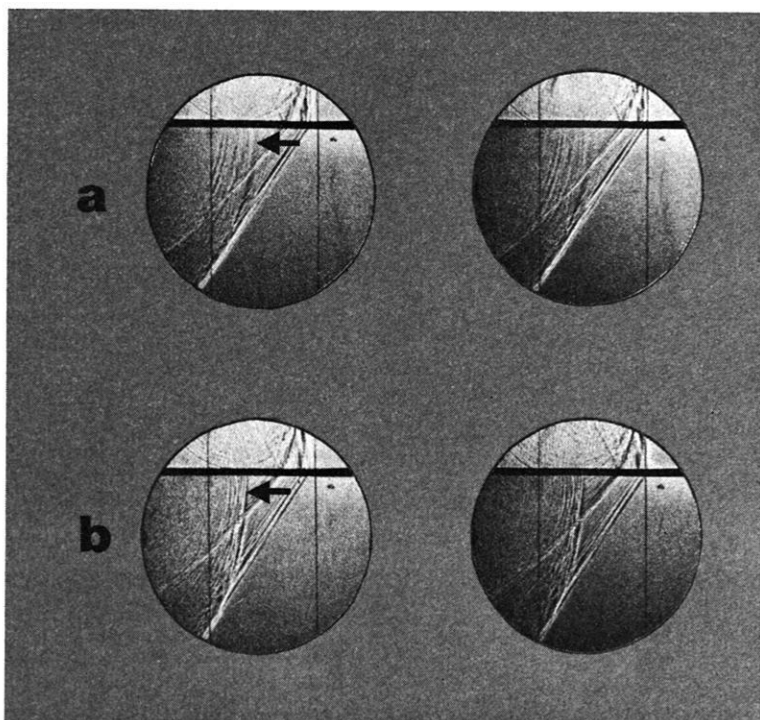


Fig. 3: Schlieren pictures of the wave field in a two-layer gel model ($\alpha_1 > \alpha_2$) with the plane velocity boundary. The source lies in the upper layer, at the distance h above the boundary. Regular refracted wave is first from the right, the pseudospherical wave (denoted by an arrow) can be seen behind it.

a $h = 20$ mm, b $h = 6$ mm.

20 mm above the boundary, in the second case 6 mm. The wave fronts of several waves can be easily seen in the figure. In the first medium (above the boundary) there is a direct wave (P_1), then a wave reflected from the boundary which practically interferes with the wave P_1 , and finally a wave reflected from the surface of the model (P_1P_1). In the second (lower) medium it is possible to observe a regular refracted wave (P_{12}), and a wave with a spherical wave front (\bar{P}_{12})¹. The wave \bar{P}_{12} in Fig. 3a (for $h = 20$ mm) is much less intensive than that in Fig. 3b (for $h = 6$ mm).

¹) There is also another wave in the second medium which is connected with the surface of the model. This wave has no importance for our study and therefore it will not be discussed in this paper.

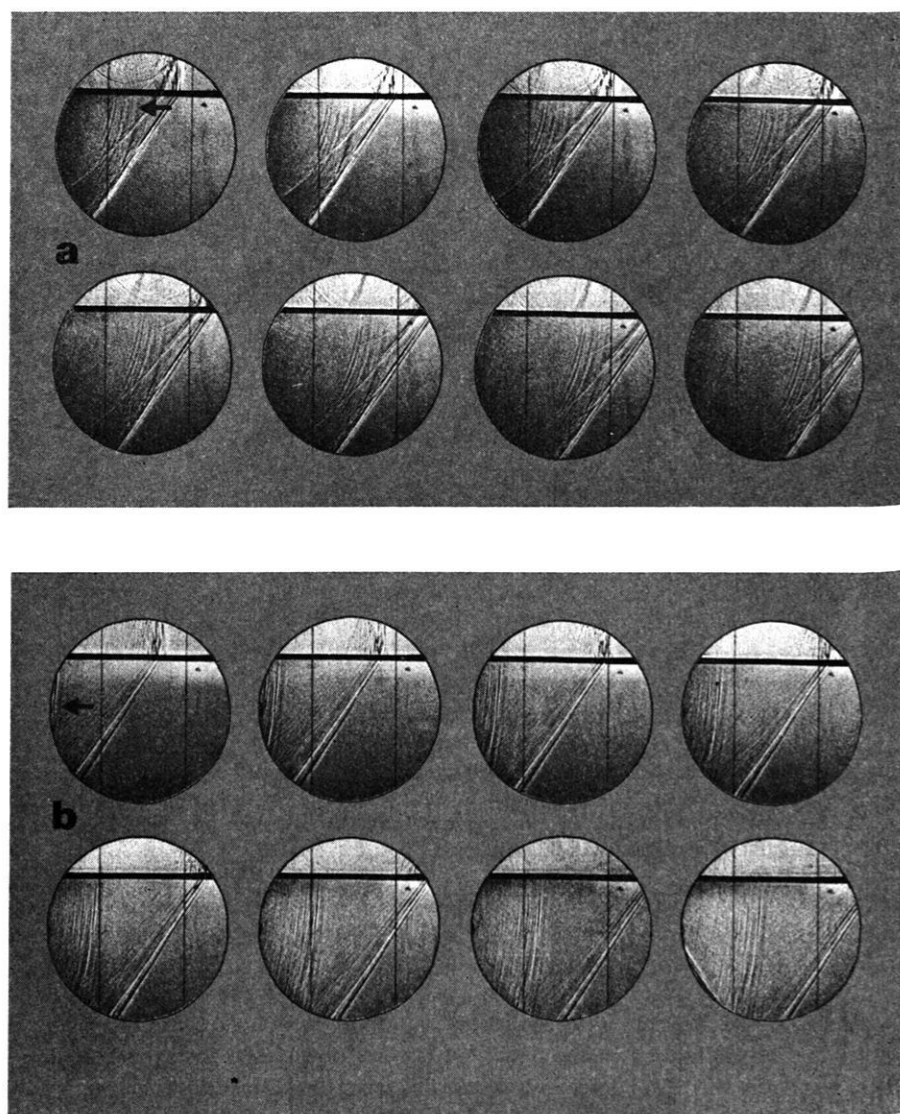


Fig. 4: Two time series of schlieren pictures of the wave field in a two-layer gel model ($\alpha_1 > \alpha_2$). The source lies in the upper layer, at the distance of 20 mm above the boundary. Pseudospherical waves are denoted by arrows at first pictures of both time series. The first time series (a) corresponds to the epicentral distance $x_0 = 250$ mm, the other (b) to $x_0 = 650$ mm.

The main object of the experiment was to investigate the properties of the wave \bar{P}_{12} , especially the dependence of its intensity on the distance h of the source from the boundary. Much valuable information has already been provided by the evaluation of the time series of schlieren frames obtained. In Fig. 4 pseudospherical waves recorded at smaller and greater epicentral distances are given.

The visual evaluation of schlieren frames allows to formulate several important conclusions:

- a) Two qualitatively different types of waves propagate in the lower medium: P_{12} and \bar{P}_{12} wave.
- b) Wave P_{12} can always be observed as first onsets. It has an approximately conical wave front (straight line in a plane section) in the vicinity of the boundary. The wave front forms an angle with the boundary the sine of which is close to α_2/α_1 .
- c) \bar{P}_{12} -wave can never be observed as first onsets. It exists only in a certain zone close to the boundary. The \bar{P}_{12} -wave kept two important features throughout all measurements. First: Its intensity decreased considerably with increasing distance h of the source from the boundary. Second: Wave fronts of \bar{P}_{12} -waves were always approximately spherical. A number of wave fronts of \bar{P}_{12} -waves were measured geometrically and we always succeeded in finding a corresponding circle by which the wave front would be adequately well approximated. The angle which the wave fronts formed with the boundary was also measured. The angle was always very close to $\pi/2$.

The above mentioned properties corresponded fully to the most important properties of a pseudospherical wave as described earlier. Further, travel-time curves were measured for selected time series of schlieren frames at different depths below the boundary. These measured travel time curves correspond to the theoretically predicted ones.

Great attention has also been paid to the question of the position of fictitious centres of circles by which the wave fronts of \bar{P}_{12} -waves were approximated. The results of the measurements of the wave fronts of pseudospherical waves indicated that these (fictitious) centres did not lie exactly in the projection of the source on the boundary, but rather in the first medium closer to the source.

A number of selected frames were evaluated densitometrically. All densitograms presented in the following correspond to greater epicentral distances ($x_0 = 650$ mm). Fig. 5 shows densitograms measured for $h = 65, 40, 20, 6, 2$ and 0 mm always at six different depths below the boundary. A relatively high noise is caused by the granularity of the recording material of high sensitivity. Here again the feature 4 is quite evident, i.e. a fast decrease of intensities of \bar{P}_{12} -waves with increasing distance h of the source from the boundary. (In the case of $h = 40$ mm the \bar{P}_{12} -wave already practically vanishes in the noise, although it can be identified without difficulties

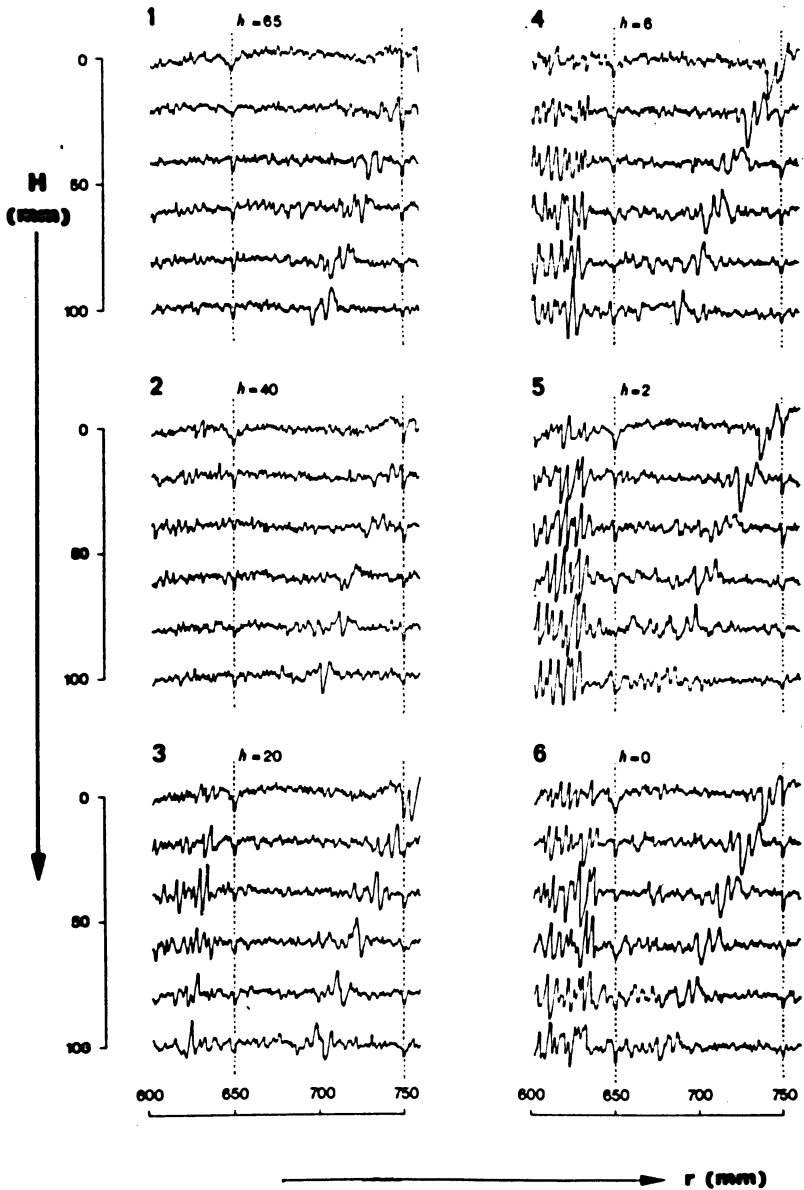


Fig. 5: Densitograms of elastic waves in the lower layer of a two-layer gel model $\alpha_1 > \alpha_2$. Densitograms were measured in the direction parallel to the velocity boundary, always at six depths H below the boundary. Measurements were carried out for 6 different distances h of the source from the boundary. r epical distance. Dashed lines denote the position of distance lines. The first wave from the right is P_{12} -wave, after it (on the left) pseudospherical P_{12} -wave comes.

under visual observation.) The intensity of P_{12} -waves changes only little in dependence on h . The strong decrease of the amplitudes of pseudospherical waves was experimentally verified on other numerous models and always qualitatively proved. The decrease of \bar{P}_{12} -waves, however, was not the same in all the cases—there are many factors which affect it (among them also certain experimental factors). Weaker attenuation of \bar{P}_{12} -wave with increasing distance h of the source from the boundary can be well seen in Fig. 6; this diagram was also constructed on the basis of densitometric amplitude measurements of \bar{P}_{12} -waves when different values of h were chosen.

When we are looking at schlieren frames an interesting analogy is evident: The geometry of wave fronts of P_{12} - and \bar{P}_{12} -waves in the lower medium resembles wave fronts of a reflected and a head wave (the straight wave front of a P_{12} -wave resembles a head wave and the circular wave front of a \bar{P}_{12} -wave resembles a reflected wave). In our case the head wave cannot exist due to the velocity conditions and the position of the source. If, however, the source should lay in the lower medium a similar arrangement of wave fronts (in accordance with the above mentioned analogy) would result. Thus, when the source passes through the boundary from a medium of lower velocity into a medium of higher velocity, the reflected wave (corresponding to the ray conception) changes into an irregular one which attenuates quickly with increasing distance of the source from the boundary. On the contrary, the head wave (which does not exist in the zeroth approximation of the ray theory) changes continuously into a regular refracted wave, corresponding to the ray conception, when the source crosses the boundary.

The results of measurements show very good agreement with theoretical conclusions specified above: Two waves with quite different properties would propagate

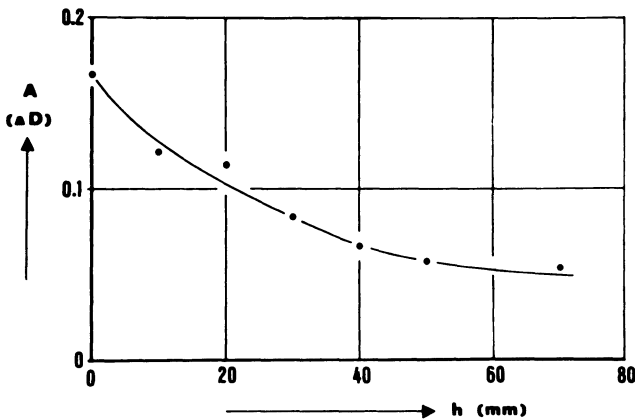


Fig. 6: Amplitudes of pseudospherical wave versus h . A amplitude in degrees of optical density D , h distance of the source from the velocity boundary.

in the lower medium. The P_{12} -wave may clearly be identified as a refracted wave which corresponds to the ray conception. No ray explanation has been found for the \bar{P}_{12} -wave existing only at smaller distance from the boundary. It appears, however, that its most typical properties fully correspond to the properties of a pseudospherical wave.

4. Conclusions

Results of laboratory measurements presented above proved quite clearly the existence of pseudospherical waves and also their importance in certain cases.

These results indicate that there are also numerous situations in seismology when these waves can be observed on the Earth's surface. For instance, when the source is located under the M -discontinuity or under another 1st order discontinuity (not far from it) the direct wave could be followed by the pseudospherical wave. However, it is necessary to be careful not to confuse this wave with a reflected wave, and a regular refracted wave with a head wave.

In this paper only compressional waves are discussed as the schlieren-method does not allow to investigate shear waves. In reality, on the other hand, also shear pseudospherical waves should exist [ČERVENÝ 1956].

It is also evident that the pseudospherical waves propagate in low velocity layers if the seismic sources is located not far from the channel. In such a case these waves can play an important role in the study of low velocity channels.

Pseudospherical waves and their properties are analysed in greater detail by ČERVENÝ et al. [1972] where also their significance in seismology is discussed.

References

- BREKHOVSKIKH, L. M.: *Waves in Layered Media*. Academic Press, New York, 1960
- ČERVENÝ, V.: *The Reflection of Spherical Elastic Waves at a Plane Boundary*. Travaux Inst. Géophys. Acad. Tchécosl. Sci., No 44. Geofysikální sborník 1956, NČSAV, Prague, 343–366, 1957
- ČERVENÝ, V., J. KOZÁK, and I. PŠENČÍK: *Refraction of Elastic Waves into a Medium of Lower Velocity – Pseudospherical Waves*. Pure and Appl. Geophys. 92, 115–132, 1972
- KOZÁK, J.: *Kinematic and Dynamic Parameters of Elastic Waves Investigated on Seismic Models by Means of the Schlieren Method*. Travaux Inst. Géophys. Acad. Tchécosl. Sci., No 354. Geofysikální sborník 1971, Academia, Praha (in press)
- OTT, H.: *Reflexion und Brechung von Kugelwellen; Effekte 2. Ordnung*. Ann. d. Phys. 41, 443–466, 1942

Model Investigations on Low Velocity Layers

J. BEHRENS, Clausthal¹⁾ and J. SIEBELS, Wolfsburg²⁾

Eingegangen am 12. Februar 1972

Summary: In the present paper the results of travel-time and amplitude investigations on low velocity layers are described. The investigated channel-structures are characterized by different velocity-depth distributions. The comparison of the amplitude-distance curves one with another and with the amplitudes, obtained from a discontinuity of first order, shows that an identification of the true structure of the intermediate low velocity layers may only be possible, if the velocity-depth distribution is unsymmetrical and the contrast between the *P*-wave velocities of the channel and the medium below the channel is high.

Zusammenfassung: In der vorliegenden Arbeit werden die Resultate von Laufzeit- und Amplitudenuntersuchungen an Kanälen niedriger Geschwindigkeit beschrieben. Die untersuchten Kanalstrukturen besitzen unterschiedliche Geschwindigkeitstiefenverteilungen. Ein Vergleich der an den Kanalmodellen gewonnenen Amplitudenentfernungskurven untereinander und mit den an einer Diskontinuität erster Ordnung gemessenen Amplituden zeigt, daß nur bei unsymmetrischer Geschwindigkeitstiefenverteilung und hohem Kontrast zwischen der *P*-Wellengeschwindigkeit im Kanal und in der darunterliegenden Schicht eine Charakterisierung der wahren Kanalstruktur möglich sein kann.

1. Introduction

In the last time the existence of low velocity layers in the Earth's crust and upper mantle has been concluded from the results of seismological observations by many authors.

Basing on the models of low velocity channels or wave guides in the Earth's crust and upper mantle derived from seismological data, a series of model investigation has been carried out recently [KAPCAN, KISLOVSKAJA 1966; SHAMINA 1966]. One of the aims of these two- and three-dimensional model experiments was to verify the velocity-depth distributions presumed in the nature and to select the most probable channel structures with first approximation.

The propagation of elastic waves inside and in the vicinity of low velocity layers has been studied by means of another group of model experiments [CHOWDHURY, DEHLINGER 1963; KHOROSHEVA 1962]. These measurements—using the *S*-wave parameters additionally—aimed at investigating the energy distribution of the direct and reflected waves in dependence of focus depths. The propagation of the

¹⁾ Prof. Dr. JÖRN BEHRENS, Institut für Geophysik der Technischen Universität Clausthal, 3392 Clausthal-Zellerfeld, Adolf-Römer-Straße 2 A, BRD.

²⁾ Dipl. Geophys. JOHANN SIEBELS, Volkswagenwerk AG, 318 Wolfsburg, Heinrich-Nordhoffstraße, BRD; früher: Institut für Geophysik der Technischen Universität Clausthal.

channel-wave has been also studied in detail by frequency measurements [KHOROSHEVA 1962].

By means of the model investigations on two- and three-dimensional "testmodels" [BEHRENS, DRESEN, WANIEK 1971 a, b], travel-time and amplitude measurements on a simple low velocity channel could be presented.

In order to enlarge the knowledge of the wave propagation on low velocity layers and to test the possibilities of identification, the velocity-depth distribution of intermediate low velocity layers recommendations were made at the General Assembly of the "European Seismological Commission" in Luxembourg 1970 to carry out further detailed model experiments on low velocity channels. The kinematic and dynamic parameters of reflected and refracted *P*- and *S*-waves should be studied on different types of low velocity layers and compared with the parameters of seismic signals from a discontinuity of first order.

Moreover the wavefield inside the low velocity layer and in the vicinity of it should be studied by means of the schlieren-method and two-dimensional model experiments.

This paper deals with the first results of investigations on simple two-dimensional models of different types of low velocity channels. Special attention was given to the travel-time curves and amplitude-distance curves of reflected and refracted *P*-waves with respect to a comparison of the investigated different channel structures. The results of the *S*-wave studies and the frequency measurements will be published later.

2. Investigated models

Figure 1 shows the designations, the dimensions, the mechanical structure and the velocity-depth distribution of the investigated models. N is the ratio of the wave velocities for the respective interface.

All models except the last one (*S4*) are characterized by an overlying layer of Plexiglas with a thickness h_1 of 30 cm (*P*-wave velocity: 2.32 mm/ μ s), a channel of various velocity-depth distribution with a thickness h_2 of 10 cm realized particularly by a combination of Plexiglas and PVC (*P*-wave velocity: 1.85 mm/ μ s), and a half space h_3 with a thickness of 100 cm of Plexiglas or Aluminium (*P*-wave velocity: 5.4 mm/ μ s). The thickness of the plates D was 3 mm. The predominant wave-length λ_1 of the incident wave was generally about 4 cm, the ratio h_2 (thickness of the channel) thereof to λ_1 (wave-length of the incident wave) results to about 2.5 to 3.

The first model *CHS* is a model with a symmetrical low velocity channel¹⁾. In the used code *CHS* the channel is marked by *CH*, the symmetrical velocity-depth distribution by the letter *S*.

¹⁾ The model *CHS* corresponds in its structural and acoustical properties with the testmodel TM - 5 (2d) [BEHRENS, DRESEN, WANIEK 1971 b].

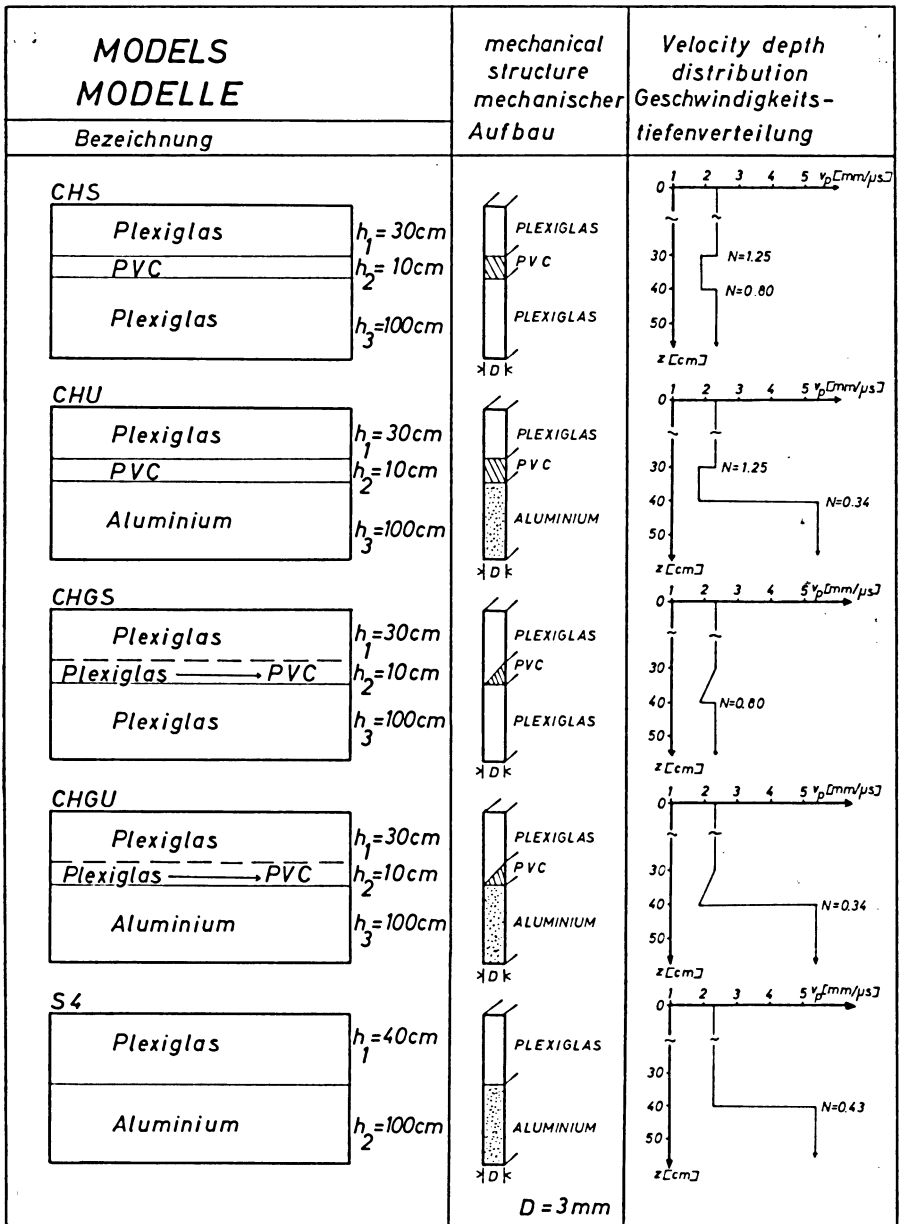


Fig. 1: Investigated models.

The model *CHU* is characterized by an unsymmetrical (*U*) low velocity channel (*CH*) with a high contrast between the *P*- and *S*-wave velocities of the channel and the medium below the channel.

The model *CHGS* represents a channel (*CH*) of a constant negative velocity gradient (*G*), symmetrically (*S*) embedded in two homogeneous media with the same acoustical properties.

The model *CHGU* is called a model of an unsymmetrical (*U*) channel (*CH*) of a constant negative velocity gradient (*G*) and a high velocity contrast to the medium below the intermediate layer. The velocity-depth distribution of the gradient layers of the models *CHGS* and *CHGU* has been controlled by several crossing profiles.

The model *S4* is the reference model of a straight (*S*) interface of first order. The thickness (40 cm) of the upper layer of Plexiglas results from the combined thicknesses of the channel and the overlying layer.

2.1 Procedure of measurements

Fig. 2 illustrates the procedure of measurements and the designation of the observed onsets.

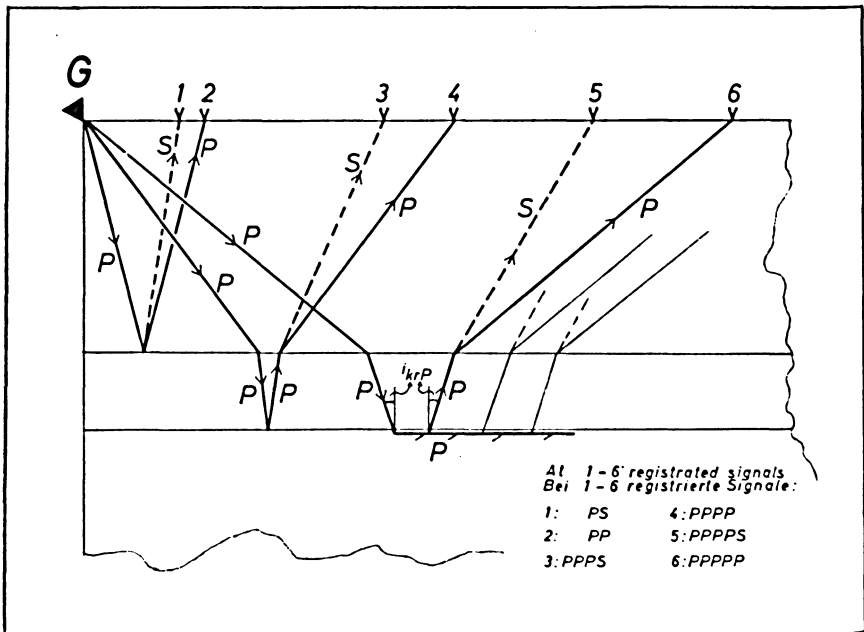


Fig. 2: Scheme of a low velocity layer and the examples of six types of signals and their designation according to their travel paths

G = source.

The elastic waves were generated by a piezoelectric source (G) at the surface of the two-dimensional models. The receiver was moved along the surface of the models in steps of 1 or 2 cm. Both, the vertical and the horizontal components of the acceleration amplitude were observed.

In Fig. 2 there are shown as an example six types of signals and their designation according to their travelpaths within the model—the reflected PS - and PP -waves (1 and 2) from the upper side of the low velocity layer, the $PPPP$ - and $PPPS$ -waves (3 and 4) from the lower boundary of the channel and in the case of an unsymmetrical channel structure the head-waves $PPPPS$ and $PPPPP$ (5 and 6).

The wave propagation within a gradient layer is marked by a crossline (\bar{P}).

3. Results

3.1 Homogeneous low velocity layers (models CHS and CHU)

3.1.1 Travel-time curves

The computed travel-time curves for the models of the symmetrical and unsymmetrical channel are shown in Fig. 3. All possible travel-time curves between the curves of the P -wave and SS -wave are listed up. The curves of the reflected waves are valid for both models—symmetrical and unsymmetrical channel—the curves of the head-waves of course only for the models of an unsymmetrical channel. For these models the vertical distances are marked by circles on the travel-time curves.

The course of the travel-time curves of the P -wave, of the reflected PP -wave and PS -wave from the upper side of the channel and of the $PPPP$ -wave from the lower boundary of the low velocity layer as well as of the $PPPPP$ -head-wave has been confirmed by measurements.

In case of an unsymmetrical velocity-depth distribution (model CHU) the superposition of several travel-time curves produces a confused picture of the travel-time graph. Therefore difficulties in the interpretation of P - and $PPPP$ -waves amplitudes must be expected at the interference zone of Rayleigh-wave, PS - and S -wave and at larger profile distances, even when the amplitudes of the disturbing waves are weak.

3.1.2 Amplitude-distance curves (models CHS and CHU)

The amplitude-distance curves of the vertical component of the reflected P -waves from the upper and lower boundary of the symmetrical (CHS) and unsymmetrical (CHU) low velocity channel are shown in Fig. 4.

The amplitudes taken from the seismograms are adjusted with respect to the preamplification of the apparatus and the directivity pattern of the source. All amplitude-distance curves published in this paper are not smoothed. The values of amplitudes of all figures are quantitatively comparable.

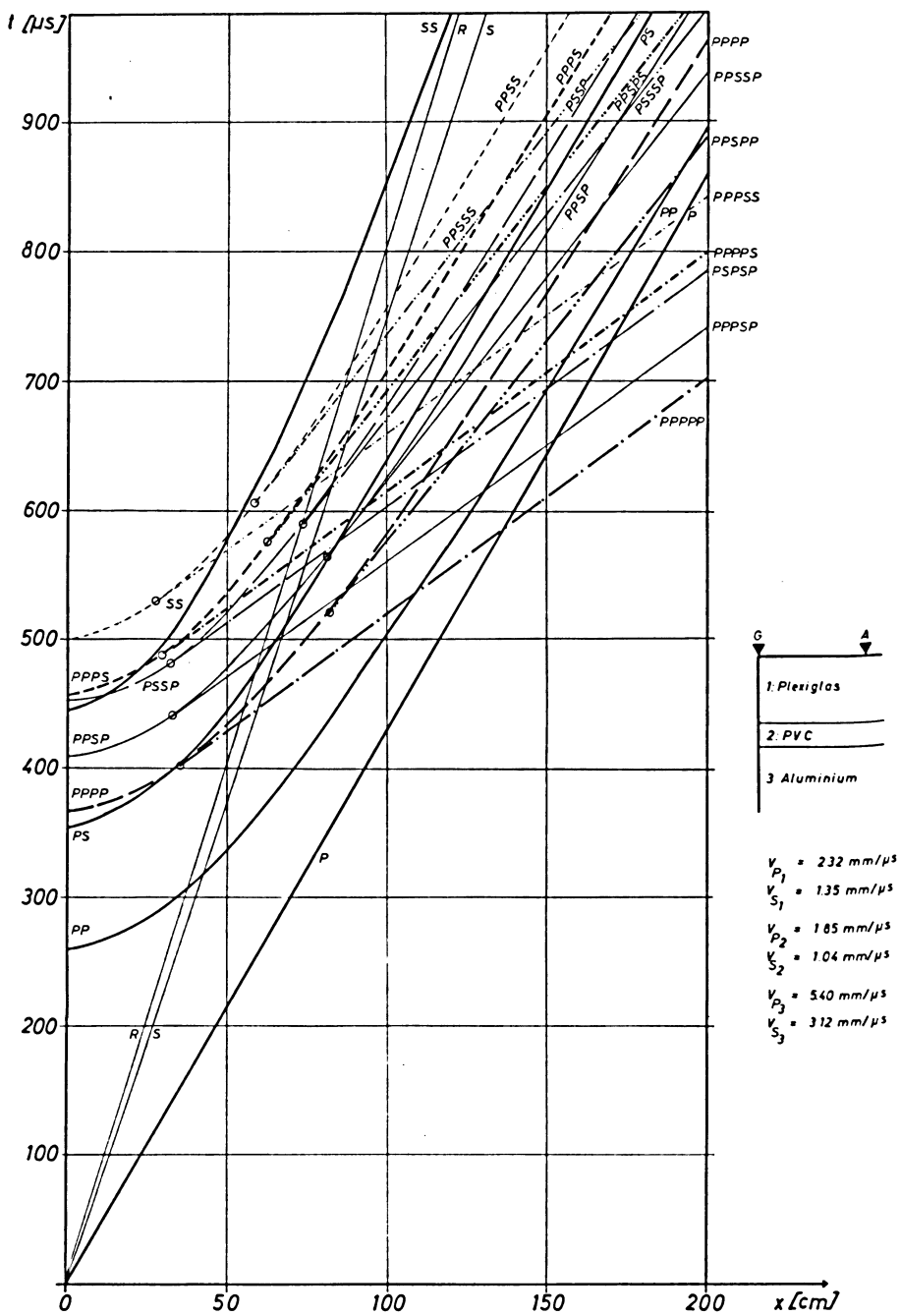


Fig. 3: Computed travel-time curves (models CHS and CHU).

AMPLITUDENENTFERNUNGSKURVEN
AMPLITUDE DISTANCE CURVES

Modelle: CHS: symmetrischer Kanal
Models: niedriger Geschwindigkeit
symmetrical low velocity channel

CHU: unsymmetrischer Kanal
niedriger Geschwindigkeit
unsymmetrical low velocity channel

(Vertikalkomponente)
(vertical component)

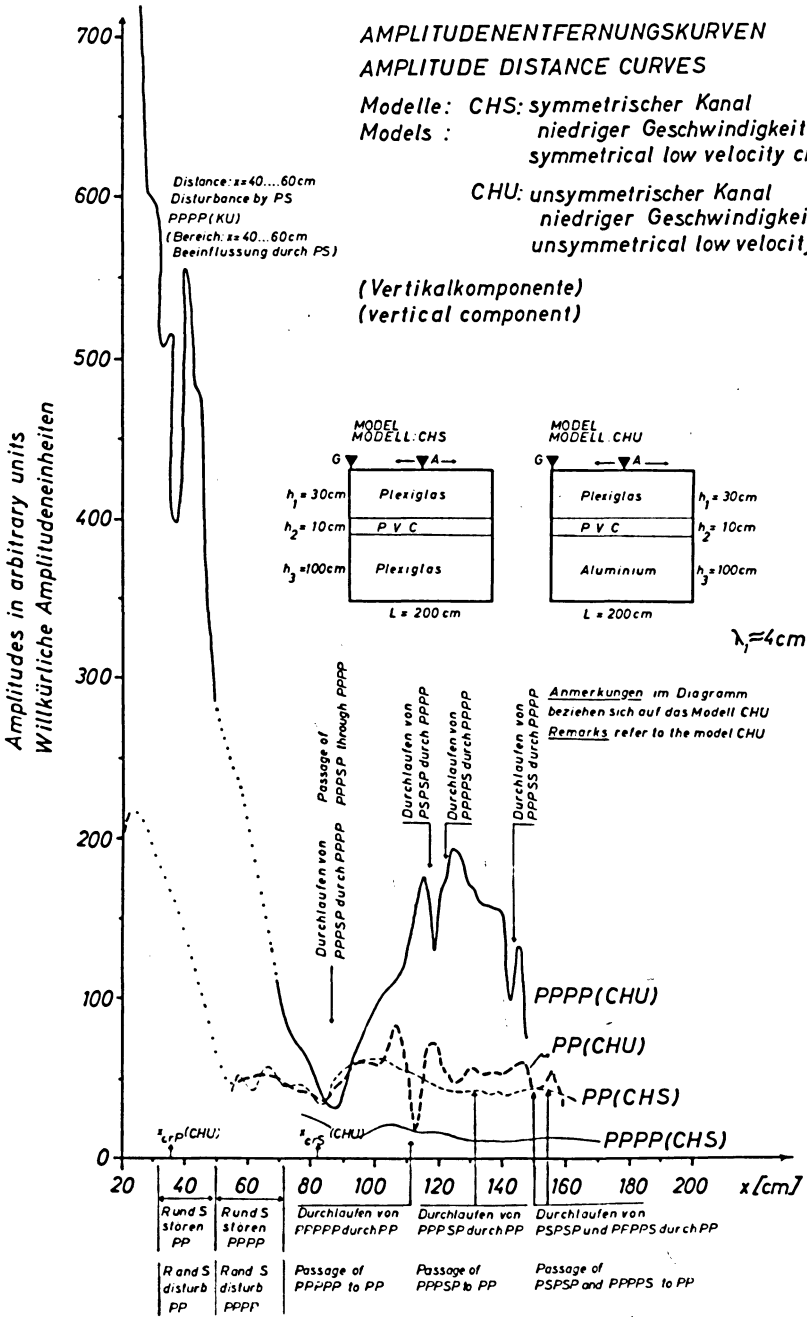


Fig. 4: Amplitude-distance curves, vertical component (models CHS and CHU).

The amplitude-distance curves of the *PP*-reflections from the upper boundary of both channels (*CHS* and *CHU*) have, of course, the same shape—except for some disturbances of the amplitude-distance curve of the model *CHU*, effected by the passage of head-waves as described above. The undulations of the amplitude-distance curve of the *PP*-reflections from the upper side of the channel (which are not caused by passing head-waves) are very typical. They were observed independently at 2- and 3-dimensional models [BEHRENS, DRESEN, WANIEK 1971 b; KOZÁK, WANIEK 1970].

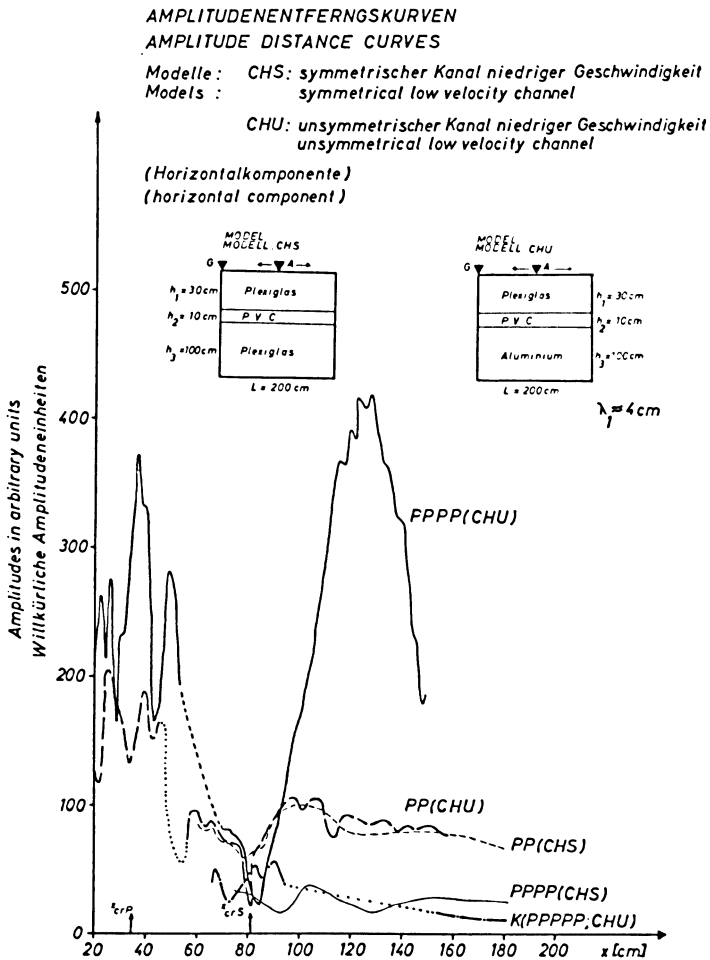


Fig. 5: Amplitude-distance curves, horizontal component (models *CHS* and *CHU*).

The amplitudes of the *PPPP*-reflection from the lower boundary of the symmetrical channel *CHS* are two or three times smaller than those from the upper side of the low-velocity layer.

The amplitude-distance curve of the *PPPP*-reflections from the lower boundary of the unsymmetrical channel *CHU* shows the wellknown course of an amplitude-distance curve of a first order discontinuity *without* a channel [BEHRENS, DRESEN, HINZ 1969; BEHRENS 1971]. The curve contains a first critical maximum near the critical distance x_{cr_p} (*CHU*) and—because of the chosen high velocity contrast between PVC and Aluminium—a strong second critical maximum, too.

Fig. 5 shows the amplitude distance curves of the horizontal component of the reflected *P*-waves for the models *CHS* and *CHU* and of the *PPPP*-head-wave *K* for the model *CHU*.

3.1.3 Amplitude-distance curves (models *CHU* and *S4*)

The similarity of the amplitude curves of the models of an unsymmetrical channel *CHU* and the model of a discontinuity of first order *S4* becomes obvious in Fig. 6. Here the model *CHU* (solid lines) and the model *S4* (dashed lines) are compared. The amplitudes of the subcritical reflected waves of the model *S4* are larger, the first critical maximum is stronger—both effects in this case are possibly caused by the disturbing *PS*-wave. The amplitude decrease behind the first critical maximum is the same for both models.

The second critical maxima are nearly of the same amount. Therefore the effect of the low velocity channel on the amplitude curves can only be noticed by the spreading of the second maximum region. This result is confirmed by the observations of the horizontal component (Fig. 7).

At greater distances ($x > 100$ cm) the amplitudes of the head-wave *K* (*PPPPP*) of the model *CHU* with the unsymmetrical low velocity channel is larger than those of the head-wave *K* of the model *S4*. This is true for the vertical component (Fig. 6). A comparison of the horizontal components (Fig. 7) is possible only up to $x = 100$ cm.

3.2 Low velocity layer with a negative velocity gradient (models *CHGS* and *CHGU*)

For the models *CHGS* and *CHGU* the homogeneous low velocity channel was replaced by a layer of a negative velocity gradient. The properties of this layer are presented in Fig. 1.

3.2.1 Travel-time curves

The computed travel-time curves of the direct *P*-wave, the reflected *PP*- and *PS*-waves from the upper side of the intermediate layer, the reflected *PP̄PP*-wave from the bottom of the layer and—in case of the unsymmetrical velocity-depth distribution—the *PP̄PP̄P*- and the *PP̄S̄PP̄P*-head-waves are shown in Fig. 8. The computed travel-time curves have been confirmed by time measurements (solid points). The open points indicate the critical distances. On the right side of Fig. 8 there are shown the velocity-depth distributions of the two models *CHGS* and *CHGU*.

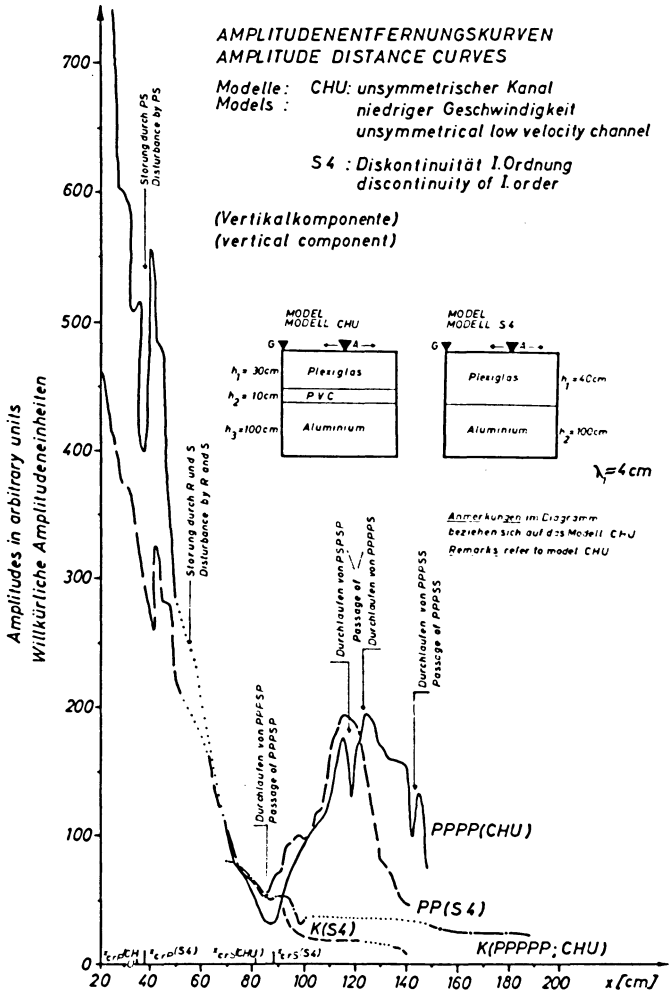


Fig. 6: Amplitude-distance curves, vertical component (models CHU and S4).

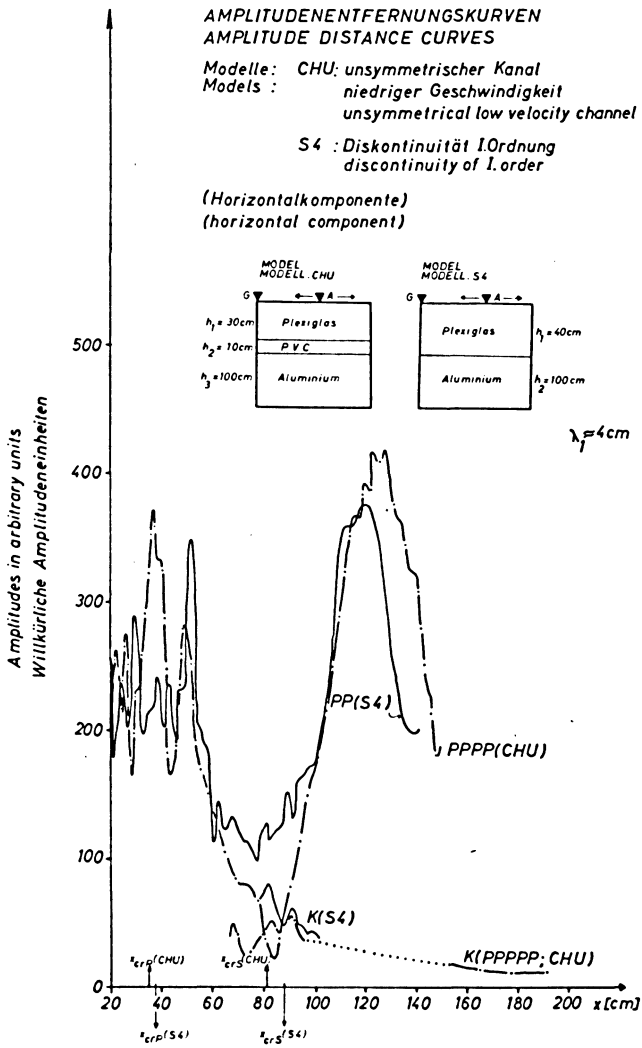


Fig. 7: Amplitude-distance curves, horizontal component (models CHU and S4).

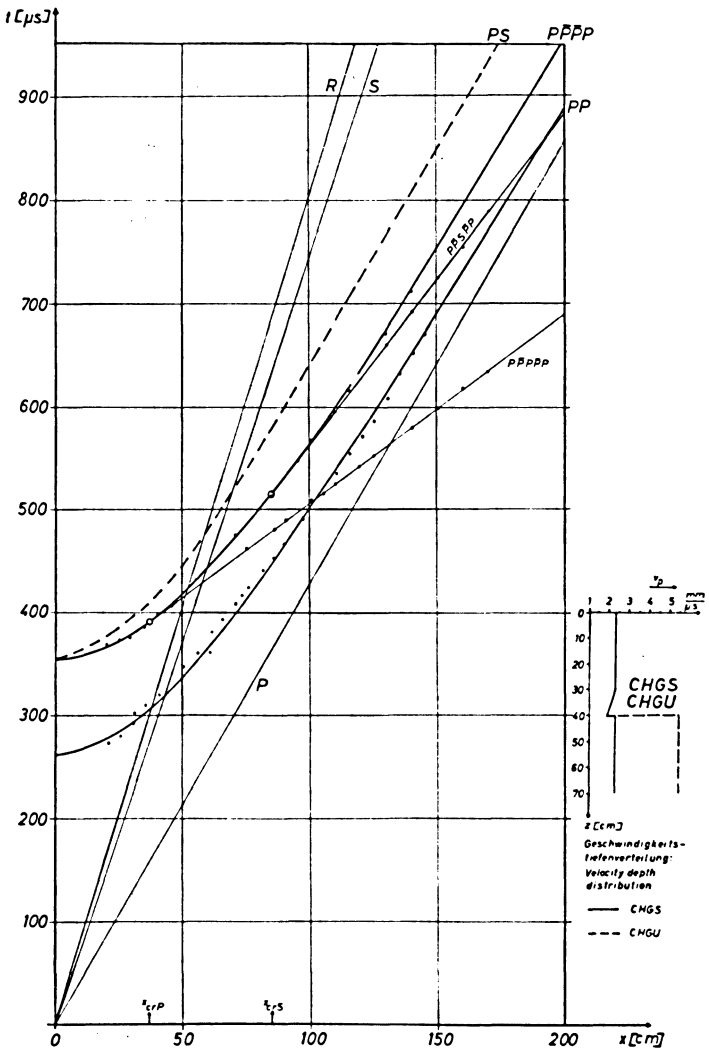
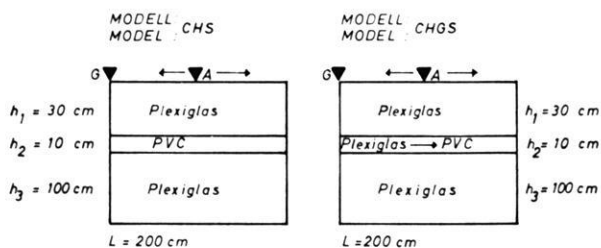
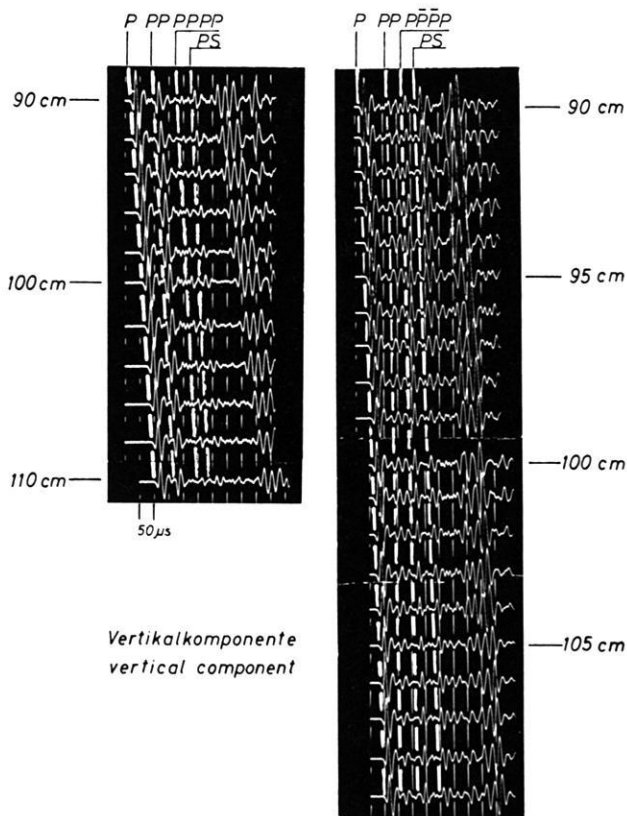


Fig. 8: Computed travel-time curves (models CHGS and CHGU).

Fig. 9: Seismogram-sections, vertical component (models CHS and CHGS). ▶



CHS : symmetrischer Kanal niedriger Geschwindigkeit
symmetrical low velocity channel

CHGS : symmetrischer Kanal mit negativem
Geschwindigkeitsgradienten
symmetrical channel with negative
velocity gradient

3.2.2 Seismograms

The influence of the negative velocity gradient (model *CHGS*), instead of a low velocity channel, on the seismograms of a model with a symmetrical velocity depth distribution (model *CHS*) is not very impressive (Fig. 9). The seismograms enclose the observations of the vertical component of the *P*-, *PP*-, *PPPP*- and *PS*-waves at distances from 90 cm to 110 cm. The amplitudes are quantitatively comparable.

On the left there are the seismograms of the symmetrical low velocity channel (*CHS*), on the right the seismograms of the gradient layer (*CHGS*).

At the shown distances the amplitude of the *PP*-reflection from the upper side of a homogeneous low velocity channel is larger than from the intermediate gradient layer. The *PPPP*-reflection from the lower boundary of a channel is smaller than from the lower boundary of the gradient layer. The *PS*-reflection from the top of the channel (model *CHS*) is somewhat smaller than of the model *CHGS*.

3.2.3 Amplitude-distance curves (models *CHS* and *CHGS*)

The shown amplitude proportions however are not valid for the whole profil. Fig. 10 shows the comparison of the amplitude-distance curves of the models *CHS* and *CHGS*. The amplitudes of the *PP*-reflection from the upper boundary and the *PPPP*-reflection from the lower boundary of the gradient layer are of the same amount in the vicinity of the shotpoint.

The curves are not smoothed over, the disturbances are generated by interference with the *PS*-, *R*- and *S*-waves.

At greater distances we observe nearly the amplitude ratio shown in the seismograms before (Fig. 9). From the form of the amplitude-distance curves however for a symmetrical velocity-depth distribution no indubitable conclusions can be drawn with regard to the existence of a negative velocity gradient instead of a low velocity channel.

3.2.4 Amplitude-distance curves (models *CHU* and *CHGU*)

For an unsymmetrical velocity-depth distribution (Fig. 11) the influence of the negative velocity gradient (model *CHGU*) on the form of the amplitude-distance curve can be seen a little better. Besides the different amplitudes near the shotpoint and the unlike form of the first critical maximum—effected mainly by the interference with the *PS*-wave—the only clear difference between the amplitude-distance curves of these two types of an unsymmetrical channel is the amount of the second critical maximum.

The amplitudes of the head-waves are equivalent at greater distances.

3.2.5 Amplitude-distance curves (models *CHGU* and *S4*)

The comparison of the unsymmetrical negative gradient layer (model *CHGU*) with the first order discontinuity (model *S4*) is shown in Fig. 12. The absolute

AMPLITUDENENTFERNUNGSKURVEN
 AMPLITUDE DISTANCE CURVES

Modelle: CHS: symmetrischer Kanal niedriger
 Geschwindigkeit
 Models: symmetrical low velocity channel

CHGS: symmetrischer Kanal mit negativem
 Geschwindigkeitsgradienten
 symmetrical channel with negative
 velocity gradient

(Vertikalkomponente)
 (vertical component)

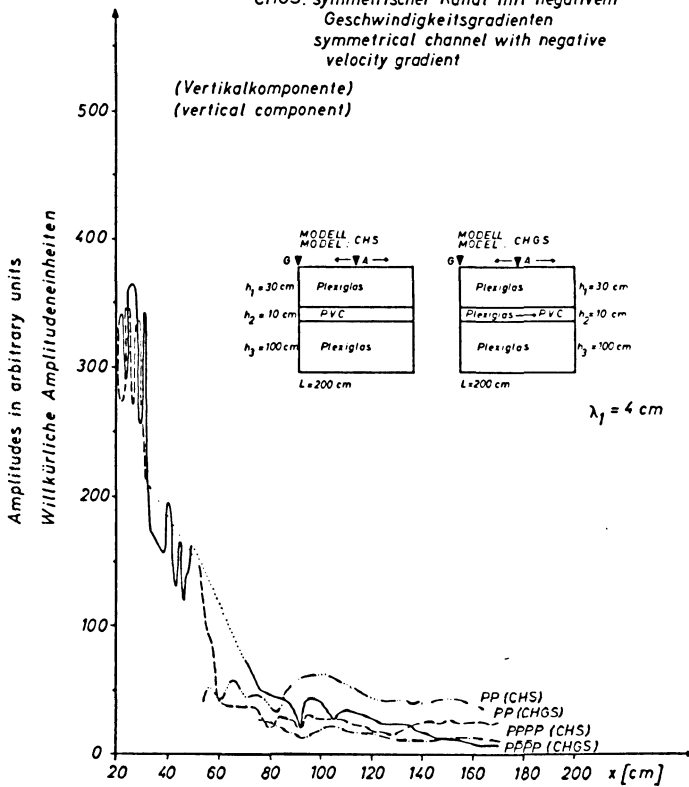


Fig. 10: Amplitude-distance curves, vertical component (models CHS and CHGS).

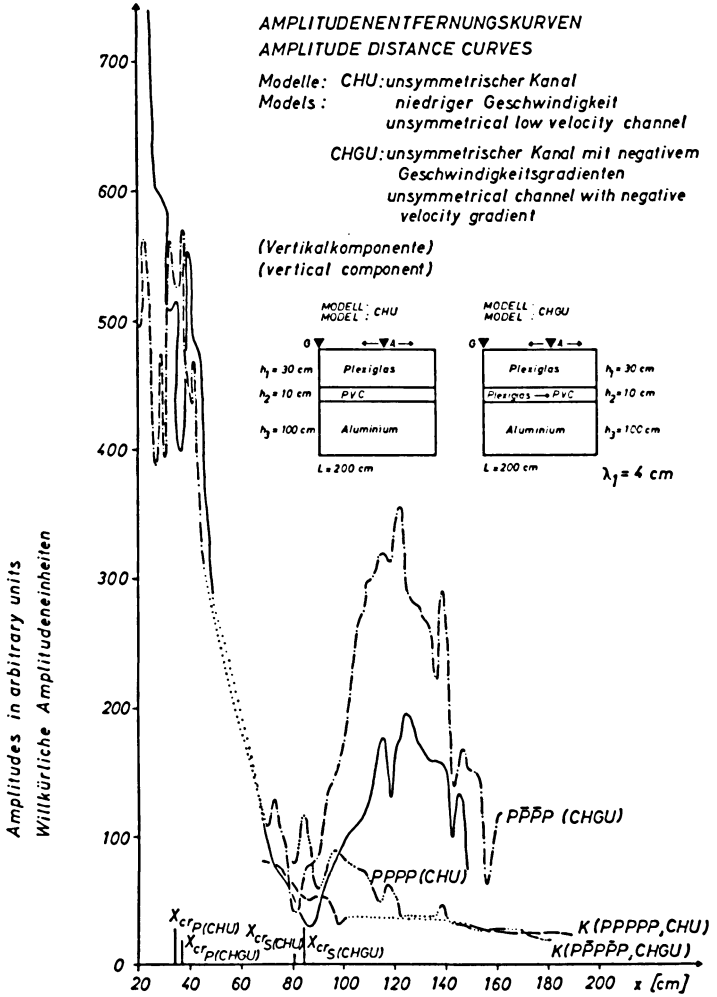


Fig. 11: Amplitude-distance curves, vertical component (models CHU and CHGU).

AMPLITUDENENTFERNUNGSKURVEN
 AMPLITUDE DISTANCE CURVES

Modelle : CHGU : unsymmetrischer Kanal mit negativem
 Geschwindigkeitsgradienten
 Models : unsymmetrical channel with negative
 velocity gradient

S4 : Diskontinuität 1. Ordnung
 discontinuity of 1 order

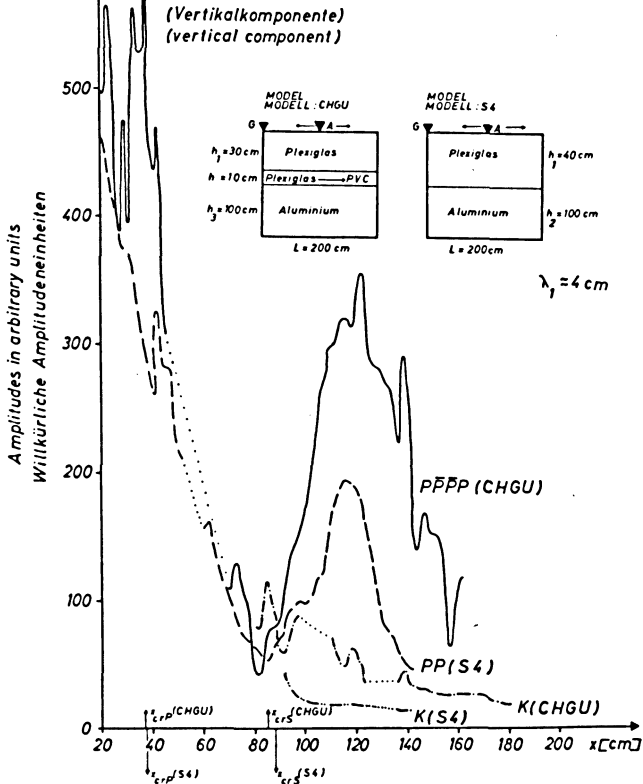


Fig. 12: Amplitude-distance curves, vertical component (models CHGU and S4).

AMPLITUDENENTFERNUNGSKURVEN
 AMPLITUDE DISTANCE CURVES

Modelle : CHGU: unsymmetrischer Kanal mit negativem
 Models : Geschwindigkeitsgradienten
 unsymmetrical channel with negative
 velocity gradient

S4 : Diskontinuität 1. Ordnung
 discontinuity of 1. order

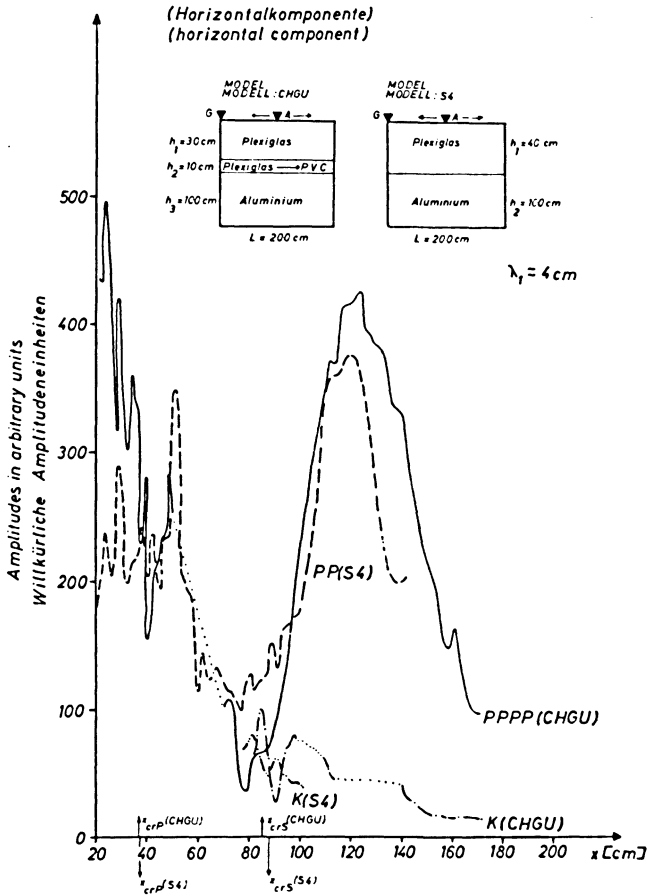


Fig. 13: Amplitude-distance curves, horizontal component (models CHGU and S4).

amplitude values of the vertical component of the subcritical reflection are not very different, but the shape and the amount of the first and second critical maxima of the considered models are quite different.

As indicated in 3.1 (Fig. 6), the second critical maximums of the models *CHU* (unsymmetrical low velocity channel) and *S4* (first order discontinuity) are of the same amount. The strong second maximum of the model *CHGU* (Fig. 12) therefore represents a characteristic property of an intermediate layer of this kind of velocity-depth distribution.

The amplitudes of the head-wave of the model *CHGU* are larger at all distances than of the model of the interface of first order *S4*.

The large amplitude indicate that—as described in the papers of BEHRENS, SHAMINA and WANIEK [1972] and BEHRENS and GOMMLICH [1972]—this head-wave originates at a poorly defined interface.

It is interesting, that the difference of the maximum amplitudes in the region of the second critical maximum can be only observed by means of the *vertical* component. The amplitudes of the *horizontal* component in the second critical region are nearly equivalent for both models (Fig. 13).

4. Conclusions

In this paper some aspects of the interpretation of low velocity layers by means of two-dimensional models of different velocity-depth distribution are described. Comparing the amplitude-distance curves it could be pointed, that there exist only few possibilities to identify the presence of a low velocity channel—especially of a symmetrical low velocity layer.

Furthermore it could be shown that the identification of an intermediate layer of a *negative* velocity gradient is very difficult, too—even by amplitude measurements. The discrimination between a symmetrical low velocity layer and an intermediate layer of a *positive* velocity-depth distribution (transition layer) by means of amplitude investigations has a better chance [BEHRENS, DRESEN, WANIEK 1971 a].

With regard to obtaining more detailed possibilities to identify the real structure of presumed low velocity layers, the *S*-wave propagation on the concerned layers will have to be studied in future.

5. Acknowledgements

The results reported in this paper are part of the results of investigations sponsored generously by the “*Deutsche Forschungsgemeinschaft*” (German Research Association).

The authors are indebted to Prof. Dr.-Ing. O. ROSENBACH for the kind support of the investigations and to their colleagues A. MÜLLER, H. HEMSCHEMEIER and G. MÜLLER for the accurate fabrication of the models.

Literatur

- BEHRENS, J.: Model investigations on the boundary structure Earth's crust/mantle. Proc. 12th Assembly ESC, Luxembourg, 1971
- BEHRENS, J., L. DRESEN und E. HINZ: Modellseismische Untersuchungen der dynamischen Parameter von Kopfwelle und Reflexion im überkritischen Bereich. *Z. Geophys.* 35, 43–68, 1969
- BEHRENS, J., L. DRESEN und L. WANIEK: Modellseismische Untersuchungen an zwei- und drei-dimensionalen Testmodellen. Teil 1, *Studia geophys. et geod.* 15, 147–160, 1971 a
- : Investigation on two- and three-dimensional testmodels. Proc. 12th Assembly ESC, Luxembourg, 1971 b
- BEHRENS, J., and G. GOMMLICH: Model investigations with respect to the interpretation of complicated seismic discontinuities. *Z. Geophys.*, 38, 481–498, 1972
- BEHRENS, J., O. G. SHAMINA, and L. WANIEK: Interpretation of discontinuities by seismic modelling methods. *Z. Geophys.* 38, 579–593, 1972
- CHOWDHURY, D. K., and P. DEHLINGER: Elastic wave propagation along layers in two-dimensional models. *Bull. Seism. Soc. Am.* 53, 593–618, 1963
- KAPCAN, A. D., and V. V. KISLOVSKAJA: Investigation of a wave guide with weak boundaries in two-dimensional perforated models. *Studia geoph. et geod.* 10, 360–369, 1966
- KHOROSHEVA, V. V.: The study of a wave guide on a solid two-dimensional model with sharp boundaries. *Bull. (Izv.) Acad. Sci. USSR. Geophys. Ser.* 8, 657–661, 1962
- KOZÁK, J., und L. WANIEK: Schlierenoptische Untersuchungen an seismischen Gelmodellen mit photometrischer Auswertung des Wellenfeldes. *Z. Geophys.* 36, 175–192, 1970
- SHAMINA, O. G.: Experimental investigation of necessary and sufficient characteristics of a wave guide. *Studia geophys. et geod.* 10, 341–350, 1966
- SIEBELS, J.: Modellseismische Untersuchungen der kinematischen und dynamischen Parameter von Reflexion und Kopfwelle an einfachen Erdkrustenmodellen. Diplomarbeit. Technische Universität Clausthal, 1971

Model Studies of Wave Propagation in Low Velocity Layers with Sharp Boundaries

L. WANIEK, Prague¹⁾

Eingegangen am 22. Februar 1972

Summary: Simple gel and liquid models of low velocity layers ($v_1 = v_3 > v_2$, $v_3 > v_1 > v_2$) with sharp boundaries were investigated by means of the schlieren method using high speed camera recording system. The nearly complete space and time distribution of the P -wave field could be observed in detail. Two basic positions of the seismic exploding wire source were used – on the surface and in the middle of the low velocity layer. Kinematic and dynamic parameters of the main wave groups were derived from schlieren-photographs. In agreement to the results of former model studies typical oscillations in the amplitude distance curve of the P -wave reflected on the upper channel boundary could be proved. When the source was located in the middle of the low velocity layer the propagation of the channel wave could be investigated.

Zusammenfassung: Mit Hilfe einer schlierenoptischen Modellapparatur wurden einfache Gel- und Flüssigkeitsmodelle mit Kanälen niedrigerer Geschwindigkeit ($v_1 = v_3 > v_2$, $v_3 > v_1 > v_2$) mit scharfen Grenzflächen untersucht. Die Benutzung einer Hochgeschwindigkeitskamera erlaubte es, nahezu das gesamte P -Wellenfeld im Detail zu erfassen. Die Quelle, ein explodierender Draht, lag an der Oberfläche des Modells und in der Mitte des Kanales. Die kinematischen und dynamischen Parameter der wesentlichsten Wellengruppen wurden aus den Schlieraufnahmen abgeleitet. In Übereinstimmung mit den Resultaten früherer Modelluntersuchungen zeigten die gewonnenen Amplitudenentfernungskurven für die an der Kanaloberkante reflektierten P -Wellen auch hier typische Oszillationen. Bei der Anregung in der Kanalmitte konnte die Ausbreitung der Kanalwelle untersucht werden.

1. Introduction

Recently a great amount of work in seismology has been done to obtain the basic criteria to evidence low velocity channels. Therefore it is quite understandable that also seismic modelling methods have been used for attaining this goal. Some of the principal phenomena of wave propagation along the layers in question were treated by two-dimensional model technique [CHOROSHEVA 1962; KAPCAN, KISLOVSKAJA 1966]. Simple wave guide models with sharp and soft boundaries were studied. Owing to the importance of investigations along this line, two of the six test models recommended for detailed studies by the European Seismological Commission in 1967 deal with basic types of low velocity layers [BERCKHEMER, WANIEK 1967]. The first systematic studies proved e.g. the existence of typical oscillations in the shape of

¹⁾ Dr. LUDVÍK WANIEK, Geofyzikální ústav ČSAV, Praha 4—Spořilov, Boční II, ČSSR.

the amplitude-distance curves of reflected *P*-wave both on three-dimensional and on two-dimensional models.

An attempt from another direction was made by investigating three-dimensional models containing low velocity layers with more complex velocity-depth function. The results obtained by SHAMINA [1966, 1967] led to the formulation of necessary and sufficient conditions for the existence of a wave guide. Seismological data were successfully interpreted on the basis of model experiments. In particular the predicted minimum of amplitude-depth curves observed in the shadow zone confirmed the possibility of a low velocity channel in the region investigated [SHAMINA 1967].

All these efforts, however, do not as yet provide a complete picture of all the typical wave phenomena connected with low velocity layers. Therefore it seemed to be useful to continue systematic model studies of these layers. The object of the present paper is to complete our knowledge of wave propagation in low velocity layers with sharp boundaries by direct, visual observation of the *P*-wave field by means of the schlieren-method.

2. Model Technique and Data Processing

Most details of the modelling apparatus and schlieren data processing are described in [KOZÁK, WANIEK 1970]. High speed camera records were obtained using super sensitive Kodak 2475 emulsion. A series of 30 schlieren frames ($0.5 \mu\text{s}$ exposure time) with time distance of $4 \mu\text{s}$ represent the result of one experiment. Distance markers (100 mm) are exposed simultaneously to every frame for correct location of the observed wave groups.

The model of a homogeneous half space with an embedded homogeneous low velocity layer was constructed respecting all the parameters proposed for the test model No 5 [BEHRENS, DRESEN, WANIEK 1971]. Gels of the system water-glycerol-gelatine were used [WANIEK 1966]. The velocity-depth distribution for this model, denoted by TM_5 , is shown in Fig. 1a. By iM_j is denoted the gel substance, where i is the concentration of glycerol in water, j is the concentration of gelatine in the water-glycerol mixture ($85M_3 - v_p = 1.85 \text{ km/s}$, $5M_3 - v_p = 1.52 \text{ km/s}$). For the gel substance $85M_3$ the predominant frequency of *P*-waves generated by the exploding wire source is 0.3 Mc/s , which corresponds to the wave length of 6.2 mm [KOZÁK 1972]. All the other parameters can be interpreted from Fig. 1a.

The second model, M—K, enables to study a homogeneous low velocity layer between two homogeneous layers of different velocities. Two liquids over a mighty gel layer form the required velocity-depth function (Fig. 1b). Water ($v_p = 1.48 \text{ km/s}$), chlorine ($v_p = 0.94 \text{ km/s}$) and gel $80M_5$ ($v_p = 1.83 \text{ km/s}$) were used for the fabrication of this model. The observed predominant frequency of 0.24 Mc/s in water corresponds to the wave length of 6.2 mm in the upper layer [KOZÁK 1972]. Two variants differing only in the thickness of the low velocity layer were studied. In the first case a thin layer the thickness of which was comparable with the wave

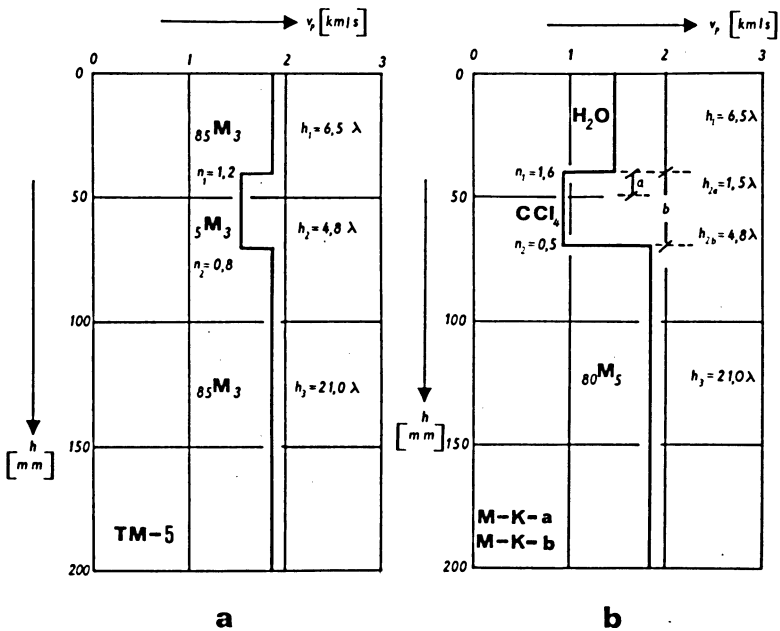


Fig. 1: Velocity-depth distribution of the investigated models. *a* test model TM-5, *b* models M-K-a and M-K-b. v_p *P*-wave velocity, h model depth, h_i thickness of the individual layers, λ wave length of the incident *P*-wave, n index of refraction.

length of the incident *P*-wave was treated (Model M-K-a). In the other case a mighty layer of about 5 wave lengths, comparable with the former model TM-5, was studied (Model M-K-b).

The used modelling device made it possible to study in detail the *P*-wave field in space and time. A high degree of the reproducibility of kinematic parameters was reached. It is impossible, however, to observe the wave field in a wide epicentral distance range by one experiment only. Therefore all model experiments which are necessary for covering the required distance range were linked up in time on the basis of the observed travel-time curve of the direct *P*-wave (Fig. 2). The time distance between individual frames is given by the high speed camera rotating mirror, the corresponding epicentral distance is evaluated directly from the obtained schlieren pictures.

For studying the dynamic properties of the observed waves microphotometric treatment of schlieren pictures can be used. However, all experimental conditions prescribed for the dynamic analysis of the observed schlieren pattern have to be respected [Kozák 1972]. It must be borne in mind that microphotometric profiles—so called densitograms—represent a spatial function of the elastic process at par-

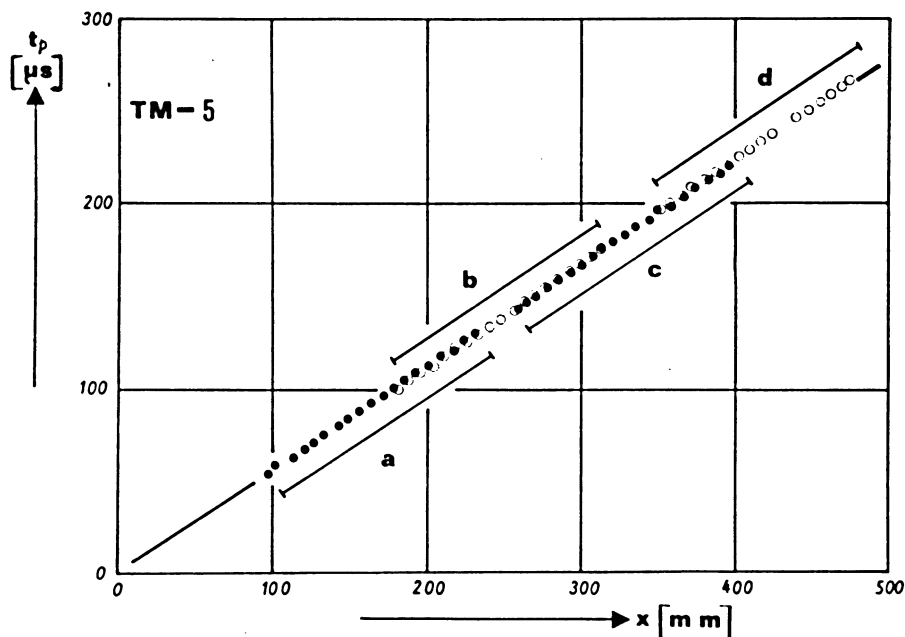


Fig. 2: Travel-time curve of the direct P -wave for the model TM-5. x epicentral distance, t_p travel time, a , b , c , d useful distance range of particular model experiments.

ticular moment contrary to seismograms (model oscillograms) that are a time function in a particular point of observation.

Dynamic parameters of P -waves presented in this paper were derived from densitograms fixing the maximum amplitude of the wave group in question. Due to the relatively high scatter of the optical density level of the undisturbed field in the different high speed camera frames, dynamic studies are possible only in relation to the direct P -wave.

The notation and meaning of all physical quantities as well as of different wave groups used in this paper is identical with KOZÁK, WANIEK [1970].

3. Results

3.1 Test Model TM-5

A number of model experiments were carried out to study the wave propagation for two of the basic positions of the seismic source, i.e. on the surface and in the middle of the low velocity layer. The wave field observed can be seen in Fig. 3, where selected schlieren frames show the quite different wave pattern in either case. A

narrow untransparent zone (black stripe) occurs along the boundary between individual layers. It is caused by the diffusion of media on the glass windows of the model cuvette in the course of the fabrication of the model.

The wave field generated by the source acting on the surface of the model (upper part of Fig. 3) is without any significant changes with increasing distance. Clear groups of reflected and refracted waves are propagating in the model. A more complex picture can be seen if seismic waves are generated from the middle of the low velocity layer (lower part of Fig. 3). Most part of seismic energy is transferred to the channel wave propagating with the velocity corresponding to this layer. The monotonous character of this wave in the schlieren pictures is caused probably by the insufficient resolution power of the high speed camera used, because strong multiple interference effects can be expected in this case. The *P*-waves refracted in the surrounding media have a simple wave pattern, not affected by the channel wave propagation. The only possible explanation is that they are generated only in the close vicinity of the source. In the schlieren frames also the forming process of head waves generated by the refracted waves is clearly visible. In the beginning they are coupled with the front of the channel wave, in greater distances the head waves are ahead of the channel wave and form a separate wave group.

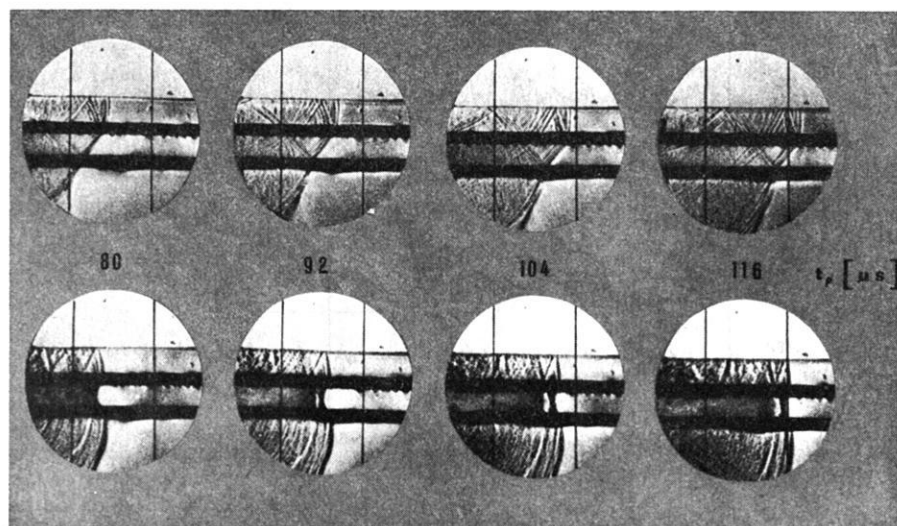


Fig. 3: Propagation of *P*-waves in the test model TM-5. The upper part corresponds to position of the source on the surface of the model, the lower part to the position of the source in the middle of the low velocity layer. t_p time scale derived from *P*-wave travel-time.

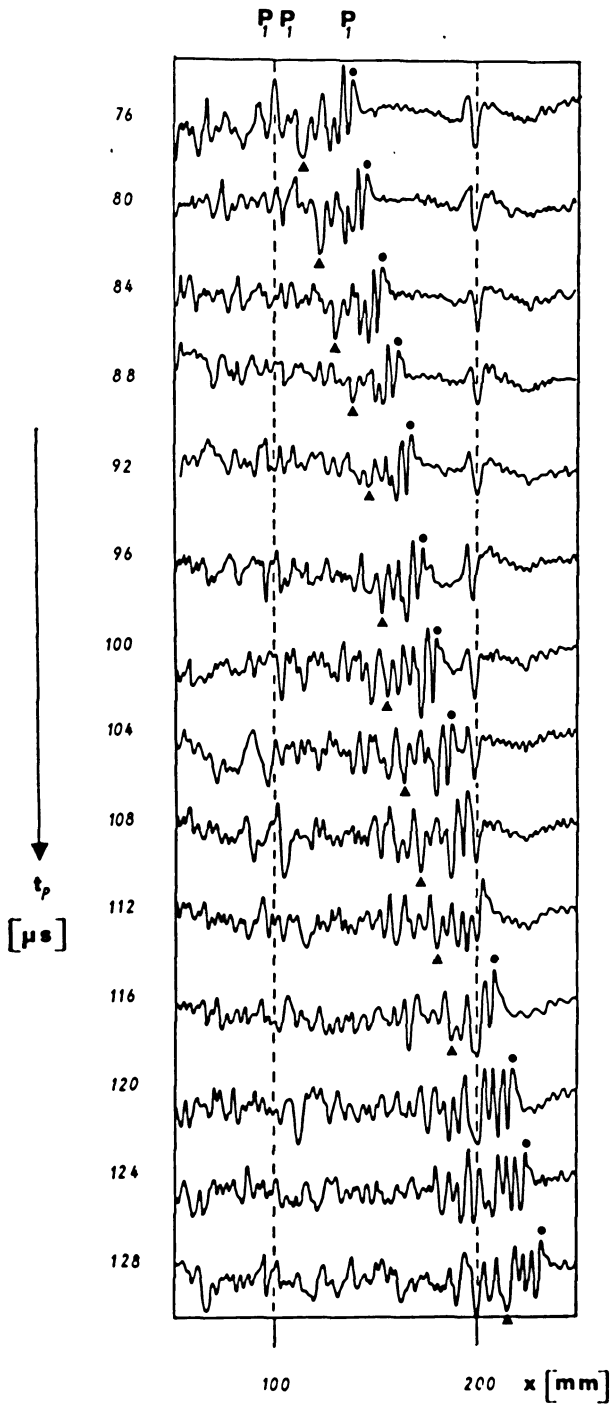


Fig. 4:
 Near surface densitograms
 of schlieren frames on test
 model TM-5. Source on the
 surface of the model. x
 epicentral distance, t_p travel
 time, P_1 direct P -wave, P_1P_1
 P -wave reflected on the upper
 boundary of the low velocity
 layer.

All observations were repeated several times in a wide distance range. In all results the above mentioned findings were confirmed.

With respect to former investigations of the dynamics of P -waves reflected on the low velocity layer boundaries when the source is located on the surface of the model [BEHRENS et al. 1972] an attempt was made to continue these investigations on the particular model. For this purpose microphotometric profiles of the corresponding schlieren pictures were made close under the surface. An example of these measurements is shown in Fig. 4, where the epicentral distance range covered by a particular model experiment (one high speed camera record) is treated. By analogous processing of model experiments from different distances it was possible to deduce the amplitudes of direct and reflected P -waves in the whole epicentral distance range. In this way only the reflection on the upper boundary of the low velocity channel can be studied; the wave reflected on the lower boundary arriving to the surface is in the photometric representation too weak for quantitative analysis.

In Fig. 5 the amplitude-distance curve of the P -wave reflected on the upper boundary of the low velocity channel is given. Neglecting the small attenuation in the model medium used and taking into account all the conditions mentioned in Chap. 2, the resulting amplitude can be expressed as

$$A^* = (A_{P_1}/\bar{A}_{P_1}) \cdot A_{P_1P_1},$$

where A_{P_1} and $A_{P_1P_1}$ are the measured amplitudes of the direct and reflected P -wave in individual frames, and \bar{A}_{P_1} is the mean value of the amplitudes of the direct P -wave. A clear oscillatory character of the curve investigated can be proved.

The first steps in dynamic analysis of the observed channel wave were carried out by microphotometric profiling along the wave guide axis (Fig. 6). The source energy is the same as in Fig. 4, the monotonous wave pattern of this wave denoted as P_2 , is

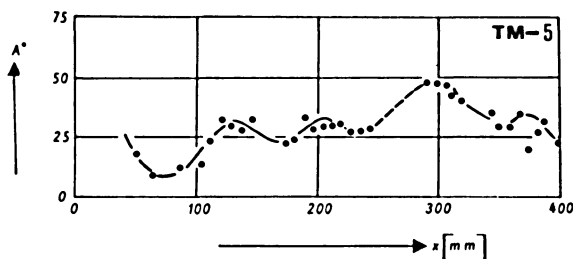


Fig. 5: Amplitude distance-curve of the P -wave reflected on the upper boundary of the low velocity layer derived from microphotometric data (test model TM-5). x epicentral distance, A^* normalized amplitude.

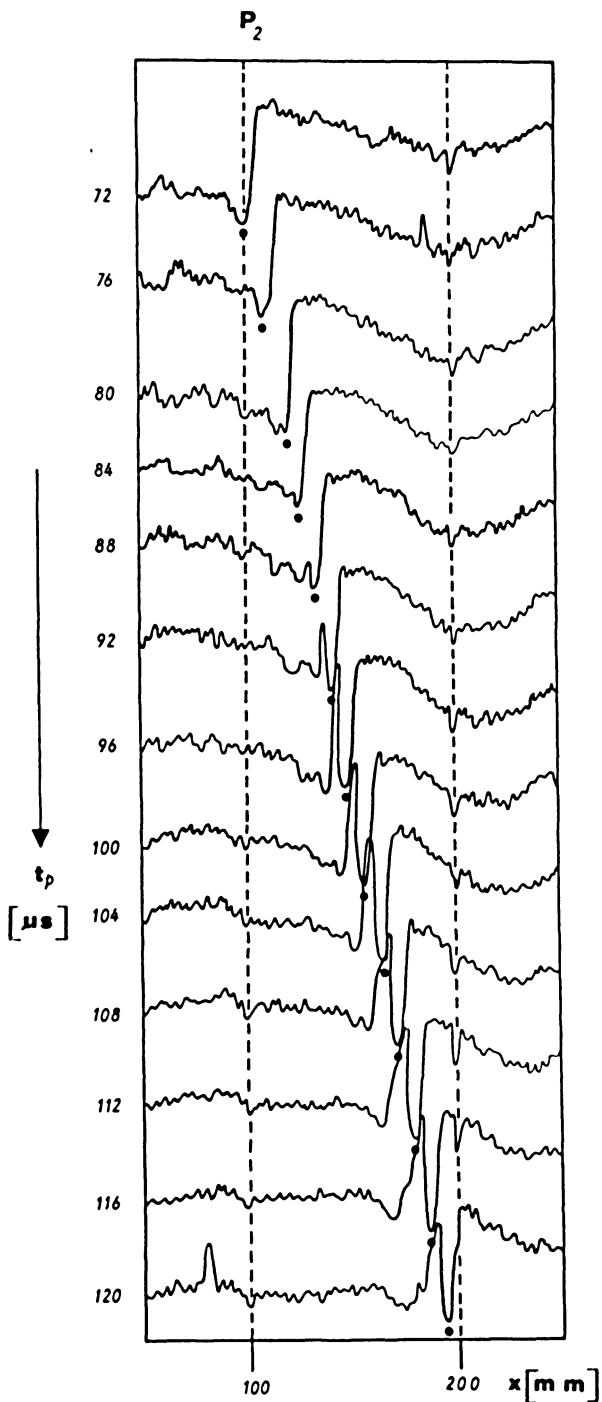


Fig. 6:
 Densitograms along the wave
 guide axis on test model
 TM-5. Source in the middle
 of the low velocity layer.
 x epicentral distance, t_p travel
 time, P_2 channel wave.

probably due as mentioned above by insufficient high speed camera parameters, which do not allow to see the complex interference field of multiple reflections forming this wave. This, however, cannot distort the energy level of this wave in comparison with all other propagating wave groups. Attention should be paid also to the wave group composed of head waves the parameters of which can be interpreted from the densitograms.

3.2 Models $M-K-a$ and $M-K-b$

The nonsymmetric wave guide model was treated in an analogous way as the previous one. The influence of the low velocity layer thickness on the wave field if source is located on the surface is shown in Fig. 7. In the upper part the narrow wave guide ($9 \text{ mm} = 1.5 \lambda$) coincides with the untransparent gel boundary zone ($M-K-a$). In the lower part in nearly the same time distances a series of schlieren pictures obtained for the model with the low velocity layer thickness of $30 \text{ mm} = 4.8 \lambda$ is given ($M-K-b$). The thickness of the upper layer as well as the source parameters are in both cases the same. A quite different energy distribution in the wave field can be observed. The thin low velocity layer generates a strong refracted wave in the third layer whilst the reflected wave in the upper layer is very weak. The thick low velocity layer causes a dynamically more uniform wave pattern. However, for detailed studies along this

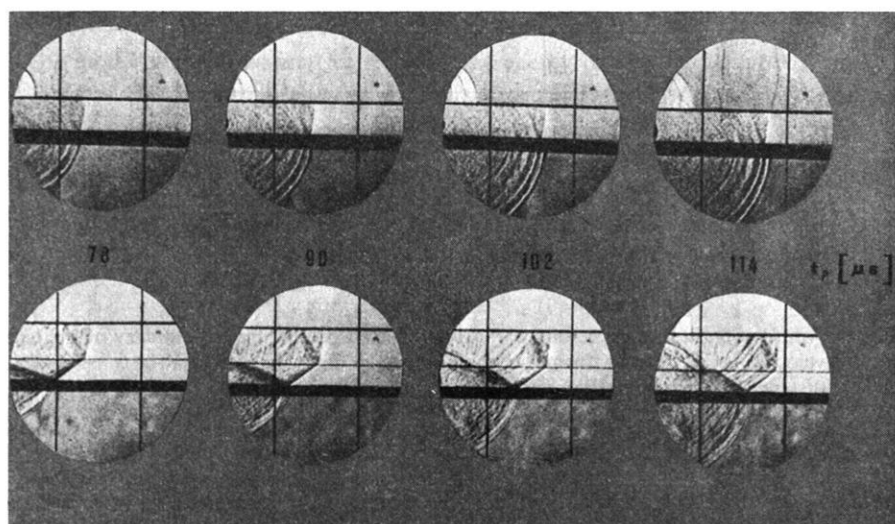


Fig. 7: P -wave field in dependence of the low velocity layer thickness. Source on the surface of the model. In the upper part thickness 1.5λ (model $M-K-a$), in the lower part thickness 4.8λ (model $M-K-b$). t_p time scale.

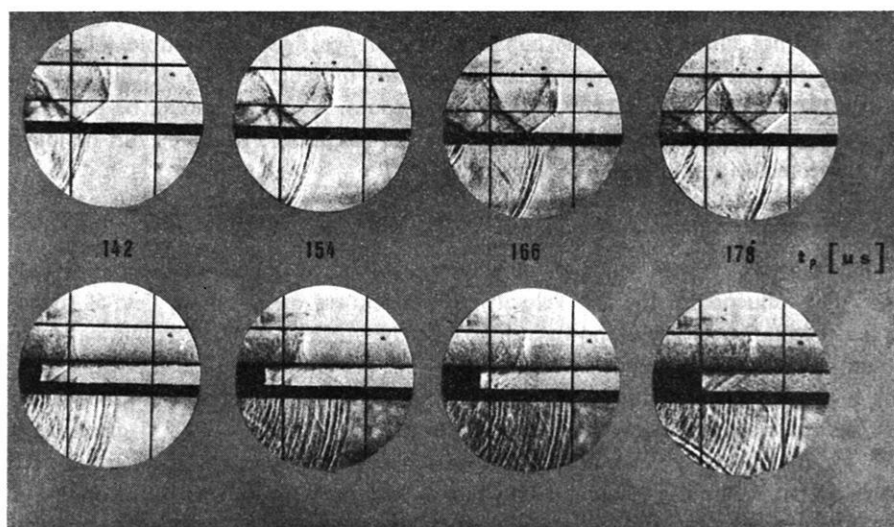


Fig. 8: Propagation of P -waves in the model M-K-b. The upper part corresponds to the position of the source on the surface of the model, the lower part to the position of the source in the middle of the low velocity layer. t_p time scale derived from P -wave travel time.

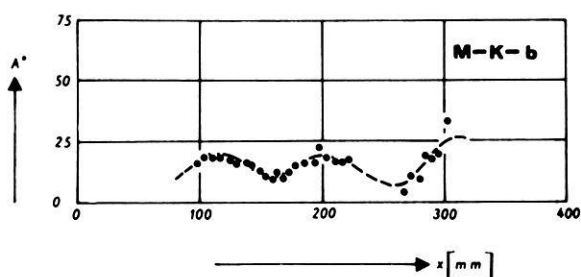


Fig. 9: Amplitude-distance curve of the P -wave reflected on the upper boundary of the low velocity layer derived from microphotometric data (Model M-K-b) x epicentral distance, A^* normalized amplitude.

line a better modelling technology has to be developed, because the wave processes in thin layers are not visible as yet, due to the diffusion and capilar effects on the glass windows.

The influence of the source depth on the P -wave field for the model M-K-b is demonstrated in Fig. 8. The arrangement of this figure is analogous to that in

Fig. 3, also most of the above mentioned findings can be confirmed. The only difference are very weak head waves generated by refracted waves with the source in the middle of the low velocity layer. As in the symmetric wave guide model TM-5 the head waves formed a separate wave group in this case no similar effect can be proved. The nonsymmetry of the velocity-depth distribution and very high velocity contrasts could account for it.

The same system of model measurements and data processing as in p. 3.1 was used with the model M-K-b. The resulting amplitude-distance curve of the *P*-wave reflected on the upper boundary of the low velocity layer shows Fig. 9. Also here a clear oscillatory character of the observed curve was confirmed. A dynamic comparison of corresponding curves with different thickness of low velocity layers is not possible on the basis of the existing experimental material.

4. Conclusions

Summarizing this paper the following conclusions can be drawn:

- 1) There exists a typical oscillation of the amplitude-distance curve of the *P*-wave reflected on the upper channel boundary. The absolute value of reflected amplitudes depends on the channel thickness.
- 2) Seismic sources located in low velocity channels produce a very strong channel wave. A close investigation of kinematic and dynamic properties is the object of further investigation.
- 3) The model set-up used enables to study the energy balance of all types of body *P*-waves. For the formulation of general statements further studies are necessary.

5. Acknowledgement

Grateful acknowledgement is made to Dr. J. KOZÁK for his friendly cooperation and particularly to Mrs. N. PICKOVÁ for her assistance in performing the experiments and treating the results.

References

- BEHRENS, J., L. DRESEN, and L. WANIEK: Investigations on two- and three-dimensional test-models. Proc. 11th Assembly ESC, Luxembourg, 1971
- BERCKHEMER, H., und L. WANIEK: Entwurf seismischer Testmodelle. Rundschreiben der Arbeitsgruppe für Modellseismik d. Europ. Seism. Komm., Herbst 1967
- CHOROSHEVA, V. V.: The study a wave guide on a solid two-dimensional model with sharp boundaries. Bull. (Izv.) Acad. Sci. USSR, Geophys. Ser. 8, 1025-1033, 1962

- KAPCAN, A. D., and V. V. KISLOVSKAJA: Investigation of wave guide with weak boundaries in two-dimensional perforated models. *Studia geoph. et geod.* 10, 360–369, 1966
- KOZÁK, J.: Kinematic and dynamic properties of elastic waves investigated on seismic models by means of the schlieren-method. *Travaux Inst. Géophys. Acad. Tchécosl. Sci.*, No. 354, *Geofyzikální sborník 1971*, Academia Praha, 1972
- KOZÁK, J., und L. WANIEK: Schlierenoptische Untersuchungen an seismischen Gelmodellen mit photometrischer Auswertung des Wellenfeldes. *Z. Geophys.* 36, 175–192, 1970
- SHAMINA, O. G.: Experimental investigation of necessary and sufficient characteristics of a wave guide. *Studia geoph. et geod.* 10, 341–350, 1966
- : Dependence of the amplitude of longitudinal waves on the depth of focus. *Bull. (Izv.) Acad. Sci. USSR, Geophys. Ser.* 9, 23–44, 1967
- WANIEK, L.: The system water-glycerol-gelatine as a medium for three-dimensional seismic models. *Studia geoph. et geod.* 10, 273–281, 1966

Model Investigations with Respect to the Interpretation of Complicated Seismic Discontinuities

J. BEHRENS and G. GOMMLICH, Clausthal¹⁾

Eingegangen am 12. Februar 1972

Summary: This paper investigates four two-dimensional models with different types of interface structures. The following models are chosen as examples: straight interface of first order, laminated interface, transition layer and a sinusoidal corrugated interface. The travel-time curves and amplitude-distance curves of the reflected waves and head-waves from these models are compared to find out the possibilities for differing them.

It can be seen, that neither the travel-time curves nor the amplitude-distance curves of the subcritical or the overcritical area yield sufficient characteristics to infer the true interface structure from those results. Only complete information of all interpretation components can be successful. The presented curves of the four investigated models show conspicuous variations which can be used for the interpretation.

Zusammenfassung: Es werden Untersuchungen an vier zweidimensionalen Modellen mit verschiedenen Grenzflächenstrukturen beschrieben. Folgende vier Modelle wurden als Beispiele gewählt: Diskontinuität 1. Ordnung, laminierte Grenzschicht, Übergangsschicht und sinusförmig gewellte Grenzfläche. Die Laufzeitkurven und Amplitudenentfernungskurven der reflektierten Wellen und der Kopfwellen dieser Modelle werden verglichen, um Unterscheidungsmöglichkeiten herauszustellen.

Es kann gezeigt werden, daß weder die Laufzeitkurven noch die Amplitudenentfernungskurven des unterkritischen oder überkritischen Bereichs für sich ausreichende Charakteristika enthalten, aus denen auf die wirkliche Grenzfläche geschlossen werden kann. Nur die gemeinsame Auswertung aller der Interpretation dienenden Parameter wird zum Erfolg führen. Die dargestellten Meßkurven der vier Modelle zeigen auffällige Verschiedenheiten, die zu einer Interpretation herangezogen werden können.

1. Introduction

At the present time, the question of the structure of seismic boundaries is of more and more importance. The two-dimensional model technique is one of the methods to investigate those problems and is turned to good account. Diverse papers have been published on first results [BEHRENS 1969b, BEHRENS 1971, BEHRENS, KOZÁK, WANIEK 1971, GOMMLICH, KITTER 1971]. These investigations aim at showing the possibilities of structure-characterization, independent to similarities with Earth's crust models.

All these papers and the paper of BEHRENS, BORTFELD, GOMMLICH and KÖHLER [1972] again point out, that the main problem is to find the connection or the bridge between the parameters of the seismic signals and the true interface structures.

¹⁾ Prof. Dr. JÖRN BEHRENS und Dipl.-Geophys. GÖTZ GOMMLICH, Institut für Geophysik der Technischen Universität Clausthal. 3392 Clausthal-Zellerfeld, Adolf-Römer-Str. 2A, BRD.

2. Investigated Models

Fig. 1 shows the investigated types of interface structures. All two-dimensional models consisted of a layer of Plexiglas overlaying a halfspace of Aluminium.

The combined values of densities, P - and S -wave velocities are shown in Table 1.

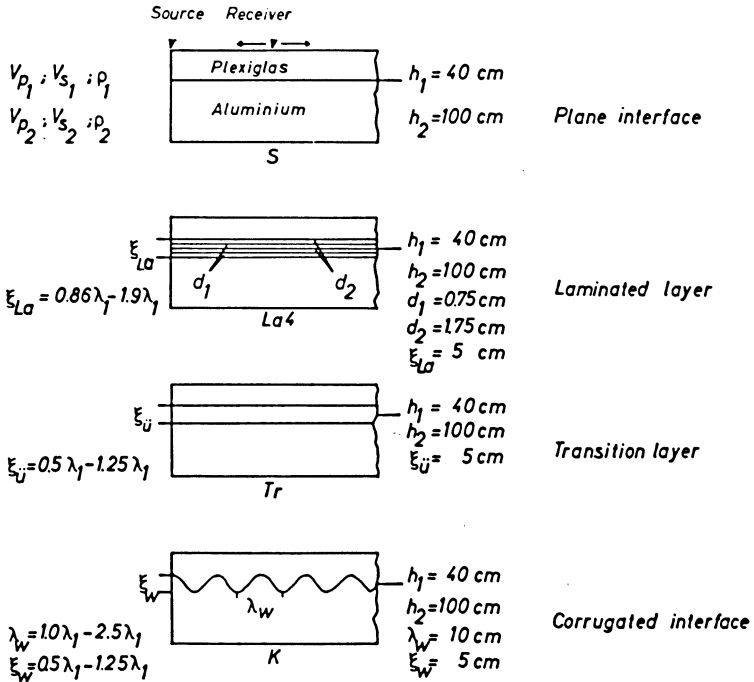


Fig. 1: Types of investigated interface-structures of the models Plexiglas/Aluminium

- λ_1 = wavelength of the incident wave
- λ_w = wavelength of the corrugation
- ξ_w = amplitude of the corrugation
- $\xi_{\bar{u}}$ = thickness of the transition layer
- ξ_{La} = thickness of the laminated layer
- d = thickness of the lamina
- V_{p_1} = P -wave velocity within the first medium
- V_{p_2} = P -wave velocity within the second medium
- V_{s_1} = S -wave velocity within the first medium
- V_{s_2} = S -wave velocity within the second medium
- ρ_1 = density of the first medium
- ρ_2 = density of the second medium

(values are stated in Table 1)

Table 1: Parameters of the models

Material for the models	Index	<i>P</i> -wave velocity V_p [mm · μ s ⁻¹]	<i>S</i> -wave velocity V_s [mm · μ s ⁻¹]	Density ρ [gr · cm ⁻³]	$\frac{V_{p1}}{V_{p2}}$	$\frac{\rho_1}{\rho_2}$
Plexiglas	1	2.32	1.35	1.2		
Aluminium	2	5.40	3.12	2.8	0.43	0.43

The ratio of *P*-wave velocities in Plexiglas and Aluminium is 0.43. This high velocity-contrast was chosen for studying the behavior of the kinematical and dynamic parameters of the signals in the region of the first and second critical point by the given length of the models.

The models have a length of 200 cm, the plathickness is 3 mm, the predominant wavelength λ_1 of the incident signal is about 4 cm.

Source and receiver are placed analogous to fieldmeasurements on the free surface of the model. The source-characteristic corresponds nearly to the theoretical characteristic of the hit on a free surface on the halfspace. The characteristic of the receiver allows to record the vertical or horizontal components of acceleration.

The first model *S* is the standard model with a straight interface of first order. The thickness h_1 of the Plexiglas-layer is 40 cm, the thickness h_2 of the Aluminium halfspace is 100 cm.

Model two has a laminated discontinuity. The laminated layer is a combination of four laminae. The designation of this model is *La4*. The laminated layer has a thickness ξ_{La} of 5 cm and consists of two laminae of Plexiglas with the thickness d_1 and two laminae of Aluminium with the thickness d_2 . The relation between the thickness d_1 and d_2 is equal to the relation between the velocities within Plexiglas and Aluminium. The thicknesses d_1 and d_2 are about a quarter of the predominant wavelength λ_1 of the incident wave.

Those models with the ratio d to λ_1 equal 0.25 and velocity-reversals were investigated theoretically by FUCHS [1969, 1970] and presumed as the structure of the MOHORVIČIĆ-discontinuity by MEISSNER [1967], DAVYDOVA, KOSMINSKAYA and MICHOTA [1970] and others.

Model three is characterized by a transition layer and is called model *Tr*. The transition layer with a nonlinear velocity-depth distribution between the upper layer of Plexiglas and the halfspace of Aluminium has a thickness $\xi_{\bar{u}}$ of 5 cm, too. It has been constructed according to the method of bimorphic models [OLIVER 1956; RIZNICHENKO, SHAMINA and KHANUTINA 1961].

The fourth model has a sinusoidal corrugated interface which is characterized by the wavelength λ_w and the amplitude ξ_w of corrugation. The wavelength λ_w is 10cm, the amplitude ξ_w is 5 cm. Models with these corrugated interfaces are called *K* models [BEHRENS 1969a, 1969b, 1971; GOMMLICH and KITTER 1971; KITTER 1971].

In Table 2 the nomenclature of the investigated models is described.

Table 2: Nomenclature of the models

Type of interface	general name of the model	special designation with respect to λ_1
straight interface	S	$S \mid \lambda_1$
laminated layer of four laminae	$La4$	$La4 \mid d_1/\lambda_1$
transition layer	Tr	$Tr \mid \xi_{\bar{u}}/\lambda_1$
corrugated interface	K	$K \mid \begin{array}{l} \xi_w/\lambda_1 \\ \lambda_w/\lambda_1 \end{array}$

λ_1 = predominant wavelength of the incident signal

d_1 = thickness of the lamina

$\xi_{\bar{u}}$ = thickness of the transition layer

λ_w = wavelength of the corrugation

ξ_w = amplitude of the corrugation

The common properties of the three last models are the thicknesses ξ of the different interface-structures. The central-lines of these structures are to be found 40 cm below the free surface of the models so that they can be compared with the straight interface model S .

3. Travel-time measurements

Fig. 2, Fig. 3 and Fig. 4 show a series of travel-time graphs for the investigated four models. On the abscissa the distance area from 10 cm to 120 cm is shown, on the ordinates the travel-time from 300 μ s to 700 μ s. X_{cr_2} and X_{cr_3} mark the first and second critical distances respectively.

Fig. 2 exemplifies the travel-time curves of model $La4$. The solid lines represent the computed travel-time curves without those of multiple reflections. The solid points mark the measured onsets of the reflected P -wave and two special types of head-waves for the model $La4 \mid 0.19$ (Table 2).

The usual branch of the P_1P_1 -reflections can be observed up to the first critical distance X_{cr_2} , whereas beyond the critical distance, the onsets of the ordinary head-wave $P_1P_2P_1$ can be observed only up to 90 cm. Parallel to the travel-time curve of the $P_1P_2P_1$ head-wave clear onsets of a second head-wave are to be found, which belong to a complicated path of propagation (Fig. 2). Onsets of a head-wave travelling in the halfspace are not clearly recognizable.

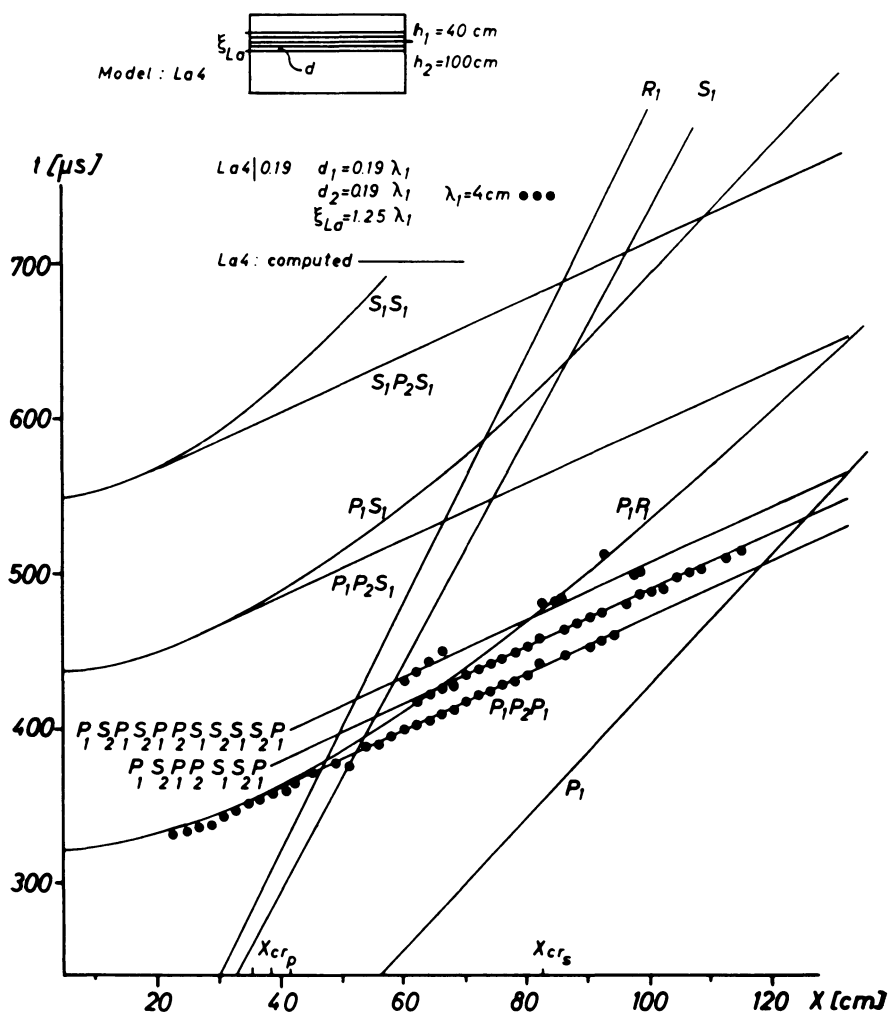


Fig. 2: Travel-time curves of the laminated model La4|0.19.

X_{cr_p} and X_{cr_s} mark the first and second critical distances respectively.

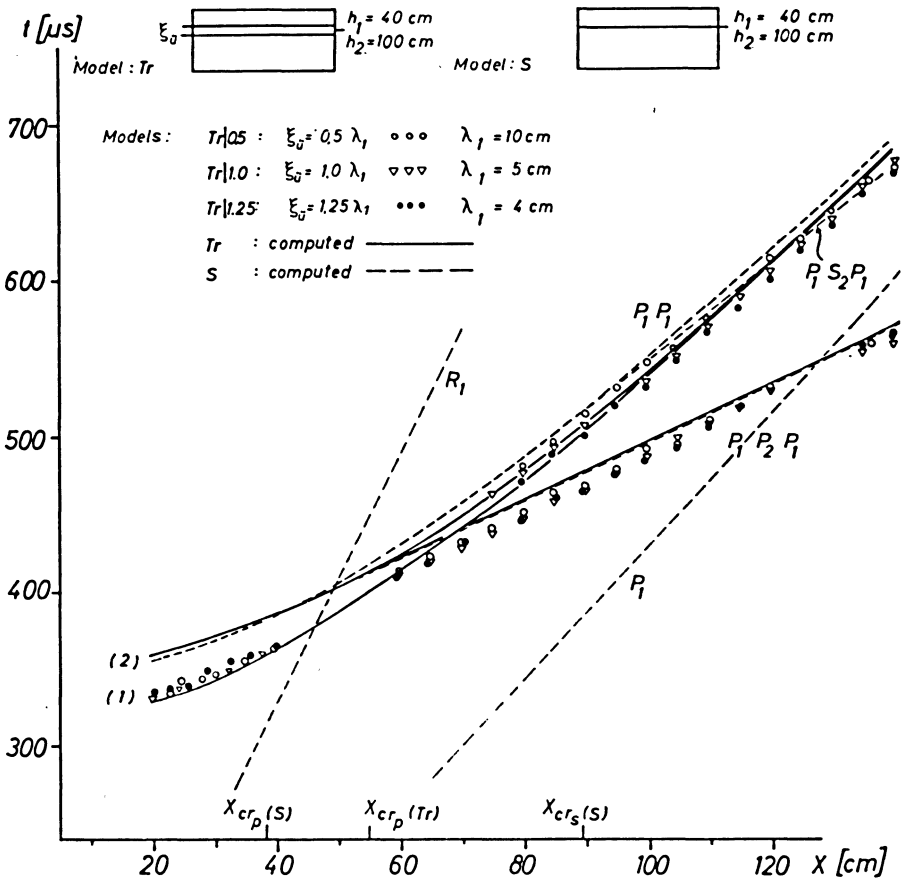


Fig. 3: Travel-time curves of the transition layer models $Tr|0.5$, $Tr|1.0$, $Tr|1.25$ and of the straight interface model S .

$X_{cr_p}(Tr)$ marks the critical distance of the models Tr .

$X_{cr_p}(S)$ and $X_{cr_s}(S)$ mark the first and second critical distances of the model S .

(1) and (2): see text.

The time measurements show that the P -wave velocity within the lamina is a few per cent slower than the expected P -wave velocity within the halfspace [RIZNICHENKO and SHAMINA 1957].

Fig. 3 shows the travel-time graphs of the model Tr . The time measurements are carried out at three different ratios $\xi_{\bar{u}}$ to λ_1 (Table 2). For comparison, there are the computed travel-time curves of the model S (straight interface) marked by dashed lines as well as of model Tr marked by solid lines.

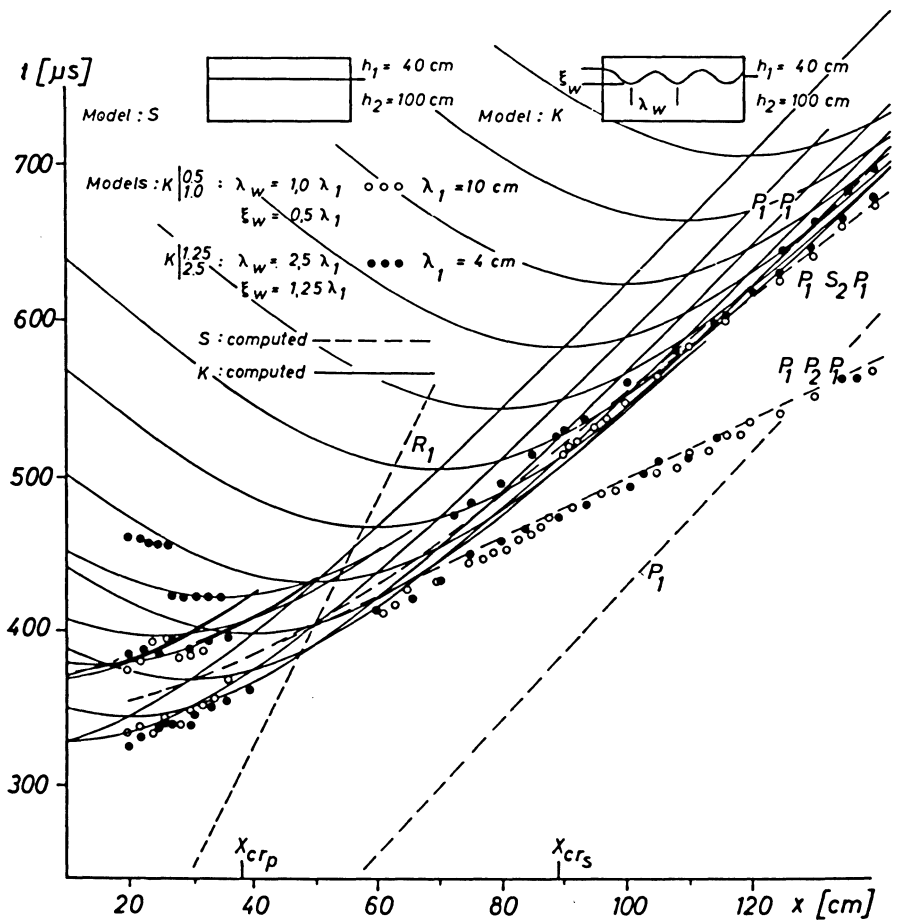


Fig. 4: Travel-time curves of the corrugated interface models $K|_{1.0}^{0.5}$, $K|_{2.50}^{1.25}$ and the straight interface model S.

X_{cr_p} and X_{cr_s} mark the first and second critical distances respectively.

Curves (1) and (2) are valid for reflections from the upper and lower boundary of the transition layer. The travel-time curve of the refracted wave is not curved as expected in the case of a transition layer. So the structure of the underground derived by the travel-time measurements only, will not be concordant with the real velocity-depth distribution of the investigated model.

Fig. 4 shows the travel-time graphs of the model K with a sinusoidal corrugated interface. The numbers beyond the vertical line of the right side of K are explained

in Table 2. The time measurements were carried out with two different predominant wavelengths λ_1 ($\lambda_1 = 10$ cm, open circles; $\lambda_1 = 4$ cm, solid points).

The dashed lines belong to model *S*, the solid lines are the computed travel-time curves for the P_1P_1 -reflections of the model *K* ($\xi_w = 5$ cm, $\lambda_w = 10$ cm) [GOMMLICH and KITTER 1971, KITTER 1971].

This diagram contains only the travel-time curves which can be observed neglecting the reflections from the interface beyond the left side of the source.

The travel-time curves of the model *K* differ much from those of other models.

The subcritical area is characterized by second onsets with travel-time curves of different apparent velocities. In this area the branches of the reflection travel-time curves are separated sufficiently—so single onsets can be identified.

The special feature of the overcritical area is characterized by the convergency of the travel-time branches. Here interferences will form the seismograms.

It is remarkable, that on the models with corrugated interfaces a clear head-wave can be observed, which appears earlier than at model *S*. This signifies that the travel path of the refracted wave is situated between the center-line and the maximums of the corrugation.

When comparing the travel-time graphs of the models *La4* and *K* with the travel-time graph of model *S*, it can be seen that there are some distinctive marks between them. Model *La4* is characterized by the second head-wave [FUCHS 1970] and the disappearance of the ordinary head-wave at short distances (90 cm). In the subcritical area model *K* shows great differences to the other models by the plurality of the travel-time curves of the P_1P_1 -reflections with different dips and the relative broad band of travel-time branches in the overcritical region.

Because of the nonlinear velocity-depth distribution of model *Tr*, the differences between the characteristics of the travel-time curves of model *Tr* and model *S* are not as obvious as in the case of the models *La4* and *K*.

4. Seismograms

The seismogram-sections of the sub- and overcritical regions for these four described models are shown in Fig. 5. The first column of this figure shows the models, their velocity-depth distribution in scheme and their special designation with respect to the predominant wavelength λ_1 of the incident signal of 4 cm (Table 2).

The next two large columns contain the pick-up distances, the seismograms of the vertical component of acceleration and the sensitivity of the amplification in order to enable a comparison of the amplitudes. The seismograms at distances of 20, 30 and 40 cm are representative of the subcritical area, the seismograms at 90, 100 and 110 cm are typical for the overcritical region. In this montage the quite different amplitudes and frequencies of the recorded signals become conspicuous.

From model *S* in the subcritical region the wellknown type of seismogram is obtained with the onsets of the direct wave P_1 , the Rayleigh wave R_1 and the reflected

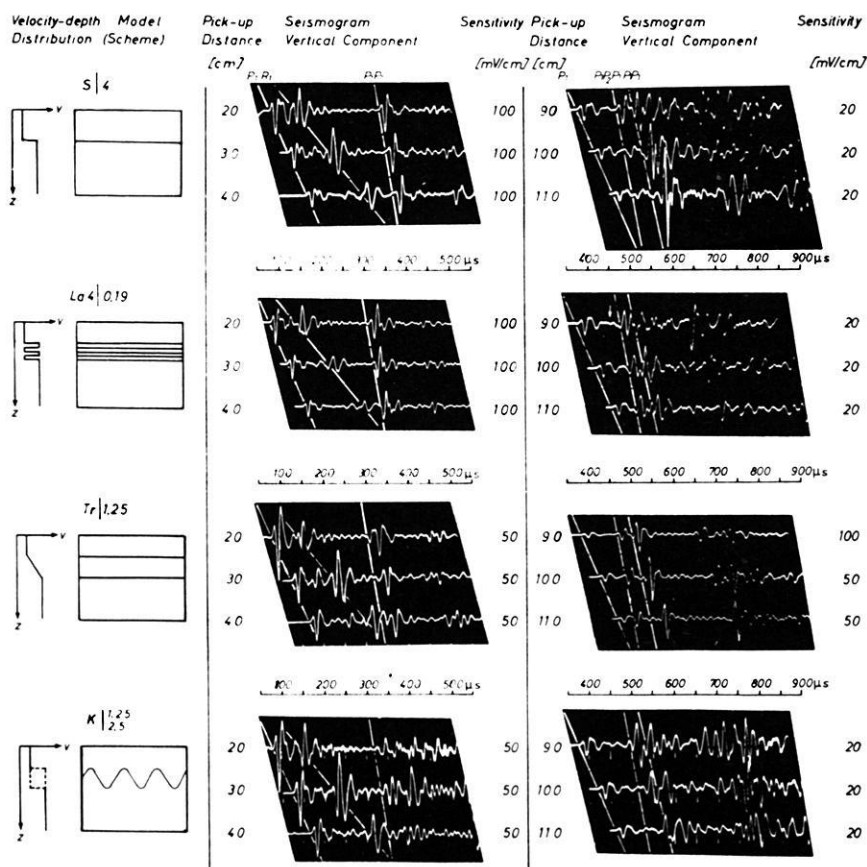


Fig. 5: Seismogram-sections of the vertical component of acceleration of the models $S|4$, $La4|0.19$, $Tr|1.25$ and $K|2.25/2.50$.

On the left: the velocity-depth distribution and the models in scheme; in the middle of the figure: the seismograms of the subcritical area; on the right side: the seismograms of the overcritical region.

arrow (model $La4|0.19$, 90 cm): onset of the $P_1P_2P_1$ -head-wave.

wave P_1P_1 . In the overcritical region, the head-wave $P_1P_2P_1$ and the reflected wave P_1P_1 can be recognized. In this region the increase of amplitudes of the P_1P_1 -reflection in the direction of the second critical maximum is clearly to be seen.

The seismograms of model $La4$ show evident differences to those of model S . The eye-catching thing in the subcritical region is the form of the reflected signal which is in correspondence with the computed seismograms by FUCHS [1969]. In the over-

critical area there is no second critical maximum of the P_1P_1 -reflections. Beside this effect there can be observed a very small onset after the P_1 wave in the seismogram at a distance of 90 cm (arrow). This onset belongs to the $P_1P_2P_1$ head-wave, which just disappears at these distances (Fig. 2). The following signal of comparable large amplitude (second white line) is caused by the second head-wave with the complicated ray path (Fig. 2).

The seismograms of model Tr are very similar to those of model S , whereas the amplitudes of the subcritical reflections are much smaller. The amplitudes of the head-waves are considerably larger than those of the model with the straight interface.

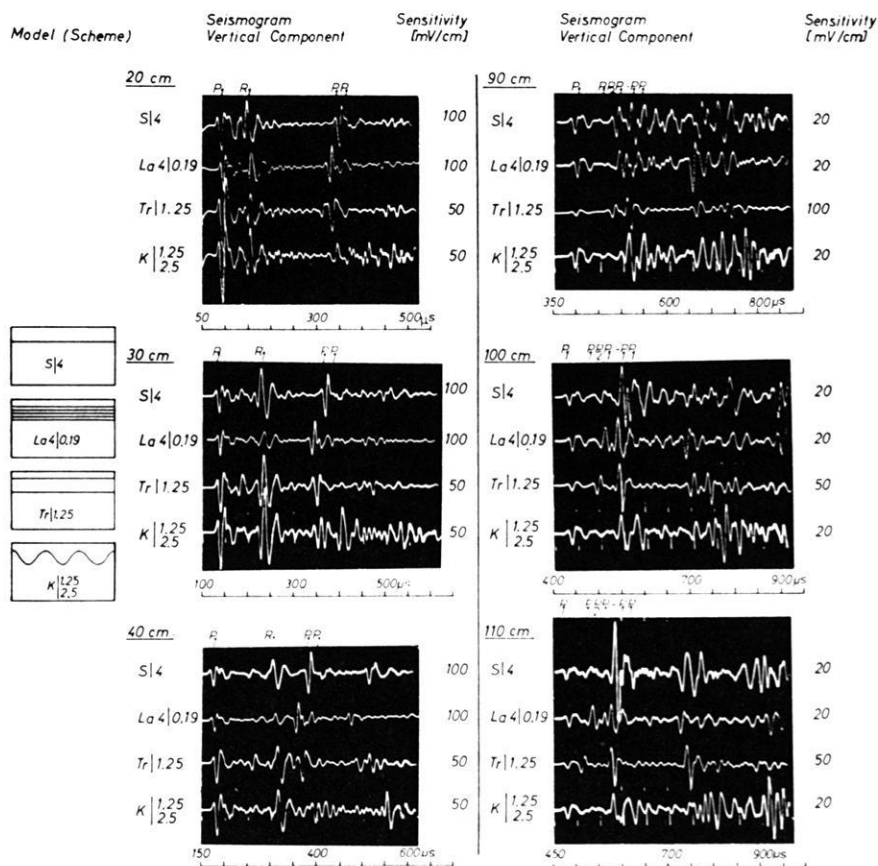


Fig. 6: Comparison of seismogram-traces of the four models $S|4$, $La|0.19$, $Tr|1.25$ and $K|1.25/2.50$ at certain distances in the sub- and overcritical region (same traces as in figure 5).

The seismograms of model *K* show quite an other picture. Beyond the first onsets of the subcritical P_1P_1 -reflections a series of subsequent onsets can be observed. It should be noted that in this case the reverberating tail of the reflected signal has a longer duration compared with the P_1P_1 -reflection from the investigated laminated interface of model *La4*. The amplitudes of the head-wave from a corrugated interface are considerably larger than those of a discontinuity of first order (model *S*). The amplitudes of the overcritical reflection and the amplitude of the head-wave are of the same order.

To point out the influence of the different interface structures on the seismograms in Fig. 6 the single seismogram-traces of the four models are compared at certain distances in the subcritical area (20, 30 and 40 cm) and in the overcritical area (90, 100 and 110 cm).

In this arrangement the interrelation of the incident signal with the concerned interface structure can be seen very clearly. Especially this is expressed by the amplitudes of the P_1P_1 -reflection in the subcritical and overcritical area. The dependence of amplitudes can be studied best by the amplitude-distance curves.

5. Amplitude-distance curves

The amplitude-distance curves of the vertical component of acceleration are shown in Fig. 7. The wavelength of the incident signal is $\lambda_1 = 4$ cm as mentioned before. On the abscissa the pick-up distances from 0 to 160 cm are plotted, on the ordinate the first maximum of the amplitudes of the P_1P_1 -reflections in arbitrary units. The amplitudes of the head-waves are shown in a separate coordinate system with the same scale (Fig. 7, upper part). For the purpose of evaluation of the amplitude-distance curves the special radiation pattern of the source was eliminated.

The amplitudes between 45 cm and 55 cm are disturbed by the *Rayleigh*- and *S*-wave and are not contained in this figure.

The amplitude-distance curve of model *S* shows the well-known behavior [ČERVENÝ 1965, COURONEAU 1965, BEHRENS, DRESEN, HINZ 1969], with the first critical maximum at ~ 45 cm, the minimum in the interference zone of the overcritical reflected wave and the head-wave and the strongly marked second critical maximum at ~ 120 cm.

The amplitude-distance curve of model *La4* | 0.19 shows an other course. At the subcritical distance X_{cr_p} the amplitudes are smaller. In the vicinity of the shotpoint the reflectivity seems to be stronger than for the model *S* | 4 in agreement to the theoretical results published by FUCHS [1969]. No critical maximums can be observed.

The amplitude-distance curves of the next two models *Tr* | 1.25 and *K* | $\frac{1.25}{2.5}$ are strongly different to the amplitude-distance curves of the previous described models in the subcritical area.

The amplitudes are considerably smaller. The undulation of the amplitudes in the subcritical region is characteristic of corrugated interfaces [BEHRENS 1969a, b; GOMMLICH, KITTER 1971; KITTER 1971]. This fact states a possibility to distinguish

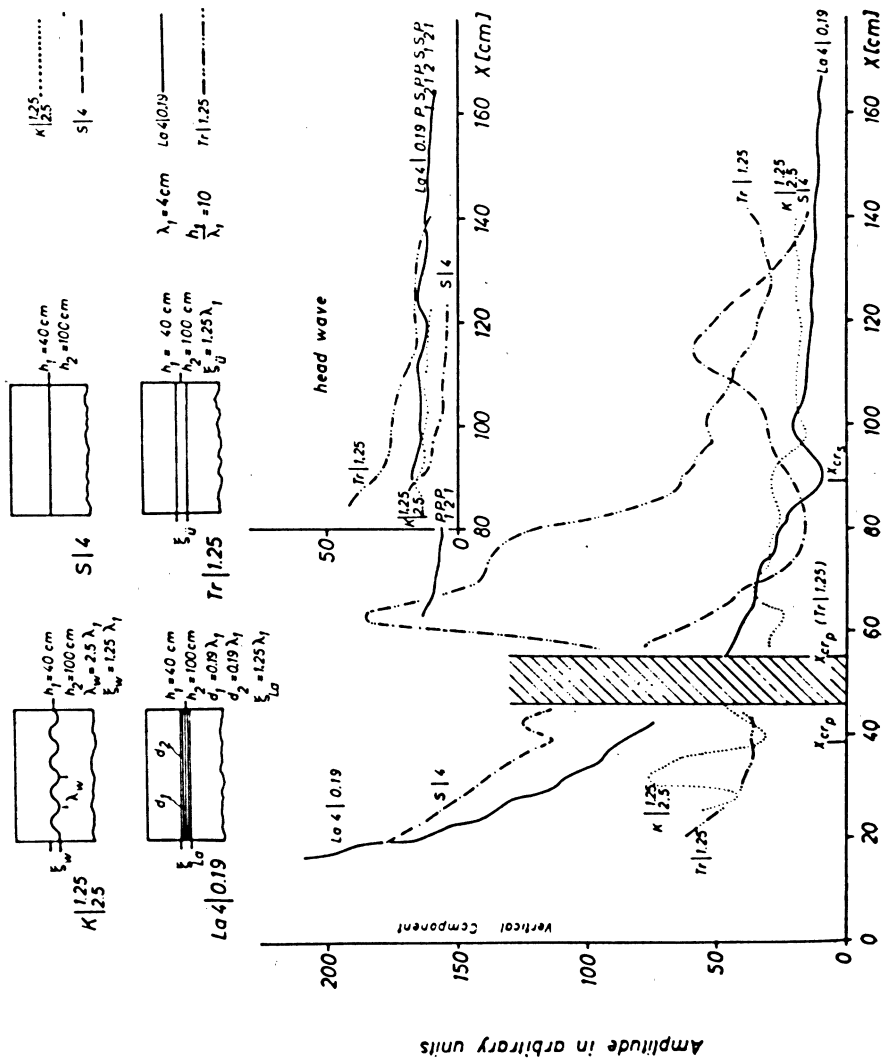


Fig. 7: Amplitude-distance curves of the vertical component of acceleration of the first maximums of the reflected (P_1P_1) and head-waves ($P_1P_2P_1$) in arbitrary units. X_{crp} and X_{crs} mark the first and second critical distance respectively.

the corrugated interface from this type of investigated transition layer. In the overcritical region a large difference in the magnitude of amplitudes can be observed. The large maximum of the amplitude-distance curve of the model $Tr | 1.25$ is produced by the nonlinear velocity-depth distribution within the investigated transition layer [BEHRENS 1971]. The amplitude curves of the P_1P_1 -reflection from the corrugated model $K |_{2.5}^{1.25}$ and from model $La4 | 0.19$ show a very similar behaviour.

The amplitudes of the head-waves of the models $K |_{2.5}^{1.25}$ and $La4 | 0.19$ seem to be equal when comparing the ordinary head-wave of model $K |_{2.5}^{1.25}$ with the second head-wave of model $La4 | 0.19$. The amplitudes of the ordinary head-wave $P_1P_2P_1$ of model $La4 | 0.19$ are only available up to 80 cm. The strong decrease is the result of wave propagation in thin layers. The amplitudes of this head-wave are much smaller than of model $S | 4$, whereas the head-wave amplitudes of the other models ($Tr | 1.25$, $K |_{2.5}^{1.25}$) are larger than those of the model $S | 4$. This is in correspondence with results of NAKAMURA [1968], BEHRENS [1969a], ABUBAKAR [1962] and others for poorly defined interfaces.

6. Conclusions

The amplitudes of head-waves serve only as an information about a possible complicated character of the structure not about the form of the structure itself.

Possible informations about the structure are to be found rather in the combined amplitude-informations of sub- and overcritical reflections.

To complete the work of interpretation of seismic discontinuities in addition to the travel-time and amplitude measurements, frequency investigations of the signals of the reflected and refracted waves are necessary. The results of these investigations, that is to say the possibilities and limits of frequency measurements have already been published by BEHRENS [1969a, b, 1971] and will not be repeated here.

The aim of the described model investigations was to show the possibilities of interpretation of complicated structures. The aim of further investigations of this kind, in connection with theoretical and field work, should be to find a bridge between seismogram and interface structure, in other words, to find a certain "black box" which combines all informations to the real picture of the discontinuity.

The combined theoretical and model investigations of BEHRENS, BORTFELD, GOMM-LICH, and KÖHLER [1972] point to a practical construction of such a "black box".

7. Acknowledgements

The results reported in this paper are part of the results of investigations sponsored generously by the "Deutsche Forschungsgemeinschaft" (German Research Association).

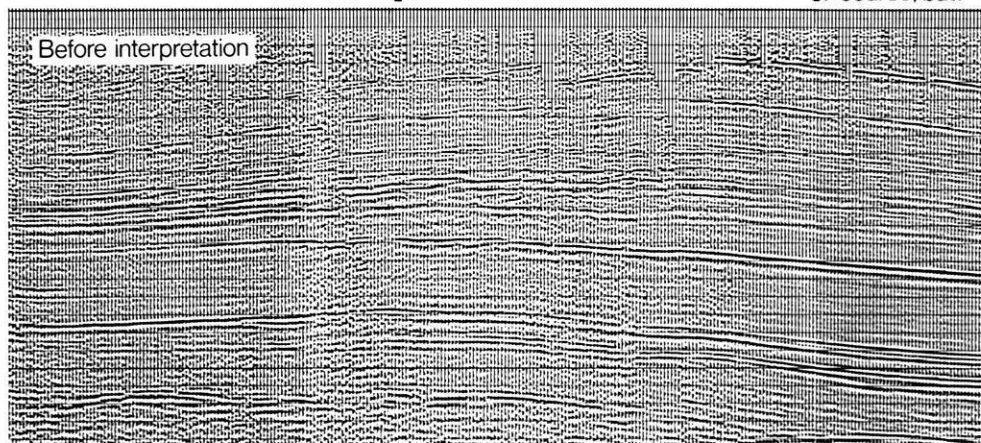
The authors are indebted to Prof. Dr.-Ing. O. ROSENBACH for the kind support of the investigations and to their colleagues A. MÜLLER, H. HEMSCHEMEIER, and G. MÜLLER for the accurate fabrication of the models.

References

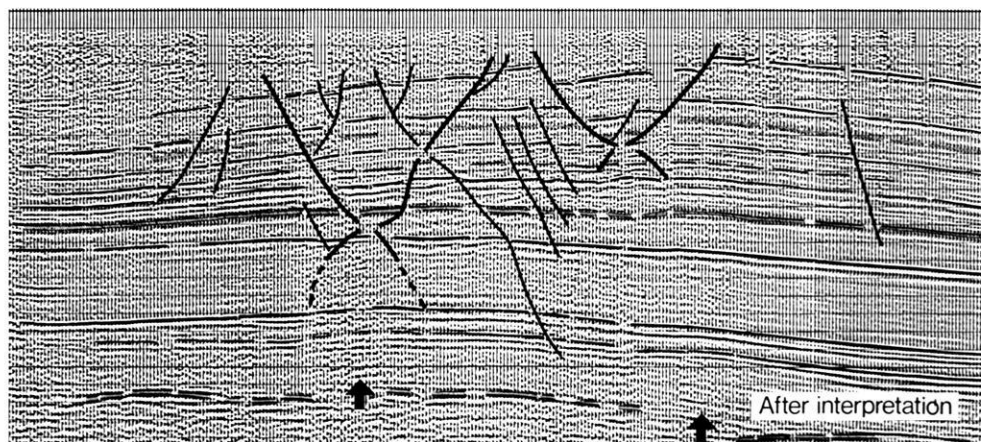
- ABUBAKAR, J.: Scattering of plane elastic waves at rough surfaces. *Proc. Cambridge Phil. Soc.* 58, 136–157, 1962
- BEHRENS, J.: Die Charakterisierung seismischer Grenzflächen mit Hilfe modellseismischer Verfahren im Hinblick auf Deutungsmöglichkeiten des Krustenaufbaus. *Habilitationschrift*, Technische Universität Clausthal, 1969a
- : Möglichkeiten zur Charakterisierung von Grenzflächenstrukturen. Paper, read on the 30th meeting of the Deutsche Geophysikalische Gesellschaft, Salzburg, 1969b
- BEHRENS, J., L. DRESEN, and E. HINZ: Modellseismische Untersuchungen der dynamischen Parameter von Kopfwelle und Reflexion im überkritischen Bereich. *Z. Geophys.* 35, 43–68, 1969
- BEHRENS, J.: Model investigations on the boundary structure Earth's crust/mantle. *Proceedings of the 12th General Assembly of the European Seismological Commission, Luxembourg*, 1971
- BEHRENS, J., J. KOZÁK, and L. WANIEK: Investigation of wave phenomena on corrugated interfaces by means of the Schlieren-method. *Proceedings of the 12th General Assembly of the European Seismological Commission, Luxembourg*, 1971
- BEHRENS, J., R. BORTFELD, G. GOMMLICH, and K. KÖHLER: Interpretation of discontinuities by seismic imaging. *Z. Geophys.* 38, 481–498, 1972
- ČERVENÝ, V.: The dynamic properties of reflected and head-waves around the critical point. *Travaux de l'Institut Géophysique de l'Académie Tschécoslovaque des Sciences, Géophysikální Sborník*, 221, 135–245, 1965
- COURONEAU, J.: Étude du "point brillant" sur modèles séismique. *Geophys. Prospect.* 13, 405–432, 1965
- DAVYDOVA, N. I., I. P. KOSMINSKAYA, and G. G. MICHOTA: The thickness and nature of seismic discontinuities based on deep seismic sounding. *Tectonophysics* 10, 561–572, 1970
- FUCHS, K.: On the properties of deep crustal reflectors. *Z. Geophys.* 35, 133–149, 1969
- : On the determination of velocity depth distributions of elastic waves from the dynamic characteristics of the reflected wave field. *Z. Geophys.* 36, 531–548, 1970
- GOMMLICH, G., and E. KITZER: Modellseismische Untersuchungen über den Entstehungs- und Ausbreitungsmechanismus reflektierter Wellen an welligen Grenzflächen. Paper, read on the 31st meeting of the Deutsche Geophysikalische Gesellschaft, Karlsruhe, 1971

- KITTER, E.: Modellseismische Untersuchungen über den Ausbreitungsmechanismus reflektierter Wellen an welligen Grenzflächen. Diplomarbeit, Technische Universität Clausthal, 1971
- MEISSNER, R.: Zum Aufbau der Erdkruste. Ergebnisse der Weitwinkelmessungen im Bayerischen Molassebecken. Teil I: Gerlands Beitr. Geophys. 76, (3), 211 – 254, Teil II: Gerlands Beitr. Geophys. 76, (4), 295 – 314, 1967
- NAKAMURA, Y.: Head waves from a transition layer. Bull. Seism. Soc. Am. 58, 963 – 976, 1968
- OLIVER, J.: Body waves in layered seismic models. Earthquake Notes 27, 29 – 38, 1956
- RIZNICHENKO, YU. V., and O. G. SHAMINA: Elastic waves in a laminated solid medium, as investigated on two-dimensional models. Bull. (Izv.) Acad. Sci. USSR, Geophys. Ser., 17 – 37, 1957
- RIZNICHENKO, YU. V., O. G. SHAMINA, and R. V. KHANUTINA: Elastic waves with generalized velocity in two-dimensional bimorphic models. Bull. (Izv.) Acad. Sci. USSR, Geophys. Ser., 321 – 334, 1961

Don't believe
that you can solve
all your seismic gas and oil problems
with good instruments
and field techniques alone. We use both of them,
of course, but.



have a look at these two pics- and you know „**why**”



35 to 40 interpretation groups
with experienced seismologists
are currently working for our clients
all over the world

PRAKLA-SEISMOS GMBH · 3 000 HANNOVER · HAARSTRASSE 5
P.O.BOX 4767 · PHONE: 80721 · TELEX: 9 22847 · CABLE: PRAKLA
GERMANY



Amsterdam · Ankara · Brisbane · Djakarta · Lima · London · Madrid
Milan · Rangoon · Rio de Janeiro · Singapore · Teheran · Tripoli · Vienna